

Synthesis and Characterisation of Chromium(III) Complexes with Polypyridyl Ligands

Inauguraldissertation

zur

Erlangung der Würde eines Doktors der Philosophie
vorgelegt der
Philosophisch-Naturwissenschaftlichen Fakultät
der Universität Basel

von

Jonas Michael Schönle

von

Bern (BE)

Basel, 2014

Originaldokument gespeichert auf dem Dokumentenserver der Universität Basel
edoc.unibas.ch



Dieses Werk ist unter dem Vertrag „Creative Commons Namensnennung-Keine
kommerzielle Nutzung-Keine Bearbeitung 3.0 Schweiz“ (CC BY-NC-ND 3.0 CH) lizenziert.
Die vollständige Lizenz kann unter

creativecommons.org/licenses/by-nc-nd/3.0/ch/
eingesehen werden.

Genehmigt von der Philosophisch-Naturwissenschaftlichen Fakultät auf Antrag von:

Prof. Dr. Edwin C. Constable

Prof. Dr. Oliver S. Wenger

Basel, den 24.06.2014

Prof. Dr. Jörg Schibler

Dekan



Namensnennung-Keine kommerzielle Nutzung-Keine Bearbeitung 3.0 Schweiz
(CC BY-NC-ND 3.0 CH)

Sie dürfen: Teilen — den Inhalt kopieren, verbreiten und zugänglich machen

Unter den folgenden Bedingungen:



Namensnennung — Sie müssen den Namen des Autors/Rechteinhabers in der von ihm festgelegten Weise nennen.



Keine kommerzielle Nutzung — Sie dürfen diesen Inhalt nicht für kommerzielle Zwecke nutzen.



Keine Bearbeitung erlaubt — Sie dürfen diesen Inhalt nicht bearbeiten, abwandeln oder in anderer Weise verändern.

Wobei gilt:

- **Verzichtserklärung** — Jede der vorgenannten Bedingungen kann **aufgehoben** werden, sofern Sie die ausdrückliche Einwilligung des Rechteinhabers dazu erhalten.
- **Public Domain (gemeinfreie oder nicht-schützbar Inhalte)** — Soweit das Werk, der Inhalt oder irgendein Teil davon zur Public Domain der jeweiligen Rechtsordnung gehört, wird dieser Status von der Lizenz in keiner Weise berührt.
- **Sonstige Rechte** — Die Lizenz hat keinerlei Einfluss auf die folgenden Rechte:
 - Die Rechte, die jedermann wegen der Schranken des Urheberrechts oder aufgrund gesetzlicher Erlaubnisse zustehen (in einigen Ländern als grundsätzliche Doktrin des **fair use** bekannt);
 - Die **Persönlichkeitsrechte** des Urhebers;
 - Rechte anderer Personen, entweder am Lizenzgegenstand selber oder bezüglich seiner Verwendung, zum Beispiel für **Werbung** oder Privatsphärenschutz.
- **Hinweis** — Bei jeder Nutzung oder Verbreitung müssen Sie anderen alle Lizenzbedingungen mitteilen, die für diesen Inhalt gelten. Am einfachsten ist es, an entsprechender Stelle einen Link auf diese Seite einzubinden.

Contents

Acknowledgements	ix
Abstract	x
Abbreviations and Explanations	xii
1 Introduction	1
1.1 Chromium	1
1.2 Coordination chemistry	2
1.2.1 Oligopyridine ligands and complexes thereof	4
1.2.2 Chromium(III) complexes with polypyridyl ligands	4
1.3 Photophysics of octahedral chromium(III) complexes	5
1.4 Sustainable materials	5
1.4.1 Dye-sensitised solar cels (DSC)	6
1.4.2 Light emitting electrochemical cell (LEC)	9
2 Tris(diimine)chromium(III) complexes	11
2.1 Synthesis of tris(diimine)chromium(III) complexes	11
2.2 Unsuccessful synthetic trials	17
2.3 Photophysical properties	19
2.3.1 Absorption spectra	19
2.3.2 Photoluminescence of the tris(diimine)chromium(III) complexes	20
2.3.2.1 Additional emission band - possible decomposition of the complexes	22
2.3.3 Electroluminescence of tris(bipyridine)chromium(III) complexes	24
2.4 Electrochemical measurements	24
2.5 Tris(diimine)chromium(III) complexes: X-ray structures	26
2.5.1 Structure of $[\text{Cr}(\text{bpy})_3][\text{PF}_6]_3 \cdot \text{MeCN}$	28
2.5.2 Structure of $4\{[\text{Cr}(\text{bpy})_2(\text{phen})][\text{PF}_6]_3\} \cdot 11\text{MeCN}$	29
2.5.3 Structure of $[\text{Cr}(\text{bpy})_2(5,5'\text{-Me}_2\text{bpy})][\text{PF}_6]_3 \cdot 3\text{Me}_2\text{CO}$	29
2.5.4 Structure of $\text{Cr}[(4,4'\text{-Me}_2\text{bpy})_2(\text{bpy})][\text{PF}_6]_3$	30
2.5.5 Structure of $[\text{Cr}(5,5'\text{-Me}_2\text{bpy})_3][\text{PF}_6]_3$	31
3 Bis(terpyridine)chromium(III) complexes	33
3.1 Synthesis of bis(terpyridine)chromium(III) complexes	33
3.2 Lability of the bis(terpyridine)chromium(III) complexes	38
3.2.1 Lability in alkaline environment	38
3.2.2 Fluoride lability	41
3.3 Ligand exchange	43
3.4 Photophysics of the bis(terpyridine)chromium(III) complexes	48
3.4.1 Absorption spectra of the bis(terpyridine)chromium(III) complexes	48
3.4.2 Photoluminescence of the bis(terpyridine)chromium(III) complexes	48
3.4.2.1 Does the emission derive from a complex or from free ligand?	50

3.5	Complexes containing 4'-diphenylaniline terpyridine ligands	52
3.5.1	Absorption spectroscopy	52
3.5.1.1	Negative solvatochromic effect	55
3.5.2	Photoluminescence measurements	57
3.6	Electrochemical measurements	59
3.7	EPR measurements	63
3.8	DSC trials with bis(terpyridine)chromium(III) complexes	65
3.8.1	Dye-sensitized solar cell trials	65
3.8.2	DSC fabrication and characterisation	65
3.8.3	DSC trials	66
3.9	X-ray structures	70
3.9.1	Homoleptic complexes	71
3.9.1.1	Structure of $2\{[\text{Cr}(\text{tpy})_2][\text{PF}_6]_3\}\cdot 5\text{MeCN}$	73
3.9.1.2	Structure of $[\text{Cr}(5,5''\text{-Me}_2\text{tpy})_2][\text{CF}_3\text{SO}_3]_3\cdot\text{H}_2\text{O}$	75
3.9.1.3	Structure of $5\{[\text{Cr}(\text{LT}3)_2][\text{PF}_6]_3\}\cdot\text{MeCN}$	77
3.9.1.4	Structure of $[\text{Cr}(4'-(4\text{-tolyl})\text{tpy})_2][\text{CF}_3\text{SO}_3]_3\cdot 2\text{MeCN}$	79
3.9.1.5	Structure of $[\text{Cr}(\text{LT}1)_2][\text{CF}_3\text{SO}_3]_3$	80
3.9.1.6	Structure of $[\text{Cr}(\text{HLT}11)(\text{LT}11)][\text{PF}_6]_4$	81
3.9.2	Heteroleptic complexes	84
3.9.2.1	$[\text{Cr}(\text{tpy})(5,5''\text{-Me}_2\text{tpy})][\text{PF}_6]_3\cdot 3\text{MeCN}$	86
3.9.2.2	$[\text{Cr}(\text{tpy})(\text{HLT}11)][\text{PF}_6]_3[\text{CF}_3\text{SO}_3]$	86
3.9.2.3	Structure of $[\text{Cr}(\text{tpy})(\text{LT}7)][\text{PF}_6]_3\cdot 3\text{Me}_2\text{CO}$	87
3.9.2.4	$[\text{Cr}(\text{tpy})(\text{LT}9)][\text{PF}_6]_3\cdot 2\text{MeCN}$	89
3.9.2.5	$[\text{Cr}(\text{tpy})(4'-(4\text{-tolyl})\text{tpy})][\text{PF}_6]_3\cdot 3\text{MeCN}$	90
3.9.2.6	Structure of $[\text{Cr}(\text{tpy})(\text{LT}8)][\text{PF}_6]_3$	92
4	Bis(terpyridine)cobalt(III) complexes	95
4.1	Synthesis of the bis(terpyridine)cobalt(III) complexes	95
5	Terpyridine ligand synthesis	97
5.1	Synthesis of the tpy ligands	97
5.1.1	2,2':6',2''-Terpyridine (tpy)	97
5.1.1.1	5,5''-Dimethyl-2,2':6',2''-terpyridine (5,5''-Me ₂ tpy)	98
5.1.1.2	2,2':6',2''-Terpyridines (tpy) substituted at the 4'-position	98
5.1.1.3	Synthesis of 4-([2,2':6',2''-terpyridin]-4'-yl)- <i>N,N</i> -diphenylaniline (LT5)	100
5.1.2	Further terpyridine ligands	101
5.2	X-ray structure	102
5.2.1	Structure of $2\{[\text{H}_2\text{LT}4][\text{CF}_3\text{SO}_3]_2\}\cdot\text{Et}_2\text{O}$	102
6	Experimental	105
6.1	General experimental	105
6.2	Synthesis of terpyridine ligands	107
6.2.1	Synthesis of precursors for terpyridine ligands	107
6.2.1.1	3-(Dimethylamino)-1-(pyridin-2-yl)prop-2-en-1-one (P1)	107
6.2.1.2	1,1'-(Pyridine-2,6-diylbis(2-oxoethane-2,1-diyl))bis(pyridin-1-ium) iodide (P2)	107
6.2.1.3	4'-(4-Bromophenyl)-2,2':6',2''-terpyridine (P3)	108
6.2.2	Terpyridine ligands	108
6.2.2.1	2,2':6',2''-Terpyridine (tpy)	108

	6.2.2.2	5,5''-Dimethyl-2,2':6',2''-terpyridine (5,5''-Me ₂ tpy)	109
	6.2.2.3	4'-(4-Tolyl)-2,2':6',2''-terpyridine (4'-(4-tolyl)tpy)	109
	6.2.2.4	4'-(4-(<i>tert</i> -Butyl)phenyl)-2,2':6',2''-terpyridine (LT1)	110
	6.2.2.5	4'-([1,1'-Biphenyl]-4-yl)-2,2':6',2''-terpyridine (LT2)	110
	6.2.2.6	4'-(Naphthalen-2-yl)-2,2':6',2''-terpyridine (LT3)	111
	6.2.2.7	6,6''-Dimethyl-4'-(<i>p</i> -tolyl)-2,2':6',2''-terpyridine (LT4)	111
	6.2.2.8	4-([2,2':6',2''-Terpyridin]-4'-yl)- <i>N,N</i> -diphenylaniline (LT5)	112
6.3		Synthesis of tris(diimine)chromium(III) complexes	113
	6.3.1	Synthesis of the {Cr(NN) ₂ Cl ₂ }Cl- type precursors	113
	6.3.1.1	[Cr(bpy) ₂ Cl ₂]Cl	113
	6.3.1.2	[Cr(phen) ₂ Cl ₂]Cl	113
	6.3.1.3	[Cr(5,5'-Me ₂ bpy) ₂ Cl ₂]Cl	114
	6.3.1.4	[Cr(4,4'-Me ₂ bpy) ₂ Cl ₂]Cl	114
	6.3.2	Synthesis of the {Cr(NN) ₂ (CF ₃ SO ₃) ₂ }(CF ₃ SO ₃)- type precursors	115
	6.3.2.1	[Cr(bpy) ₂ (CF ₃ SO ₃) ₂][CF ₃ SO ₃]	115
	6.3.2.2	[Cr(phen) ₂ (CF ₃ SO ₃) ₂][CF ₃ SO ₃]	115
	6.3.2.3	[Cr(5,5'-Me ₂ bpy) ₂ (CF ₃ SO ₃) ₂][CF ₃ SO ₃]	116
	6.3.2.4	[Cr(4,4'-Me ₂ bpy) ₂ (CF ₃ SO ₃) ₂][CF ₃ SO ₃]	116
	6.3.3	Synthesis of the {Cr(NN) ₃ } complexes	117
	6.3.3.1	[Cr(bpy) ₃][PF ₆] ₃	117
	6.3.3.2	[Cr(bpy) ₂ (phen)][PF ₆] ₃	117
	6.3.3.3	[Cr(bpy) ₂ (5,5'-Me ₂ bpy)][PF ₆] ₃	118
	6.3.3.4	[Cr(bpy) ₂ (4,4'-Me ₂ bpy)][PF ₆] ₃	118
	6.3.3.5	[Cr(phen) ₃][PF ₆] ₃	119
	6.3.3.6	[Cr(phen) ₂ (5,5'-Me ₂ bpy)][PF ₆] ₃	119
	6.3.3.7	[Cr(phen) ₂ (4,4'-Me ₂ bpy)][PF ₆] ₃	120
	6.3.3.8	[Cr(5,5'-Me ₂ bpy) ₃][PF ₆] ₃	120
	6.3.3.9	[Cr(5,5'-Me ₂ bpy) ₂ (phen)][PF ₆] ₃	121
	6.3.3.10	[Cr(5,5'-Me ₂ bpy) ₂ (4,4'-Me ₂ bpy)][PF ₆] ₃	121
	6.3.3.11	[Cr(4,4'-Me ₂ bpy) ₂ (bpy)][PF ₆] ₃	122
	6.3.3.12	[Cr(4,4'-Me ₂ bpy) ₂ (5,5'-Me ₂ bpy)][PF ₆] ₃	122
6.4		Synthesis of bis(terpyridine)chromium(III) complexes	124
	6.4.1	Synthesis of the precursors of type: {Cr(tpy)Cl ₃ }	124
	6.4.1.1	[Cr(tpy)Cl ₃]	124
	6.4.1.2	[Cr(4'-(4-tolyl)tpy)Cl ₃]	124
	6.4.1.3	[Cr(LT1)Cl ₃]	125
	6.4.1.4	[Cr(LT2)Cl ₃]	125
	6.4.1.5	[Cr(LT3)Cl ₃]	126
	6.4.1.6	[Cr(5,5''-Me ₂ tpy)Cl ₃]	126
	6.4.1.7	[Cr(LT4)Cl ₃]	127
	6.4.1.8	[Cr(LT5)Cl ₃]	127
	6.4.1.9	[Cr(LT11)Cl ₃]	128
	6.4.2	Synthesis of the precursors of the type {Cr(tpy)(CF ₃ SO ₃) ₃ }	128
	6.4.2.1	[Cr(tpy)(CF ₃ SO ₃) ₃]	128
	6.4.2.2	[Cr(5,5''-Me ₂ tpy)(CF ₃ SO ₃) ₃]	128
	6.4.2.3	[Cr(LT4)(CF ₃ SO ₃) ₃]	129
	6.4.2.4	[Cr(LT5)(CF ₃ SO ₃) ₃]	129
	6.4.3	Synthesis of the bis(terpyridine)chromium(III) complexes	130
	6.4.3.1	[Cr(tpy) ₂][PF ₆] ₃	130
	6.4.3.2	[Cr(4'-(4-tolyl)tpy) ₂][CF ₃ SO ₃] ₃	130

6.4.3.3	[Cr(4'-(4-tolyl)tpy) ₂][PF ₆] ₃	131
6.4.3.4	[Cr(LT3) ₂][PF ₆] ₃	131
6.4.3.5	[Cr(5,5''-Me ₂ tpy) ₂][PF ₆] ₃	132
6.4.3.6	[Cr(LT5) ₂][CF ₃ SO ₃] ₃	132
6.4.3.7	[Cr(HLT11)(LT11)][PF ₆] ₄	133
6.4.3.8	[Cr(tpy)(4'-(4-tolyl)tpy)][PF ₆] ₃	133
6.4.3.9	[Cr(tpy)(HLT11)][PF ₆] ₄	134
6.4.3.10	[Cr(tpy)(LT7)][PF ₆] ₄	134
6.4.3.11	[Cr(tpy)(LT8)][PF ₆] ₃	135
6.4.3.12	[Cr(tpy)(LT9)][PF ₆] ₃	135
6.4.3.13	[Cr(tpy)(5,5''-Me ₂ tpy)][PF ₆] ₃	135
6.4.3.14	[Cr(LT6)(4'-(4-tolyl)tpy)][CF ₃ SO ₃] ₃	136
6.4.3.15	[Cr(4'-(4-tolyl)tpy)(LT4)][CF ₃ SO ₃] ₃	136
6.4.3.16	[Cr(4'-(4-tolyl)tpy)(LT4)][PF ₆] ₃	137
6.4.3.17	[Cr(4'-(4-tolyl)tpy)(LT5)][CF ₃ SO ₃] ₃	137
6.4.3.18	[Cr(LT2)(LT5)][CF ₃ SO ₃] ₃	138
6.4.3.19	[Cr(5,5''-Me ₂ tpy)(LT4)][CF ₃ SO ₃] ₃	138
6.4.3.20	[Cr(LT1)(LT4)][CF ₃ SO ₃] ₃	139
6.4.3.21	[Cr(LT2) ₂][PF ₆] ₃	139
6.4.3.22	[Cr(LT5)(LT10)][CF ₃ SO ₃] ₃	140
6.4.3.23	[Cr(4'-(4-tolyl)tpy)(5,5''-Me ₂ tpy)][CF ₃ SO ₃] ₃ (trial)	140
6.5	Synthesis of the bis(terpyridine)cobalt(III) complexes	141
6.5.1	[Co(tpy) ₂][PF ₆] ₃	141
6.5.2	[Co(LT3) ₂][PF ₆] ₃	141
6.5.3	[Co(4'-(4-tolyl)tpy) ₂][PF ₆] ₃	142
	Conclusion and outlook	143

Bibliography

153

Appendix A: X-ray structures: CIF file labels and CCDC numbers	154
--	-----

Acknowledgements

First of all, I thank my supervisors *Prof. Dr. Edwin C. Constable* and *Prof. Dr. Catherine E. Housecroft* for the opportunity to do my PhD project in their group. During the last four years they helped, advised and supported me on my project. It was a great pleasure to work on this wide-ranging and demanding project. I enjoyed working in the excellently equipped lab and having a lot of freedom in my work.

I thank *Prof. Dr. Oliver S. Wenger*, not only for being my co-referee and co-examiner, but also for the fruitful discussions during the last year.

I am very thankful for the collaboration with *Prof. Dr. Cornelia G. Palivan*, *Dr. Mariana Spulber* and *Dr. Renee Mayap Talom*. They made big efforts trying to measure EPR-spectra of our $\{\text{Cr}(\text{tpy})_2\}^{3+}$ complexes. I also have to thank *Prof. Dr. Silvio Decurtins* and co-workers, University of Berne, for the SQUID measurement trials.

I have to acknowledge *Dr. Henk Bolink* and *Dr. David Vonlanthen*, University of Valencia, for the manufacturing and analysis of the LEC devices.

I thank *Dr. Markus Neuburger* and *Dr. Jennifer A. Zampese* for measuring and solving several single crystals.

For the measuring of a big number of elemental analysis samples *Werner Kirsch* and *Sylvie Mittelheisser* have to be acknowledged.

I thank *PD Dr. Daniel Häussinger*, *Heiko Gsellinger* and *Kaspar Zimmerman* for their efforts keeping the NMR-spectrometers running and for their help with NMR related questions.

I am very thankful for the effort made by the supporting staff of the department, which enabled me to work on this project. *Beatrice Erismann* for managing all administrative issues, *Dr. Bernhard Jung* for his assistance in IT questions, *Markus Hauri* and *Roy Lips* for the supply of materials and the whole "*Werkstatt Team*" for the maintenance of the infrastructure.

I thank *Dr. Biljana Bozic-Weber*, *Sebastian Fürer*, *Ewald Schönhofer* and *Liselotte Siegfried* for supporting me during the preparation and measurement of the DSCs.

Dr. Collin Morris, *Dr. Gabriel Schneider*, *Ralf Schmitt* and *Steffen Müller* are acknowledged for measuring ESI-MS and MALDI-MS, respectively.

Thank you to *Ewald Schönhofer* for his assistance during the TGA measurements.

I have to thank a number of current and former members of the Constable-Housecroft group (*Nik Hostettler*, *Steffen Müller*, *Dr. Federica Reinders*, *Dr. Frank Schaeper*, *Ralph Schmitt*, *Ewald Schönhofer*) for the opportunity to use the ligands that they synthesised.

Prof. Dr. Catherine Housecroft, *Cathrin Ertl*, *Sebastian Fürer*, *Dr. Colin Martin* and *Dr. Collin Morris* are acknowledged for proofreading this thesis or parts of it.

A big thanks goes to all current and former members of the Constable-Housecroft group, especially (in alphabetical order): *Sven Brauchli*, *Andreas Bünzli*, *Annika Büttner*, *Cathrin Ertl*, *Sebastian Fürer*, *Nik Hostettler*, *Sarah Keller*, *Max Klein*, *Dr. Marzena Kocik*, *Emanuel Kohler*, *Dr. Peter Kopecky*, *Fredi Malzner*, *Dr. Colin Martin*, *Dr. Collin Morris*, *Steffen Müller*, *Daniel Ris*, *Dr. Pirmin Rösel*, *Ralph Schmitt*, *Dr. Gabriel Schneider*, *Ewald Schönhofer*, *Liselotte Siegfried*, *Dr. Marketa Smidkova*, *Dr. David Vonlanthen*, *Roché Walliser* and *Dr. Iain Wright*. I want to thank them for the good working atmosphere, the productive discussion and the nice time we spent together in- and outside the lab.

For financial support, the European Research Council (Advanced grant 267816 LiLo), the Swiss National Science Foundation and the University of Basel have to be acknowledged.

I want to close my acknowledgements and thank my family and friends for their constant support.

Abstract

Slowing down climate change is probably the biggest current global challenge for mankind. The two main strategies to achieve this are the development of new sustainable energy sources and new or improved technologies that are less energy consuming. Inorganic transition metal complexes are the basis for two technologies that address both energy production and energy saving: dye-sensitised solar cells (DSCs) and light emitting electrochemical cells (LECs). Promising results were obtained for devices based on scarce metal complexes, such as iridium and ruthenium, but the rarity of these metals is a big drawback in terms of their widespread use and commercialisation. Therefore, complexes with more abundant metals, such as zinc and copper, are now being investigated.

Since chromium(III) complexes are known to be emitting and kinetically inert, we chose $[\text{Cr}(2,2'\text{-bipyridine})_3]^{3+}$ as a model for our approach to use chromium(III) complexes as active compounds in LECs. A series of both new and known homoleptic and heteroleptic $\{\text{Cr}(\text{bpy})_3\}^{3+}$ containing complexes were synthesised. However they showed no electroluminescence in the device configuration, even though they exhibited photoluminescence in solution.

The main part of this thesis focuses on the synthesis and characterisation of $\{\text{Cr}(\text{tpy})_2\}^{3+}$ complexes, which have been rarely investigated so far. A new synthetic route was developed to synthesise homoleptic and heteroleptic $\{\text{Cr}(\text{tpy})_2\}^{3+}$ complexes. The presence of heteroleptic complexes could be shown with X-ray structures. Surprisingly, the d^3 complexes were found to be labile in solution, although chromium(III) complexes are generally considered to be kinetically inert. Ligand exchange in these complexes in alkaline solution or in the presence of F^- was investigated. Absorption and emission spectroscopic properties of the complexes have been studied. The complexes containing at least one 4'-diphenylaniline tpy ligand showed a broad and solvatochromic absorption band. They were further tested in DSC devices, but tended to be very inefficient.

Chapter 1: Introduction

Chapter 1 gives background information about chromium, polypyridyl ligands and their chromium(III) complexes. The photophysical properties of chromium(III) are introduced, along with possible applications in LECs and DSCs.

Chapter 2: Tris(diimine)chromium(III) complexes

In this chapter the synthesis and characterisation of tris(diimine)chromium(III) complexes are presented. The photophysical properties, electrochemical measurements, LEC trials and X-ray structures are discussed.

Chapter 3: Bis(terpyridine)chromium(III) complexes

In the main chapter of this thesis, the synthesis and characterisation of bis(terpyridine)chromium(III) complexes are presented. The photophysical properties, electrochemistry measurements, DSC trials and X-ray structures are reported. Furthermore, the lability and ligand exchange reactions of the $\{\text{Cr}(\text{tpy})_2\}^{3+}$ complexes are discussed.

Chapter 4: Bis(terpyridine)cobalt(III) complexes

The synthesis of the bis(terpyridine)cobalt(III) complexes and one X-ray structure are presented. These cobalt complexes were needed to prepare magnetically diluted samples for the EPR measurements.

Chapter 5: Terpyridine ligand synthesis

The synthesis routes for the tpy ligand syntheses are discussed in chapter 5.

Chapter 6: Experimental

The experimental details for all the syntheses are reported.

Parts of this work have been published:

E. C. Constable, C. E. Housecroft, M. Neuburger, J. Schönle and J. A. Zampese, *Dalton Trans.*, 2014, **43**, 7227–7235.

Abbreviations and Explanations

A	A	Ampere
	a, b, c	lattice parameters (X-ray)
	ATR	attenuated total reflection (IR)
	a.u.	arbitrary units
	aq.	aqueous
B	bpy	2,2'-bipyridine
C	°C	degree Celsius ($0\text{ }^{\circ}\text{C} = 273.15\text{ K}$) ¹
	CCDC	Cambridge Crystallographic Data Centre
	CFSE	crystal field stabilisation energy
	CHF	Swiss franc
	conc.	concentration/ concentrated
	COSY	correlation spectroscopy (NMR)
	CSD	Cambridge Structural Database
D	D	Debye ($1\text{ D} = 3.335\ 64 \cdot 10^{-30}\text{ C m}$) ²
	Dc	calculated density (X-ray)
	d	doublet (NMR)
	ddd	doublet of doublets of doublets (NMR)
	DEPT	distortionless enhancement by polarisation transfer
	DFT	density functional theory
	DMF	dimethylformamide
	DMSO	dimethylsulfoxide
	DSC	dye-sensitised solar cell
	dt	doublet of triplets (NMR)
E	<i>e.g.</i>	exempli gratia (Latin) = for example
	EA	elemental analysis
	ECD	electrochemically doped (LEC)
	ECL	electrochemiluminescence
	ED	electrodynamic (LEC)
	edn.	edition
	EPR	electron paramagnetic resonance
	eq.	equivalent
	ESSADI	estimated safe and adequate daily dietary intake
	<i>et al.</i>	et alii (Latin) = and others
	ex.	excitation
F	FF	fill factor (DSC)
	FR#	failed reaction
	FTO	fluorine doped tin oxide
G	GTF	glucose tolerance factor
	GWh	gigawatt hour
H	HDPE	high density polyethylene
	HMBC	heteronuclear multiple bond correlation
	HMQC	heteronuclear multiple quantum correlation
	HOMO	highest occupied molecular orbital
	Hppy	2-phenylpyridine
	Hz	Hertz ($1\text{ Hz} = 1\text{ s}^{-1}$) ¹
I	IC	internal conversion
	IR	infrared

	IL	interligand transition
	ISC	intersystem crossing
	I_{SC}	short-circuit current (DSC)
	iTMC	ionic transition-metal complex
	ITO	indium tin oxide
J	J_{SC}	short-circuit current density (DSC)
K	K	Kelvin
L	LC	ligand-centred
	LEC	light emitting electrochemical cell
	LED	light emitting diode
	LMCT	ligand to metal charge transfer
	L_{N-N}	general diimine ligand (bpy or phen)
	L_{N-N-N}	general tpy ligand
	LT#	ligand tpy, derivatives of 2,2':6',2''-terpyridine (LT1 to LT11, compare table 2)
	LUMO	lowest unoccupied molecular orbital
M	m	multiplet (NMR) or medium (IR)
	MALDI	matrix-assisted laser desorption/ionisation
	MC	metal-centred
	MLCT	metal to ligand charge transfer
	MS	mass spectrometry
	Mt	megaton
	mw	microwave reactor
	m/z	mass-to-charge ratio (MS)
N	naph	naphthalene
	NIR	near infrared
	NMR	nuclear magnetic resonance
	NN	general diimine ligand (bpy and phen)
	NNN	general tpy ligand
	norm.	normalised
	N719	standard for DSC measurements (figure 3.48, p. 66)
O	OLED	organic light-emitting diodes
	overn.	overnight
P	P#	precursor (ligand synthesis)
	P_{IN}	intensity of the incident light
	p.	page
	phen	1,10-phenanthroline
	PLEC	polymer light emitting electrochemical cell
	ppm	parts per million
	PPV	poly(1,4-phenylene vinylene)
	py	pyridine
R	R1	agreement factor (X-ray)
	refl.	reflections
	rel.	relative
	rt.	room temperature
S	s	singlet (NMR) or strong (IR)
	sh	shoulder (UV-VIS)
	sp. grp.	space group
	SSL	solid state lighting
T	T	temperature

	t	triplet (NMR)
	td	triplet of doublets (NMR)
	TOF	time of flight (MS)
	tpy	2,2':6',2''-terpyridine
	tt	triplet of triplets (NMR)
U	U	volume of the unit cell (X-ray)
	UV	ultraviolet
	UV-VIS	ultraviolet-visible spectroscopy
V	V	volt $\left(1V = \frac{kg \cdot m^2}{A \cdot s^3}\right)_1$
	V_{OC}	open-circuit photovoltage (DSC)
	vbpy	4-vinyl-4'-methyl-2,2'-bipyridine
W	w	weak (IR)
	wR2	weighted agreement factor (X-ray)
Z	z	formula units (X-ray)
	Å	Ångström ($1 \text{ Å} = 10^{-10} \text{ m}$)
	α, β, γ	interaxial angles (X-ray)
	η	energy conversion efficiency (DSC)
	λ	wavelength
	λ_{ex}	wavelength of the excitation wavelength
	λ_{max}	wavelength of the emission maximum
	$\mu(M-K\alpha)$	absorption coefficient of the radiation source M (X-ray)
	4'-(3,5- <i>t</i> Bu ₂ phenyl)tpy	4'-(3,5-di- <i>tert</i> -butylphenyl)-2,2':6',2''-terpyridine
	4-dmc	dimethyl [2,2'-bipyridine]-4,4'-dicarboxylate
	4'-(4-tolyl)tpy	4'-(<i>p</i> -tolyl)-2,2':6',2''-terpyridine
	4,4'-Me ₂ bpy	4,4'-dimethyl-2,2'-bipyridine
	5,5'-Me ₂ bpy	5,5'-dimethyl-2,2'-bipyridine
	5,5''-Me ₂ bpy	5,5''-dimethyl-2,2':6',2''-terpyridine

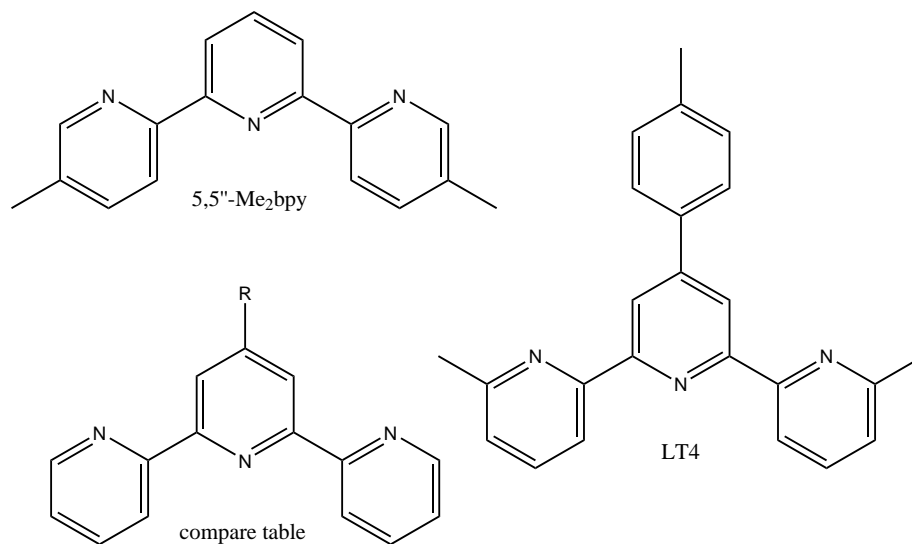
Explanations:

- The complex cations were enclosed with **two different sorts of brackets**:
 $\{\text{Cr}(\text{tpy})_2\}^{3+}$ Curly brackets indicate general complexes of this type, including derivatives of the ligands. Also heteroleptic complexes are included in this label.
- $[\text{Cr}(\text{tpy})_2]^{3+}$ Square brackets refer to the specific complex.

- **Protonated ligands** are abbreviated with the corresponding number of protons in front of the abbreviation, *e.g.*:

HLT11⁺ monoprotated ligand LT11
H₂tpy²⁺ bisprotonated tpy ligand

Table 2: Overview abbreviations 2,2':6',2''-terpyridine ligands.



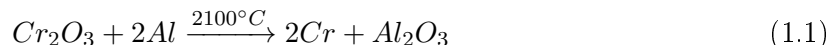
label:	R:	label:	R:
tpy	H	LT7	
4'-(4-tolyl)tpy		LT8	
LT1		LT9	
LT2		LT10	
LT3		LT11/ HLT11	
LT5		P3	
LT6			

Chapter 1

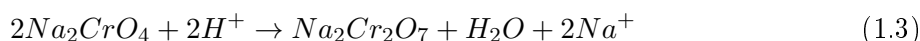
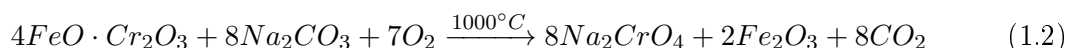
Introduction

1.1 Chromium

Louis Nicolas Vauquelin (1763 - 1829), a french chemist and pharmacist, discovered chromium in 1797. He isolated chromium(III)oxide (Cr_2O_3) by treating the mineral crocoite (PbCrO_4) with hydrochloric acid.^{3,4} One year later, in 1798, *Vauquelin* succeeded in reducing chromium(III)oxide with charcoal to elemental chromium, which was impure.⁴ He chose the name chromium, from the Greek term *chroma* meaning colour, since all compounds containing chromium are coloured.⁵ *Berzelius* named, in honour of *Vauquelin*, in 1818 the mineral $\text{Pb}_2\text{Cu}(\text{CrO}_4)(\text{PO}_4)(\text{OH})$ Vauquelinit.⁴ Nearly 100 years after the discovery, *Goldschmidt* succeeded in isolating pure elemental chromium applying the aluminothermic process:⁶⁻⁸



In the lithosphere chromium is not available in its elemental form, but mainly as chromite ($\text{FeO}\cdot\text{Cr}_2\text{O}_3$), rarer as crocoite (PbCrO_4) and chromium(III)oxide (Cr_2O_3).⁸ The first applications of chromium compounds were as pigments for dyeing (*e.g.* wallpaper or wool).⁹ Common examples are chrome red ($\text{PbCrO}_4\cdot\text{PbO}$), green chromium oxide (Cr_2O_3) and chrome yellow (PbCrO_4).^{3,10} Chrome yellow was used for many years as the official colour for the school buses in the United States.¹¹ In the "*Compendium of Pigments*"³ over 60 chromium containing pigments are listed. Nowadays chromium is mainly mined as chromite ($\text{FeO}\cdot\text{Cr}_2\text{O}_3$), where South Africa (6.8 Mt in 2011), India (4.3 Mt in 2011) and Kazakhstan (3.6 Mt in 2011) are the main mining countries. In Europe Finland is the only remaining country mining chromite. In 2011 worldwide, 23.3 Mt chromite were mined.¹² The world resources of chromite are estimated to be greater than $12\cdot 10^9$ tonnes, where 95 % are located in Kazakhstan and South Africa.¹³ Chromite is converted into dichromate (equation 1.2 and 1.3), which is the starting material for the production of the majority of chromium compounds and pure chromium metal.⁹



A further important starting material, above all for the production of stainless steel, is ferrochrome which is produced directly from chromite by carbo-thermic reduction.⁸

The main applications of chromium compounds are:⁵

- production of stainless steel
- surface treatment (to improve the appearance and/ or the resistance)
- manufacture of chemicals

An important application of chromium is in stainless steels, where corrosion resistant alloys, also

combined with other metals like vanadium, nickel and cobalt, have been developed.⁵ Chromium is also used to treat surfaces and give them an excellent hardness, protection against corrosion and an attractive appearance. To coat surfaces two methods are used: electroplating and chromising at high temperatures.⁵

Chromium compounds with chromium in several oxidation states (II, III, IV, V and VI) are known. Compounds with oxidation states IV and V are rare.¹⁴ chromium(II) compounds tend to oxidise to chromium(III) and are therefore strong reducing agents. Further they tend to form dinuclear complexes (*e.g.* $[\text{Me}_4\text{Cr}\equiv\text{CrMe}_4]^{4-}$) with multiple bonds.⁸ The chromium(VI) salts chromate $(\text{CrO}_4)^{2-}$ and dichromate $(\text{Cr}_2\text{O}_7)^{2-}$ are both strong oxidising agents.¹⁵

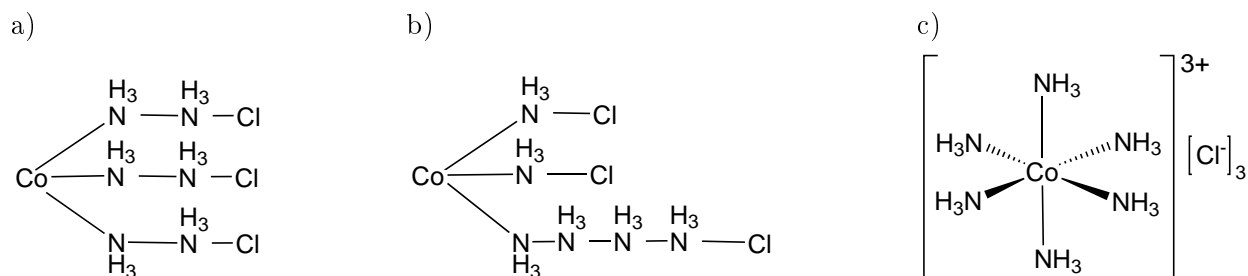
The Philips catalyst, SiO_2 supported chromium oxide, is important in the production of high density polyethylene (HDPE). The catalyst is prepared by impregnation of an aqueous solution of chromate on amorphous silica gel. By calcination the catalyst $\text{Cr(II)O}_x/\text{SiO}_2$ is formed. This catalyst is applied for the production of $1\cdot 10^6$ tonnes HDPE per year, or around half of the world's market.¹⁶ In 1960 the first ruby (Al_2O_3) lasers were produced,^{17,18} where the Al_2O_3 is doped with Cr^{3+} , whose spin forbidden transitions ($^4\text{A}_2 \rightarrow ^2\text{T}_1$ and $^4\text{A}_2 \rightarrow ^2\text{E}$) are responsible for the emission of the laser.¹⁹ Elemental chromium has few applications but is used as the base material for the production of high quality alloys, for example for the production of gas-turbines for aircraft.^{6,8} Around 90 % of the leather tanning is done nowadays with chromium(III) salts, where the collagen coordinates to the chromium(III).²⁰

Whether trivalent chromium is an essential trace element or not has been a controversial discussion for over 50 years.^{21,22} In the 1990s a chromium(III) containing glucose tolerance factor (GTF) was proposed and chromium picolinate ($[\text{Cr}(\text{C}_6\text{H}_4\text{NO}_2)_3]$) was sold as nutritional supplement to promote weight loss and increase muscle mass. Recent studies disagree with this and show that chromium(III) is not essential for mammals.^{21,22} Therefore the ESADDI (estimated safe and adequate daily dietary intake) was reduced from up to 200 mg in the 1990s to 30 mg in 2009.²¹ Compounds containing hexavalent chromium are skin and mucous membrane irritants and classified as toxic and carcinogenic.¹⁴

1.2 Coordination chemistry

Coordination chemistry concerns compounds where a central metal atom or ion is surrounded by a certain number of ligands. The ligands (from latin *ligare* = bind) share a pair of electrons with the metal centre and are therefore coordinatively bonded to the metal centre. The ligands act as *Lewis* bases and form a coordination bond with the *Lewis* acid (the metal cation). The coordination number of a metal centre specifies the possible number of coordinative bonds. A ligand can be mono- or polydentate, the latter means that one ligand provides more than one donor atom.^{23,24} If at least one polydentate ligand coordinates to a metal ion it is referred to as chelated complex. The thermodynamic stability of a chelated complex is greater than that of a complex containing comparable monodentate ligands.²³

Coordination chemistry, as we know it today, was first described in 1893 by the Swiss chemist *Alfred Werner*. Several attempts to describe the observed complexes were already done before *Werner*. The most regarded theories before *Werner's* were *Blomstrand's* and *Jørgensen's*. *Blomstrand* supposed that the coordination number is equal to the valency. He ordered all "ligands" in short chains on the metal centre (scheme 1.1a), where the number of chains was equivalent with the valence number. *Jørgensen* proposed in 1884 the chain theory (scheme 1.1b), an advancement of *Blomstrand's* proposition. After *Jørgensen* the "ligands" are ordered in chains of different length on the metal centre. *Jørgensen* justified his adaptations with the observation that one chloride precipitates much more rapidly and has therefore less influence from the cobalt central ion.²⁴⁻²⁶



Scheme 1.1: Constitutional formula of $[\text{Co}(\text{NH}_3)_6]\text{Cl}_3$, proposed by *Blomstrand* (a), *Jørgensen* (b) and *Werner* (c).

In 1892 *Werner* postulated his theory without any experimental investigations and proved it afterwards experimentally. He proposed the concept of primary and secondary valence. The primary valence, nowadays known as oxidation state, corresponded to the number of chains in *Blomstrand's* and *Jørgensen's* chain model. In the $[\text{Co}(\text{NH}_3)_6]\text{Cl}_3$ example (scheme 1.1c) the three chloride counter anions are in the primary valence, the secondary valence, nowadays called coordination number, defines the number of coordinative bonds and the geometry of the complex. In the $[\text{Co}(\text{NH}_3)_6]\text{Cl}_3$ example the coordination number is 6 and the six edges of the octahedron are occupied by one monodentate ammonia ligand each.^{24–26}

In 1913 *Werner* was awarded the Nobel Prize in Chemistry for this achievement. This Nobel Prize was the first for an inorganic chemist and the first Nobel Prize in Chemistry for a Swiss scientist.²⁶

Several compounds which were known at this time from dyes used in ancient times to observations made by alchemists and itarochemists, could be described applying *Werner's* coordination chemistry.²⁶

Chromium(III) complexes were already studied at the very beginning of the research on coordination chemistry. *Werner* for example investigated the exchange of ammonia with water in $[\text{Cr}(\text{NH}_3)_6]^{3+}$ (figure 1.1). These studies were also part of his *Nobel Lecture* (December 11, 1913).^{26,27} *Pfeiffer* studied the isomerism of trivalent chromium complexes.²⁸

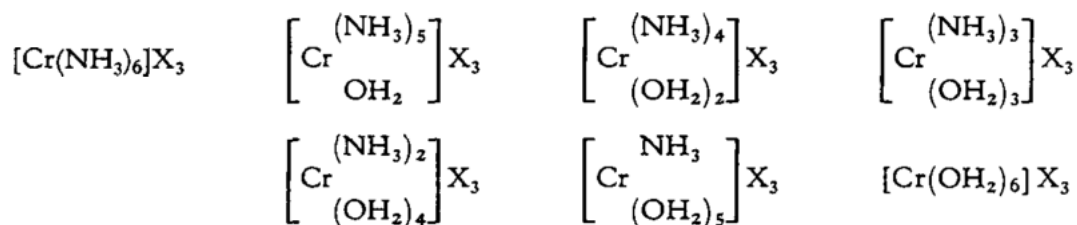
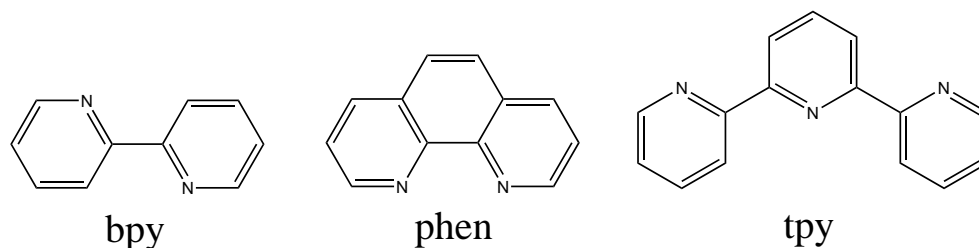


Figure 1.1: Replica of the ligand exchange experiments on $[\text{Cr}(\text{NH}_3)_6]^{3+}$ reported in *Werner's* Nobel Lecture.²⁷

1.2.1 Oligopyridine ligands and complexes thereof

2,2'-Bipyridine (bpy) and 1,10-phenanthroline (phen) were first reported by *Blau* in 1888,²⁹ and 2,2':6',2''-terpyridine (tpy) was first synthesised by *Morgan* and *Brustall* in 1932.³⁰ The oligopyridines bpy, phen and tpy and derivatives thereof (scheme 1.2) are counted among the most common polydentate ligands. Currently, more than 40'000 publications have been published containing the term "1,10-phenanthroline", over 39'000 for "2,2'-bipyridine" and over 5000 for "2,2':6',2''-terpyridine" (SciFinder³¹ research 11th May 2014). Bpy, phen and tpy and multiple derivatives thereof³²⁻³⁴ have been continuously and intensively used in both analytical^{35,36} and preparative coordination chemistry,³² including the detection of iron in water (Fe²⁺ complexes),^{35,36} dyes for DSCs (Ru²⁺, Fe²⁺, Zn²⁺ and Cu⁺ complexes),³⁷⁻³⁹ active medium for LECs (Ir³⁺, Ru²⁺ and Cu⁺ complexes),⁴⁰ and solar energy water splitting (Ru²⁺).⁴¹ Complexes with various metals are known to form complexes with bpy, phen and tpy ligands and derivatives thereof. *Schubert et al.*³⁴ showed recently that complexes with tpy ligands have been described for 63 metalsⁱ: most of the recorded complexes have ruthenium as metal centre, followed by iron and copper.

Octahedral complexes (coordination number 6) of the type {M(tpy)₂}ⁿ⁺ have advantages over {M(NN)₃}ⁿ⁺- complexes (NN= bpy or phen), namely better stability of the {M(tpy)₂}ⁿ⁺ motif. Since the number of chelate rings increases from 3 ({M(NN)₃}ⁿ⁺) to 4 ({M(tpy)₂}ⁿ⁺). Also the {M(tpy)₂}ⁿ⁺ complexes are achiral if the ligands are symmetrically substituted, whereas the {M(NN)₃}ⁿ⁺ complexes are chiral and give Δ and Λ enantiomers.⁴²



Scheme 1.2: Structures of the discussed oligopyridines 2,2'-bipyridine (bpy), 1,10-phenanthroline (phen) and 2,2':6',2''-terpyridine (tpy).

1.2.2 Chromium(III) complexes with polypyridyl ligands

Complexes containing the {Cr(bpy)₃}³⁺ core have been investigated much more intensively compared to complexes containing the {Cr(tpy)₂}³⁺ core (figure 1.2). The peak of the research activity on {Cr(bpy)₃}³⁺ was in the 1980s. The studies on {Cr(bpy)₃}³⁺ were mainly focused on electrochemical processes,^{43,44} the photochemical^{45,46} and photophysical^{47,48} properties including emission quenching⁴⁹ with O₂ and photoaquation reactions. The focus on the investigation of {Cr(tpy)₂}³⁺ lay on the electrochemical properties.⁵⁰⁻⁵²

ⁱ - all alkali metals, except francium - all alkaline earth metals, except radium - all d-block metals (rows 4 - 6), except hafnium - all lanthanides and the actinides uranium, neptunium, plutonium, americium and curium - and also aluminium, gallium, indium, tin, thallium, lead and bismuth, (based on a SCIFinder research by *Schubert et al.* on 31st December 2010 including 3890 papers).³⁴

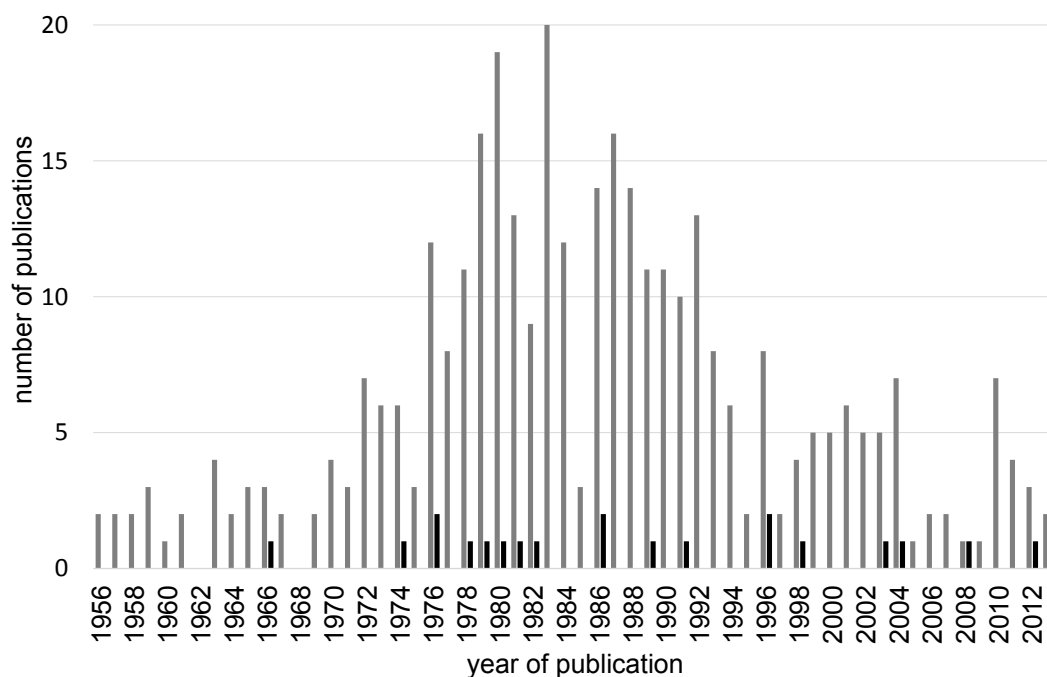


Figure 1.2: Number of papers containing tris(bipyridine)chromium(III) (grey) and bis(terpyridine)chromium(III) (black), based on a structure search with SciFinder³¹ (22th March 2014).

1.3 Photophysics of octahedral chromium(III) complexes

Nearly 150 years ago *Ed Becquerel* described the first luminescent Cr(III) containing compounds.^{53,54} The photophysics and photochemistry of octahedral chromium(III) complexes are, besides ruthenium(II) complexes, the most intensively investigated of all transition metal complexes.⁵⁵ The electronic configuration of Cr³⁺ ions is [Ar]3d³. The electronic configuration of the quartet ground state (⁴A_{2g}) is (t_{2g})³, according to *Hund's* first rule²³ (figure 1.3). The crystal field stabilisation energy (CFSE) for octahedral d³-complexes is -1.2 Δ_{oct}.²³ Three quartet excited states (⁴T_{2g}, ⁴T_{1g} ((t_{2g})²(e_g)) and ⁴T_{1g} ((t_{2g})(e_g)²)) are generated. In absorption measurements only two broad absorptions are typically observed, for ⁴T_{2g} ← ⁴A_{2g} and ⁴T_{1g} ((t_{2g})²(e_g)) ← ⁴A_{2g}, whereas the third ligand field band (⁴T_{2g} ((t_{2g})(e_g)²) ← ⁴A_{2g} is often obscured by more intense charge transfer transitions.⁵⁴ The ⁴T_{1g} excited state undergoes a fast and non radiative internal conversion (IC) to ⁴T_{2g}. Fluorescence from the ⁴T_{2g} state (⁴T_{2g} → ⁴A_{2g}) is rarely observed (in solution at room temperature), whereas intersystem crossing (ISC) to ²E_g occurs efficiently. The doublet states ²T_{1g} and ²E_g (electronic configuration: (t_{2g})³) are the lowest-lying excited states. The emissions (²E_{2g} → ⁴A_{2g} and ²T_{1g} → ⁴A_{2g}) are assigned as phosphorescence. The excitations (⁴T_{2g} ← ⁴A_{2g}) and (⁴T_{1g} ← ⁴A_{2g}) often lead to a facile substitution of ligands by solvent (at room temperature). In both excited states an electron resides in an antibonding e_g orbital (σ*).^{55,56}

The photophysics of {Cr(bpy)₃}³⁺ is introduced in section 2.3.2 (p. 20).

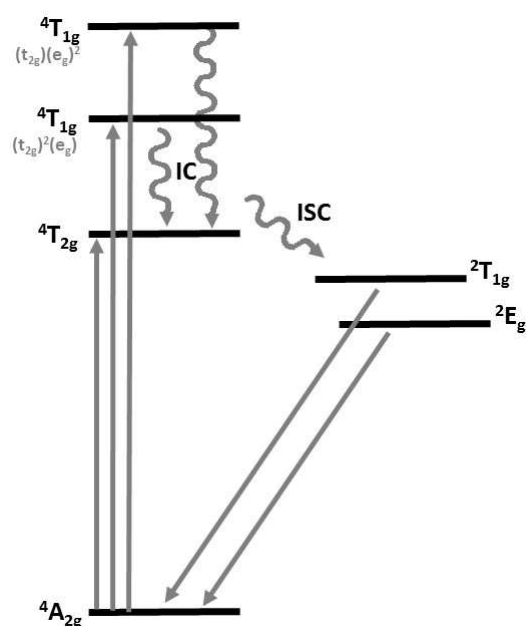


Figure 1.3: Energy level diagram for chromium(III) complexes, where IC stands for internal conversion and ISC for intersystem crossing.

1.4 Sustainable materials

Recently pinpointed by the Swiss Federal Assembly, the key points for the climate policy after the year 2020 are as follows: reducing of the energy consumption and reducing of greenhouse gas emissions.⁵⁷

The principal strategies to accomplish these objectives are:

- alternative sustainable energy sources
- new technologies which are less energy consuming

In the following sections two promising applications of ionic transition metal complexes covering each one of the above mentioned strategies are discussed: dye-sensitised solar cells (DSC) (section 1.4.1) and light emitting electrochemical cells (LEC) (section 1.4.2, p. 9). Both techniques were intensively investigated and developed but they have a significant common disadvantage: they are based on ionic transition metal complexes (iTMC) of the scarce metals ruthenium and iridium. Since these metals are counted among the scarcest elements in the Earth's crust they are very expensive (table 1.1) and as such a wide application is not possible. Therefore recently the replacement of the platinum group elements by first row transition metals has become a growing research area. Promising results were obtained with DSCs based on copper(I) and zinc(II) complexes.³⁹ In LEC devices ionic copper(I) complexes are a promising alternative to iridium(III) complexes, but still very little explored.^{40,58}

Chromium, also an abundant and relatively cheap transition metal, is known to form light emitting complexes in trivalent oxidation state.^{54,56} The potential of chromium(III) complexes to do solar energy conversion was already discussed for quite some time.^{61,62} Chromium(III) (d^3) complexes are a text-book example of kinetically inert compounds.²³ Therefore chromium(III) complexes with polypyridyl ligands could be potential candidates as emitting materials in LECs and sensitisers in DSCs.

Table 1.1: Abundances and market prices of the elements used in LEC and DSC devices

element	abundance in Earth's crust [ppm] ⁵⁹	market price [CHF/kg] (April 2014) ⁶⁰
iridium	$3.7 \cdot 10^{-5}$	~ 29948
ruthenium	$3.7 \cdot 10^{-5}$	~ 2543
zinc	72	~ 1.8
copper	27	~ 6.2
chromium	135	~ 8.5

1.4.1 Dye-sensitised solar cells (DSC)

Photovoltaic energy production is a rapidly increasing market, with the solar energy production in Switzerland increasing by more than 220 times between 1990 and 2012, but the total production of 320 GWh (2012) is only around 0.5 % of the total electrical energy consumption.^{63,64} Silicon-based systems are the dominant photovoltaic devices on the market. The energy consumption and therefore expensive production of these cells is a big disadvantage.⁶⁵ One promising alternative is the dye-sensitised solar cell (DSCⁱⁱ). It was first reported by *Grätzel et al.* in 1991,⁶⁶ and is also known as the *Grätzel* cell. One of the crucial parts of these cells is the dye. Therefore several categories of dyes have been investigated:

Transition metal complexes:

This category of dyes has been investigated intensively, in particular for Ru(II) dyes. Further sensitizers with Os(II), Re(I), Fe(II), Pt(II) and Cu(I) have been investigated.^{67,68}

Porphyrins and phthalocyanines:

In contrast to the metal complex dyes, porphyrin and phthalocyanine dyes have intense spectral response bands in the near-IR region. Both metal free compounds and complexes (mainly Zn(II)) were applied.⁶⁸

Organic dyes:

The main advantage of organic dyes is that they are usually cheaper and more environmentally friendly than metal complex dyes, especially compared with the scarce metals ruthenium and osmium.

The architecture (figure 1.4) of a DSC consists of two electrodes. The anode, FTO (fluorine doped tin oxide) or ITO (indium tin oxide) coated conducting glass, is covered with a TiO₂ layer upon which the dye is absorbed. The counter electrode, usually platinised conducting glass, is connected to the anode via an electrolyte.^{68,69} The photosensitizer, or simplified: dye, is excited by sunlight ①. The excited electron is then injected into the conduction band of the semiconductor ② and forwarded to the conducting glass ③. The sensitizer is regenerated by oxidation of the electrolyte ⑥, which is then reduced at the cathode ⑤. The circuit is closed by electron migration from the anode through the external load to the cathode ④.^{68,69}

ⁱⁱThe abbreviation DSSC is also used.

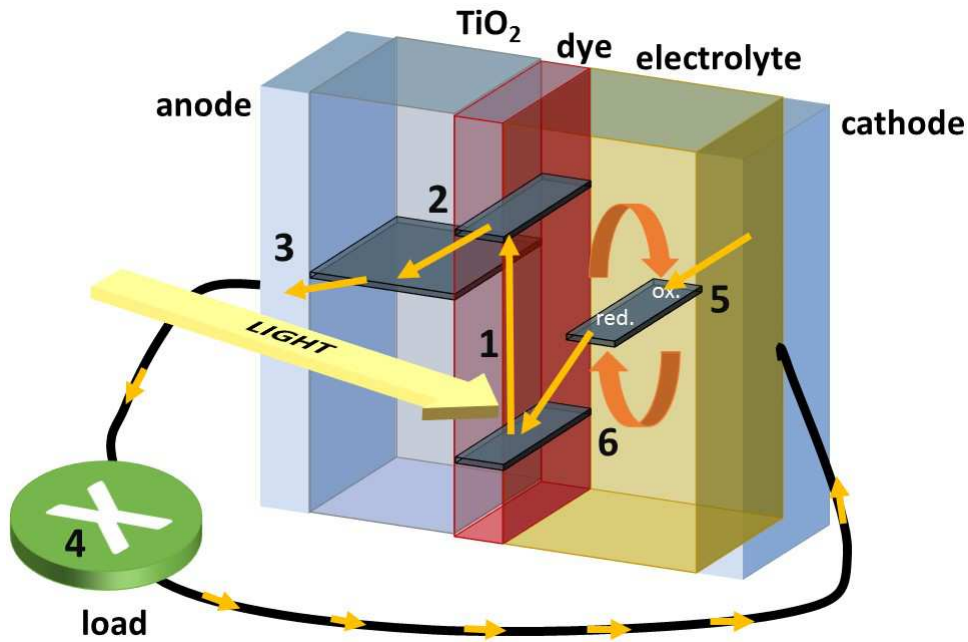


Figure 1.4: Architecture and working principle of a DSC: ①: The dye is excited by sunlight. ②: The electron is injected into the conducting band of the TiO_2 . ③: The electron is forwarded to the conducting glass. ④: The circuit is closed through an external load. ⑤: The electrolyte is reduced at the cathode. ⑥: The dye is regenerated by oxidation of the electrolyte. (figure: adapted from Grätzel⁶⁹).

Solar cells are characterised by the following parameters:⁶⁸

J_{SC} short-circuit current density

The current which flows through the external circuit when the electrodes are short circuited is the short circuit current, I_{SC} . The short circuit current density is the current produced per unit area.

⇒ maximum current density that a solar cell can deliver

V_{OC} open-circuit voltage

The voltage at which no current flows through the external circuit.

⇒ maximum voltage that a solar cell can deliver

FF fill factor

The maximum power generated by the solar cell (P_{max}) per unit area divided by the product of J_{SC} and V_{OC} .

$$FF = \frac{P_{max}}{J_{SC} \cdot V_{OC}}$$

η conversion efficiency

The efficiency of the conversion from solar to electrical energy (P_{in} : intensity of incident light).

$$\eta = \frac{J_{SC} \cdot V_{OC} \cdot FF}{P_{in}} = \frac{P_{max}}{P_{in}}$$

1.4.2 Light emitting electrochemical cell (LEC)

The main lighting techniques which are currently under development are based on the solid-state lighting (SSL) principle. In traditional light sources (*e.g.* light bulbs or fluorescent lamps) the light emission is only a byproduct of heating or discharging, leading to low efficiency. In SSL a semiconducting material emits light upon stimulation by an electric field, which injects electrons (on the cathode) and generates holes (on the anode). Holes and electrons migrate through the film and form an excited state when they meet. In this electrochemiluminescence (ECL) process, a photon is released upon recombination to the ground state. A considerable advantage of SSL is the possibility to tune the spectrum, the polarisation, the colour temperature, the modulation and the emission pattern.^{40,70–72}

LEDs (light-emitting diodes) based on light emitting inorganic semiconductors and OLEDs (organic light-emitting diodes) derive the ECL from a non charged compound (light emitting layer) which is embedded in charge transport and injection layers. LEDs and OLEDs have in common that they are much more efficient than conventional light sources, but also that the production is complex and therefore expensive. Apart from the widespread and applied LED and OLED technologies, LECs (light emitting electrochemical cellsⁱⁱⁱ) have been developed as a possible alternative technique^{40,71,72}

The advantage of LECs is the much simpler architecture (figure 1.5) and in contrast to OLEDs, they do not have to be rigorously encapsulated as the components are not air and moisture sensitive. This leads to simpler and easier production.⁴⁰ In the LEC device the light emitting layer is sandwiched between the two electrodes. Two rationales were proposed to explain the mechanism of operation:⁴⁰

Electrodynamical (ED):

Formation of electrical double layers at the electrodes which cause a drop in the electrical potential near the electrodes and simplify charge injection. The light emission occurs in the region between the electrodes (field free region) where the anions and cations are still joined.

Electrochemically doped (ECD):

Accumulation of ions on the anode and cathode leads to the formation of negatively and positively doped regions around the electrodes. In the junction region between the the two doped regions the potential drops. This favours charge recombination with light emission.

The LEC application was first presented by *Pei et al.* in 1995.^{73,74} They presented a LEC, nowadays categorised as a polymer-LEC (PLEC), based on a semiconducting and emitting polymer (*e.g.* poly(1,4-phenylene vinylene) (PPV)).^{40,73,74} In the second group of LECs, referred to as iTMC- LECs, an ionic transition-metal complex (iTMC) is the luminescent material.⁴⁰ The first approach to iTMC-LEC was reported by *Murry, Wightmann et al.* using poly[Ru(vbpy)₃][PF₆]₂ (vbpy = 4-vinyl-4'-methyl-2,2'-bipyridine) as luminescent material.⁷⁵ The best investigated iTMC-LEC are those with iridium(III) as the metal centre and mainly derivatives of the archetypal complex {Ir(ppy)₂(bpy)}⁺ (Hppy = 2-phenylpyridine). The first Ir-iTMC-LEC was reported 10 years ago by *Bernhard, Malliaras et al.*⁷⁶ The major advantage of Ir-iTMC-LECs is that the emission colour can be readily tuned, and thanks to intensive research in recent years, the hole visible range can be covered.^{40,76–82} Besides Ir- and Ru-iTMC-LECs^{83–86}, copper(I) complexes as light emitting materials have also been investigated. The first LECs with copper as the metal ion were reported by *Armaroli et al.*,⁸⁷ using homoleptic copper(I) diphenylphosphines. Several attempts were tried with heteroleptic complexes containing a bpy ligand and one diphenylphosphine or two phosphane ligands. The

ⁱⁱⁱThe abbreviation LEEC is also used.

performance levels achieved with copper(I) complexes are moderate, but are comparable to ruthenium(II) and iridium(III) complexes based LECs with similar luminance levels.^{58,88-91}

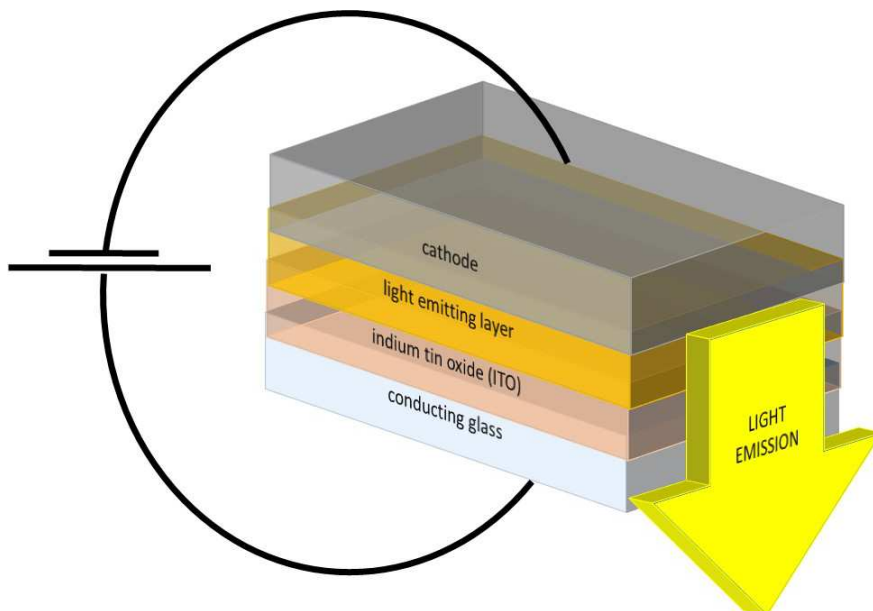
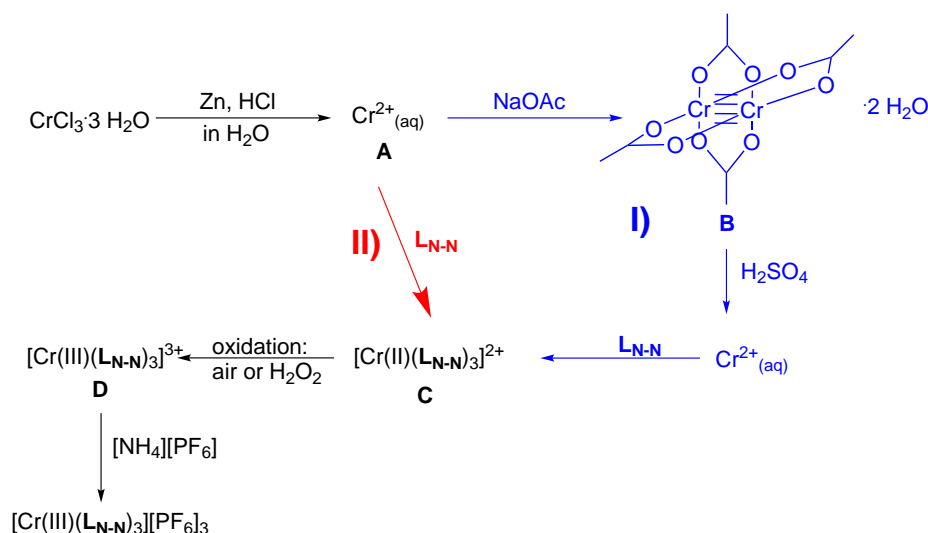


Figure 1.5: Architecture of a LEC (figure: adapted from *Armaroli, Bolink et al.*⁴⁰).

Chapter 2

Tris(diimine)chromium(III) complexes

2.1 Synthesis of tris(diimine)chromium(III) complexes



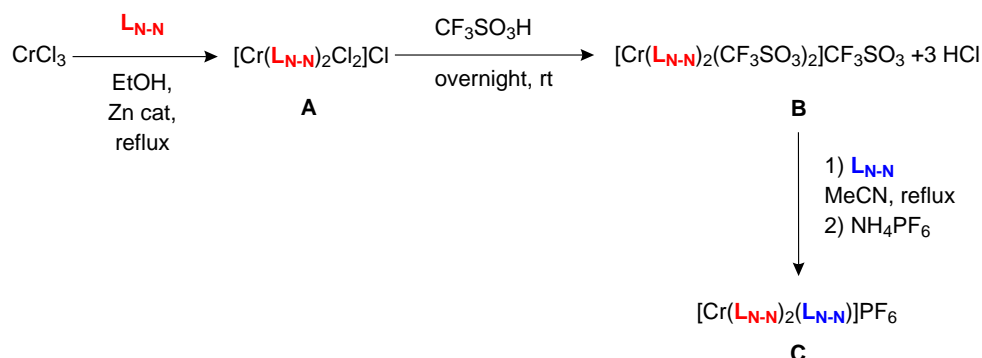
Scheme 2.1: First synthetic approaches, where $\text{L}_{\text{N-N}}$ stands for the diimine (bpy or phen) ligand.

The majority of the reported synthesis strategies contain at least an intermediate with perchlorate as counter anion.^{92,93} Since complexes with perchlorate counter anions are potentially explosive⁹⁴ the aim was to use an alternative synthesis approach. The first approaches (scheme 2.1, variant I) to synthesise $\{\text{Cr}(\text{bpy})_3\}^{3+}$ started with chromium(III) chloride trihydrate. In the first step chromium(II) acetate was synthesised following the protocol of *Block et al.*⁹⁵ Chromium(III) is reduced in the presence of zinc to chromium(II). In the presence of sodium acetate the dinuclear chromium(II) acetate ($[\text{Cr}(\text{CH}_3\text{COO})_2(\text{H}_2\text{O})]_2$) forms. The dinuclear chromium(II) acetate is stable under air.⁹⁶ After treatment with sulfuric acid, instead of perchloric acid, the bipyridine ligand was added to produce a tris(bipyridine)chromium(II) intermediate which was then oxidised with air or H_2O_2 . In the final step the counter anion (Cl^-) was exchanged with NH_4PF_6 to PF_6^- .⁹²

As an alternative to the reaction pathway shown in variant I an approach with a shortcut (scheme 2.1, variant II) was performed in which the bipyridine ligand was added directly to the Cr^{2+} after the reduction step.

The above described approaches starting with $\text{CrCl}_3 \cdot 3\text{H}_2\text{O}$ did not work well or reproducibly.

Therefore an alternative synthesis strategy was applied.



Scheme 2.2: Applied synthesis strategy for the synthesis of tris(diimine)chromium(III) complexes.

This three step synthesis (scheme 2.2) starts with anhydrous chromium(III) chloride. In the first step CrCl_3 and the bipyridine ligand are refluxed in EtOH in the presence of catalytic amounts of zinc.⁹⁷ The metal centre of intermediate **A** coordinates two diimine ligands and two chlorides, and an additional chloride acts as counter anion. This intermediate, was usually not characterised, but was used directly in the next step. The good elemental analyses for $[\text{Cr}(5,5'\text{-Me}_2\text{bpy})_2\text{Cl}_2]\text{Cl}$ and $[\text{Cr}(4,4'\text{-Me}_2\text{bpy})_2\text{Cl}_2]\text{Cl}$ gave evidence for the synthesis of the desired intermediates $\{\text{Cr}(\text{bpy})\text{Cl}_2\}\text{Cl}$. Almost all single crystal growing trials were not successful (see below).

In the next step the chloride ions were exchanged by stirring **A** overnight at room temperature in trifluoromethanesulfonic acid.⁹⁸ Intermediate **B**, was not characterised, and used directly in the next step. In the third step, **B** and the third equivalent of bipyridine ligand were refluxed in acetonitrile and in the final step the CF_3SO_3^- anions were exchanged with NH_4PF_6 to PF_6^- .⁹⁹ A merit of this synthetic strategy is the possibility to synthesise heteroleptic complexes. An other alternative was to perform the last step in the microwave reactor instead of heating under reflux.

From one crystal growing trial of $[\text{Cr}(\text{bpy})_2\text{Cl}_2]\text{Cl}$ two differently coloured (yellow and red) types of crystals were obtained. The crystals grew by storing an EtOH solution of $[\text{Cr}(\text{bpy})_2\text{Cl}_2]\text{Cl}$ during 6 weeks in the fridge. Both structures were of poor quality, but the preliminary data confirmed the gross structural features of the cations.

The structural data for the reddish crystals show that beside the two bpy ligands, one chloride and one oxygen atom coordinate to the metal centre. The oxygen containing ligand could not be determined conclusively as OH^- or H_2O (figure 2.1). The overall charge of the complexes is therefore either 3+ or 2+. Since the solvent molecules and counter ions could not be determined it was not possible to match a charge to the complex.

The second, yellow, type of crystals (figure 2.2), contained the $[\text{Cr}(\text{bpy})_3]^{3+}$ cation. The preliminary data show unambiguously the structure of the cation core. Three anions (Cl^-) balance the charge on the cation. But the solvent molecules could not be identified.

The structure determination confirmed that $[\text{Cr}(\text{bpy})_3]^{3+}$ can be formed directly from CrCl_3 in one step. Since an excess of bpy (3.1 eq.) was used in this synthesis one possibility is that some $[\text{Cr}(\text{bpy})_3]^{3+}$ was formed in the first step of the reaction. Or as a second possibility, a ligand exchange between two complexes happened in the EtOH solution (single crystal growing trial).

Table 2.1: Crystallographic data of solvated $[\text{Cr}(\text{bpy})_3][\text{Cl}]_3$

formula moiety	$\text{C}_{120}\text{H}_{123}\text{Cl}_{12}\text{Cr}_4\text{N}_{24}\text{O}_{16}$	$\mu(\text{Mo-K}\alpha)$ [mm^{-1}]	0.658
formula weight	2790.82	T [K]	173(2)
crystal colour and habit	yellow, block	refln. collected	94136
crystal system	orthorhombic	unique refln.	6744
space group	Pnma	refln. for refinement	6410
		parameters	459
a, b, c [\AA]	23.223(5) 20.329(6) 13.448(3)	threshold	$I > 2.0\sigma$
α, β, γ [$^\circ$]	90 90 90	R1 (R1 all data)	0.0553 (0.0577)
U [\AA^3]	6349(3)	wR2 (wR2 all data)	0.1637 (0.1681)
Dc [Mg m^{-3}]	1.46	goodness of fit	1.054
		crystal growing:	EtOH (fridge)

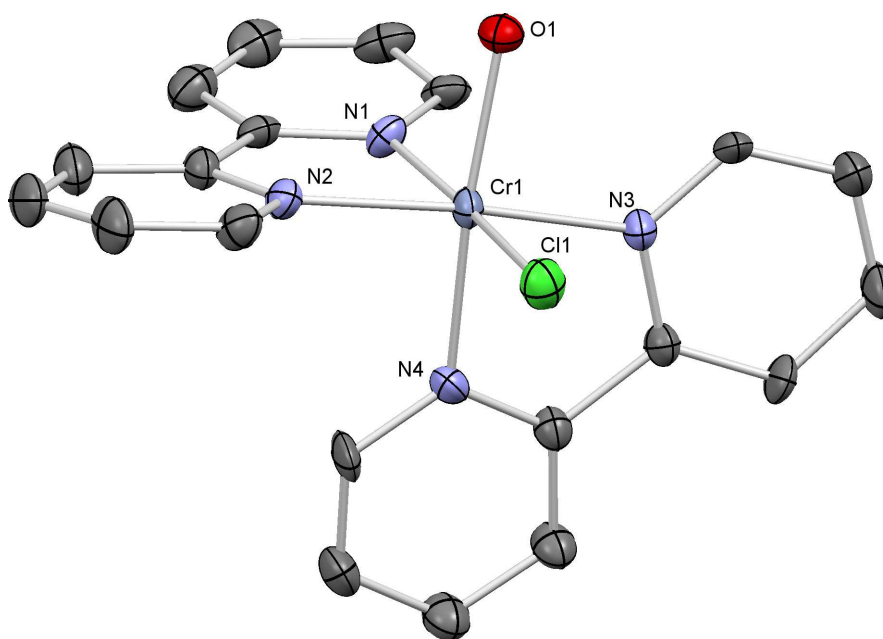


Figure 2.1: Structure of the cation $[\text{Cr}(\text{bpy})_2(\text{OH or H}_2\text{O})\text{Cl}]^{+2}$ with ellipsoids plotted at 50 % probability level. H atoms, counter ions and solvent molecules are omitted for clarity. Selected bond lengths [\AA]: Cr1-O1 = 1.976(5), Cr1-N1 = 2.052(6), Cr1-N3 = 2.041(5), Cr1-N2 = 2.053(5), Cr1-N4 = 2.067(6), Cr1-Cl1 = 2.279(2), and bond angles [$^\circ$]: N1-Cr1-N2 = 79.3(2), N3-Cr1-N4 = 79.4(2). Angle between the two bpy (least squares planes): 86.48 $^\circ$.

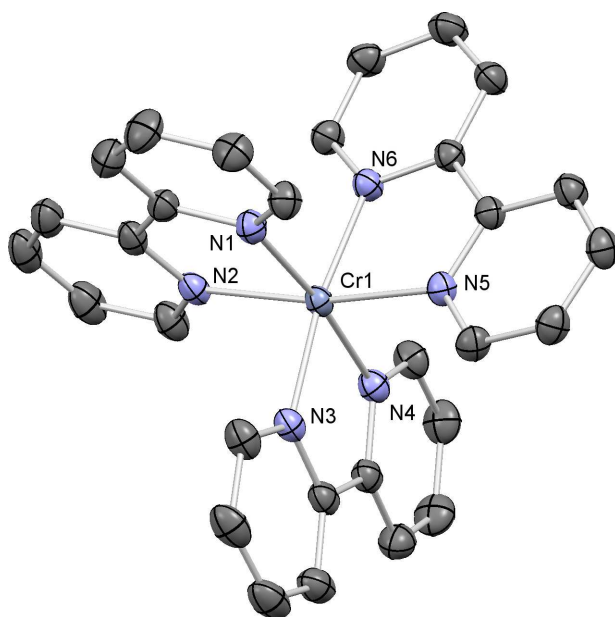


Figure 2.2: Structure of the cation in solvated $[\text{Cr}(\text{bpy})_3]\text{Cl}_3$ with ellipsoids plotted at 50 % probability level. H atoms, counter ions and solvent molecules are omitted for clarity. Selected bond lengths [\AA]: $\text{Cr1-N1} = 2.049(2)$, $\text{Cr1-N2} = 2.047(2)$, $\text{Cr1-N3} = 2.041(2)$, $\text{Cr1-N4} = 2.046(2)$, $\text{Cr1-N5} = 2.050(2)$, $\text{Cr1-N6} = 2.046(2)$, and bond angles [$^\circ$]: $\text{N1-Cr-N2} = 79.99(9)$, $\text{N3-Cr-N4} = 79.93(9)$, $\text{N5-Cr-N6} = 80.00(9)$; angles between the bpy (least squares planes)[$^\circ$]: between bpy containing N1 and N3: 80.83, N3 and N5: 85.08, N1 and N5: 59.62.

A microwave reaction (2.5 h, 110 $^\circ\text{C}$, 8 bar, solvent: CH_2Cl_2) with $[\text{Cr}(5,5'\text{-Me}_2\text{bpy})_2(\text{CF}_3\text{SO}_3)_2][\text{CF}_3\text{SO}_3]$ and 2.5 eq. of bpy yielded an unexpected product. Single crystals grew by slow diffusion of Et_2O in a MeCN solution of the crude product. The preliminary data (figure 2.3) show unambiguously a dimer core of the cation. The position of the two ligands is disordered (0.503 : 0.497) in the coordination sphere of Cr1, therefore an anisotropic refinement of the methyl groups of 5,5'- Me_2bpy was not possible. Since the asymmetric unit contains four anions (PF_6^-) per dimeric cation, the charge is equalised if the bridging ligands are interpreted as OH^- : $(\text{Cr}(\text{bpy})(5,5'\text{-Me}_2\text{bpy}))_2(\mu\text{-OH})_2[\text{PF}_6]_4$.

The two monomers $\{\text{Cr}(\text{bpy})(5,5'\text{-Me}_2\text{bpy})\}^{3+}$ are additionally connected by π - π interactions between the pyridine rings containing N1 and N8 (angle between the least squares planes: 9.4° , distance between the centroids: 3.68 \AA , shortest distance between a centroid and a least squares plane: 3.15 \AA) plus N4 and N5 (angle between the least squares planes: 5.0° , distance between the centroids: 3.80 \AA , shortest distance between a centroid and a least squares plane: 3.17 \AA). In the coordination sphere of Cr1 is the position of the two bpy units disordered in a ratio of 0.503(19) to 0.497(19). Also one of the four anions is disordered (0.519(9) : 0.481(9)). The distance between the two chromium(III) centres is 3.02 \AA . The distances and angles in $[(\text{Cr}(\text{bpy})(5,5'\text{-Me}_2\text{bpy}))_2(\mu\text{-OH})_2][\text{PF}_6]_4$ are consistent with the data published for the phenanthroline complex $[(\text{Cr}(\text{phen})(5,5'\text{-Me}_2\text{phen}))_2(\mu\text{-OH})_2][\text{PF}_6]_4$.^{100,101}

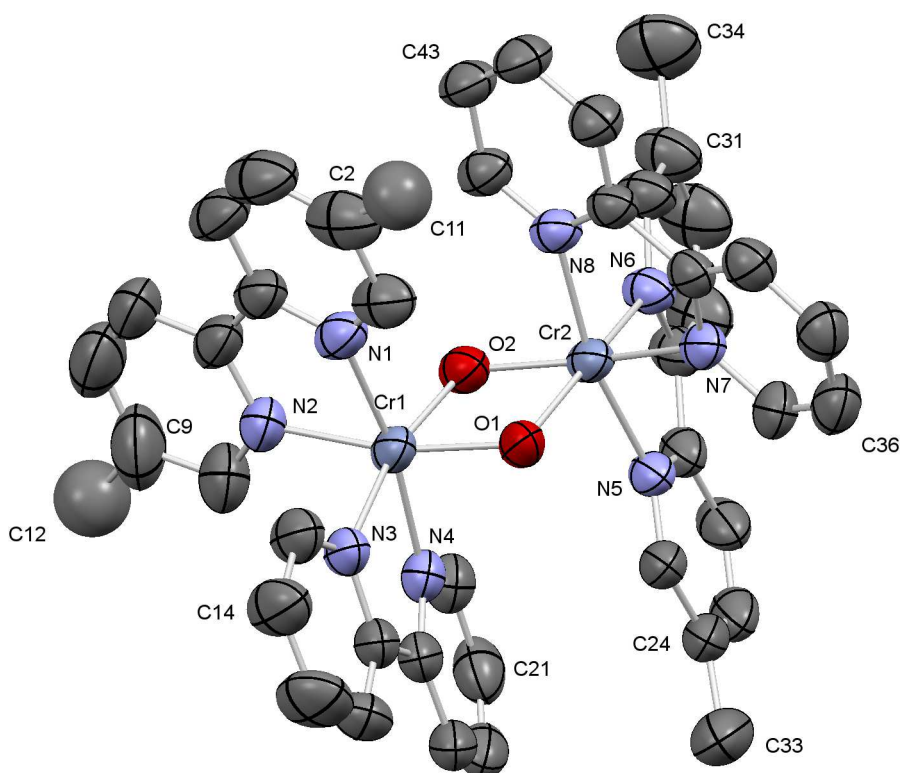
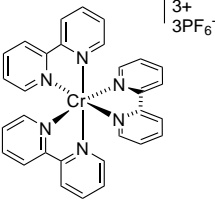
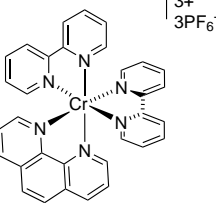
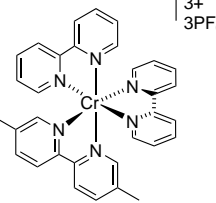
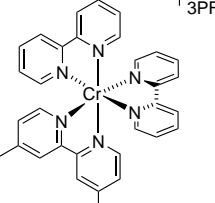
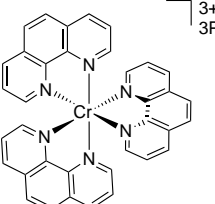
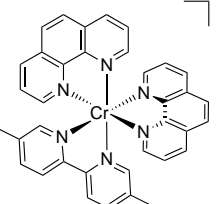
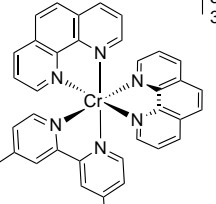
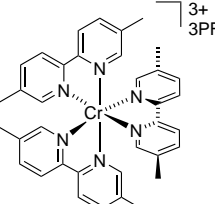
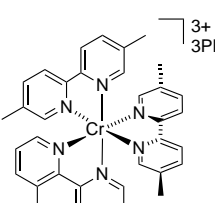
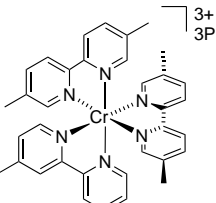
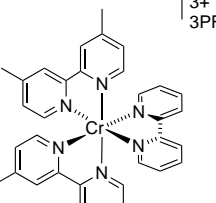
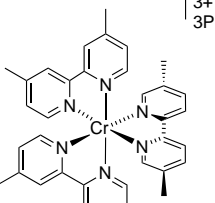


Figure 2.3: Structure of the cation in $[(\text{Cr}(\text{bpy})(5,5'\text{-Me}_2\text{bpy}))_2(\mu\text{-OH})_2][\text{PF}_6]_4$ with ellipsoids plotted at 50 % probability level. H atoms, counter ions and solvent molecules are omitted for clarity. Selected bond lengths [\AA]: Cr1-N1 = 2.063(6), Cr1-N2 = 2.048(6), Cr1-N3 = 2.063(5), Cr1-N4 = 2.054(6), Cr1-O1 = 1.950(5), Cr1-O2 = 1.951(4), Cr2-N5 = 2.059(5), Cr2-N6 = 2.075(5), Cr2-N7 = 2.068(6), Cr2-N8 = 2.055(5), Cr2-O1 = 1.947(4), Cr2-O2 = 1.940(5), and bond angles [$^\circ$]: Cr2-O1-Cr1 = 101.5(2), Cr2-O2-Cr1 = 101.7(2), N1-Cr1-N2 = 78.2(3), N3-Cr1-N4 = 78.5(2), N5-Cr2-N6 = 78.1(2), N7-Cr2-N8 = 78.9(2), angles between the bpy (least squares planes)[$^\circ$]: between bpy containing N1 and N3: 65.90, N5 and N7: 60.39.

Table 2.2: Crystallographic data of $[(\text{Cr}(\text{bpy})(5,5'\text{-Me}_2\text{bpy}))_2(\mu\text{-OH})_2][\text{PF}_6]_4$

formula sum	$\text{C}_{34}\text{H}_{32}\text{CrF}_{18}\text{N}_6\text{OP}_3$	$\mu(\text{Mo-K}\alpha)$ [mm^{-1}]	0.574
formula weight	1027.57	T [K]	173(2)
crystal colour and habit	red, block	refn. collected	98671
crystal system	monoclinic	unique refn.	12716
space group	$\text{P}2_1/\text{n}$	refn. for refinement	9549
		parameters	737
	13.671(3)	threshold	$I > 2.0\sigma$
a, b, c [\AA]	21.231(4)	R1 (R1 all data)	0.1125 (0.1346)
	19.973(4)	wR2 (wR2 all data)	0.3182 (0.3430)
	90	goodness of fit	1.042
α, β, γ [$^\circ$]	107.18(3)	crystal growing	overlying
	90		$\text{Me}_2\text{CO}/ \text{Et}_2\text{O}$
U [\AA^3]	5538.6(19)		
Dc [Mg m^{-3}]	1.848		

Table 2.3: Synthesised tris(diimine)chromium(III) complexes (exp. = link to the experimental part, str. = link to the structure discussion).

 <p>[Cr(bpy)₃][PF₆]₃ exp.: 6.3.3.1 (p. 117) str.: 2.5.1 (p. 28) known, e.g. <i>Hallok et al.</i>¹⁰²</p>	 <p>[Cr(bpy)₂(phen)][PF₆]₃ exp.: 6.3.3.2 (p. 117) str.: 2.5.2 (p. 29) known, <i>Kane-Maguire et al.</i>⁹⁹</p>	 <p>[Cr(bpy)₂(5,5'-Me₂bpy)][PF₆]₃ exp.: 6.3.3.3 (p. 118) str.: 2.5.3 (p. 29)</p>	 <p>[Cr(bpy)₂(4,4'-Me₂bpy)][PF₆]₃ exp.: 6.3.3.4 (p. 118)</p>
 <p>[Cr(phen)₃][PF₆]₃ exp.: 6.3.3.5 (p. 119) known, e.g. <i>Kane-Maguire et al.</i>⁹⁹</p>	 <p>[Cr(phen)₂(5,5'-Me₂bpy)][PF₆]₃ exp.: 6.3.3.6 (p. 119)</p>	 <p>[Cr(phen)₂(4,4'-Me₂bpy)][PF₆]₃ exp.: 6.3.3.7 (p. 120) known as ClO₄⁻-salt: <i>Ronco et al.</i>⁴³</p>	 <p>[Cr(5,5'-Me₂bpy)₃][PF₆]₃ exp.: 6.3.3.8 (p. 120) str.: 2.5.5 (p. 31)</p>
 <p>[Cr(5,5'-Me₂bpy)₂(phen)][PF₆]₃ exp.: 6.3.3.9 (p. 121) known, e.g. <i>Kane-Maguire et al.</i>⁹⁹</p>	 <p>[Cr(5,5'-Me₂bpy)₂(4,4'-Me₂bpy)][PF₆]₃ exp.: 6.3.3.10 (p. 121)</p>	 <p>[Cr(4,4'-Me₂bpy)₂(bpy)][PF₆]₃ exp.: 6.3.3.11 (p. 122) str.: 2.5.4 (p. 30)</p>	 <p>[Cr(4,4'-Me₂bpy)₂(5,5'-Me₂bpy)][PF₆]₃ exp.: 6.3.3.12 (p. 122)</p>

2.2 Unsuccessful synthetic trials

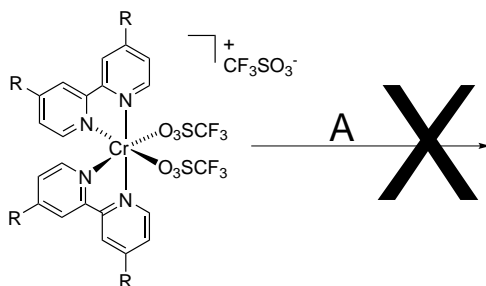
Besides the successful synthesis of tris(diimine)complexes, several additional attempts with mono- and bidentate ligands were done. All the trials were unsuccessful (FR1a - FR2) with bipyridine substituted in the 6-position (table 2.4). With 6-methyl-2,2'-bipyridine several trials in different solvents and using both reflux and microwave techniques (FR1a-e) were executed. But the desired product could not be isolated. As obvious reason could be the steric hindrance of the methyl groups which are adjacent to the N-coordination sites.

In a further series two monodentate ligands were inserted: pyridine (FR4a-c) and 2,6-lutidine (FR5). Also in these trials no desired product could be isolated.

Dreves reported the synthesis of the neutral homoleptic $\text{Cr}(\text{ppy})_3$,¹⁰³ where Hppy stands for 2-phenylpyridine. One tried therefore to coordinate one ppy^- instead of a bipyridine in the last step of the reaction. But all attempts (FR3a-c) were unsuccessful.

The bipyridine ligands (6-methyl-2,2'-bipyridine and 6-phenyl-2,2'-bipyridine) were synthesised by *Ewald Schönhofer*,¹⁰⁴⁻¹⁰⁷ all the other ligands were available commercially.

Table 2.4: Overview of the unsuccessful synthetic trials:



label:	A:	R=	eq. of A:	solvent:	reaction conditions:
FR1a		H	2.0	CH ₂ Cl ₂	refluxing for 7 h
FR1b	<i>see FR1a</i>	H	3.0	MeCN	refluxing for 6 h
FR1c	<i>see FR1a</i>	H	3.0	MeCN	refluxing for 10 h
FR1d	<i>see FR1a</i>	H	3.0	CH ₂ Cl ₂	microwave 100 °C, 8 bar, 3 h
FR1e	<i>see FR1a</i>	H	3.0	CH ₂ Cl ₂ / MeCN	refluxing for 5.5 h
FR2a		H	1.5	MeCN	refluxing for 6 h
FR2b	<i>see FR2a</i>	H	3.0	MeCN	microwave 140 °C, 11 bar, 2 h
FR3a		H	3.0	MeCN	refluxing for 6 h
FR3b	<i>see FR3a</i>	H	2.5	CH ₂ Cl ₂	microwave 110 °C, 9 bar, 2 h
FR3c	<i>see FR3a</i>	H	1.5	THF	refluxing for 2 h
FR4a		H	12	MeCN	refluxing for 5.5 h
FR4b	<i>see FR4a</i>	H	8.2	CH ₂ Cl ₂	microwave 110 °C, 9 bar, 2 h
FR4c	<i>see FR4a</i>	H	2.5	CH ₂ Cl ₂	microwave 110 °C, 9 bar, 1.5 h
FR5		Me	2.1	MeCN	refluxing for 6 h

2.3 Photophysical properties

Data reported in the literature as wavenumbers have been converted to wavelengths ($\bar{\nu} = \frac{1}{\lambda}$) and the original value reported in brackets.

2.3.1 Absorption spectra

The tris(diimine)chromium(III) complexes are all yellow coloured and absorb in the UV and in the visible range. The absorption spectra are well structured (figure 2.4). *Kliger et al.* assigned the absorptions for $[\text{Cr}(\text{bpy})_3]^{3+}$ as dd- transitions, intraligand transitions (IL), ligand to metal charge transfers (LMCT) and metal to ligand charge transfers (MLCT) (table 2.5).⁴⁸ In the absorption spectrum a significant difference in the UV region is noticeable between the complexes containing a phen ligand and those not. The complexes containing phen show a broad absorption at around 270 nm, illustrated by $[\text{Cr}(\text{phen})_3]^{3+}$ (figure 2.5, dashed line). This is consistent with the UV-VIS for $[\text{Cr}(\text{phen})_3]^{3+}$ by *Marusak et al.*¹⁰⁸ In contrast to the free bpy ligand, the free phen ligand also shows a broad absorption band at 269 nm (in MeCN).

Table 2.5: Assignment of the ground state transitions of $[\text{Cr}(\text{bpy})_3]^{3+}$ according to *Kliger et al.*⁴⁸

λ [nm]	assignment
466	⁴ dd (⁴ A ₂ → ⁴ T ₂)
455, 427, 398	³ IL ($\pi\pi^* \setminus ^4,2d$)
359, 346, 330	⁴ LMCT ($\pi \rightarrow t_2$)
312, 299	¹ IL (¹ $\pi\pi^*$)
281, 265	⁴ LMCT ($\pi \rightarrow e$), ⁴ MLCT ($t_2 \rightarrow e$)
237	¹ IL (¹ $\pi\pi^*$)

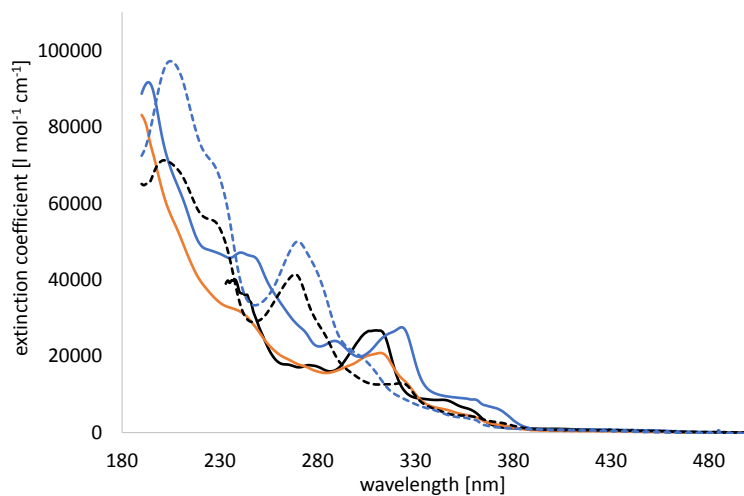


Figure 2.4: Absorption spectra in aqueous solution ($1 \cdot 10^{-5} \text{ M}$) of $[\text{Cr}(\text{bpy})_3][\text{PF}_6]_3$ (black, solid line), $[\text{Cr}(5,5'\text{-Me}_2\text{bpy})_3][\text{PF}_6]_3$ (blue, solid line), $[\text{Cr}(\text{bpy})_2(5,5'\text{-Me}_2\text{bpy})][\text{PF}_6]_3$ (orange, solid line), $[\text{Cr}(\text{phen})_2(5,5'\text{-Me}_2\text{bpy})][\text{PF}_6]_3$ (black, dashed line), $[\text{Cr}(\text{phen})_2(4,4'\text{-Me}_2\text{bpy})][\text{PF}_6]_3$ (blue, dashed line).

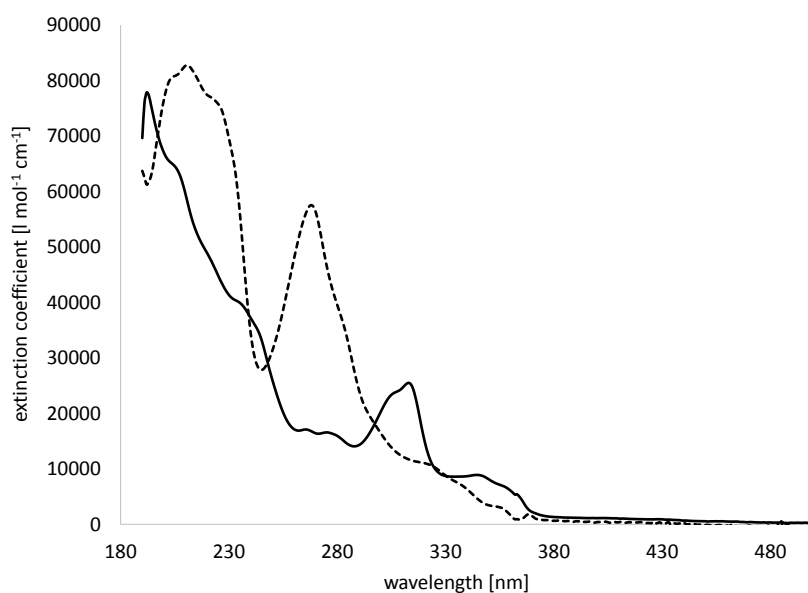


Figure 2.5: Absorption spectra in MeCN solution ($1 \cdot 10^{-5} \text{ M}$) of $[\text{Cr}(\text{bpy})_3][\text{PF}_6]_3$ (solid line) and $[\text{Cr}(\text{phen})_3][\text{PF}_6]_3$ (dashed line).

2.3.2 Photoluminescence of the tris(diimine)chromium(III) complexes

The photoluminescence spectra of the reported $\{\text{Cr}(\text{bpy})_3\}^{3+}$ complexes all have similar emission maxima, independent of the substituents on the bpy ligand (table 2.6 and figure 2.6). They are also consistent with the data reported¹⁰⁹ for $[\text{Cr}(\text{bpy})_3][\text{PF}_6]_3$ (699 nm ($14'300 \text{ cm}^{-1}$) and 728 nm ($13'740 \text{ cm}^{-1}$)), measured in $\text{CH}_2\text{Cl}_2/\text{water}$ 1:1^{47,110} and $[\text{Cr}(\text{phen})_3][\text{PF}_6]_3$ (700 nm and 730 nm), measured in water.¹⁰⁸

This is consistent with the fact that the emission originates from the transitions of two metal-centred excited states (${}^2\text{T}_1$ and ${}^2\text{E}$). In so much as the lifetimes of the two emission peaks (at ~ 700 nm and ~ 730 nm) are identical, these two excited states are thermally equilibrated (figure 2.7).^{47,108,110} Balzani, Hofmann *et al.* showed that the emission is not dependent from the excitation wavelength (312 to 450 nm, figure 2.7 A - D) and that the inter system crossing (ISC) ${}^4\text{T}_2 \rightsquigarrow {}^2\text{E}$ takes place with almost unitary efficiency.⁴⁷

An additional emission band at higher energies was observed if the complexes in this investigation were excited at higher energies (≤ 280 nm). If $[\text{Cr}(5,5'\text{-Me}_2\text{bpy})_3][\text{PF}_6]_3$ was excited at 280 nm, an additional emission band was also observed (figure 2.8). The additional emission band showed two maxima ($\lambda_{max} = 343$ and 384 nm) and these wavelengths do not correspond to half of the wavelengths of the bands observed at 700 nm and 731 nm (figure 2.8). The relative intensities (figure 2.8) of the 343/384 nm and 700/731 nm bands also indicate that the two sets of bands are not related as harmonics. Exciting ($\lambda_{ex} = 280$ nm) free 5,5'-Me₂bpy in MeCN results in an emission with $\lambda_{max} = 343$ nm. This leads to the supposition that this emission is ligand based. Since a decomposition of the complex in solution is likely to occur. (compare 2.3.2.1, p. 22), the presence of free ligand in solution is also possible. We could find no evidence for the second emission maximum at 384 nm.

The photoluminescence lifetimes of the excited states ${}^2\text{T}_1$ and ${}^2\text{E}$ were long (in the μs range)¹¹¹ and surpass the measurement and evaluation range of our instruments. Using the following approach we were nevertheless able to estimate the lifetimes. The logarithmic number of counts of the accessible part of the decay, using the longest possible time range (50 μs), was plotted against the time. The slope (D) of the decay was determined by linear regression and the lifetime determined using equation 2.1.¹¹²

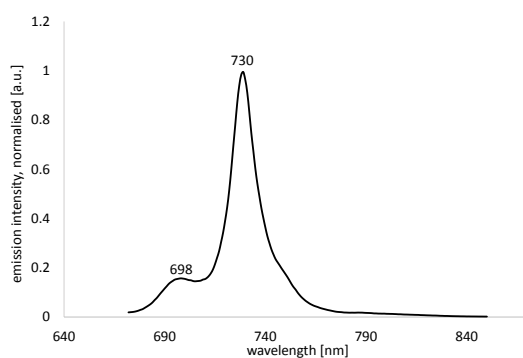
$$D = -\frac{1}{\tau} \quad (2.1)$$

Applying the above procedure, we determined for $[\text{Cr}(\text{bpy})_3][\text{PF}_6]_3$ in aqueous solution a photoluminescence lifetime of 58 μs , which is consistent with the reported value of 60 μs .¹¹¹ Also the photoluminescence lifetimes of some additional complexes were determined, using the approach described above: $[\text{Cr}(5,5'\text{-Me}_2\text{bpy})_3][\text{PF}_6]_3$: 107 μs , $[\text{Cr}(\text{bpy})_2(5,5'\text{-Me}_2\text{bpy})][\text{PF}_6]_3$: 71 μs and $[\text{Cr}(\text{bpy})_2(4,4'\text{-Me}_2\text{bpy})][\text{PF}_6]_3$: 107 μs (all in N₂ degassed aqueous solution).

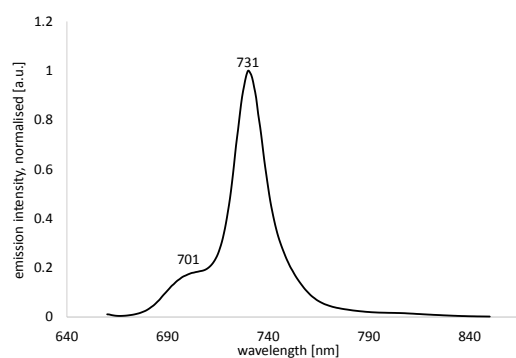
Table 2.6: Overview of photoluminescence data for four different $\{\text{Cr}(\text{NN})_3\}^{3+}$ complexes in different solvents and excited at different wavelengths.

complex	λ_{ex} [nm]	λ_{em} [nm]	solvent	concentration
$[\text{Cr}(\text{bpy})_3][\text{PF}_6]_3$	280	703, 730	water	$1.0 \cdot 10^{-4}$ M
	313	702, 727	MeCN	$1.0 \cdot 10^{-4}$ M
	330	701, 728	MeCN	$1.0 \cdot 10^{-4}$ M
$[\text{Cr}(\text{bpy})_2(5,5'\text{-Me}_2\text{bpy})][\text{PF}_6]_3$	280	701, 730	water	$5.0 \cdot 10^{-5}$ M
	320	703, 730	water	$5.0 \cdot 10^{-5}$ M
$[\text{Cr}(5,5'\text{-Me}_2\text{bpy})_3][\text{PF}_6]_3$	280	703, 731	water	$1.0 \cdot 10^{-4}$ M
	320	702, 730	water	$1.0 \cdot 10^{-4}$ M
	280	701, 730	MeCN	$1.0 \cdot 10^{-4}$ M
$[\text{Cr}(\text{phen})_2(5,5'\text{-Me}_2\text{bpy})][\text{PF}_6]_3$	280	702, 730	water	$1.0 \cdot 10^{-4}$ M
	320	705, 731	water	$1.0 \cdot 10^{-4}$ M
	325	702, 730	MeCN	$1.0 \cdot 10^{-4}$ M

a)



b)

Figure 2.6: Typical band shapes of the photoluminescence band of the $\{\text{Cr}(\text{NN})_3\}^{3+}$ complexes. a) $[\text{Cr}(\text{bpy})_3][\text{PF}_6]_3$ ($1.0 \cdot 10^{-4}$ M in MeCN, ex. 330 nm); b) $[\text{Cr}(\text{phen})_2(5,5'\text{-Me}_2\text{bpy})][\text{PF}_6]_3$ ($1.0 \cdot 10^{-4}$ M in water, ex. 320 nm).

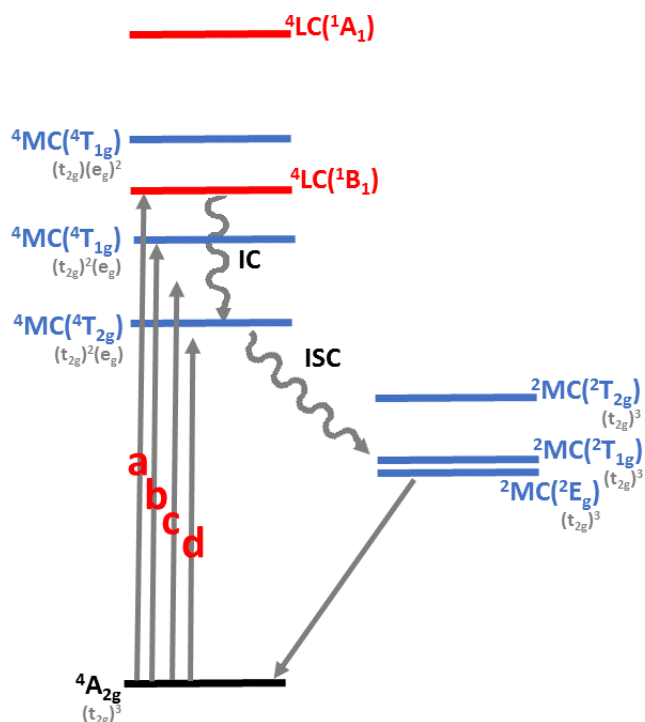


Figure 2.7: Energy level diagram of $[\text{Cr}(\text{bpy})_3]^{3+}$. Where MC stands for metal-centred states, LC for ligand-centred, IC for internal conversion and ISC inter system crossing. The excitation arrows stand for λ_{ex} : 313 nm (a), 365 nm (b), 405 nm (c) and 465 nm (d). The figure is adapted from *Balzani, Hoffman, et al.*⁴⁷

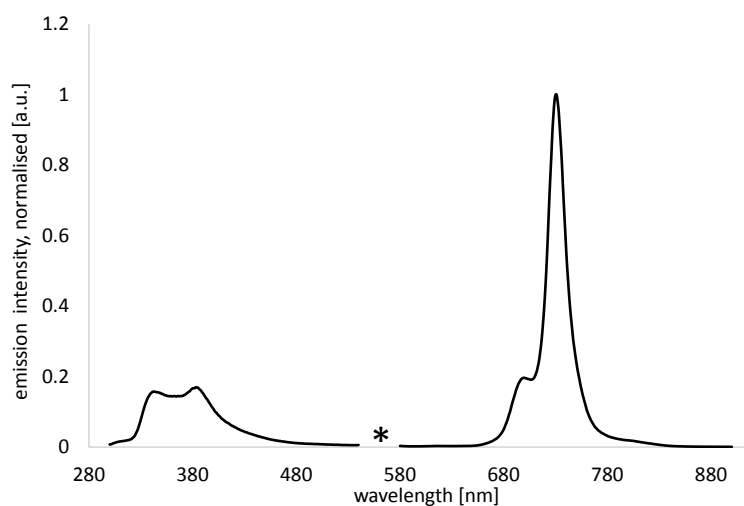


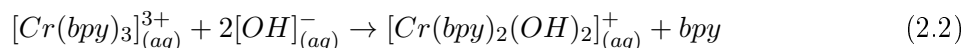
Figure 2.8: Photoluminescence spectrum for $[\text{Cr}(5,5'\text{-Me}_2\text{bpy})_3][\text{PF}_6]_3$ excited at 280 nm in water ($1.0 \cdot 10^{-4}$ M). The first harmonic of the excitation is omitted and its position is marked with an asterisk.

2.3.2.1 Additional emission band - possible decomposition of the complexes

An additional emission band was observed at around 660 nm in aged aqueous and MeCN solutions. Therefore was the following experiment performed: A cuvette, containing an MeCN solution of $[\text{Cr}(\text{bpy})_3][\text{PF}_6]_3$, was gently heated at 50 °C in an air stream (figures 2.9a and 2.9b). The heating was interrupted every 10 minutes and a photoluminescence spectrum taken. An increase in the emission band at 660 nm and a decrease in the signal at 730 nm (figure 2.9a) was observed. The increase of the band at 660 nm compared with the initial emission (730 nm) is presented in figure 2.9b. Figure 2.9c shows the photoluminescence spectra for a reference sample, which was not heated between the measurements. In this sample only minimal changes in the intensity of the band at 660 nm could be observed.

A corresponding experiment was also performed using an MeCN solution of $[\text{Cr}(5,5'\text{-Me}_2\text{bpy})_3][\text{PF}_6]_3$ (figures 2.10a and 2.10b), here an increase in the emission band between 650 and 710 nm could also be observed. However the increase of the emission band at around 660 nm is less compared with $[\text{Cr}(\text{bpy})_3][\text{PF}_6]_3$. This suggests that the Cr(III) complexes with sterically more demanding ligands are less labile than those with bpy, since the metal ion is less available for solvent attack.

A possible explanation is decomposition of the complex. Base-catalysed ligand loss (equation 2.2) is known and is proposed to follow an associative mechanism involving a seven coordinate intermediate $[\text{Cr}(\text{bpy})_3\text{OH}][\text{PF}_6]_2$.^{113,114}



The additional emission band may be assigned as the first harmonic of the emission of monoprotonated bpy ligand (Hbpy^+ , $\lambda_{max} = 335$ nm, in MeCN)¹¹⁵ and/or the hydrate ($\text{bpy}\cdot\text{H}_2\text{O}$, $\lambda_{max} = 328$ nm, in water).¹¹⁵ The emission of Hbpy^+ is observed even in very dilute solutions as reported by *Hoffmann et al.*¹¹⁵ (measured in H_2SO_4 at $< 10^{-6}$ M). Since the emission maximum of the additional emission lies at 657 nm ($= 2\cdot 328.5$ nm, figure 2.9) it could be associated with the reported emission for $\text{bpy}\cdot\text{H}_2\text{O}$. The presence of protonated Hbpy^+ is also a contradiction of the presence of base needed for the base-catalysed ligand loss (equation 2.2).

No further investigations were performed and therefore we have no definitive evidence for the postulated decomposition. However for the $\{\text{Cr}(\text{tpy})_2\}^{3+}$ we could prove the decomposition and determine $\{\text{Cr}(\text{tpy})(\text{OH})_3\}$ as the residue of the decomposition (compare 3.2, p. 38).

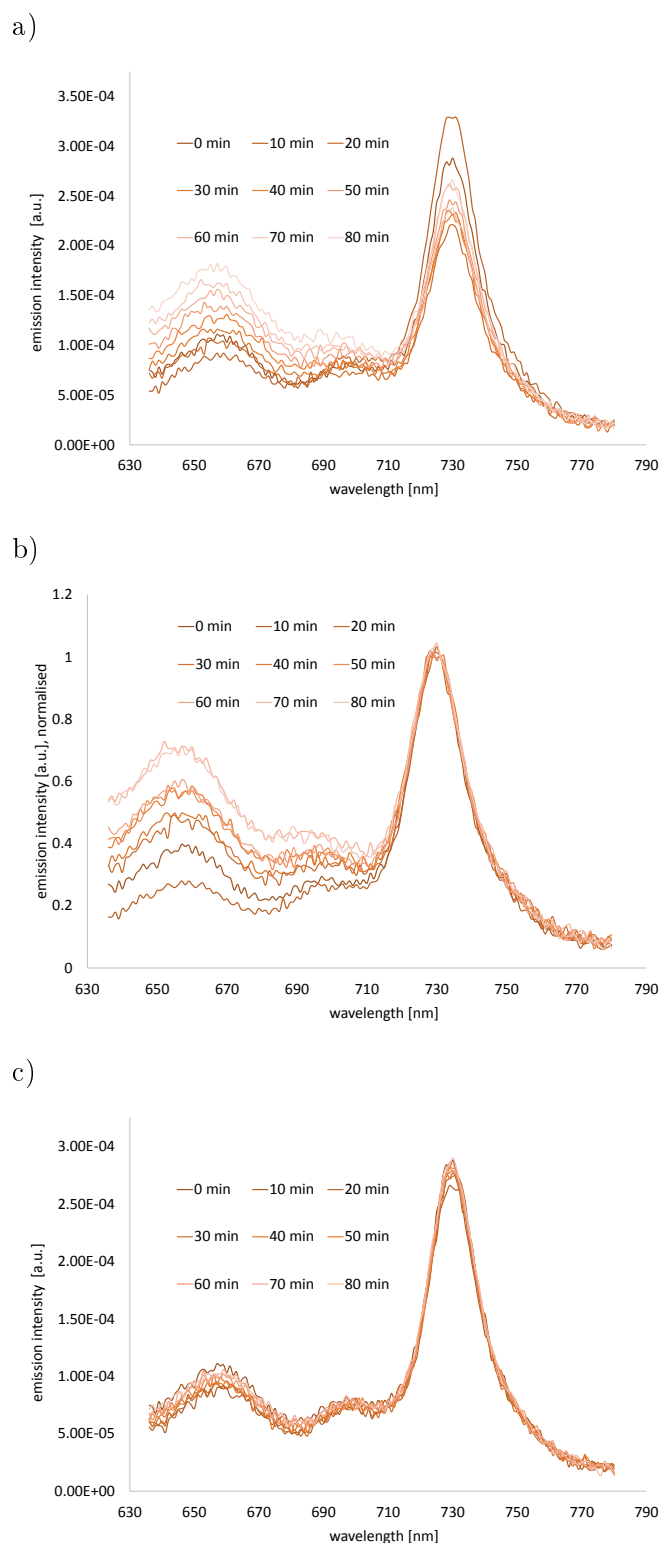


Figure 2.9: Photoluminescence spectra of $[\text{Cr}(\text{bpy})_3][\text{PF}_6]_3$ in MeCN ($5 \cdot 10^{-6}$ M), and excited at 300 nm. Between the measurements the sample was heated gently in an air stream (50°C). Spectrum a) shows the crude data whereas spectrum b) is normalised at 730 nm. Spectrum c) shows a spectrum where the sample was not heated between the measurements.

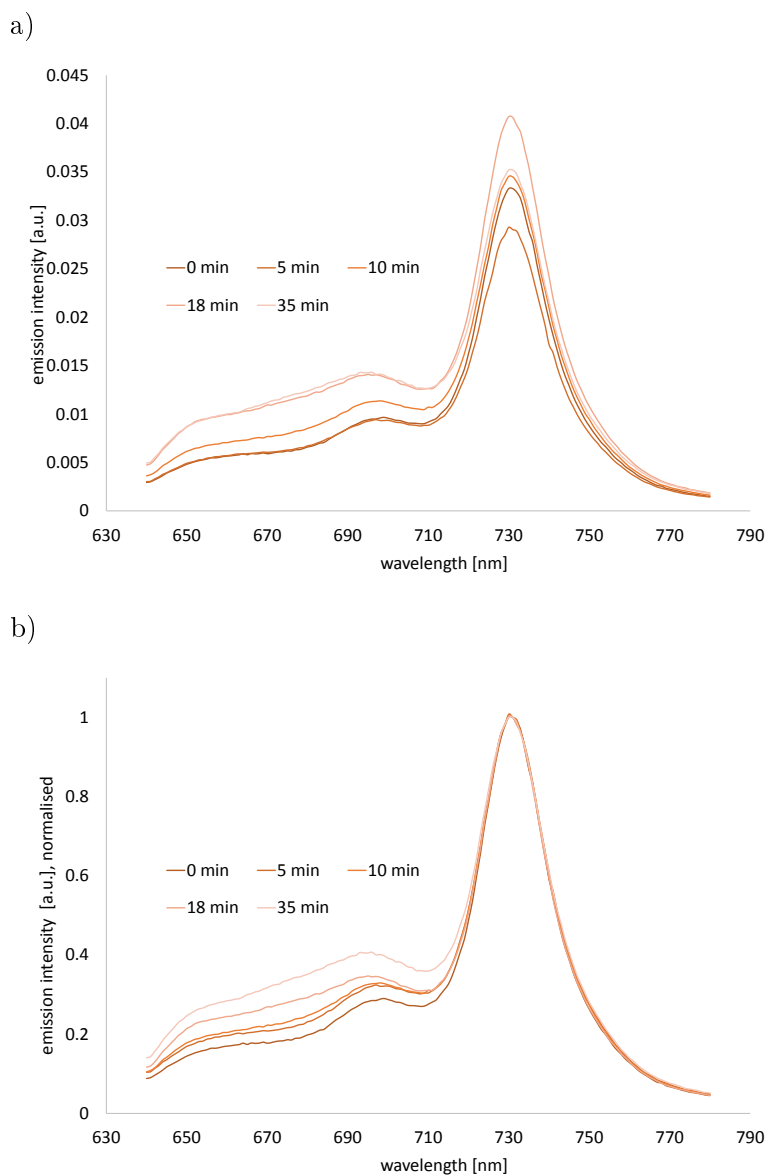


Figure 2.10: Photoluminescence spectra of $[\text{Cr}(5,5'\text{-Me}_2\text{bpy})_3][\text{PF}_6]_3$ in MeCN ($1 \cdot 10^{-5}$ M), excited at 300 nm. Between the measurements the sample was heated gently in an air stream (50 °C). Spectrum a) shows the raw data whereas spectrum b) is normalised at 730 nm.

2.3.3 Electroluminescence of tris(bipyridine)chromium(III) complexes

Two of our complexes ($[\text{Cr}(\text{bpy})_3][\text{PF}_6]_3$ and $[\text{Cr}(5,5'\text{-Me}_2\text{bpy})_3][\text{PF}_6]_3$) were tested in LEC configuration (LEC = Light Emitting Electrochemical Cell, see section 1.4.2, p. 9).^{40,73} This work was carried out by the group of *Dr. Henk Bolink* (Instituto de Ciencia Molecular, University of Valencia, Spain). Neither of the complexes showed any electroluminescence in the device configuration. But photoluminescence was also measured in the LEC configuration, with the emission maximum at 728 nm.¹¹⁶

2.4 Electrochemical measurements

The electrochemical processes of some of the $\{\text{Cr}(\text{bpy})_3\}^{3+}$ complexes were studied using cyclic voltammetry and square wave techniques (table 2.7). The complexes show four reversible one-electron transfer waves (figures 2.11, 2.12, 2.13). For two complexes square wave measurements were necessary to determine the potential of the fourth reduction. All complexes showed no oxidation peaks and the reported reduction potentials correspond to the literature.^{43,44}

The small changes in the reduction potentials of the complexes are negligible. Figures 2.12 and 2.13 show that the one-electron transfer waves of the complexes are often broad or express a shoulder. A possible explanation for this observation is that the reduction potentials for the two different ligands of the heteroleptic complexes are slightly different.

The observed redox processes were, in the literature, commonly assigned as reductions of both the metal centre and the ligands.^{43,117,118} *Wieghardt et al.*⁴⁴ recently published that the reduction processes are all ligand centred and the oxidation state of the metal centre does not change. As a model compound, these authors selected $[\text{Cr}(^t\text{Bu}_2\text{bpy})_3][\text{PF}_6]_3$ ($^t\text{Bu}_2\text{bpy}$ = 4,4'-di-tert-butyl-2,2'-bipyridine). $^t\text{Bu}_2\text{bpy}$ was chosen since higher quality X-ray crystals could be grown compared to the complex with an unsubstituted tpy ligand. In addition to X-ray structures, magnetic susceptibility measurements, UV-VIS/NIR spectra and DFT calculations were performed to determine the composition of the different oxidation states of $\{\text{Cr}(\text{bpy})_3\}^n$ (table 2.8). The bpy ligand can exist in three different oxidation levels: neutral (bpy^0), π - radical monoanionic ($\text{bpy}^{\bullet-}$) or as dianionic (bpy^{-2}).⁴⁴ We have not confirmed whether this formulation will also hold for the complexes discussed in this thesis.

Table 2.7: Cyclic voltammometric data for $\{\text{Cr}(\text{bpy})_3\}^{3+}$ complexes. Measured in MeCN with $[\text{nBu}_4\text{N}][\text{PF}_6]$ as supporting electrolyte and a scan rate of 0.1 V s^{-1} . Referenced to Fc/Fc^+ .

compound	$E_{1/2}^{3+/2+}$ [V]	$E_{1/2}^{2+/1+}$ [V]	$E_{1/2}^{1+/0}$ [V]	$E_{1/2}^{0/1-}$ [V]
$[\text{Cr}(\text{bpy})_3][\text{PF}_6]_3$	-0.549	-1.068	-1.634	-2.256
$[\text{Cr}(5,5'\text{-Me}_2\text{bpy})_3][\text{PF}_6]_3$	-0.744	-1.299	-1.901	(-2.216)*
$[\text{Cr}(\text{phen})_2(5,5'\text{-Me}_2\text{bpy})][\text{PF}_6]_3$	-0.694	-1.213	-1.762	-2.207
$[\text{Cr}(\text{phen})_2(4,4'\text{-Me}_2\text{bpy})][\text{PF}_6]_3$	-0.675	-1.195	-1.763	(-2.291)*
$[\text{Cr}(5,5'\text{-Me}_2\text{bpy})_2(\text{bpy})][\text{PF}_6]_3$	-0.670	-1.257	-1.839	-2.443
$[\text{Cr}(5,5'\text{-Me}_2\text{bpy})_2(\text{phen})][\text{PF}_6]_3$	-0.683	-1.214	-1.798	-2.315

*: determined using square wave measurement

Table 2.8: The composition of $\{\text{Cr}(\text{tBu}_2\text{bpy})_3\}^n$ ($n = 3+, 2+, 1+$ and 0) according to *Wieghardt et al.*⁴⁴

3+	2+	1+	0
$[\text{Cr}^{\text{III}}(\text{tBu}_2\text{bpy})_3][\text{PF}_6]_3$	$[\text{Cr}^{\text{III}}(\text{tBu}_2\text{bpy})_3][\text{PF}_6]_2$	$[\text{Cr}^{\text{III}}(\text{tBu}_2\text{bpy})_3][\text{PF}_6]$	$[\text{Cr}^{\text{III}}(\text{tBu}_2\text{bpy})_3]$
$S = 3/2$	$S = 1$	$S = 1/2$	$S = 0$

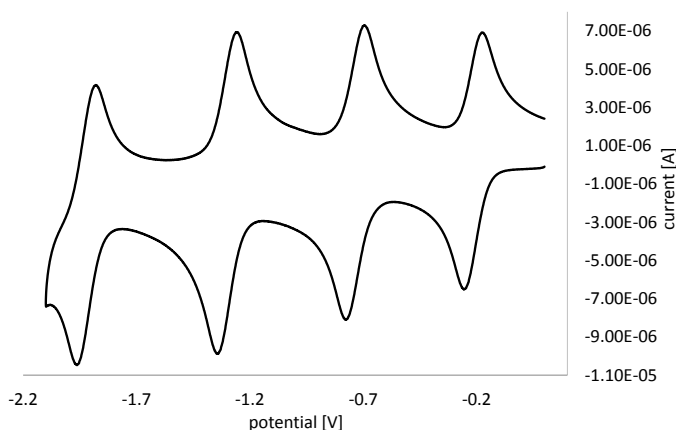


Figure 2.11: Cyclic voltammogram for $[\text{Cr}(\text{bpy})_3][\text{PF}_6]_3$, measured in MeCN solution with $[\text{nBu}_4\text{N}][\text{PF}_6]$ as supporting electrolyte, with respect to Fc/Fc^+ and a scan rate of 0.1 V s^{-1} .

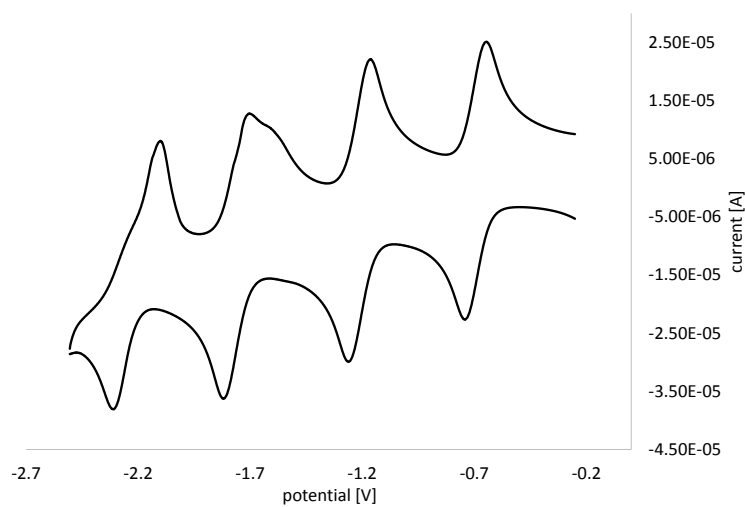


Figure 2.12: Cyclic voltammogram for $[\text{Cr}(\text{phen})_2(5,5'\text{-Me}_2\text{bpy})][\text{PF}_6]_3$, measured in MeCN solution with $[\text{nBu}_4\text{N}][\text{PF}_6]$ as supporting electrolyte, with respect to Fc/Fc^+ and a scan rate of 0.1 V s^{-1} .

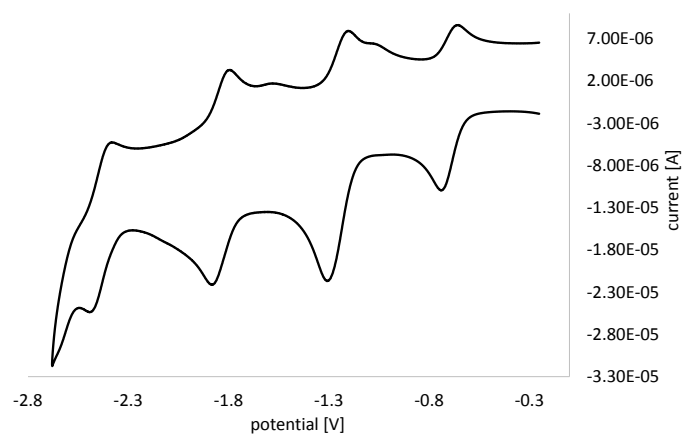


Figure 2.13: Cyclic voltammogram for $[\text{Cr}(5,5'\text{-Me}_2\text{bpy})_2(\text{bpy})][\text{PF}_6]_3$. Measured in MeCN solution with $[\text{nBu}_4\text{N}][\text{PF}_6]$ as supporting electrolyte, with respect to Fc/Fc^+ and a scan rate of 0.1 V s^{-1} .

2.5 Tris(diimine)chromium(III) complexes: X-ray structures

Single crystals of several cations out of the tris(diimine)chromium(III) series were received. They were grown using the overlaying technique. The complex was dissolved in either MeCN or acetone and then overlaid in a thin vial with Et₂O or *n*-hexane (for details compare tables 2.9 and 2.10).

All examples show no interactions between the cations, since the distances between them are too big.¹¹⁹ Because the space between the cations is filled with anions and solvent molecules, the main interactions in the packing are therefore CH...N and CH...F. The angles between the diimine ligands are between 71.6° and 90.0° (table 2.11).

Table 2.9: Crystallographic data of {Cr(NN)₃}³⁺ complexes, part I

compound	[Cr(bpy) ₃][PF ₆] ₃	[Cr(bpy) ₂ (phen)][PF ₆] ₃	[Cr(4,4'-Me ₂ bpy) ₂ (bpy)][PF ₆] ₃
formula moiety	C ₃₂ H ₂₄ CrN ₆ , 3(F ₆ P), C ₂ H ₃ N	4(C ₃₂ H ₂₄ CrN ₆), 12(F ₆ P), 11(C ₂ H ₃ N)	4(C ₃₄ H ₃₂ CrN ₆), 12(F ₆ P), 12(C ₂ H ₃ N), H ₂ O
formula weight	996.52	4369.52	4556.93
crystal colour and habit	yellow, block	yellow, block	yellow, block
crystal system	rhombohedral	monoclinic	monoclinic
space group	R3c	P2 ₁ /c	C2/c
a, b, c [Å]	31.535(5) 31.535(5) 21.523(4)	10.2863(9) 34.025(4) 13.0344(12)	24.4712(17) 12.9795(8) 31.013(2)
α, β, γ [°]	90.00 90.00 120.00	90.00 94.356(7) 90.00	90.00 95.608(6) 90.00
U [Å ³]	18536(10)	4548.8(8)	9803.4(12)
Dc [Mg m ⁻³]	1.607	1.595	1.543
Z	18	1	2
μ(Mo-Kα) [mm ⁻¹]	0.511	0.471	0.476
T [K]	173(2)	173(2)	173(2)
refln. collected	69367	43616	14484
unique refln.	8531	9061	8641
refln. for refinement	7726	8430	7928
parameters	572	681	720
threshold	I > 2.0σ	I > 2.0σ	I > 2.0σ
R1 (R1 all data)	0.0569 (0.0633)	0.0487 (0.0521)	0.0684 (0.0730)
wR2 (wR2 all data)	0.1502 (0.1558)	0.1632 (0.1607)	0.1632 (0.1607)
goodness of fit	1.085	1.131	1.131
crystal growing	overlaying MeCN/ Et ₂ O	overlaying MeCN/ Et ₂ O	overlaying MeCN/ Et ₂ O

Table 2.10: Crystallographic data of $\{\text{Cr}(\text{NN})_3\}^{3+}$ complexes, part II

compound	$[\text{Cr}(4,4'\text{-Me}_2\text{bpy})_2(\text{bpy})][\text{PF}_6]_3$	$[\text{Cr}(5,5'\text{-Me}_2\text{bpy})_3][\text{PF}_6]_3$	$\text{Cr}[(\text{bpy})_2(5,5'\text{-Me}_2\text{bpy})][\text{PF}_6]_3$
formula moiety	$\text{C}_{34}\text{H}_{32}\text{CrN}_6$, 3(F ₆ P), 2(C ₂ H ₃ N)	$2(\text{C}_{36}\text{H}_{36}\text{CrN}_6)$, 6(F ₆ P), 2(C ₃ H ₆ O), (H ₂ O)	$2(\text{C}_{33}\text{H}_{30}\text{CrN}_6)$, 6(F ₆ P), 5(C ₃ H ₆ O)
formula weight	1093.65	2211.39	2285.47
crystal colour and habit	yellow, plate	yellow, block	yellow, block
crystal system	monoclinic	trigonal	monoclinic
space group	P2 ₁ /c	P3 ₂ 21	P2 ₁ /c
a, b, c [Å]	19.290(2) 13.2160(16) 18.703(3)	19.115(3) 19.115(3) 23.453(5)	11.174(2) 18.538(4) 24.374(5)
α, β, γ [°]	90.00 109.351(4) 90.00	90.00 120.00 90.00	90.00 90.78(3) 90.00
U [Å ³]	4498.7(10)	7421(2)	5048.3(17)
Dc [Mg m ⁻³]	1.615	1.484	1.504
Z	4	3	2
$\mu(\text{Mo-K}\alpha)$ [mm ⁻¹]	0.476	0.435	0.430
T [K]	123	173(2)	173(2)
refln. collected	25201	209659	56481
unique refln.	10115	8763	8943
refln. for refinement	5222	7871	6257
parameters	613	629	831
threshold	I > 1.0 σ	I > 2.0 σ	I > 2.0 σ
R1 (R1 all data)	0.1457 (0.2564)	0.0668 (0.0741)	0.0946 (0.1255)
wR2 (wR2 all data)	0.0982 (0.1819)	0.1716 (0.1776)	0.2502 (0.2813)
goodness of fit	1.0892	1.098	1.052
crystal growing	overlying MeCN/ Et ₂ O	overlying hexane/ acetone	overlying hexane/ acetone

Table 2.11: Angles between the bipyridine ligands, where A represents the ligand containing N1, and similarly B(N3) and C(N5).

compound	A and B [°]	B and C [°]	A and C [°]
$[\text{Cr}(\text{bpy})_3][\text{PF}_6]_3$	85.6	85.7	80.3
$[\text{Cr}(\text{bpy})_2(\text{phen})][\text{PF}_6]_3$	71.6	88.1	85.8
$[\text{Cr}(4,4'\text{-Me}_2\text{bpy})_2(\text{phen})][\text{PF}_6]_3$ (sp. grp.: C2/c)	89.4	81.6	89.6
$[\text{Cr}(4,4'\text{-Me}_2\text{bpy})_2(\text{phen})][\text{PF}_6]_3$ (sp. grp.: P2 ₁ /c)	86.4	85.7	89.4
$[\text{Cr}(5,5'\text{-Me}_2\text{bpy})_2(\text{phen})][\text{PF}_6]_3$	89.1	85.6	90.0

2.5.1 Structure of $[\text{Cr}(\text{bpy})_3][\text{PF}_6]_3 \cdot \text{MeCN}$

$[\text{Cr}(\text{bpy})_3][\text{PF}_6]_3 \cdot \text{MeCN}$ crystallises in the rhombohedral space group R3c (figure 2.14). The unit cell contains 18 cations ($Z = 18$) (figure 2.15). A pseudo-polymorphic structure has already been reported by *Petersen et al.*¹²⁰ with the same space group however without solvent in the lattice and with a smaller Z value ($Z = 6$). An additional structure in the space group R32 of $[\text{Cr}(\text{bpy})_3][\text{PF}_6]_3$ has been reported earlier by *Ferguson et al.*⁹³

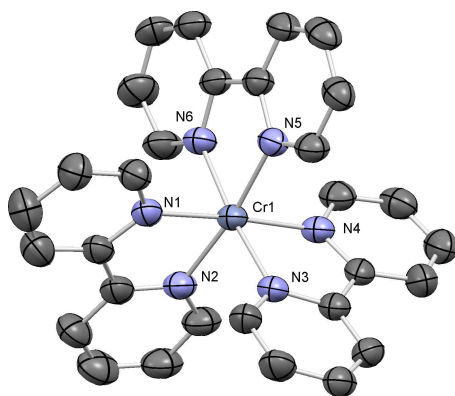


Figure 2.14: Structure of the cation in $[\text{Cr}(\text{bpy})_3][\text{PF}_6]_3 \cdot \text{MeCN}$ with ellipsoids plotted at 50 % probability level. H atoms, counter ions and solvent molecules are omitted for clarity. Selected bond lengths [\AA]: Cr1-N1 = 2.048(4), Cr1-N2 = 2.042(4), Cr1-N3 = 2.047(4), Cr1-N4 = 2.047(4), Cr1-N5 = 2.046(4), Cr1-N6 = 2.067(4); and bond angles [$^\circ$]: N1-Cr1-N2 = 80.06(16), N3-Cr1-N4 = 79.99(15), N5-Cr1-N6 = 79.99(15).

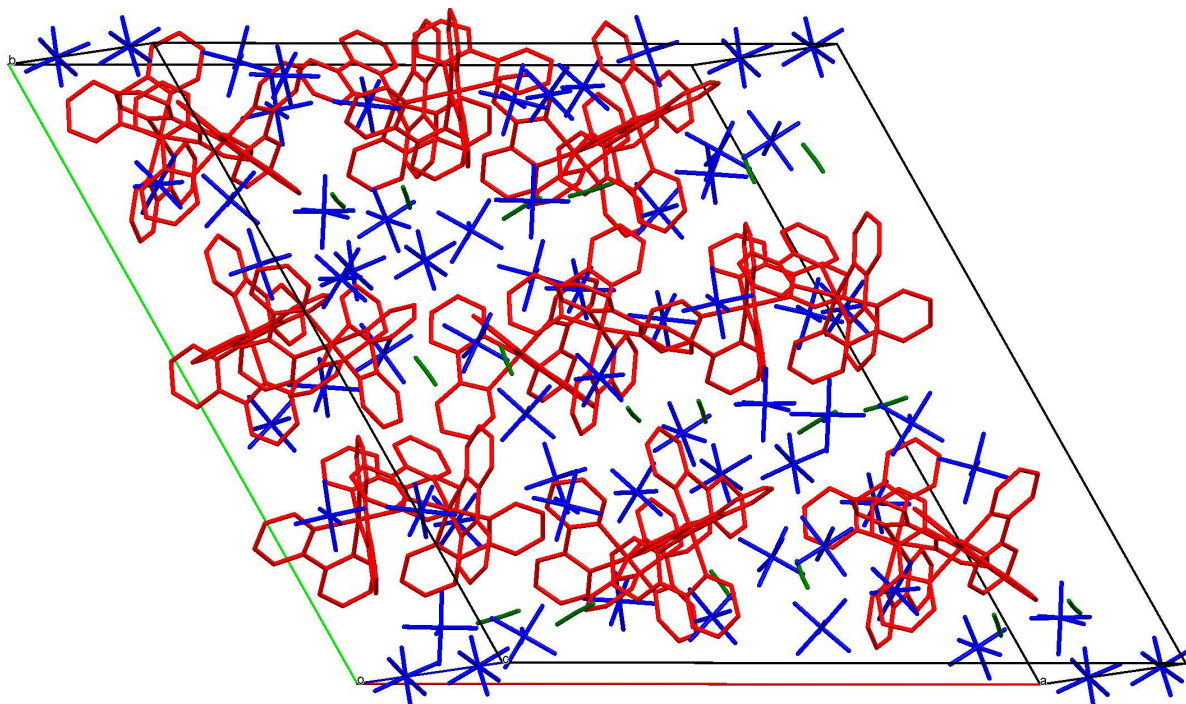


Figure 2.15: Unit cell packing of $[\text{Cr}(\text{bpy})_3][\text{PF}_6]_3 \cdot \text{MeCN}$. Colour code: cations (red), anions (PF_6^- , blue) and solvent molecules (MeCN, green).

2.5.2 Structure of $4\{[\text{Cr}(\text{bpy})_2(\text{phen})][\text{PF}_6]_3\}\cdot 11\text{MeCN}$

$4\{[\text{Cr}(\text{bpy})_2(\text{phen})][\text{PF}_6]_3\}\cdot 11\text{MeCN}$ crystallises as yellow blocks (figure 2.17) in the monoclinic space group $P2_1/c$ (figure 2.16). Two of the MeCN molecules in the asymmetric unit are disordered and have been modelled over two sites. The third solvent position has a fractional occupancy.

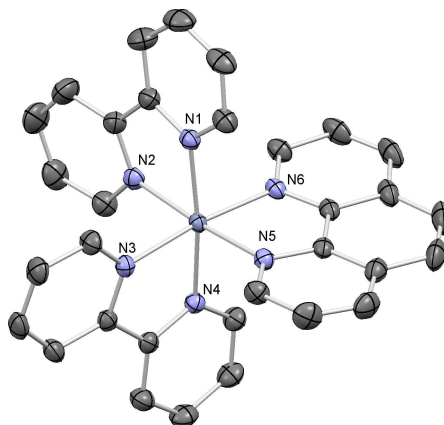


Figure 2.16: Structure of the cation in $[\text{Cr}(\text{bpy})_2(\text{phen})][\text{PF}_6]_3$ with ellipsoids plotted at 50 % probability level. H atoms, counter ions and solvent molecules are omitted for clarity. Selected bond lengths [Å]: Cr1-N1 = 2.0506(19), Cr1-N2 = 2.0527(19), Cr1-N3 = 2.0361(18), Cr1-N4 = 2.0373(19), Cr1-N5 = 2.0494(19), Cr1-N6 = 2.0468(18); and bond angles [°]: N1-Cr1-N2 = 79.53(8), N3-Cr1-N4 = 79.81(8), N5-Cr1-N6 = 80.75(8).

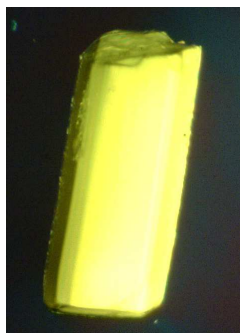


Figure 2.17: Picture (optical microscope) of a crystalline block of $[\text{Cr}(\text{bpy})_2(\text{phen})][\text{PF}_6]_3$.

2.5.3 Structure of $[\text{Cr}(\text{bpy})_2(5,5'\text{-Me}_2\text{bpy})][\text{PF}_6]_3\cdot 3\text{Me}_2\text{CO}$

$[\text{Cr}(\text{bpy})_2(5,5'\text{-Me}_2\text{bpy})][\text{PF}_6]_3\cdot 3\text{Me}_2\text{CO}$ crystallises in the monoclinic space group $P2_1/c$ (figure 2.18). Preliminary data confirmed the gross structural features of the cation. However, there was disordering of the methyl group over two positions. In figure 2.18 the cation with the 5,5'-Me₂bpy ligand containing N1 and N2 is presented. The second position includes N5 and N6. The PF₆⁻ anions were heavily disordered and could not be modelled in a satisfactory manner.

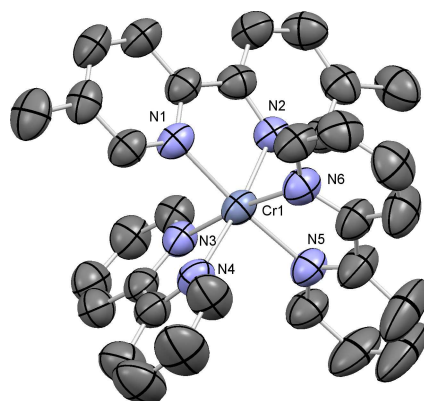


Figure 2.18: Structure of the cation in $[\text{Cr}(\text{bpy})_2(5,5'\text{-Me}_2\text{bpy})][\text{PF}_6]_3 \cdot \text{Me}_2\text{CO}$ with ellipsoids plotted at 50 % probability level. H atoms, counter ions and solvent molecules are omitted for clarity. Selected bond lengths [\AA]: Cr1-N1 = 2.042(3), Cr1-N2 = 2.041(3), Cr1-N3 = 2.050(3), Cr1-N4 = 2.039(4), Cr1-N5 = 2.037(3), Cr1-N6 = 2.049(4); and bond angles [$^\circ$]: N1-Cr1-N2 = 80.38(13), N3-Cr1-N4 = 79.49(14), N5-Cr1-N6 = 80.16(14).

2.5.4 Structure of $\text{Cr}[(4,4'\text{-Me}_2\text{bpy})_2(\text{bpy})][\text{PF}_6]_3$

The heteroleptic complex $\text{Cr}[(4,4'\text{-Me}_2\text{bpy})_2(\text{bpy})][\text{PF}_6]_3$ crystallised in two different space groups depending on the number of solvent molecules in the lattice.

$4\{\text{Cr}[(4,4'\text{-Me}_2\text{bpy})_2(\text{bpy})][\text{PF}_6]_3\} \cdot 12\text{MeCN} \cdot \text{H}_2\text{O}$ crystallises in the monoclinic space group $\text{C}2/c$ (figure 2.19), whereas $[\text{Cr}[(4,4'\text{-Me}_2\text{bpy})_2(\text{bpy})][\text{PF}_6]_3] \cdot 2\text{MeCN}$ crystallises in the monoclinic space group $\text{P}2_1/c$ (figure 2.20).

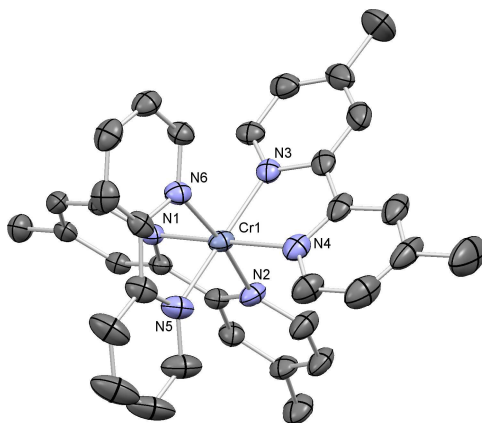


Figure 2.19: Structure of the cation in $4\{\text{Cr}[(4,4'\text{-Me}_2\text{bpy})_2(\text{bpy})][\text{PF}_6]_3\} \cdot 12\text{MeCN} \cdot \text{H}_2\text{O}$ (space group: $\text{C}2/c$) with ellipsoids plotted at 50 % probability level. H atoms, counter ions and solvent molecules are omitted for clarity. Selected bond lengths [\AA]: Cr1-N1 = 2.044(3), Cr1-N2 = 2.044(3), Cr1-N3 = 2.038(3), Cr1-N4 = 2.031(3), Cr1-N5 = 2.041(3), Cr1-N6 = 2.032(3); and bond angles [$^\circ$]: N1-Cr1-N2 = 79.56(12), N3-Cr1-N4 = 80.15(13), N5-Cr1-N6 = 79.34(13).

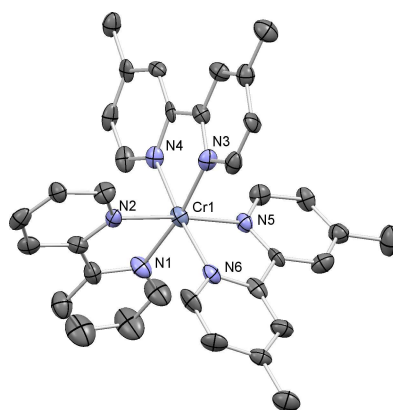


Figure 2.20: The structure of the cation in $[\text{Cr}(4,4'\text{-Me}_2\text{bpy})_2(\text{bpy})][\text{PF}_6]_3 \cdot 2\text{MeCN}$ (space group: $P2_1/c$) with ellipsoids plotted at 50 % probability level. H atoms, counter ions and solvent molecules are omitted for clarity. Selected bond lengths [\AA]: Cr1-N1 = 2.038(7), Cr1-N2 = 2.068(6), Cr1-N3 = 2.027(7), Cr1-N4 = 2.059(7), Cr1-N5 = 2.039(6), Cr1-N6 = 2.048(7); and bond angles [$^\circ$]: N1-Cr1-N2 = 80.1(3), N3-Cr1-N4 = 79.4(3), N5-Cr1-N6 = 80.1(3).

2.5.5 Structure of $[\text{Cr}(5,5'\text{-Me}_2\text{bpy})_3][\text{PF}_6]_3$

Since the crystals were highly twinned, the structure was difficult to solve. Preliminary data confirmed the structure (figure 2.21) of the cation as well as the number and identity of the anions. The presence of solvent (Me_2CO) could also be confirmed, but the molecules could not be modelled completely.

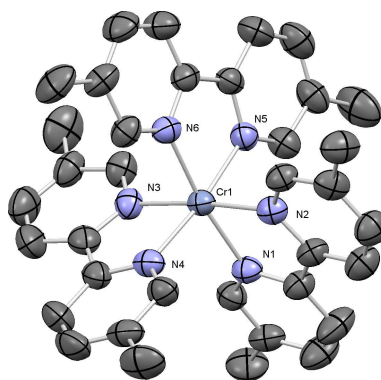


Figure 2.21: Structure of the cation in $[\text{Cr}(5,5'\text{-Me}_2\text{bpy})_3][\text{PF}_6]_3$ with ellipsoids plotted at 50 % probability level. H atoms, counter ions and solvent molecules are omitted for clarity. Selected bond lengths [\AA]: Cr1-N1 = 2.050(4), Cr1-N2 = 2.041(4), Cr1-N3 = 2.052(4), Cr1-N4 = 2.043(4), Cr1-N5 = 2.050(4), Cr1-N6 = 2.048(4); and bond angles [$^\circ$]: N1-Cr1-N2 = 80.14(15), N3-Cr1-N4 = 79.93(17), N5-Cr1-N6 = 80.01(15).

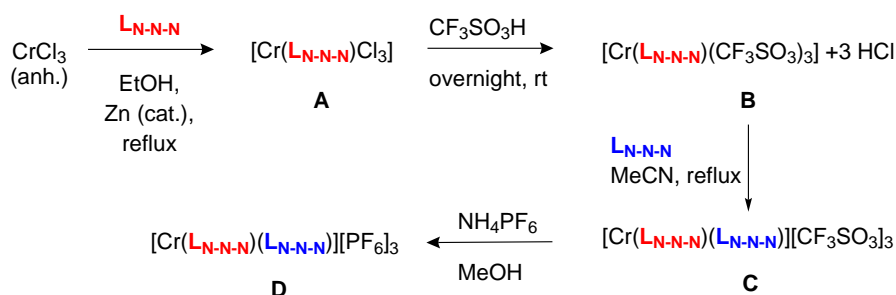
Chapter 3

Bis(terpyridine)chromium(III) complexes

3.1 Synthesis of bis(terpyridine)chromium(III) complexes

The majority of the previously reported syntheses start with a chromium(II) compound and include a $[\text{Cr}(\text{tpy})_2]^{2+}$ -intermediate.^{51,52,121,122} *Wallace et al.* published a protocol starting with $\text{CrCl}_3 \cdot \text{H}_2\text{O}$ which was treated with zinc amalgam to form a chromium(II) intermediate and following the same procedure as the examples above.¹²³

We developed a new synthesis based on the synthesis strategy known for the synthesis of tris(bipyridine)chromium(III) complexes (scheme 2.2, p. 12). This three step synthesis (scheme 3.1) starts with anhydrous chromium(III) chloride. In the first step CrCl_3 and the first equivalent of the terpyridine ligand are refluxed in EtOH in the presence of catalytic amounts of zinc. Since the intermediate is neutral and poorly soluble, the separation of the zinc powder and intermediate **A** by recrystallisation, analogous to $\{\text{Cr}(\text{bpy})_2\text{Cl}_2\}^+$, is not possible. Therefore granular zinc was used in place of the zinc powder. As a consequence, the amount had to be increased. The separation was now possible since the intermediate **A** precipitates as a fine powder and could be filtered carefully, however the granular zinc remained in the reaction flask. $[\text{Cr}(\text{tpy})]\text{Cl}_3$ was first synthesised by *Broomhead et al.*¹²⁴



Scheme 3.1: Three step synthesis strategy to homoleptic and heteroleptic bis(terpyridine)chromium(III) complexes.

In the following step the chlorides were exchanged by stirring **A** overnight at room temperature in trifluoromethanesulfonic acid. Since the intermediate **B** was sometimes not stable while storing in an oxygen containing atmosphere, the reaction strategy was adapted and intermediate **B** no longer isolated. Instead **B** was, after it was precipitated with Et_2O , filtered in a *Schlenk*-frit and redissolved directly in the reaction flask for step three. Also the third step was performed

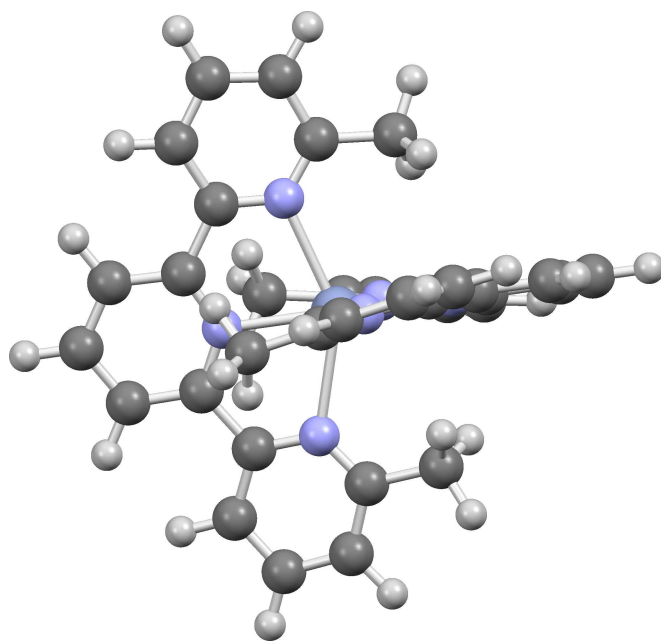
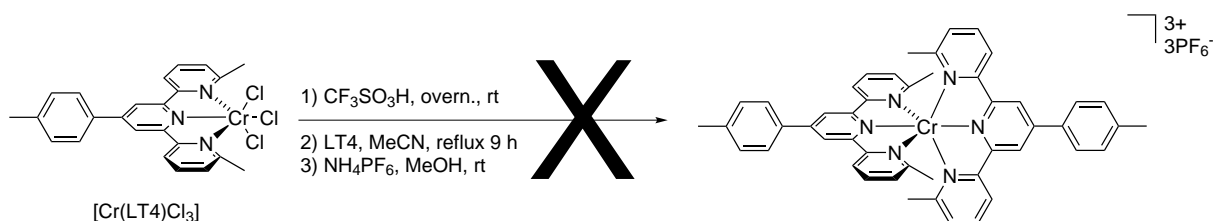


Figure 3.1: Calculated structure for $[\text{Cr}(6,6''\text{-Me}_2\text{tpy})_2]^{3+}$ (Spartan '4 V.1.1.3).

in an analogous manner to the tris(bipyridine)chromium(III) synthesis. **B** and the second equivalent tpy ligand were refluxed in acetonitrile. The third step could also be performed using the microwave reactor instead of refluxing the reaction mixture.

Since the two tpy ligands were introduced in two separate steps it is also possible to synthesise heteroleptic $\{\text{Cr}(\text{tpy}_A)(\text{tpy}_B)\}^{3+}$ complexes. To the best of our knowledge, no heteroleptic complexes with $\{\text{Cr}(\text{tpy})_2\}^{3+}$ cores have been reported before.

We achieved the synthesis of heteroleptic complexes with the sterically demanding ligand



Scheme 3.2: Attempted route to the homoleptic complex with the sterically demanding ligand LT4, which could not be isolated.

LT4 ($[\text{Cr}(4'-(4\text{-tolyl})\text{tpy})(\text{LT4})][\text{CF}_3\text{SO}_3]_3$ and $[\text{Cr}(\text{LT1})(\text{LT4})][\text{CF}_3\text{SO}_3]_3$), but the homoleptic complex $[\text{Cr}(\text{LT4})_2]^{3+}$ could not be isolated (scheme 3.2). The colour of the reaction mixture changed from greenish to yellow suggesting the formation of $[\text{Cr}(\text{LT4})_2]^{3+}$ in solution, but after anion exchange with NH_4PF_6 in MeOH, a dark green precipitate formed and there was no evidence for the formation of the desired complex.

Calculations for $[\text{Cr}(6,6''\text{-Me}_2\text{tpy})_2]^{3+}$ show that the tpy units have to be quite deformed to fit in the complexes. The structure was modelled using molecular mechanics (Spartan '4 V.1.1.3) and the modelled structure is shown in figure 3.1.

Anion exchange with an excess of NH_4PF_6 in MeOH was not complete with all complexes. An

example is the crystal structure of $[\text{Cr}(\text{HLT11})(\text{tpy})][\text{PF}_6]_3[\text{CF}_3\text{SO}_3]$ (3.9.2.2 , p. 86). In this example only three of the four anions were exchanged. The second reason is that all complexes containing at least one of the *N,N*-diphenylanyline tpy were too soluble to precipitate them with NH_4PF_6 .

The analysis methods to determine the composition of the complexes were limited to elemental analysis and X-ray structures. As presented in section 3.7 (p. 63) EPR measurements were unsuccessful. All attempts to use mass spectrometry (ESI-MS and MALDI-MS) to characterise the $\{\text{Cr}(\text{tpy})_2\}^{3+}$ complexes failed.

Table 3.1: Synthesised bis(terpyridine)chromium(III) complexes, part I: homoleptic complexes (exp. = link to the experimental part, str. = link to the structure discussion)

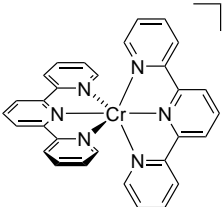
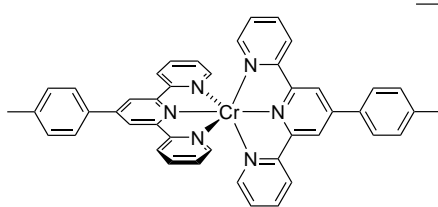
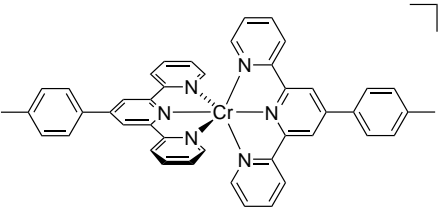
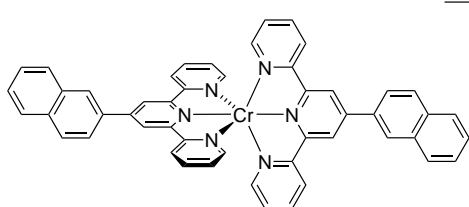
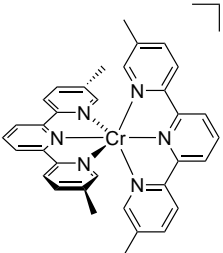
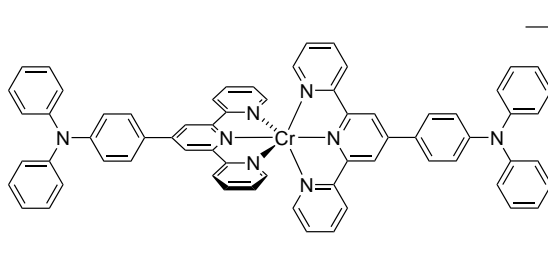
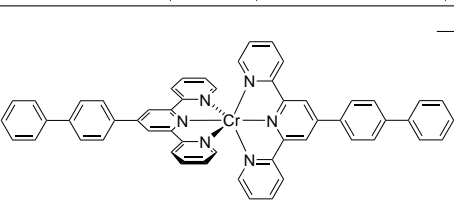
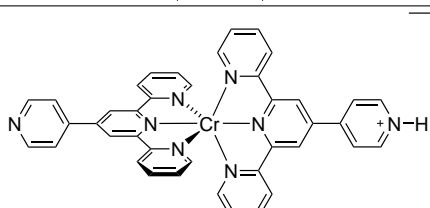
 <p>[Cr(tpy)₂][PF₆]₃ exp.: 6.4.3.1 (p. 130); str.: 3.9.1.1 (p. 73) reported by <i>Wiegardt et al.</i>⁵²</p>	 <p>[Cr(4'-(4-tolyl)tpy)₂][CF₃SO₃]₃ exp.: 6.4.3.2 (p. 130); str.: 3.9.1.4 (p. 79) reported as CF₃SO₃ salt by <i>Nair et al.</i>⁵¹</p>
 <p>[Cr(4'-(4-tolyl)tpy)₂][PF₆]₃ exp.: 6.4.3.3 (p. 131); reported as CF₃SO₃ salt by <i>Nair et al.</i>⁵¹</p>	 <p>[Cr(LT3)₂][PF₆]₃ exp.: 6.4.3.4 (p. 131); str.: 3.9.1.3 (p. 77)</p>
 <p>[Cr(5,5''-Me₂tpy)₂][PF₆]₃ exp.: 6.4.3.5 (p. 132); str.: 3.9.1.2 (p. 75)</p>	 <p>[Cr(LT5)₂][CF₃SO₃]₃ exp.: 6.4.3.6 (p. 132)</p>
 <p>[Cr(LT2)₂][PF₆]₃ exp.: 6.4.3.21 (p. 139);</p>	 <p>[Cr(HLT11)(LT11)][PF₆]₄ exp.: 6.4.3.7 (p. 133); str.: 3.9.1.6 (p. 81)</p>

Table 3.2: Synthesised bis(terpyridine)chromium(III) complexes, part II: heteroleptic complexes I (exp. = link to the experimental part, str. = link to the structure discussion).

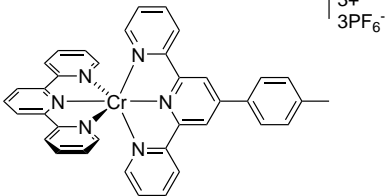
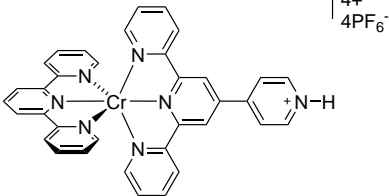
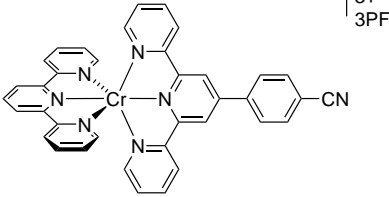
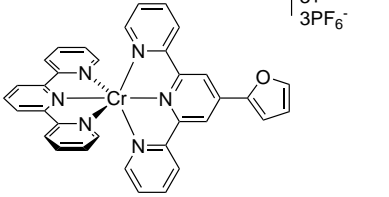
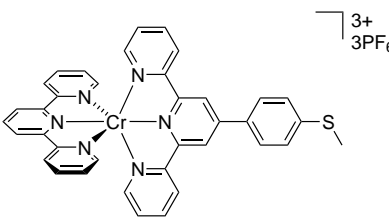
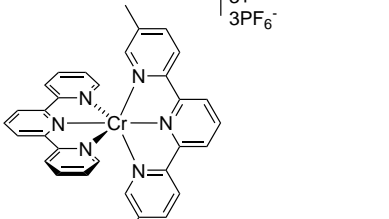
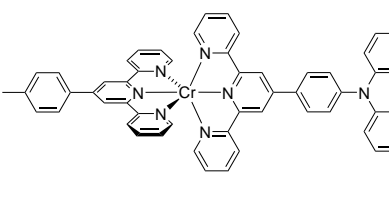
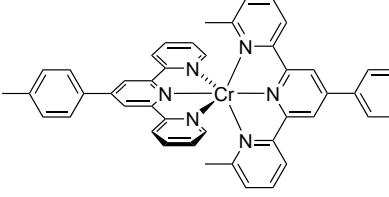
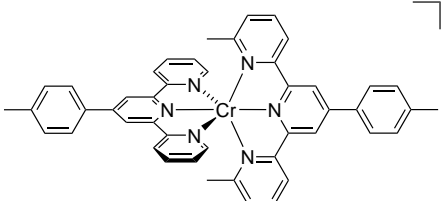
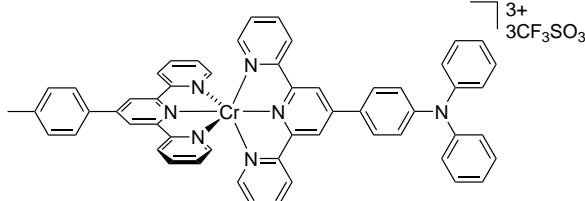
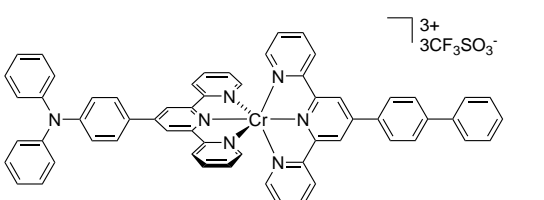
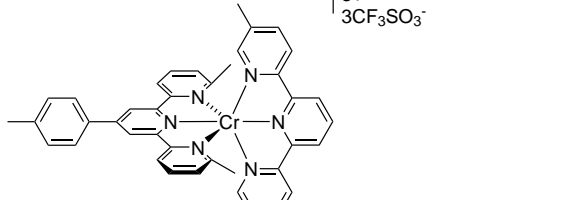
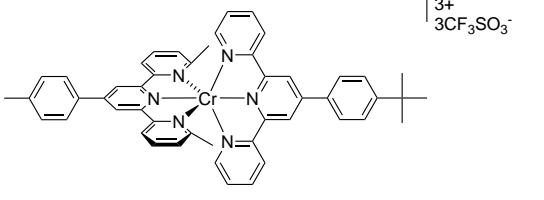
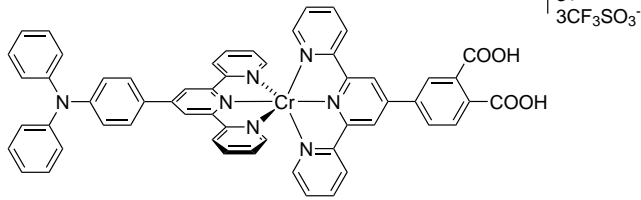
 <p>[Cr(tpy)(4'-(4-tolyl)tpy)][PF₆]₃ exp.: 6.4.3.8 (p. 133); str.: 3.9.2.5 (p. 90)</p>	 <p>[Cr(tpy)(HLT11)][PF₆]₄ exp.: 6.4.3.9 (p. 134); str.: 3.9.2.2 (p. 86)</p>
 <p>[Cr(tpy)(LT7)][PF₆]₃ exp.: 6.4.3.10 (p. 134); str.: 3.9.2.3 (p. 87)</p>	 <p>[Cr(tpy)(LT8)][PF₆]₃ exp.: 6.4.3.11 (p. 135); str.: 3.9.2.6 (p. 92)</p>
 <p>[Cr(LT9)(tpy)][PF₆]₃ exp.: 6.4.3.12 (p. 135); str.: 3.9.2.4 (p. 89)</p>	 <p>[Cr(tpy)(5,5''-Me₂tpy)][PF₆]₃ exp.: 6.4.3.13 (p. 135); str.: 3.9.2.1 (p. 86)</p>
 <p>[Cr(4'-(4-tolyl)tpy)(LT6)][CF₃SO₃]₃ exp.: 6.4.3.14 (p. 136);</p>	 <p>[Cr(4'-(4-tolyl)tpy)(LT4)][CF₃SO₃]₃ exp.: 6.4.3.15 (p. 136)</p>

Table 3.3: Synthesised bis(terpyridine)chromium(III) complexes, part III: heteroleptic complexes II (exp. = link to the experimental part, str. = link to the structure discussion).

 <p>[Cr(4'-(4-tolyl)tpy)(LT4)][PF₆]₃ exp.: 6.4.3.16 (p. 137)</p>	 <p>[Cr(4'-(4-tolyl)tpy)(LT5)][CF₃SO₃]₃ exp.: 6.4.3.17 (p. 137)</p>
 <p>[Cr(LT2)(LT5)][CF₃SO₃]₃ exp.: 6.4.3.18 (p. 138)</p>	 <p>[Cr(5,5''-Me₂tpy)(LT4)][CF₃SO₃]₃ exp.: 6.4.3.19 (p. 138)</p>
 <p>[Cr(LT1)(LT4)][CF₃SO₃]₃ exp.: 6.4.3.20 (p. 139)</p>	 <p>[Cr(LT5)(LT10)][CF₃SO₃]₃ exp.: 6.4.3.22 (p. 140)</p>

3.2 Lability of the bis(terpyridine)chromium(III) complexes

Chromium(III) (d^3) is a text-book²³ example of a kinetically inert metal ion with respect to ligand exchange. We observed a sensitive lability in alkaline environment or in the presence of F^- ions.

3.2.1 Lability in alkaline environment

The original aim was to replace the singly charged anions ($CF_3SO_3^-$ and PF_6^-) by threefold charged PO_4^{3-} . However we observed the decomposition of $[Cr(tpy)_2][CF_3SO_3]_3$ when Na_3PO_4 was added. The solution turned from yellow to greenish and a white precipitate formed. The white precipitate was found to be free ligand by 1H NMR spectroscopy. Since a decomposition of the complex in an alkaline environment was supposed, the following experiments were conducted.

Figure 3.2 shows a titration of an aqueous solution of $[Cr(tpy)(4'-(4-tolyl)tpy)][PF_6]_3$ with aqueous NaOH, monitored by UV-VIS spectroscopy. The decomposition can be observed in

the decay of the characteristic absorption with two maxima at 350 and 364 nm. The decrease of the absorption intensity after adding 0.25 eq. NaOH is considerable. After the addition of three equivalents of NaOH, conversion was essentially complete.

In contrast, the $\{\text{Cr}(\text{tpy})_2\}^{3+}$ complexes are stable in neutral aqueous solution. Figure 3.3 shows a 2 month monitoring of $[\text{Cr}(\text{tpy})_2][\text{PF}_6]_3$ in a neutral aqueous solution (deionised water, $\text{pH} = 6.36$). The minimal variances in the spectrum are caused by evaporation of solvent and a minimal decomposition between day 35 and day 67.

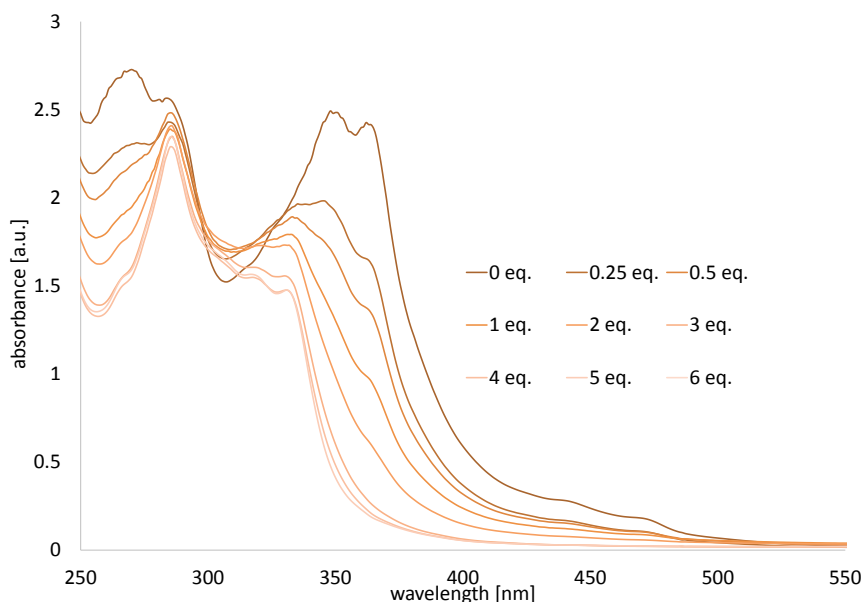
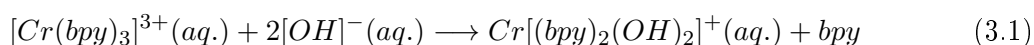


Figure 3.2: Absorption spectra of an aqueous solution of $[\text{Cr}(\text{tpy})(4'-(4\text{-tolyl})\text{-tpy})][\text{PF}_6]_3$ ($1.0 \cdot 10^{-4} \text{ mol l}^{-1}$) during a titration with aqueous NaOH ($1.0 \cdot 10^{-2} \text{ mol l}^{-1}$).

This correlates with the behaviour described for $[\text{Cr}(\text{bpy})_3][\text{ClO}_4]_3$ in aqueous solutions ($\text{pH} < 7$).¹¹³ Further decomposition (according to equation 3.1) has also been reported.^{113,114}



An associative mechanism has been proposed for this base-catalysed aquation reaction involving a seven coordinate intermediate $[\text{Cr}(\text{bpy})_3(\text{OH}_2)]^{3+}$, that is deprotonated under basic conditions and forms $[\text{Cr}(\text{bpy})_2(\text{OH})_2]^{+}$ and free bpy. The same process has also been described for photoaquation reactions under basic conditions.^{47,125}

For comparison, $[\text{Cr}(\text{bpy})_3][\text{PF}_6]_3$ was titrated with NaOH under the same conditions as used for the $\{\text{Cr}(\text{tpy})_2\}^{3+}$ complexes. The decomposition is minimal (figure 3.4) compared with the corresponding $\{\text{Cr}(\text{tpy})_2\}^{3+}$ complexes (figure 3.2).

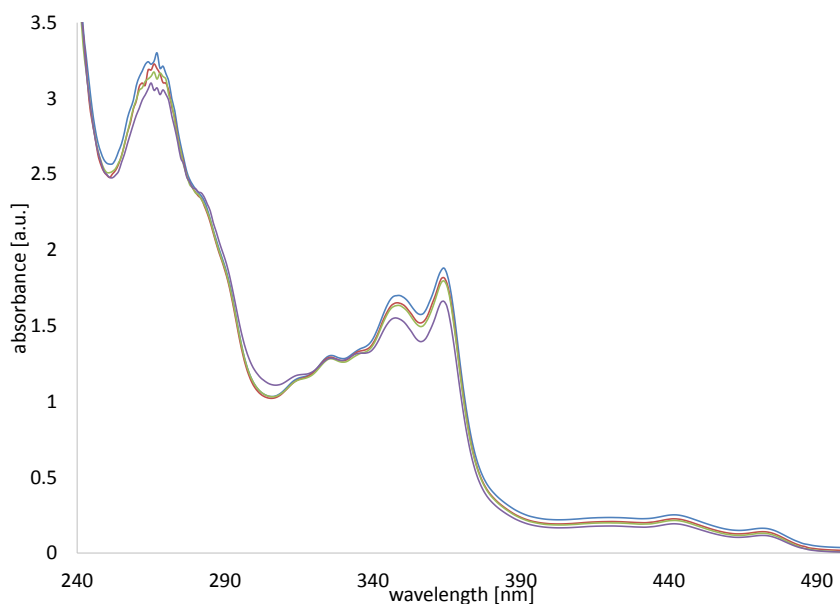


Figure 3.3: Absorption spectra of an aqueous solution of $[\text{Cr}(\text{tpy})_2][\text{PF}_6]_3$ ($1.0 \cdot 10^{-4} \text{ mol l}^{-1}$) over a period of 67 days. Blue: fresh, red: after 29 days, green: after 35 days and purple: after 67 days.

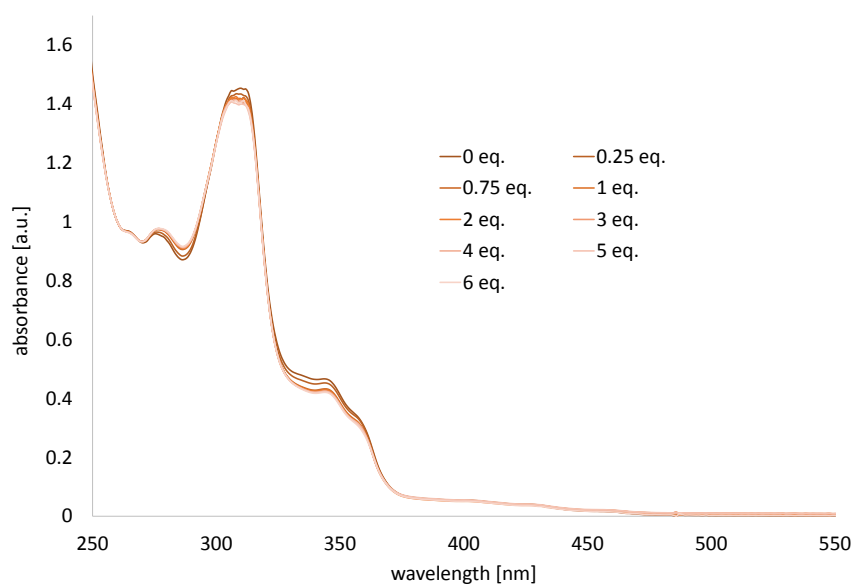


Figure 3.4: Absorption spectra of an aqueous solution of $[\text{Cr}(\text{bpy})_3][\text{PF}_6]_3$ ($1.0 \cdot 10^{-4} \text{ mol l}^{-1}$) during a titration with aqueous NaOH ($1.0 \cdot 10^{-2} \text{ mol l}^{-1}$).

Since $\{\text{Cr}(\text{tpy})_2\}^{3+}$ complexes containing a diphenylaniline tpy ligand (here LT5) show a broad absorption with maxima at 512 and 670 nm, the decomposition of $[(4'-(4\text{-tolyl})\text{-tpy})(\text{LT5})][\text{CF}_3\text{SO}_3]_3$ was observable by the naked eye when NaOH was added (figure 3.5). After the addition of 4 equivalents of NaOH, decomposition was nearly complete and was complete after adding 8 equivalents.

To determine the composition of the residues, 3.10 mg of $[\text{Cr}(\text{tpy})(4'-(4\text{-tolyl})\text{-tpy})][\text{PF}_6]_3$ in

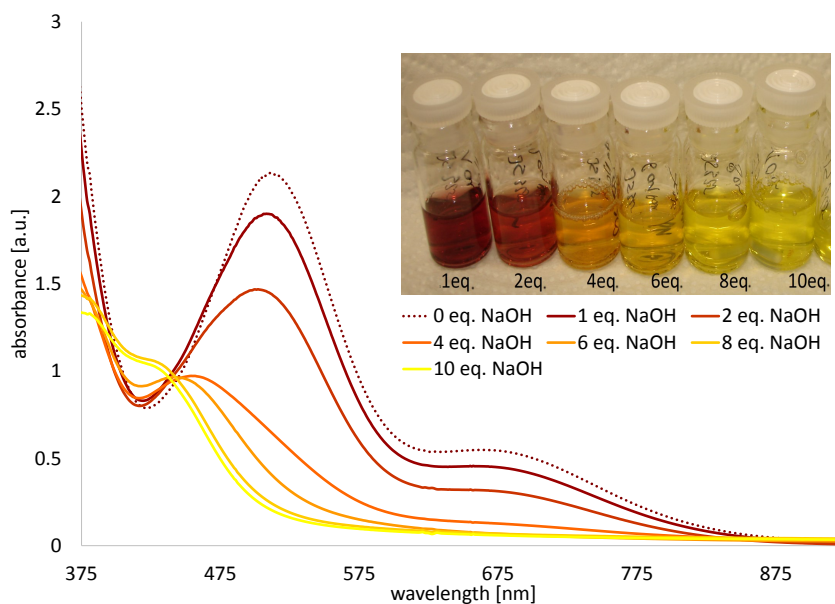


Figure 3.5: Absorption spectra of an aqueous solution of $[\text{Cr}(4'-(4\text{-tolyl})\text{-tpy})(\text{LT5})][\text{CF}_3\text{SO}_3]_3$ ($1.0 \cdot 10^{-4}$ mol l^{-1}) during a titration with aqueous NaOH ($1.0 \cdot 10^{-2}$ mol l^{-1}). *Inset*: Picture of the solutions with the particular equivalents of NaOH.

20 ml water was treated with an excess of NaOH (aqueous solution, 7.25 eq.) and stirred for 1 h at room temperature. The pale green solution with a flaky white precipitate was evaporated to dryness. Then CHCl_3 was added and the suspension was sonicated for 20 min. After filtration, the clear filtrate was evaporated and a ^1H NMR spectrum of the CDCl_3 soluble part of the residue was measured. The ^1H NMR is shown in figure 3.6a and shows that the CDCl_3 soluble material is a mixture of the two ligands of the former complex. In this experiment the ratio 1 : 0.9 ($4'-(4\text{-tolyl})\text{-tpy}$: tpy), was determined from the integrals of the signals labelled with I and II in figure 3.6a. In a corresponding experiment with $[\text{Cr}(4'-(4\text{-tolyl})\text{-tpy})(\text{LT5})][\text{CF}_3\text{SO}_3]_3$ (10 eq. NaOH, in water) the ratio of the two ligands was 1 : 1.

In an independent experiment $[\text{Cr}(\text{tpy})(4'-(4\text{-tolyl})\text{-tpy})][\text{CF}_3\text{SO}_3]_3$ (3.6 mg in 2.5 ml MeCN) was treated with a large excess (48 eq.) of tetrabutylammonium hydroxide ($^n\text{Bu}_4\text{NOH}$). The mixture was stirred for 1 h at room temperature, the solvent was removed by evaporation and the residue redissolved in CH_2Cl_2 with a drop of MeOH for the preparation of the MALDI-MS sample. The main signal at m/z 425.6 fits well with the calculated isotopic pattern for $\{[\text{Cr}(4'-(4\text{-tolyl})\text{-tpy})(\text{OH})_3\text{-H}]^+\}$ (figure 3.7). This is a strong evidence that the chromium containing residue is $\{\text{Cr}(\text{tpy})(\text{OH})_3\}$ when OH^- was added to the solution. A further hint are the three additional bands in the IR spectrum at 3216, 2958 and 2872 cm^{-1} after the addition of NaOH. The O–H vibration¹²⁶ pattern matches with that reported for chromium(III) hydroxide $(\text{Cr}(\text{OH})_3)$.¹²⁷ However the wavenumbers $(\text{Cr}(\text{OH})_3)$: 3410, 2954 and 2866 cm^{-1} ¹²⁷ are only partly consistent.

The results of the UV-VIS monitoring (figures 3.2 and 3.5) are consistent with the postulated formation of $\{\text{Cr}(\text{tpy})(\text{OH})_3\}$. When NaOH is added to $[\text{Cr}(\text{tpy})(4'-(4\text{-tolyl})\text{-tpy})][\text{PF}_6]_3$, three equivalents are needed to essentially complete the decomposition (figure 3.2). In the second example the decomposition is essentially completed after the addition of 8 equivalents, but the main part of the decomposition took place after adding the first 4 equivalents of NaOH. Combined with the fact that the ratio of the free ligand is roughly 1:1, one can estimate a statistical elimination independent of functional groups on the ligand (figure 3.5).

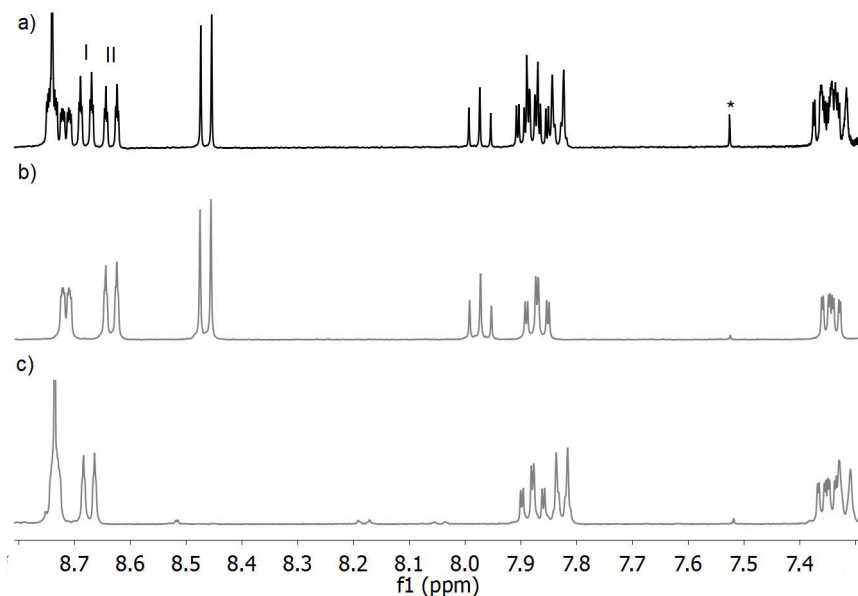


Figure 3.6: ^1H NMR spectra in CDCl_3 of: a) the chloroform-soluble part of the residue of $[\text{Cr}(\text{tpy})(4'-(4\text{-tolyl})\text{-tpy})][\text{CF}_3\text{SO}_3]_3$ (see text); b) tpy, c) $4'-(4\text{-tolyl})\text{-tpy}$. Signal marked with an asterisk arises from one of the ^{13}C satellite peaks of residual CHCl_3 .

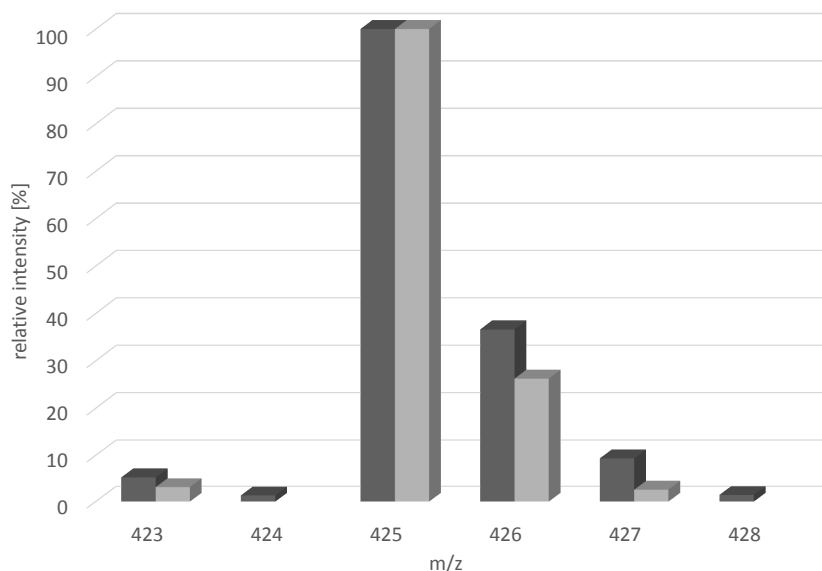


Figure 3.7: Comparison of the calculated (dark grey) and measured (light grey) isotope pattern for $\{[\text{Cr}(4'-(4\text{-tolyl})\text{-tpy})(\text{OH})_3\text{-H}]^+\}$.

3.2.2 Fluoride lability

While carrying out ligand exchange experiments (see 3.3, p. 43) we realised that complexes with a PF_6^- anion decompose when heated in the microwave reactor, whereas those containing CF_3SO_3^- seem to be stable respectively undertake a ligand exchange.

Therefore, the following experiments were executed: Solutions (3 mg compound in 1.5 ml MeCN) of $[\text{Cr}(\text{LT3})_2][\text{PF}_6]_3$ (figure 3.8.A.I) and $[\text{Cr}(\text{LT3})_2][\text{CF}_3\text{SO}_3]_3$ (figure 3.8.A.II) were heated in the microwave reactor for 1 h at 150 °C and 8 bar. Figure 3.8.B shows that no change is visible in vial II ($[\text{Cr}(\text{LT3})_2][\text{CF}_3\text{SO}_3]_3$), whereas $[\text{Cr}(\text{LT3})_2][\text{PF}_6]_3$ (vial 1) changed colour to pale purple.

It is obvious that a decomposition has occurred. To determine the composition of the residue, additional experiments were performed. $[\text{Cr}(\text{tpy})_2][\text{PF}_6]_3$ (around 3 mg) in MeCN (1.5 ml) was heated under the same conditions (microwave reactor, 1 h, 150 °C, 8 bar) as in the experiment described above. The UV-VIS spectrum shows a weak absorption with a maximum at 550 nm (figure 3.9: blue curve).

As a blank, a 0.1 M solution of NH_4PF_6 in MeCN was heated in the microwave reactor under the same conditions as the complexes described before (1 h, 150 °C, 8 bar). $^{19}\text{F}\{^1\text{H}\}$ NMR spectroscopy shows a complete decomposition of the PF_6^- ion (figure 3.10). According to the $^{19}\text{F}\{^1\text{H}\}$ NMR spectrum, heating in the microwave reactor yielded four different compounds. The two doublets around -85 ppm fit with the reported spectra¹²⁸ for POF_4^- , POF_3 and PO_2F_2^- . Since the published data are not measured in the same solvent, a precise assignment is not possible. *Otero et al.*¹²⁸ report further "the ^{19}F spectra showed several single peaks from -165 to -125 ppm." The additional signals that could not be assigned fit in this range. Therefore a hydrolysis, as discussed in the literature,¹²⁸ can be proposed as decomposition of the PF_6^- in the microwave reactor. The resulting F^- ions coordinate then to the Cr(III) ion and replace one tpy ligand.

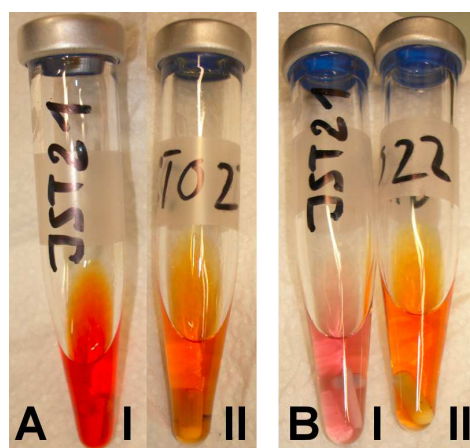


Figure 3.8: Pictures of the samples before (A) and after (B) heating in the microwave reactor. I: $[\text{Cr}(\text{LT}3)_2][\text{CF}_3\text{SO}_3]_3$ II: $[\text{Cr}(\text{LT}3)_2][\text{PF}_6]_3$.

In a further experiment $[\text{Cr}(\text{tpy})_2][\text{PF}_6]_3$ (3.0 mg in 2.5 ml MeOH) was treated with an excess (32 eq.) of tetrabutylammonium fluoride (${}^n\text{Bu}_4\text{NF}$). The mixture was stirred for 1 h and yielded a pale purple solution. The UV-VIS spectrum shows a weak absorption with a maximum at 570 nm (figure 3.9: red curve).

These maxima and the shapes of the absorption bands agree with those reported for $[\text{Cr}(\text{tpy})\text{F}_3]$ ($\lambda_{\text{max}} = 581$ nm in propan-2-ol and 556 nm in water).¹²⁹ It could also be confirmed that the pale purple colour does not arise from $\{\text{Fe}(\text{tpy})_2\}^{2+}$ since the distinctive shape¹³⁰ (figure 3.9: green curve) of its absorption band is missing. That was considered since tpy is known as a sensitive reagent to detect iron cations. Impurities of iron cations can derive for example from the spatula.¹³¹ The subsequent addition of tetrabutylammonium fluoride and FeSO_4 to a MeOH solution of $[\text{Cr}(\text{tpy})_2][\text{PF}_6]_3$ showed (figure 3.12) clearly the different shape of the absorption. The fact that $\{\text{Fe}(\text{tpy})\}^{2+}$ is formed confirmed the presence of free tpy ligand in the solution after adding tetrabutylammonium fluoride.

In a similar experiment $[\text{Cr}(\text{tpy})_2][\text{PF}_6]_3$ (3.0 mg in 2.5 ml CHCl_3) was treated with an excess (32 eq.) of tetrabutylammonium fluoride (${}^n\text{Bu}_4\text{NF}$). After stirring for 1 h the solvent was evaporated and a MALDI-MS was measured (sample preparation with CH_2Cl_2 , matrix: 4-nitroaniline). The MALDI-MS shows one pattern with the most intense peak at m/z 323 (figure 3.11). This corresponds to $[\text{Cr}(\text{tpy})\text{F}_2]^+$ and, as shown in figure 3.11, the match between measured and calculated isotopic patterns is good. As reported above, a decomposition of the $\{\text{Cr}(\text{tpy})_2\}^{3+}$ complexes was observed when ${}^n\text{Bu}_4\text{NF}$ was added to a MeOH or CHCl_3 solution, whereas no change was observed in the absorption spectrum when an aqueous solution was treated with ${}^n\text{Bu}_4\text{NF}$. We postulate the greater number of hydrogen bonds between F^- and water compared to F^- in MeOH makes it act as a weaker nucleophile.

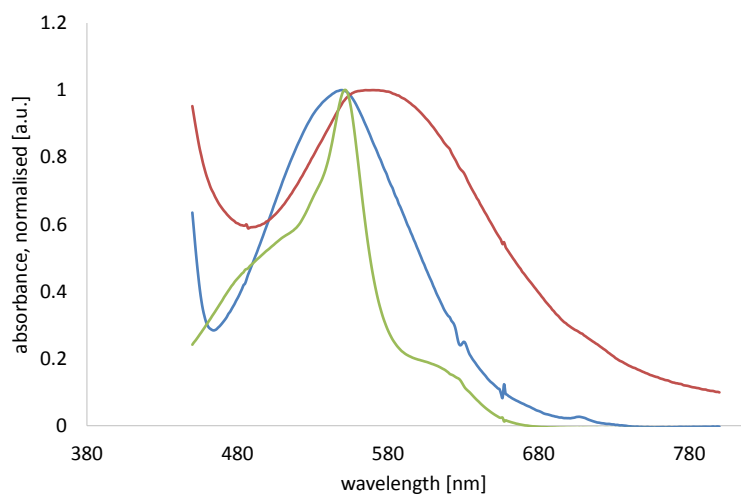


Figure 3.9: Normalised UV-VIS spectrum. Blue: proposed $[\text{Cr}(\text{tpy})\text{F}_3]$ in MeCN ($[\text{Cr}(\text{tpy})_2][\text{PF}_6]_3$ heated in the mw, $\lambda_{\text{max}} = 550$ nm); red: proposed $[\text{Cr}(\text{tpy})\text{F}_3]$ in MeOH (addition of ${}^n\text{Bu}_4\text{NF}$ to $[\text{Cr}(\text{tpy})_2][\text{PF}_6]_3$, $\lambda_{\text{max}} = 570$ nm); green: control experiment $[\text{Fe}(\text{tpy})_2]^{2+}$.

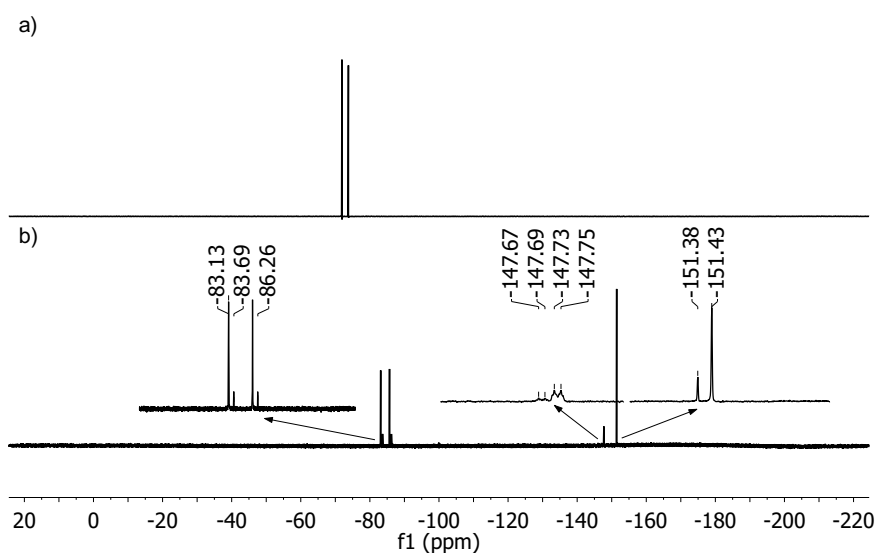


Figure 3.10: ${}^{19}\text{F}\{{}^1\text{H}\}$ NMR spectra in $d_3\text{-MeCN}$ of: a) NH_4PF_6 before heating in the microwave reactor; b) decomposition products of NH_4PF_6 after heating in the microwave reactor for 1 h at 150 °C and 8 bar.

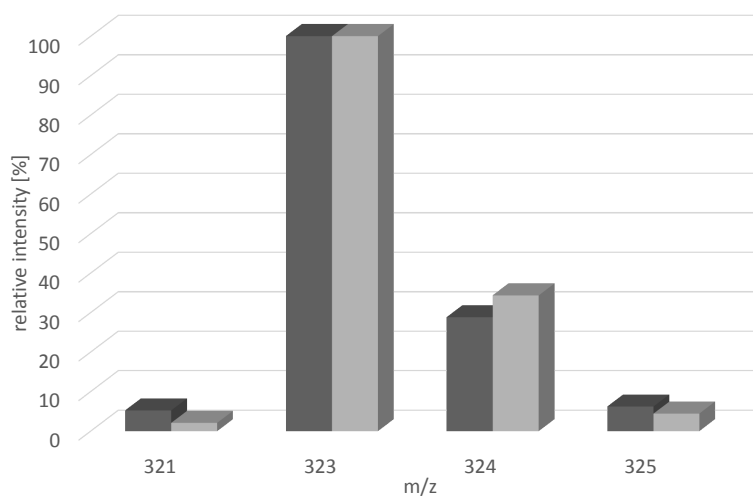


Figure 3.11: Comparison of the calculated (dark grey) and measured (light grey) isotope pattern for $[\text{Cr}(\text{tpy})\text{F}_2]^+$.

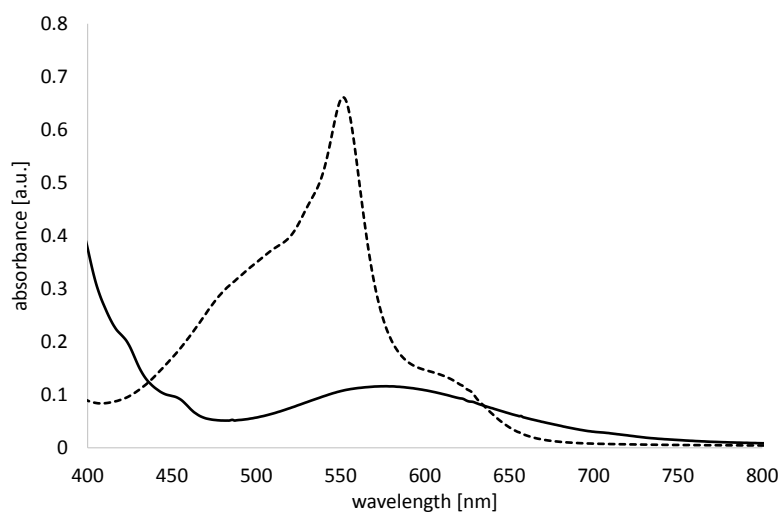
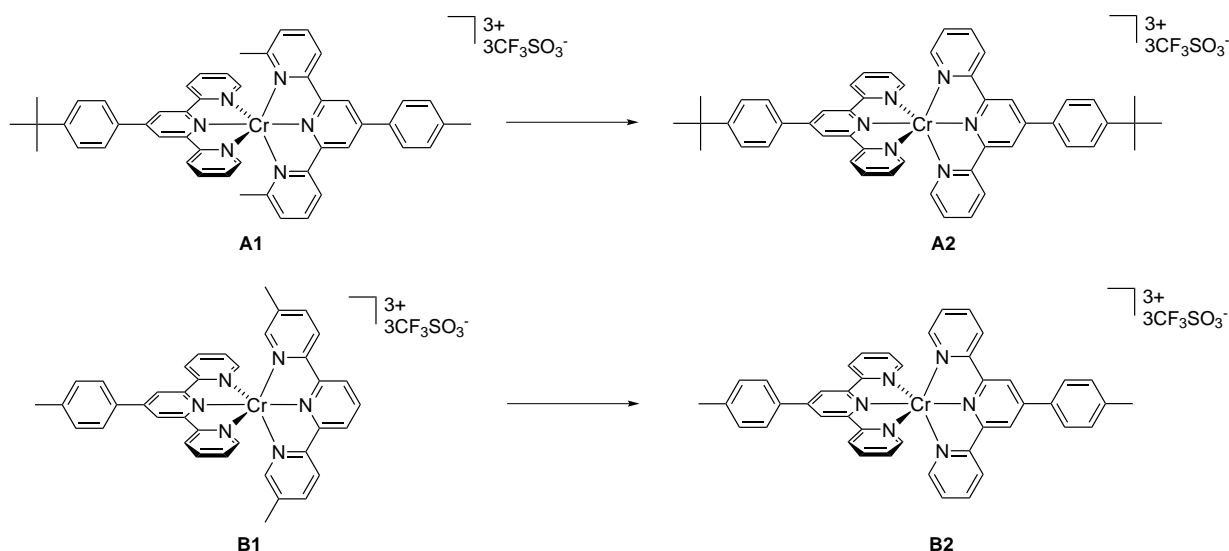


Figure 3.12: Absorption spectra of $[\text{Cr}(\text{tpy})_2][\text{PF}_6]_3$ in MeOH after it has been treated with $n\text{Bu}_4\text{NF}$ (solid line) and after additional adding of FeSO_4 (dotted line).

3.3 Ligand exchange

In two cases, crystal structures of homoleptic complexes were obtained from a bulk product that was assumed to be heteroleptic (scheme 3.3). Therefore we had to consider a ligand exchange between the heteroleptic complexes and the formation of homoleptic complexes. But we have also a definitive evidence for the existence of heteroleptic $\{\text{Cr}(\text{tpy}_A)(\text{tpy}_B)\}^{3+}$ complexes, the X-ray structures (compare 3.9, p. 70).



Scheme 3.3: Assumed heteroleptic structures in the bulk product (**A1** and **B1**) and the homoleptic structures (**A2** and **B2**), which were confirmed by X-ray crystallography.

In example **A** (scheme 3.3) the bulk compound **A1** was characterised by elemental analysis (6.4.3.20, p. 139). This was not the case in example **B**, since this complex could not be obtained pure. In both examples a sterically demanding ligand is exchanged for a less sterically demanding one. However, single crystal structures of complexes containing one sterically demanding ligand were also obtained ($[\text{Cr}(\text{tpy})(5,5''\text{-Me}_2\text{tpy})][\text{PF}_6]_3$ and $[\text{Cr}(4'-(4\text{-tolyl})\text{tpy})(\text{LT4})][\text{CF}_3\text{SO}_3]_3$. The crystal structure of $[\text{Cr}(\text{tpy})(5,5''\text{-Me}_2\text{tpy})][\text{PF}_6]_3$ is discussed in 3.9.2.1 on page 86. The data for $[\text{Cr}(4'-(4\text{-tolyl})\text{tpy})(\text{LT4})][\text{CF}_3\text{SO}_3]_3$ are only preliminary, but the data confirmed the main structural features of the cation (figure 3.13).

As a consequence of these observations a series of exchange experiments was conducted. To easily monitor a ligand exchange, LT5 was added to $[\text{Cr}(4'-(4\text{-tolyl})\text{tpy})_2][\text{CF}_3\text{SO}_3]_3$, since $\{\text{Cr}(\text{tpy})_2\}^{3+}$ complexes with this diphenylaniline tpy (LT5) appear dark in contrast to the yellow $[\text{Cr}(4'-(4\text{-tolyl})\text{tpy})_2][\text{CF}_3\text{SO}_3]_3$ (3.5.1, p. 52). Scheme 3.4 summarises the performed ligand exchange experiments I to III. An obvious change in the absorption spectra, and also visible to the naked eye, occurred only under harsh conditions (figure 3.14). Figure 3.15 shows that the pattern of the normalised UV-VIS spectrum for I is consistent with that for $[\text{Cr}(4'-(4\text{-tolyl})\text{tpy})(\text{LT5})][\text{CF}_3\text{SO}_3]_3$. A close look at the UV-VIS spectrum (figure 3.14) of trial II (refluxing for 7 h) also shows a slight increase of the absorption intensity at around 500 nm.

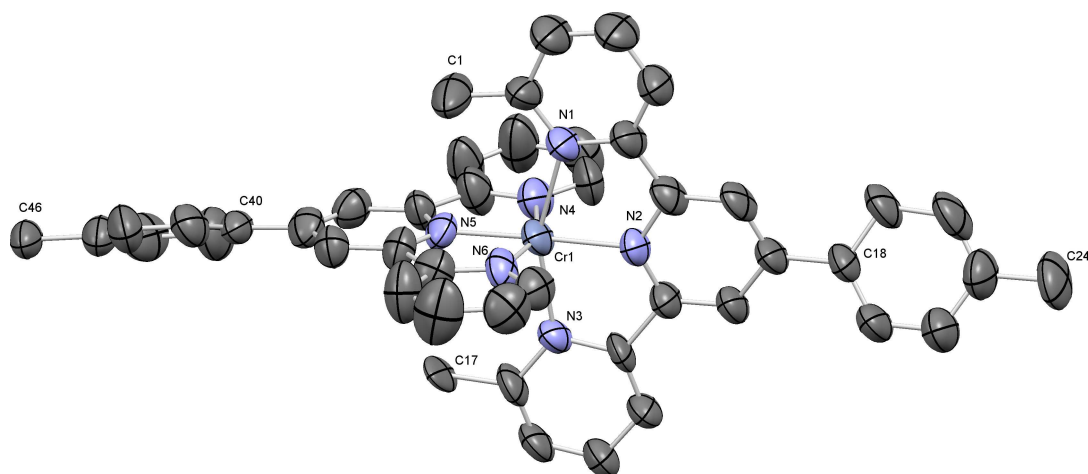


Figure 3.13: The cation of $[\text{Cr}(4'-(4\text{-tolyl})\text{tpy})(\text{LT4})][\text{CF}_3\text{SO}_3]_3$ with ellipsoids plotted at 50 % probability level. Anions, H atoms and solvent molecules are omitted for clarity. (R1: 0.1572)

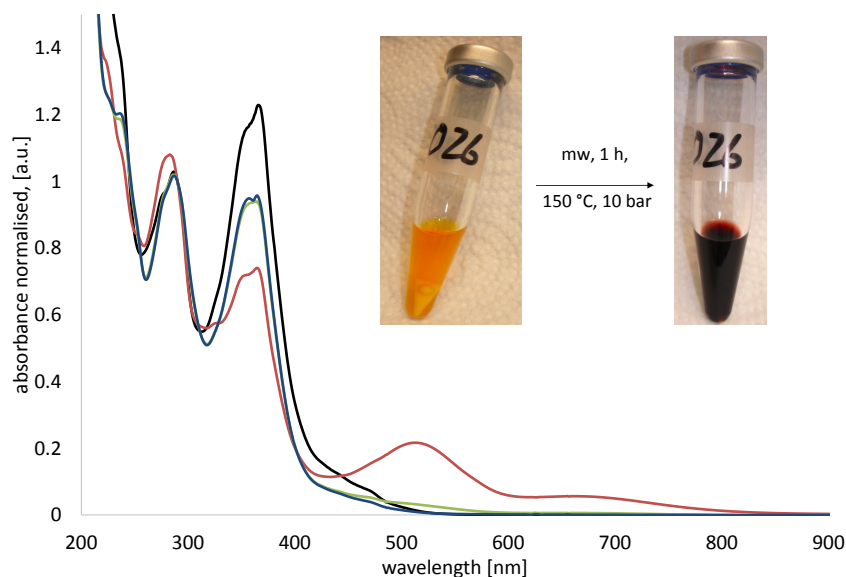
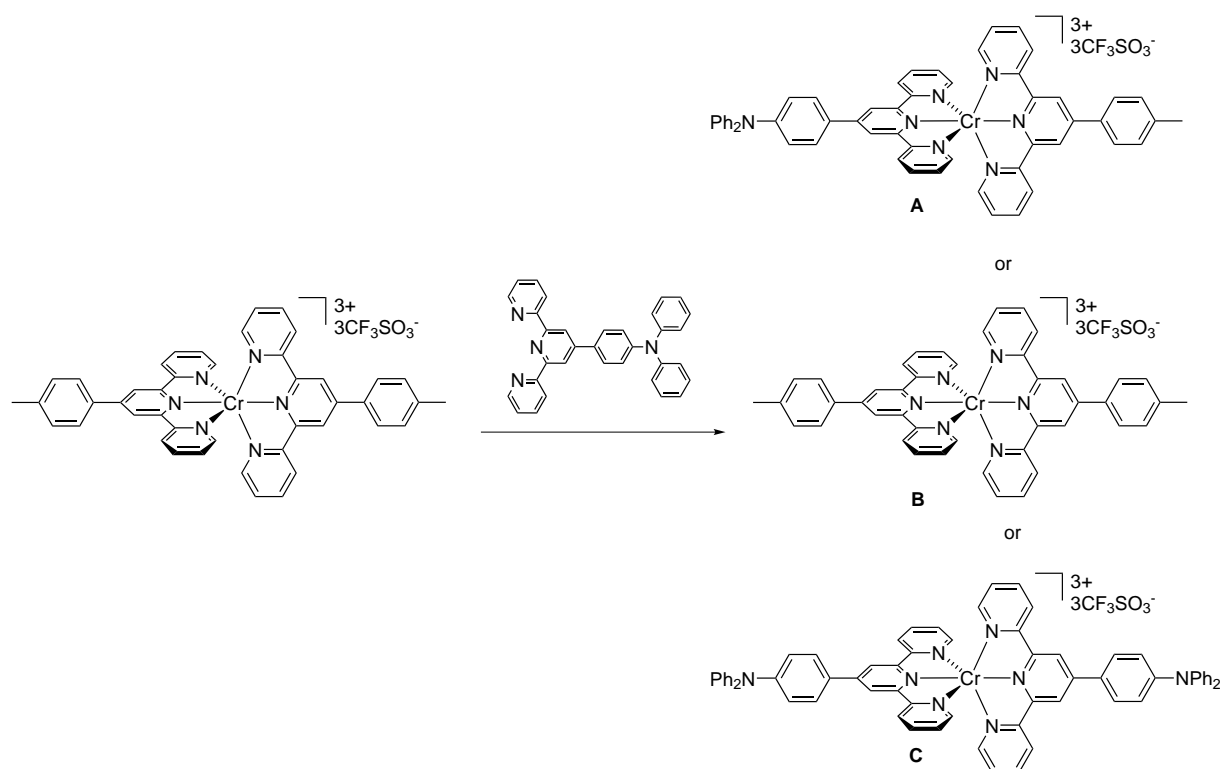


Figure 3.14: UV-VIS spectra in MeCN of $[\text{Cr}(5,5''\text{-Me}_2\text{tpy})_2][\text{PF}_6]_3$ (black) and the ligand exchange trials (compare scheme 3.4) I (red), II (green) and III (blue). The inset shows the colour change of ligand exchange experiment I.



label	additional ligand	reaction conditions	solvent	observations	conclusion
I	LT5, 1 eq.	mw, 1 h, 150 °C, 10 bar	MeCN	dark red solution	some or all ligands exchanged (A, B and/ or C possible)
II	LT5, 1 eq.	reflux, 7 h	MeCN	no colour change detectable, small change in UV-VIS	minimal exchange (mainly B, A and/ or C possible)
III	LT5, 1 eq.	stirring at rt, 2 days	MeCN	no colour change detectable	no exchange (B)

Scheme 3.4: Overview of the ligand exchange experiments I to III.

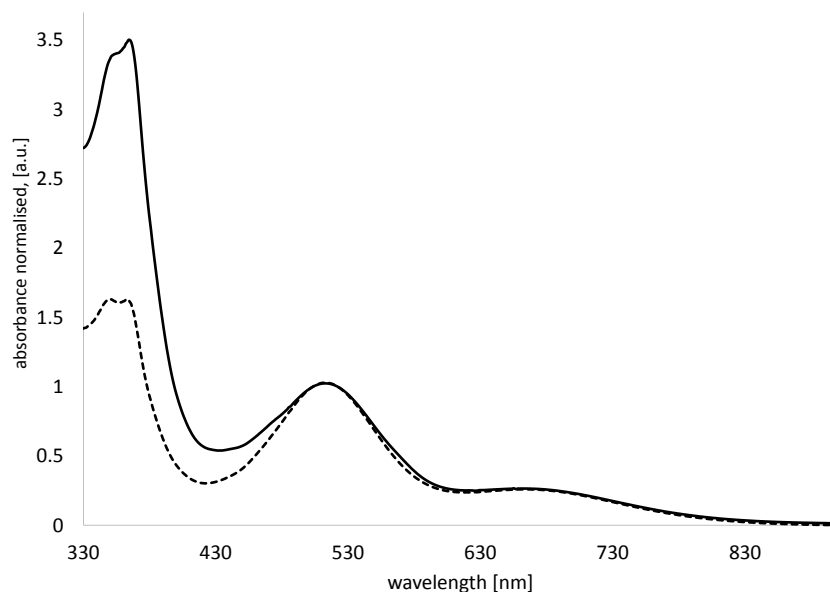
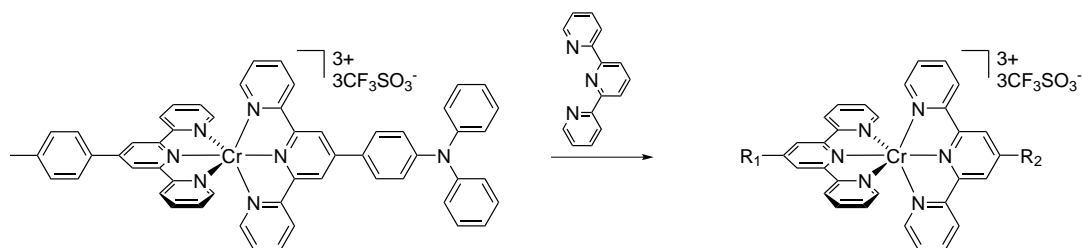


Figure 3.15: UV-VIS spectra in MeCN of exchange trial I (solid line) (compare scheme 3.4) compared with $[\text{Cr}(4'-(4\text{-tolyl})\text{tpy})(\text{LT5})][\text{CF}_3\text{SO}_3]_3$ (dotted line).

In a further ligand exchange experiment (IV, scheme 3.5) a reverse exchange was performed, in which the heavier ligands $4'-(4\text{-tolyl})\text{tpy}$ and LT5 could potentially be exchanged by tpy . The decrease in the absorption intensity between 440 and 840 nm indicates that some of the $4'$ -diphenylaniline tpy ligand has been replaced by tpy (figure 3.16).



label	additional ligand	reaction conditions	solvent	observations
IV	tpy, 5 eq.	mw, 1 h, 150 °C, 10 bar	MeCN	dark red solution, change observable in UV-VIS spectrum

Scheme 3.5: Ligand exchange experiment IV. The products of the ligand exchange reaction could not be determined in detail, therefore R_1 and R_2 stand for H, Me, 4'-(4-tolyl) and *N,N*-diphenylaniline.

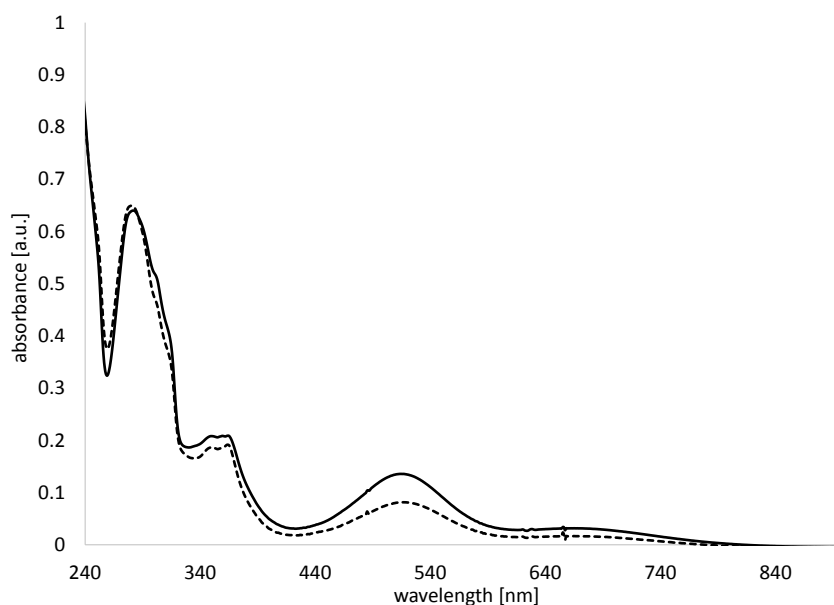
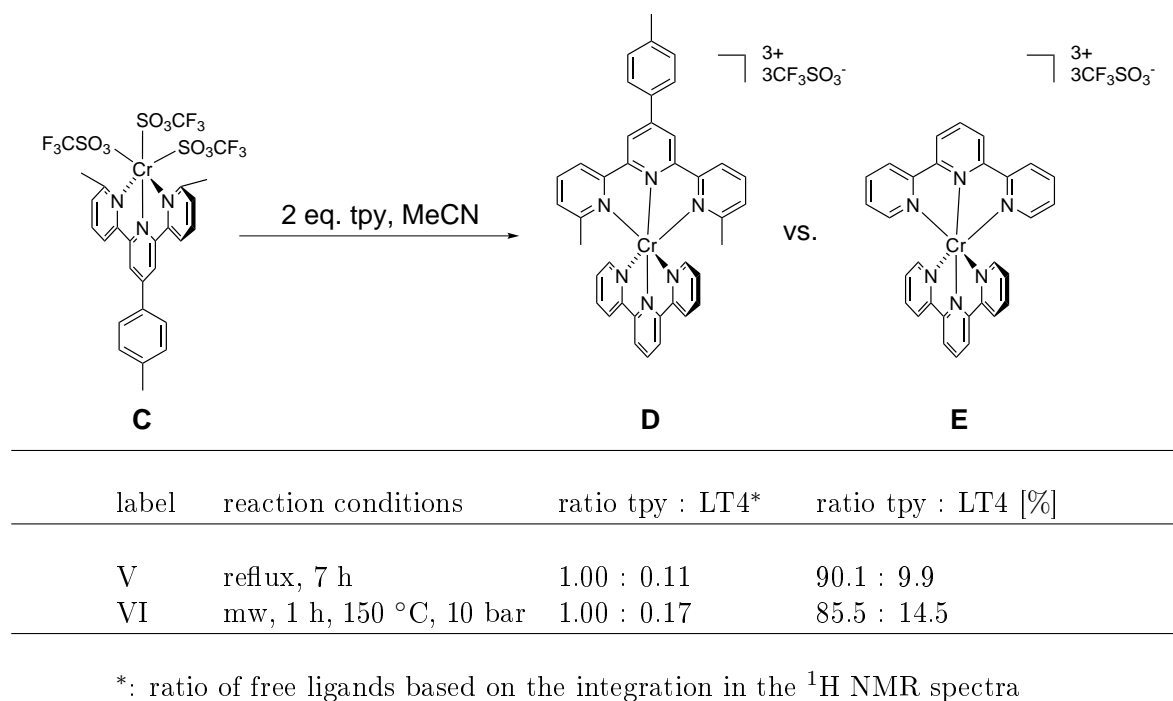


Figure 3.16: UV-VIS spectra in MeCN of the exchange trial IV: before the microwave reaction (additional ligand already added) (solid line) and after the reaction (dotted line).

In an ancillary experiment, a possible ligand exchange in the $\{\text{Cr}(\text{tpy})(\text{CF}_3\text{SO}_3)_3\}$ -moiety during the last reaction step (adding of the second ligand, compare 3.1 p. 33) was tested. To a MeCN solution of $[\text{Cr}(\text{LT4})(\text{CF}_3\text{SO}_3)_3]$ (scheme 3.6, **C**) an excess of tpy (2.0 eq.) was added. The reaction was done under reflux conditions (V) and by heating in the microwave reactor (VI). After the reaction, the crude product was washed with CH_2Cl_2 and in this way free ligand collected, since the chromium complexes are not soluble therein. The CH_2Cl_2 was evaporated and a ^1H NMR (in CDCl_3) of the residue measured. The ratio of tpy to LT4 was determined by ^1H NMR spectroscopy. The ratios are 1.00 : 0.11 (V) and 1.00 : 0.17 (VI) respectively (scheme 3.6). Therefore one can estimate that mainly the target complex $(\text{tpy})(\text{LT4})][\text{CF}_3\text{SO}_3]_3$ (**D**) was formed. But the presence of free LT4 in the reaction mixture points to a ligand exchange and the formation of the homoleptic $[\text{Cr}(\text{tpy})_2][\text{CF}_3\text{SO}_3]_3$ (**E**). A ligand exchange in the last step of the reaction was therefore proved. These observations agree with the observations done before for the complexes containing the sterically demanding ligand LT4. Also the fact that the exchange rate is higher under harsher conditions (microwave reactor) is consistent with previous observations.



Scheme 3.6: Ligand exchange experiments V and VI.

3.4 Photophysics of the bis(terpyridine)chromium(III) complexes

Since the complexes containing one of the 4'-diphenylaniline tpy ligands LT5 or LT6 have quite different photophysical properties, they are discussed separately in section 3.5 (p. 52).

3.4.1 Absorption spectra of the bis(terpyridine)chromium(III) complexes

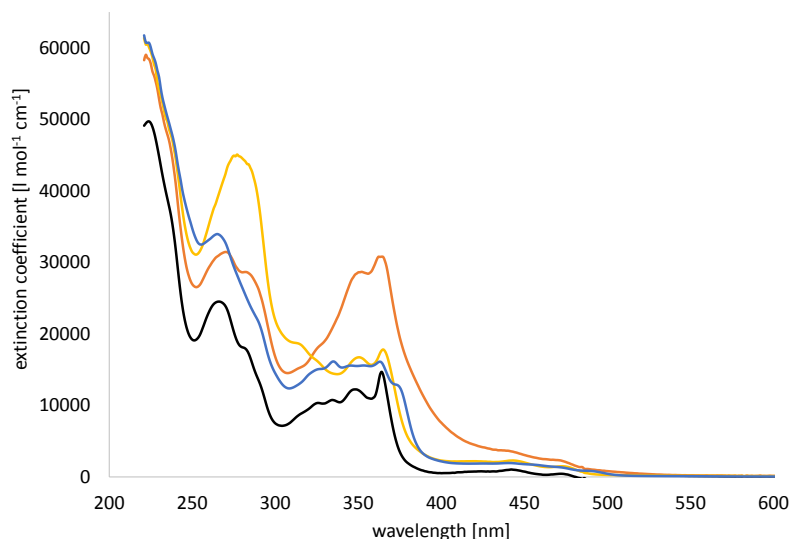


Figure 3.17: UV-VIS spectra measured in aqueous solution of $[\text{Cr}(\text{tpy})_2][\text{PF}_6]_3$ (black, $1 \cdot 10^{-5}$ M), $[\text{Cr}(\text{tpy})(4'-(4\text{-tolyl})\text{tpy})][\text{PF}_6]_3$ (orange, $5 \cdot 10^{-5}$ M), $[\text{Cr}(\text{tpy})(\text{HLT11})][\text{PF}_6]_4$ (yellow, $5 \cdot 10^{-5}$ M) and $[\text{Cr}(\text{tpy})(5,5''\text{-Me}_2\text{tpy})][\text{PF}_6]_3$ (blue, $5 \cdot 10^{-5}$ M).

The complexes which do not include a 4'-diphenylaniline tpy ligand absorb mainly in the UV-range. They show two absorption bands at around 270 nm and 365 nm (figure 3.17). The absorption in the visible range is weak (figure 3.17). $[\text{Cr}(\text{tpy})(4'-(4\text{-tolyl})\text{tpy})][\text{PF}_6]_3$ has a substantially more intense absorption between 300 and 500 nm, compared to the other complexes. The data are comparable with those reported in the literature for $[\text{Cr}(\text{tpy})_2][\text{ClO}_4]_3$ in MeCN¹³² and aqueous HCl solution.¹⁰⁹

3.4.2 Photoluminescence of the bis(terpyridine)chromium(III) complexes

In the literature little has been reported about the photoluminescence of $\{\text{Cr}(\text{tpy})_2\}^{3+}$ complexes. The reported emission maxima of the $\{\text{Cr}(\text{tpy})_2\}^{3+}$ complexes lie between 700 and 800 nm (table 3.4). However in our measurements we see bands at higher energies several times more intense than those reported. The emission bands at higher energies appear at exactly half of the wavelength of those at lower energies (figure 3.18). As figure 3.19 shows, the emission around 350 nm was also observed when the complex was excited at lower energies. We supposed therefore that the emission bands at around 700 nm are the 1st harmonic of the emissions at around 350 nm. As shown in figure 3.20, the excitation spectra for both emissions are identical. The identical fluorescence lifetime (for $[\text{Cr}(\text{tpy})_2][\text{PF}_6]_3$, $\tau = 2.8$ ns, in MeCN) of both emissions is a further hint to substantiate the proposition that the emission at higher energies is the first harmonic of those at lower energies. *Sutin et al.* reported that the lifetime of $[\text{Cr}(\text{tpy})_2]^{3+}$ is three orders of magnitude shorter compared with $[\text{Cr}(\text{bpy})_3]^{3+}$

complexes ($\sim 0.05 \mu\text{s}$ for $[\text{Cr}(\text{tpy})_2]^{3+}$ and $66 \mu\text{s}$ for $[\text{Cr}(\text{bpy})_3]^{3+}$, both measured in 1 M HCl).¹³³ We observed a difference of even four orders of magnitude (2.8 ns for $[\text{Cr}(\text{tpy})_2][\text{PF}_6]_3$ (in MeCN, see above) and $58 \mu\text{s}$ for $[\text{Cr}(\text{bpy})_3][\text{PF}_6]_3$ (in water, see 2.3.2, p. 20)).

Maestri et al. explained the shorter fluorescence lifetime by the fact that the tpy ligand is stiffer than the bpy ligand. They supposed that the *mer*-form of the cation $\{\text{Cr}(\text{tpy})_2\}^{3+}$ has to be highly distorted. This makes the metal ion more exposed to solvent approaches, which can result in a direct vibrational coupling between the solvent molecules and the metal core. This results in an increase of non radiative processes.¹⁰⁹ In our crystal structures we found that the chelate angles are between 77.39° and 79.41° , the tpy are ligands only little distorted from planarity and nearly orthogonal to each other (3.9 on page 70).

Table 3.4: Reported emission wavelengths for $\{\text{Cr}(\text{tpy})_2\}^{3+}$

compound	emission [nm]	excitation [nm]	solvent	source
$[\text{Cr}(\text{tpy})_2]^{3+}$ *	775	-	1 M HCl	<i>Sutin et al.</i> ¹³³
$[\text{Cr}(4'-(4\text{-tolyl})\text{tpy})_2][\text{ClO}_4]_3$	773	340	water	<i>Nair et al.</i> ⁵¹
$[\text{Cr}(\text{P3})_2][\text{ClO}_4]_3$	707	340	water	<i>Nair et al.</i> ⁵¹

* = The anions are not defined in the paper.

P3 = 4'-(4-Bromophenyl)-2,2':6',2''-terpyridine (6.2.1.3, p. 108)

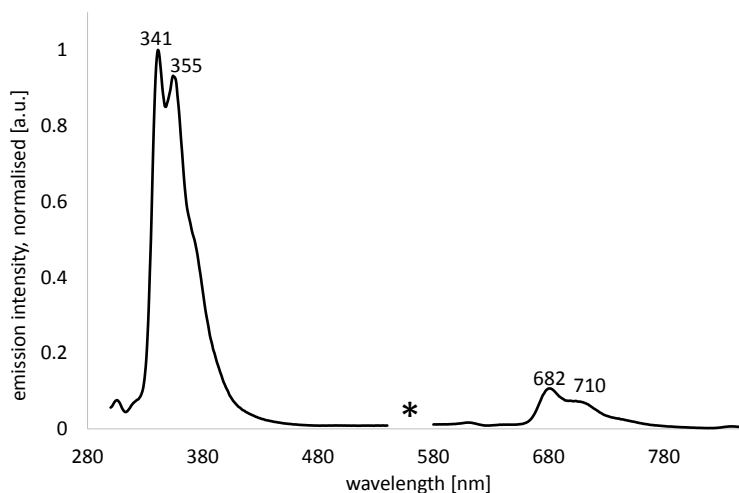


Figure 3.18: Photoluminescence spectrum of $[\text{Cr}(\text{tpy})_2][\text{PF}_6]_3$ in MeCN ($1 \cdot 10^{-5}$ M), excited at 280 nm. The first harmonic of the excitation is omitted and its position is marked with an asterisk.

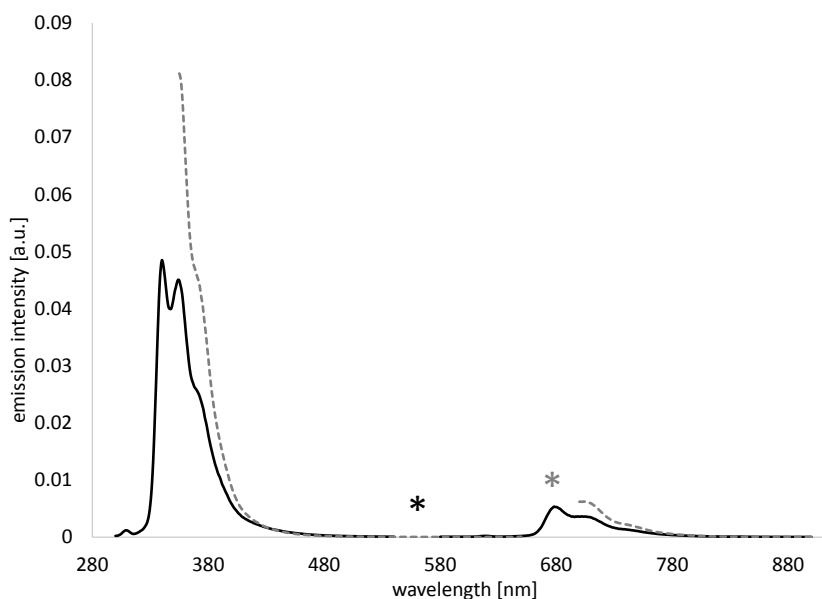


Figure 3.19: Photoluminescence spectra of $[\text{Cr}(\text{tpy})_2][\text{PF}_6]_3$ in water ($5 \cdot 10^{-5}$ M), excited at 280 nm (black solid line), 335 nm (grey dashed line). The first harmonics of the excitations are omitted and their positions are marked with asterisks.

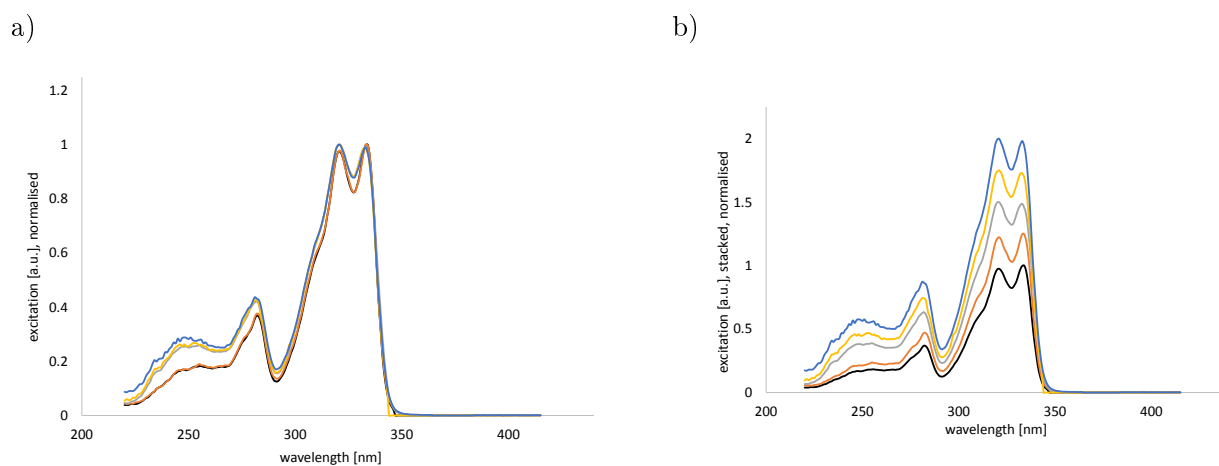
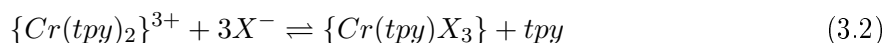


Figure 3.20: Excitation spectra of $[\text{Cr}(\text{tpy})_2][\text{PF}_6]_3$ in MeCN for different wavelengths. The spectra are normalised. Since they are one above the other they were plotted in b) in a stacked manner. The excitation spectra for emissions at 356 nm (black), 376 nm (orange), 679 nm (grey), 706 nm (orange) and 748 nm (blue) are presented.

3.4.2.1 Does the emission derive from a complex or from free ligand?

Figure 3.21 shows that the emission pattern depends upon the concentration of the solution. Further it was found that the broad band of $[\text{Cr}(\text{tpy})_2][\text{PF}_6]_3$ ($\lambda_{max} = 390$ nm) disappears after the addition of FeSO_4 (figure 3.22). The iron(II) cations act as a trap for free tpy, leading to the formation of non-luminescent $[\text{Fe}(\text{tpy})_2]^{2+}$. The observations described above and the fact that the $\{\text{Cr}(\text{tpy})_2\}^{3+}$ complexes are not kinetically inert (3.2, p. 38) lead to the assumption that we observe mainly the emission of the free ligand. Therefore we compared the emission for the complex with the reported data for tpy and 4'-(4-tolyl)tpy in the neutral and protonated states.^{134,135}

Figure 3.22 shows an emission spectrum of $[\text{Cr}(\text{tpy})_2][\text{PF}_6]_3$ in MeCN excited at 280 nm. This spectrum shows three emission maxima at 340 nm, 356 nm and 390 nm and a shoulder at 412 nm. The broad band with the maximum at 390 nm and a shoulder at 412 nm can be assigned to tpy in its mono- and diprotonated forms. The band with the maxima at 340 nm and 365 nm belong to the emission of tpy in its neutral state (compare table 3.5). Upon addition of one drop of FeSO_4 (concentrated in MeOH) the broad band at 390 nm vanishes. Additionally a band at 378 nm appears. The residual emission band can then be interpreted as the ligand based emission of $\{\text{Cr}(\text{tpy})_2\}^{3+}$ and/or $\{\text{Cr}(\text{tpy})(\text{X})_3\}$, where $\{\text{Cr}(\text{tpy})(\text{X})_3\}$ stands for a possible decomposition product (3.2, p. 38). Therefore the emission of free tpy, neutral or protonated, has to be considered as several times more intense than a possible emission arriving from the complex. The formation of $[\text{Fe}(\text{tpy})_2]^{2+}$, and therefore a trapping of free ligand, was confirmed by UV-VIS measurements. Figure 3.23 shows the characteristic absorption bands for $[\text{Fe}(\text{tpy})_2]^{2+}$ at 320 and 530 nm. The proposed decay of the $\{\text{Cr}(\text{tpy})_2\}^{3+}$ complex and protonation of the tpy ligand is shown in equations 3.2 to 3.4. Consideration of figure 3.21 leads to the conclusion that the position of the equilibrium depends on the concentration. For more concentrated samples ($1 \cdot 10^{-4}$ and $5 \cdot 10^{-5}$ M) the presence of $\text{H}_2\text{tpy}^{2+}$, Htpy^+ and tpy can be affirmed, whereas the less concentrated samples show only the emissions bands of tpy and $\text{H}_2\text{tpy}^{2+}$.



where $\text{X}^- = \text{F}^-$ or OH^-

Figure 3.24 shows that the residue $[\text{Cr}(\text{tpy})(\text{F})_3]$ of a decomposition is photoluminescent. Since the sample was prepared as described in section 3.2 (p. 38), Fe^{2+} was added to trap all free ligand to enable the emission of the complex to be measured.

Since the emission derived from the free tpy ligand (neutral or protonated), is many times more intense than that of the complex, small amounts of free ligand make it difficult or impossible to observe the emission from the complex.

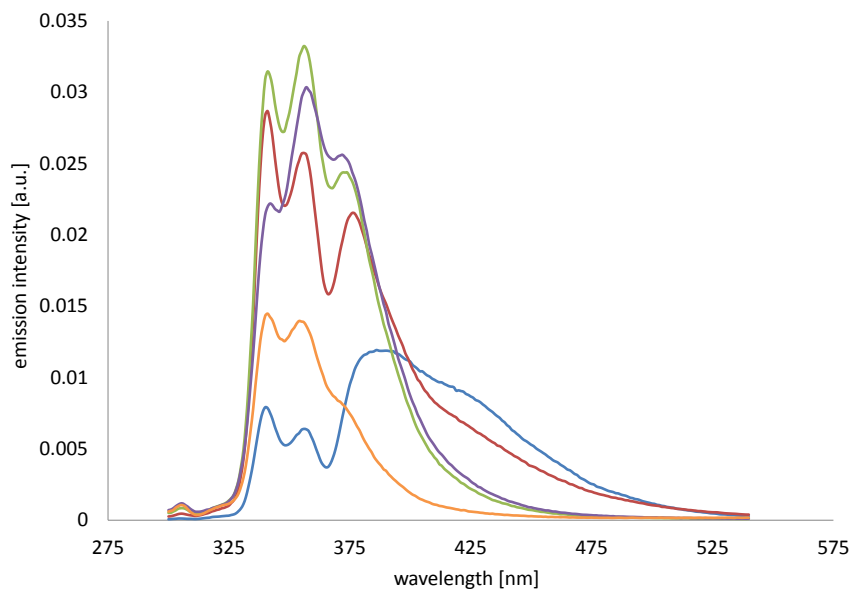


Figure 3.21: Photoluminescence spectrum of $[\text{Cr}(\text{tpy})_2][\text{PF}_6]_3$ in MeCN solutions of different concentrations, excited at 280 nm. Key: $1 \cdot 10^{-4}$ M: blue, $5 \cdot 10^{-5}$ M: red, $2.5 \cdot 10^{-5}$ M: green, $1.25 \cdot 10^{-5}$ M: purple, $1 \cdot 10^{-5}$ M: orange.

Table 3.5: Emission wavelengths for tpy and 4'-(4-tolyl)tpy in the neutral and protonated states in MeCN.

complex	emission [nm]	source
tpy	340	<i>Yoshikawa et al.</i> ¹³⁴
[tpyH][PF ₆]	412 (ex. 313 nm)	<i>Yoshikawa et al.</i> ^{134,135}
[tpyH ₂][PF ₆][Cl]	395 (ex. 278 nm)	<i>Yoshikawa et al.</i> ¹³⁵
4'-(4-tolyl)tpy	386	<i>Yoshikawa et al.</i> ¹³⁵
[4'-(4-tolyl)tpyH ₂][PF ₆][Cl]	436 (ex. 285 nm)	<i>Yoshikawa et al.</i> ¹³⁵
\hookrightarrow no excitation wavelength reported for tpy and 4'-(4-tolyl)tpy		

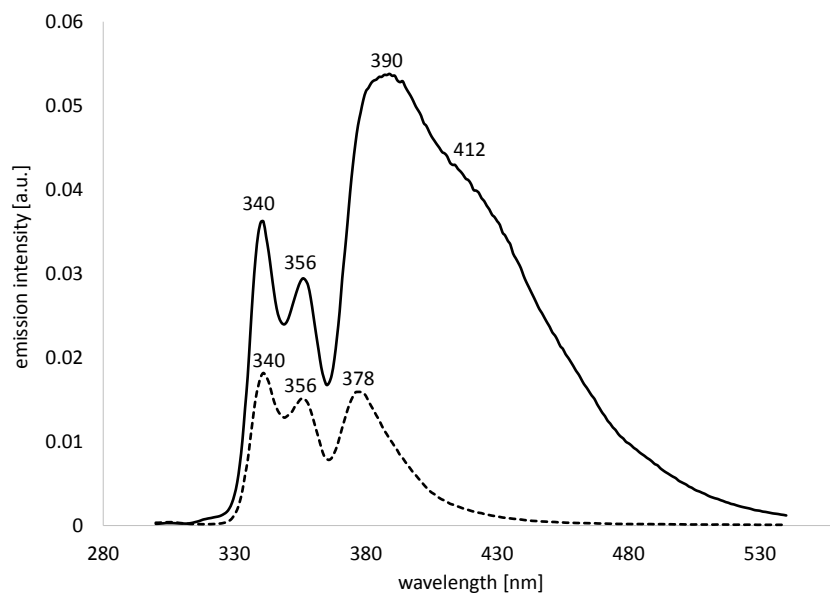


Figure 3.22: Photoluminescence spectrum of $[\text{Cr}(\text{tpy})_2][\text{PF}_6]_3$ in MeCN ($1 \cdot 10^{-4}$ M), excited at 280 nm. Solid line: before adding FeSO_4 , dashed line: after adding 1 drop of a concentrated solution of FeSO_4 in MeOH.

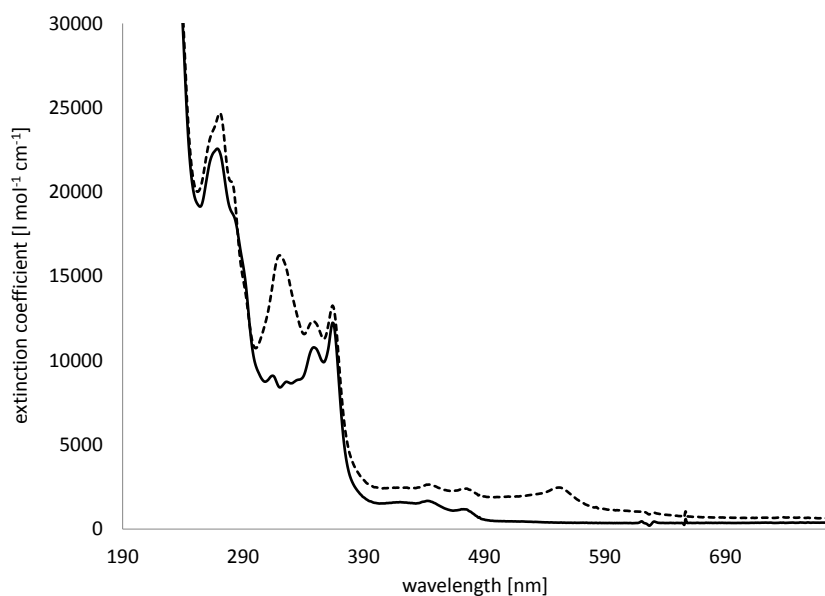


Figure 3.23: UV-VIS spectrum of $[\text{Cr}(\text{tpy})_2][\text{PF}_6]_3$ in MeCN ($1 \cdot 10^{-5}$ M), excited at 280 nm. Key: solid line: before adding FeSO_4 , dashed line: after adding 1 eq. FeSO_4 .

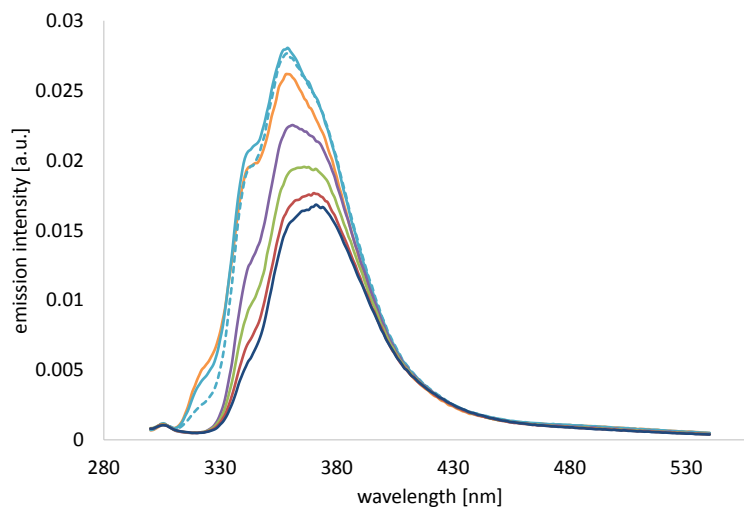
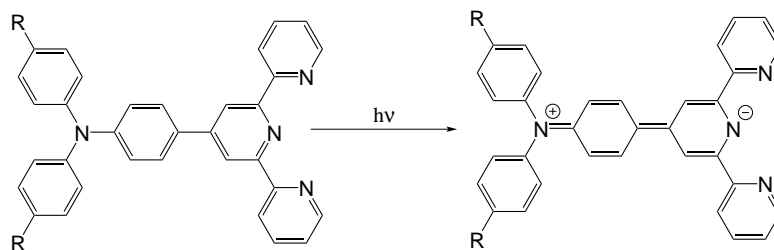


Figure 3.24: Photoluminescence spectrum of $[\text{Cr}(\text{tpy})(\text{F})_3]$ in MeCN ($1 \cdot 10^{-5}$ M). Adding FeSO_4 : 0 eq.: orange, 0.5 eq.: clear blue - dotted, 1.0 eq.: clear blue, 2.0 eq.: purple, 3.0 eq.: green, 4.0 eq.: red, 5.0 eq.: dark blue.

3.5 Complexes containing 4'-diphenylaniline terpyridine ligands

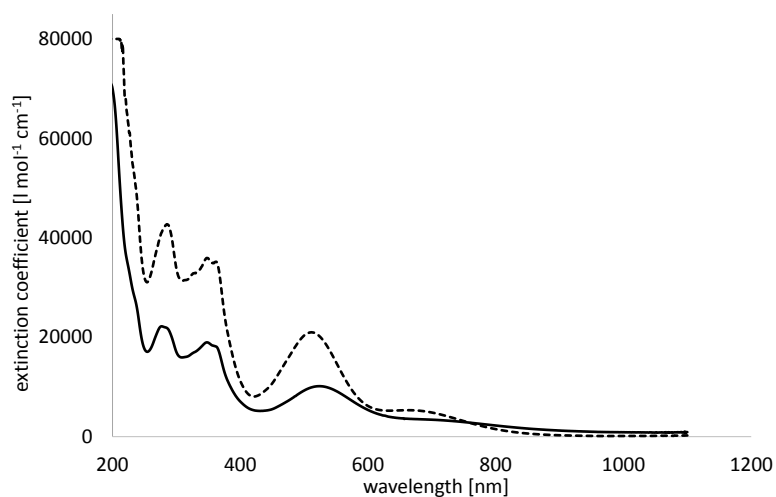
3.5.1 Absorption spectroscopy

All synthesised $\{\text{Cr}(\text{tpy})_2\}^{3+}$ complexes containing one of the 4'-diphenylaniline tpy ligands LT5 or LT6 (scheme 3.7) have a dark red colour. The broad absorption in the visible range (figure 3.25) is assigned to the intra-molecular charge transfer in the 4'-diphenylaniline tpy (scheme 3.7), where the tertiary amine acts as electron donor and the pyridyl nitrogens as electron acceptors.¹³⁶ In the free ligand this charge transfer is expressed as an intense band in the near-UV (figure 3.26). If the ligand coordinates to a metal centre, the coordinated cation serves to stabilize the photo-generated negatively charged tpy fragment. The charge transfer band therefore shifts to lower energies. This effect causes a red shift in the absorption of the complex compared to the free ligands.¹³⁶⁻¹³⁹ This red shift was observed for complexes containing different transition metals (table 3.6).



Scheme 3.7: Intra-molecular charge transfer in ligand LT5 (R = -H) and LT6 (R = -OMe).

a)



b)



Figure 3.25: a) Absorption spectra in aqueous solution of $[\text{Cr}(4'-(4\text{-tolyl})\text{tpy})(\text{LT6})][\text{CF}_3\text{SO}_3]_3$ (dashed line) and $[\text{Cr}(4'-(4\text{-tolyl})\text{tpy})(\text{LT5})][\text{CF}_3\text{SO}_3]_3$ (solid line). b) Picture of the $5 \cdot 10^{-5}$ M aqueous solution of $[\text{Cr}(4'-(4\text{-tolyl})\text{tpy})(\text{LT5})][\text{CF}_3\text{SO}_3]_3$.

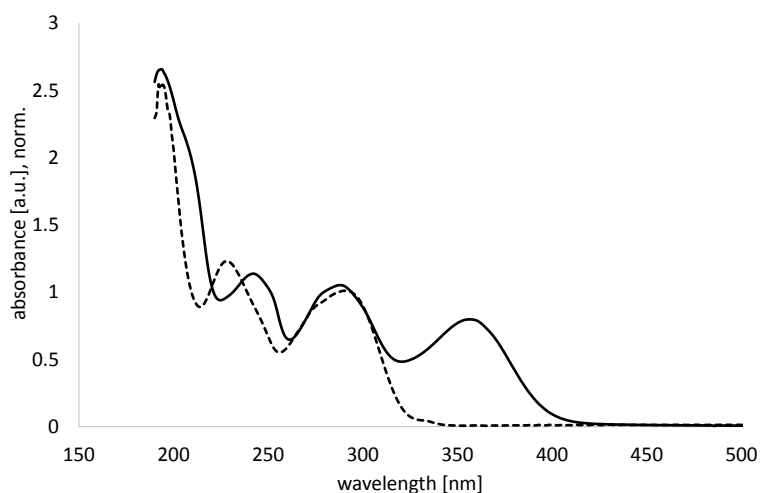


Figure 3.26: Absorption spectra, normalised at 295 nm, of aqueous solutions of LT5 (solid line) and tpy (dashed line).

Table 3.6: Absorption data of various transition metal complexes containing either LT5 or LT6.

complex	solvent	absorption max.	source
[Ru(LT5) ₂][PF ₆] ₂	CH ₂ Cl ₂	288, 356, 405 , 532	<i>Yan et al.</i> ¹⁴⁰
[Ru(tpy)(LT5)][NO ₃] ₂	MeOH	-, 414 , 493	<i>Berlinguette et al.</i> ¹⁴¹
[Ru(LT6) ₂] ^{2+‡}	MeCN	284, 310, 502	<i>Balzani, Sauvage et al.</i> ¹⁴²
[Os(LT6) ₂] ^{2+‡}	MeCN	280, 314, 504 , 672	<i>Balzani, Sauvage et al.</i> ¹⁴²
[Ir(LT5) ₂][PF ₆] ₃	CH ₂ Cl ₂	-, 492	<i>Yellowless, Gareth Williams et al.</i> ¹⁴³
	H ₂ O	-, 494	
	MeCN	253, 288, 321, 493	
[Ir(LT6)(4'-(3,5- ^t Bu ₂ phenyl)tpy)][PF ₆] ₃	MeCN	280, 322, 350, 509*	<i>Flamigni et al.</i> ¹⁴⁴
[Zn(LT5) ₂][PF ₆] ₂	DMF	289, 358, 458*	<i>Cheng et al.</i> ¹⁴⁵
[Zn(LT5) ₂][PF ₆] ₂	MeCN	284, 311 (sh), 325, 407	<i>Constable, Housecroft et al.</i> ³⁸
[Zn(LT6) ₂][PF ₆] ₂	MeCN	283, 313 (sh), 325, 420	<i>Constable, Housecroft et al.</i> ³⁸
[Cd(LT5) ₂][PF ₆] ₂	DMF	277, 359, 450*	<i>Chen et al.</i> ¹⁴⁶
4'-(3,5- ^t Bu ₂ phenyl)tpy:	4'-(3,5-di-tert-butylphenyl)-2,2':6',2''-terpyridine		
‡:	The anions are not defined in the paper.		
*:	Data measured from the reported graph		

3.5.1.1 Negative solvatochromic effect

The $\{\text{Cr}(\text{tpy})_2\}^{3+}$ complexes containing one of the diphenylaniline tpy ligands (LT5 and LT6) show a shift to higher energies in the absorption when dissolved in solvents of increasing polarity. This negative solvatochromism¹⁴⁷ was investigated in detail based on $[\text{Cr}(4'-(4\text{-tolyl})\text{tpy})(\text{LT6})]^{3+}$ (figures 3.27, 3.28 and 3.29). In some solvents a shift to higher energies in the absorption maxima (figure 3.30 a-d) over time is observed, for the investigations of the solvatochromic effect, fresh solutions of these complexes were used (figure 3.31). Whereas the observed shifting is slow in water, MeOH and DMSO, where no change was observable within one hour, it is faster in DMF (figure 3.30d) and essentially completed after 4 h. The absorption maxima shifts are:

in DMSO:	from 519 nm (fresh)	to 488 nm	(after 4 days)
in MeOH:	from 535 nm (fresh)	to 509 nm	(after 4 days)
in water:	from 524 nm (fresh)	to 452 nm	(after 4 days)
in DMF:	from 507 nm (fresh)	to 483 nm	(after 6 hours)

As the $\{\text{Cr}(\text{tpy})_2\}^{3+}$ complexes are not kinetically stable (section 3.2, p. 38) it was assumed that this is also the case here. The measurements of the fresh solutions in MeOH, DMSO and DMF fit a trend line for a dependence of absorption maximum in the visible range on polarity/dipole moment. The position of the absorption maximum in the visible range shows a correlation with the polarity of the solvent. In figure 3.31 the correlations between the absorption maximum and the dipole moment and the polarity index are shown. The only exception to the relationship is water.

Solvatochromic effects were also reported for some of the complexes in the literature (table 3.6). *Flamigni et al.* reported a significant negative solvatochromic effect (CH_2Cl_2 (λ_{max} : 557 nm) to DMSO (λ_{max} : 449 nm)) for the heteroleptic $[\text{Ir}(\text{LT6})(4'-(3,5\text{-}^t\text{Bu}_2\text{phenyl})\text{tpy})][\text{PF}_6]_3$ complex.¹⁴⁴ Whereas *Yellowless, Williams et al.* reported a small effect for the homoleptic complex $[\text{Ir}(\text{LT5})_2][\text{PF}_6]_3$ (table 3.6). They explained this observation with the fact that for the homoleptic complexes with D_{2d} symmetry, there is no dipole moment in the ground state. Therefore the increase of the polarity in the excited state will be small.¹⁴³ This is not consistent with our observations for the homoleptic $[\text{Cr}(\text{LT5})_2][\text{PF}_6]_3$ complex, where we observed a similar solvatochromic effect (CH_2Cl_2 (λ_{max} : 559 nm) to EtOAc (λ_{max} : 507 nm)) as in the heteroleptic complexes.

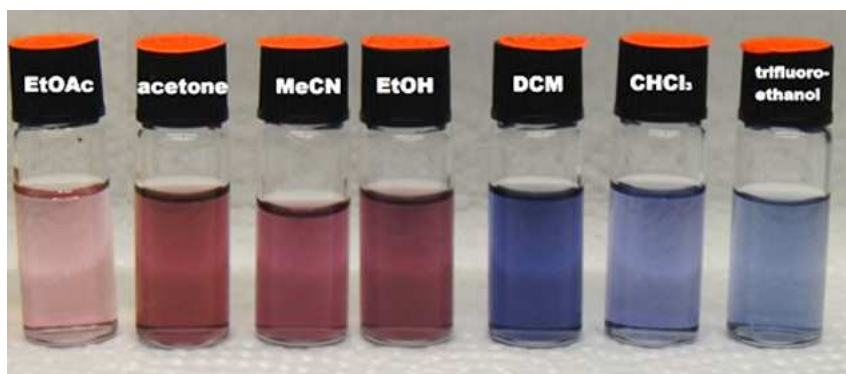


Figure 3.27: Picture of samples containing $[\text{Cr}(4'-(4\text{-tolyl})\text{tpy})(\text{LT6})][\text{CF}_3\text{SO}_3]_3$ in different solvents.

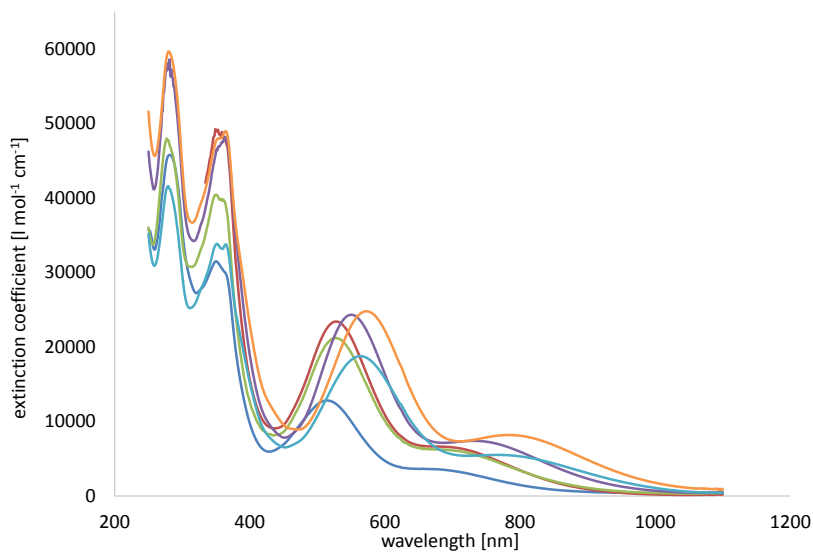


Figure 3.28: UV-VIS spectra of $[\text{Cr}(4'-(4\text{-tolyl})\text{tpy})(\text{LT6})][\text{CF}_3\text{SO}_3]_3$ measured in different solvents. EtOAc (dark blue, 514 nm), MeCN (green, 526 nm), acetone (red, 528 nm), EtOH (purple, 551 nm), CH_2Cl_2 (light blue, 563 nm) and CHCl_3 (orange, 574 nm). In brackets are the absorption maxima in the visible range noted.

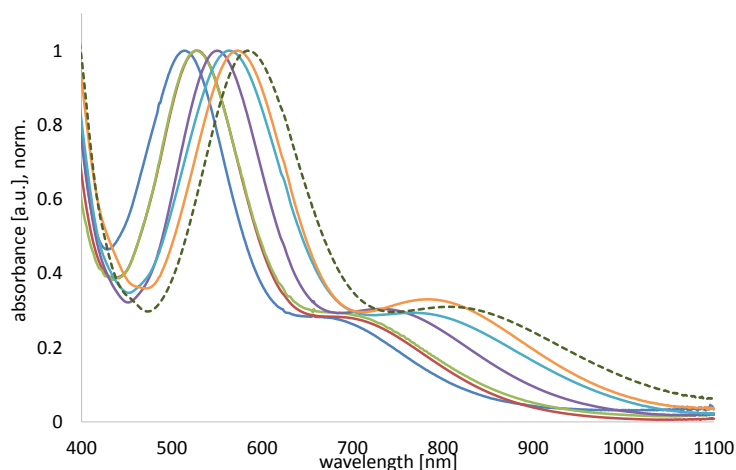


Figure 3.29: Normalised absorption spectra of $[\text{Cr}(4'-(4\text{-tolyl})\text{tpy})(\text{LT6})][\text{CF}_3\text{SO}_3]_3$ measured in different solvents. EtOAc (dark blue, 514 nm), MeCN (green, 526 nm), acetone (red, 528 nm), EtOH (purple, 551 nm), CH_2Cl_2 (light blue, 563 nm), CHCl_3 (orange, 574 nm) and $\text{CF}_3\text{CH}_2\text{OH}$ (green, dashed, 584 nm). In brackets are the absorption maxima in the visible range noted.

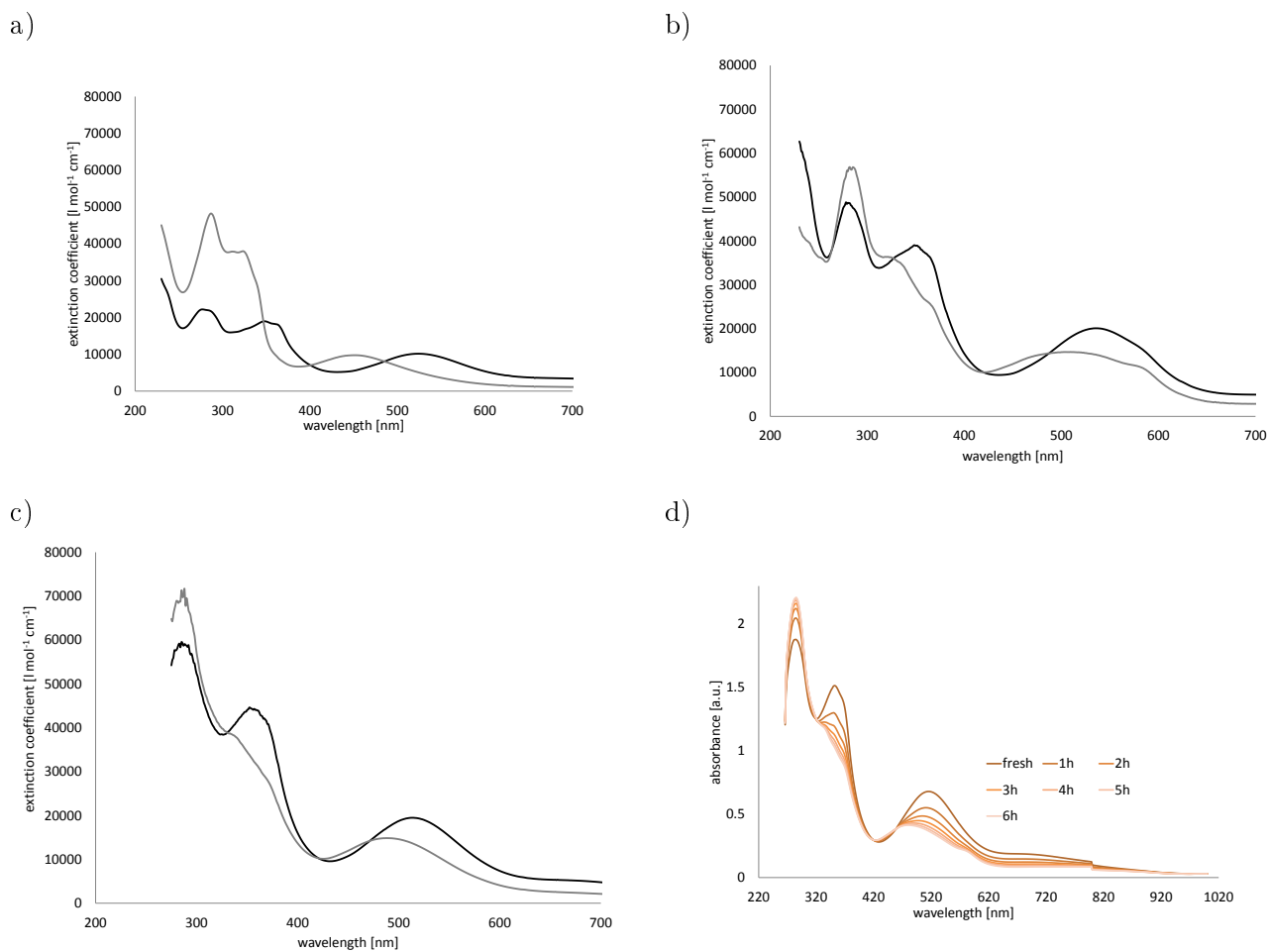


Figure 3.30: UV-VIS spectra of $5 \cdot 10^{-5}$ M solutions of $[\text{Cr}(4'-(4\text{-tolyl})\text{tpy})(\text{LT6})][\text{CF}_3\text{SO}_3]_3$ in water (a), MeOH (b), DMSO (c) and DMF (d). In a - c, the black line is for a fresh sample and the grey line is the measurement after 4 days. In d, the change of the absorption spectrum within 6 hours is shown.

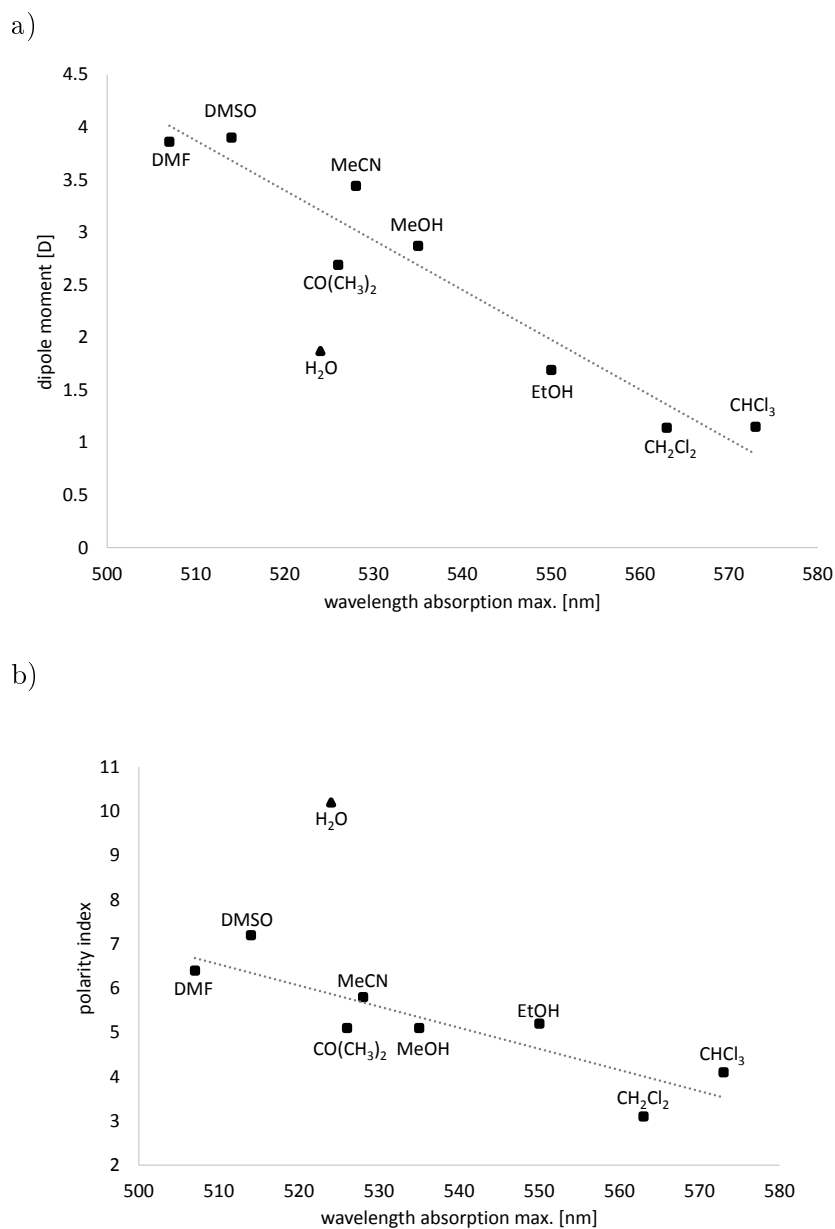


Figure 3.31: Correlations between the absorption maxima of $[\text{Cr}(4'-(4\text{-tolyl})\text{tpy})(\text{LT6})][\text{CF}_3\text{SO}_3]_3$ in the visible range and the dipole moment (a) and the polarity index (b) of the particular solvent. The coefficient of determination for the linear regressions are: 0.928 (for a) and 0.754 (for b). Water was excluded in both cases for the calculation of the coefficient of determination. Source for the solvent properties: *High Purity Solvent Guide*.¹⁴⁸

3.5.2 Photoluminescence measurements

As the emission maximum of an aqueous solution containing $[\text{Cr}(4'-(4\text{-tolyl})\text{tpy})(\text{LT5})][\text{CF}_3\text{SO}_3]_3$ is significantly different from an MeCN solution of the same complex, a titration was performed. To an MeCN solution of $[\text{Cr}(4'-(4\text{-tolyl})\text{tpy})(\text{LT5})][\text{CF}_3\text{SO}_3]_3$ water was added in small amounts (figure 3.32). A decrease in intensity of the emission band at 473 nm, which was also observed in pure MeCN, and an increasing of intensity of the emission band at around 415 nm was observed. This corresponds to the emission wavelength which was observed in pure water. The decrease in the emission intensity is fast at the beginning, and after the addition of around 5% of water the decay slows down. But the decrease in the band at 473 nm is basically finished before the intensity of the band at 415 nm starts increasing substantially. Whereas no changes were observed in the UV-VIS spectra (figure 3.34).

The corresponding homoleptic complexes $[\text{Cr}(4'-(4\text{-tolyl})\text{tpy})_2][\text{CF}_3\text{SO}_3]_3$ (figure 3.33a) and $[\text{Cr}(\text{LT5})_2][\text{CF}_3\text{SO}_3]_3$ (figure 3.33b) always showed one of the two emissions observed in the heteroleptic complex ($[\text{Cr}(4'-(4\text{-tolyl})\text{tpy})(\text{LT5})][\text{CF}_3\text{SO}_3]_3$, figure 3.32). The intensity of the emission band at 470 nm decreases when water is added to a MeCN solution of $[\text{Cr}(\text{LT5})_2][\text{CF}_3\text{SO}_3]_3$ and analogously for $[\text{Cr}(4'-(4\text{-tolyl})\text{tpy})_2][\text{CF}_3\text{SO}_3]_3$ the emission at around 420 nm increases when water is added.

In a similar experiment water was added to a MeCN solution ($1 \cdot 10^{-5}$ M) of $[\text{Cr}(\text{tpy})_2][\text{PF}_6]_3$ (figure 3.36). An approximately linear increase in the emission intensity at 352 nm was observed. Upon adding an aqueous FeSO_4 solution ($5 \cdot 10^{-4}$ M), a comparable increase of the emission intensity was observed until 0.5 eq. of the FeSO_4 had been added. Then a remarkable decrease of the intensity was observed (figure 3.36). A possible explanation is the formation of an emitting $\{\text{Cr}(\text{tpy})\text{X}_3\}$ and a subsequent trapping of the free ligand by the Fe^{2+} ions. After the addition of 0.5 eq., all free ligand is trapped, therefore the Fe^{2+} ions start to decompose the postulated $\{\text{Cr}(\text{tpy})\text{X}_3\}$ complex. The consequence is a decreasing in the emission intensity.

The two free ligands 4'-(4-tolyl)tpy and LT5 express a quite different emission maximum when excited at 280 nm (figure 3.35). The emission maxima for the free ligands are not consistent with those observed for the complex $[\text{Cr}(4'-(4\text{-tolyl})\text{tpy})(\text{LT5})][\text{CF}_3\text{SO}_3]_3$. When water was added to a MeCN solution of the free ligand 4'-(4-tolyl)tpy no change in the intensity of the emission was observed. However when the same was done with a MeCN solution of LT5 (free ligand), an increasing of the band was observed (figure 3.37), as with the complex. The same emission bands as reported above were also measured if the complexes were excited at 340 nm. Excitation in the lower energy visible absorbing band resulted in no emission.

Similar effects were also observed with several solvent mixtures, and likewise with $[\text{Cr}(4'-(4\text{-tolyl})\text{tpy})(\text{LT6})][\text{CF}_3\text{SO}_3]_3$. They are summarised in table 3.7.

Table 3.7: Overview of a series of measurements with $[\text{Cr}(\text{LT6})_2][\text{CF}_3\text{SO}_3]_3$ where the composition of the solvent was changed.

	solvent	added solvent:	shift λ_{max}^{em} [nm]	excitation λ^{ex} [nm]
I	MeCN	$\text{CF}_3\text{CH}_2\text{OH}$	597 \rightarrow 422	350
II	CH_2Cl_2	$\text{CF}_3\text{CH}_2\text{OH}$	515 \rightarrow quenched	350
III	DMSO	H_2O	588 \rightarrow 394	340
IV	CHCl_3	$\text{CF}_3\text{CH}_2\text{OH}$	505 \rightarrow 429	360
V	DMF	$\text{CF}_3\text{CH}_2\text{OH}$	600 \rightarrow 441	360

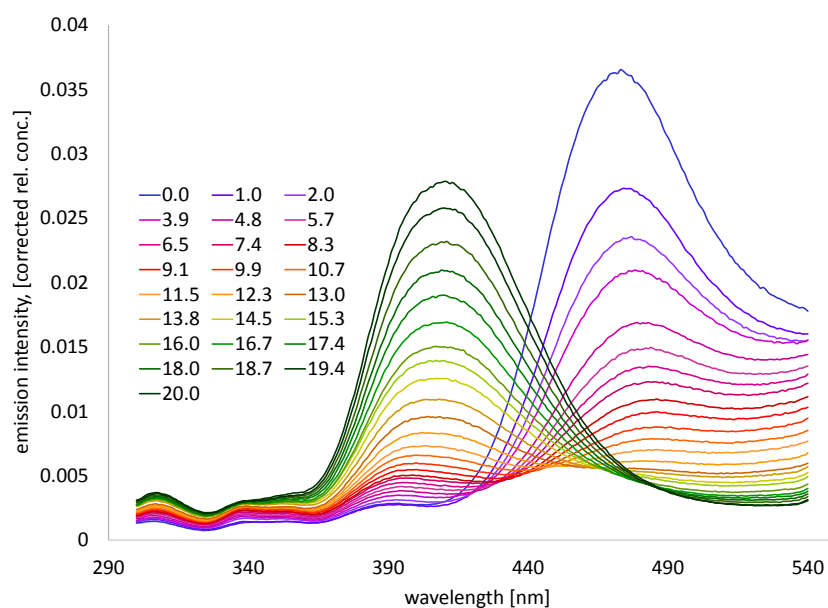


Figure 3.32: Emission spectrum of $[\text{Cr}(4'-(4\text{-tolyl})\text{tpy})(\text{LT5})][\text{CF}_3\text{SO}_3]_3$ in MeCN adding water, when excited at 280 nm. The numbers in the key correspond to the amount of water in percent.

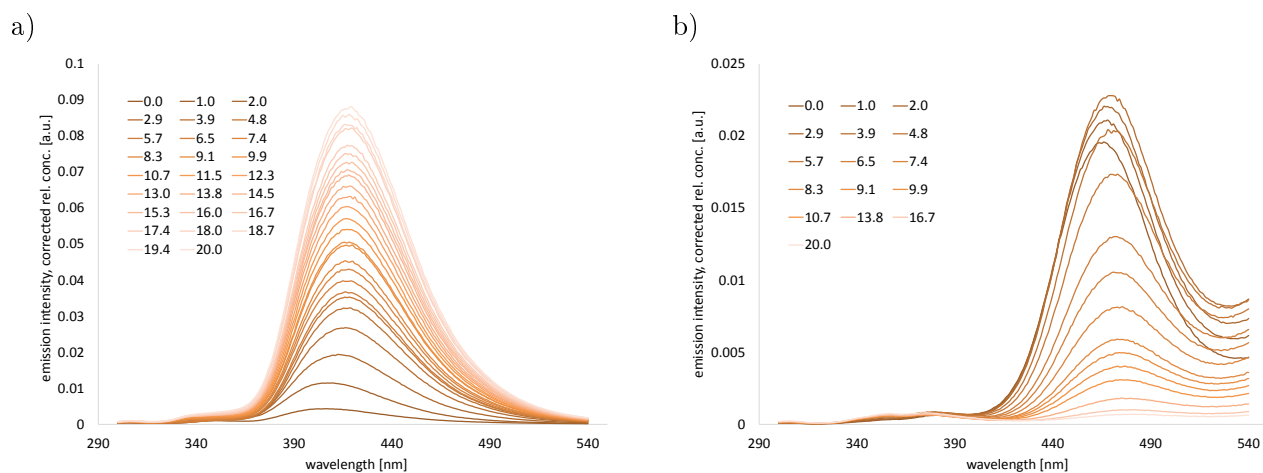


Figure 3.33: Emission spectra of $[\text{Cr}(4'-(4\text{-tolyl})\text{tpy})_2][\text{CF}_3\text{SO}_3]_3$ (a) and $[\text{Cr}(\text{LT5})_2][\text{CF}_3\text{SO}_3]_3$ (b) in MeCN upon the addition of water, when excited at 280 nm. The numbers in the key correspond to the amount of water in percent by volume.

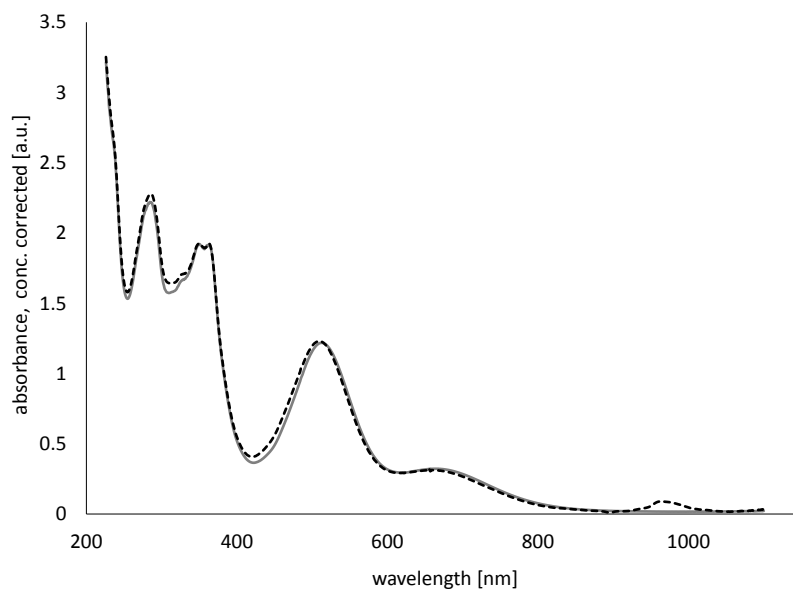


Figure 3.34: UV-VIS spectra of $[\text{Cr}(4'-(4\text{-tolyl})\text{tpy})(\text{LT5})][\text{CF}_3\text{SO}_3]_3$ in MeCN. The spectra were recorded before (grey, solid line) and after (black, dashed line) the addition of 20 % water by volume.

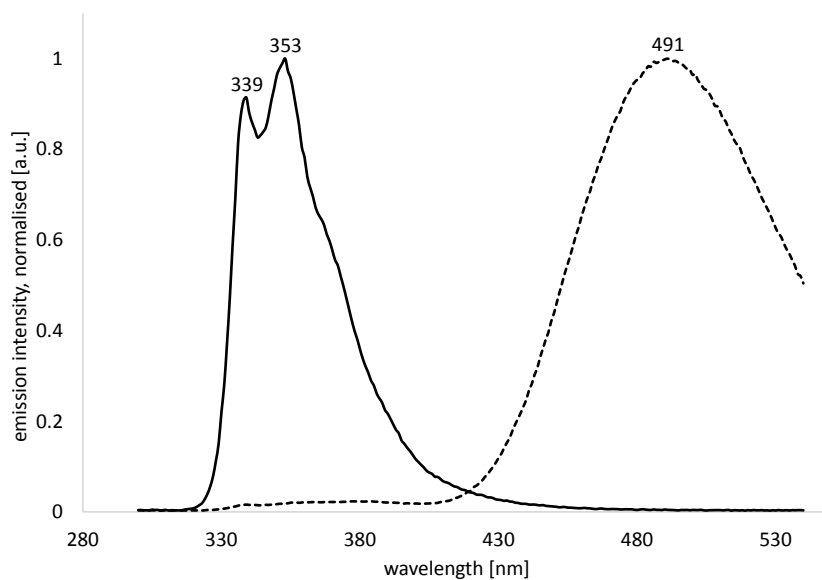


Figure 3.35: Photoluminescence spectra of 4'-(4-tolyl)tpy (solid line) and LT5 (dashed line) in MeCN, excited at 280 nm.

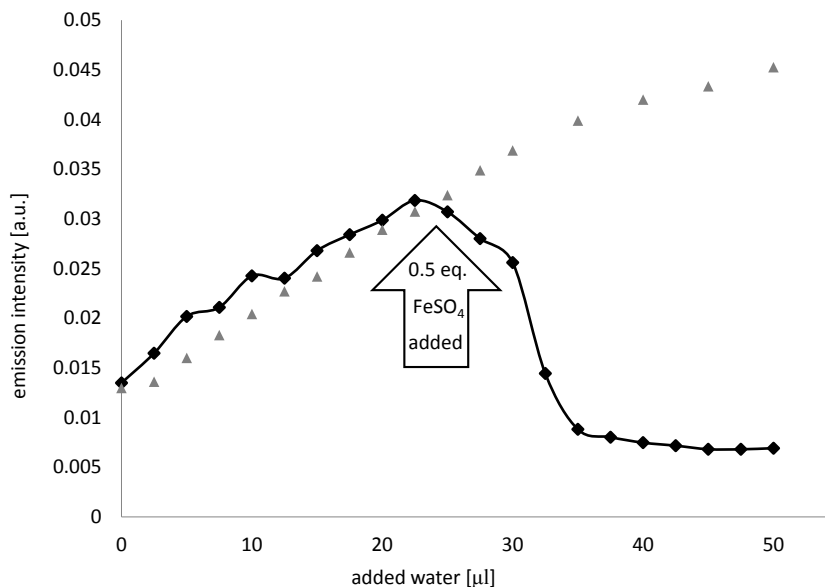


Figure 3.36: Emission intensity at 352 nm of $[\text{Cr}(\text{tpy})_2][\text{PF}_6]_3$ (in MeCN, $1 \cdot 10^{-5}$ M) plotted against amount of water added; 25 μl correspond to 1 % water in MeCN. The grey triangles represent pure water addition, and the black squares the addition of a $5 \cdot 10^{-4}$ M aqueous solution of FeSO_4 .

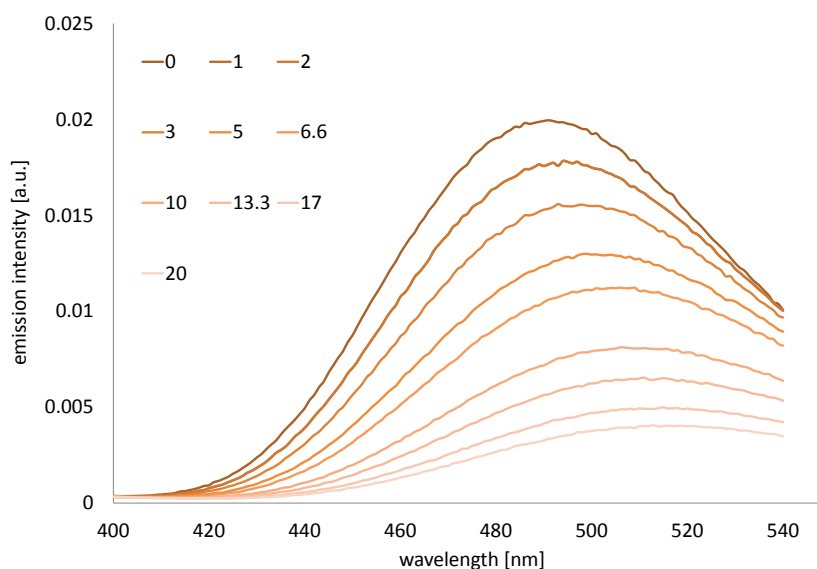


Figure 3.37: Photoluminescence spectrum of LT5 in MeCN adding water, when excited at 280 nm. The numbers in the key correspond to the amount of water in percent by volume.

As shown in table 3.7, the emission maxima depend on the solvent. In figure 3.38 the emission maxima in pure solvents are plotted against the dipole moment (a) and the polarity (b) of the solvents. As already observed for the solvatochromic effect in the absorption spectra (figure 3.31), an approximately linear correlation is observed with exception of the point for water. The emission maxima for the free ligand (LT6) also depend on solvent. The emission maxima were 565 nm in MeCN ($\lambda_{ex} = 350$ nm) and 523 nm in CHCl_3 ($\lambda_{ex} = 360$ nm). The emissions measured for the complex containing solution (λ_{em}^{max} : 597 nm (MeCN) and 505 nm (CHCl_3)) are therefore not identical to those for the free ligand.

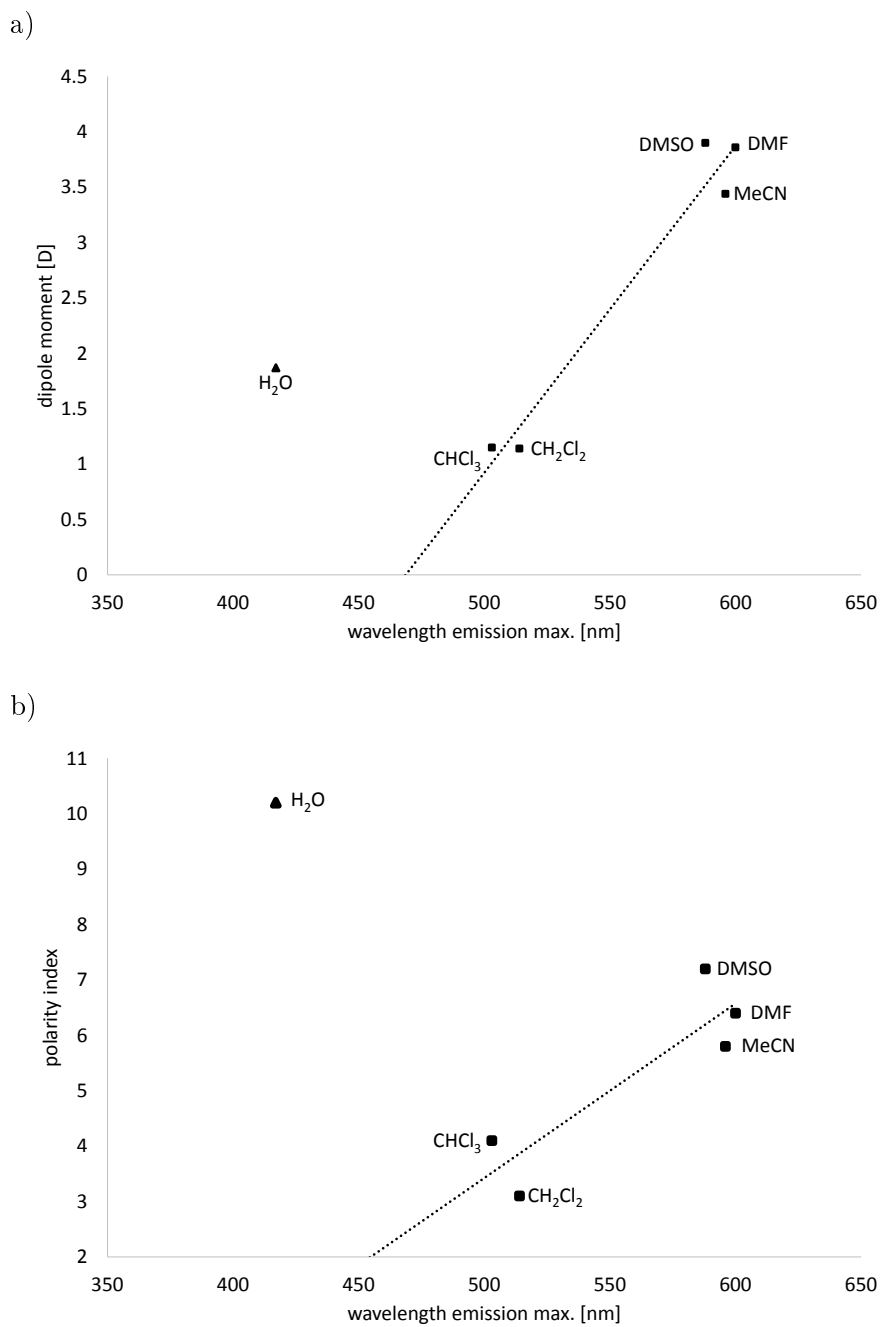


Figure 3.38: Correlations between the emission maxima of $[\text{Cr}(4'-(4\text{-tolyl})\text{tpy})(\text{LT6})][\text{CF}_3\text{SO}_3]_3$ and the dipole moment (a) and the polarity index (b) of the particular solvent. The coefficient of determination for the linear regressions are: 0.963 (for a) and 0.790 (for b). Water was excluded in both cases for the calculation of the coefficient of determination. Source for the solvent properties: *High Purity Solvent Guide*.¹⁴⁸

3.6 Electrochemical measurements

The electrochemical processes of some of the $\{\text{Cr}(\text{tpy})_2\}^{3+}$ complexes were studied using cyclic voltammetry techniques. Each complex showed three reversible redox processes (table 3.8, figures 3.39, 3.40 and 3.41). The fourth reversible reduction and two irreversible reductions mentioned in the literature^{52,118,149} were not observed for all complexes (figure 3.43). Whereas the potentials for $E_{1/2}^{3+/2+}$, $E_{1/2}^{2+/1+}$ and $E_{1/2}^{1+/0}$ are at comparable values to those of the $\{\text{Cr}[\text{bpy}]_3\}^{3+}$ complexes (2.4, p. 24), the $E_{1/2}^{0/1-}$ reduction occurs at a significantly more negative potential. The difference between the potentials $E_{1/2}^{1+/0}$ and $E_{1/2}^{0/1-}$ is around 1 V, between the three higher reduction potentials only around 0.5 V. The influence of the substitution on tpy is negligible. The results are consistent with those in the literature for $[\text{Cr}(\text{tpy})_2][\text{ClO}_4]_3$ ^{51,52,118,132} and $[\text{Cr}(4'-(4\text{-tolyl})\text{tpy})_2][\text{ClO}_4]_3$.⁵¹

Table 3.8: Cyclic voltammetric data for $\{\text{Cr}(\text{tpy})_2\}^{3+}$ complexes. Measured in MeCN with $[\text{nBu}_4\text{N}][\text{PF}_6]$ as supporting electrolyte and a scan rate of 0.1 V s^{-1} . Referenced to Fc/Fc^+ .

compound	reductions [V]				oxidation [V]
	$E_{1/2}^{3+/2+}$	$E_{1/2}^{2+/1+}$	$E_{1/2}^{1+/0}$	$E_{1/2}^{0/1-}$	$E_{1/2}^{3+/4+}$
$[\text{Cr}(\text{tpy})_2][\text{PF}_6]_3$	-0.533	-0.953	-1.469	-2.388	-
$[\text{Cr}(4'-(4\text{-tolyl})\text{tpy})_2][\text{CF}_3\text{SO}_3]_3$	-0.581	-0.949	-1.278		-
$[\text{Cr}(\text{LT}5)_2][\text{CF}_3\text{SO}_3]_3$	-0.601	-0.955	-1.431	-2.341	0.683
$[\text{Cr}(\text{tpy})(4'-(4\text{-tolyl})\text{tpy})][\text{PF}_6]_3$	-0.544	-0.946	-1.463	-2.367	-
$[\text{Cr}(\text{tpy})(5,5''\text{-Me}_2\text{tpy})][\text{PF}_6]_3$	-0.537	-0.957	-1.457	-2.338	-
$[\text{Cr}(\text{tpy})(\text{HLT}11)][\text{PF}_6]_4$	-0.400	-0.855	-1.338		-
$[\text{Cr}(4'-(4\text{-tolyl})\text{tpy})(\text{LT}4)][\text{PF}_6]_3$	-0.599	-1.095	-1.583		-
$[\text{Cr}(4'-(4\text{-tolyl})\text{tpy})(\text{LT}5)][\text{CF}_3\text{SO}_3]_3$	-0.587	-0.955	-1.276	-2.343	0.660
$[\text{Cr}(\text{tpy})(\text{LT}6)][\text{CF}_3\text{SO}_3]_3$	-0.601	-0.938	-1.254		*
$[\text{Cr}(\text{LT}5)(\text{LT}10)][\text{CF}_3\text{SO}_3]_3$	-0.507	-0.880	-1.393		0.547

*: This complex exhibits two oxidation potentials at 0.382 and 0.933 V

One exception is the protonated complex $[\text{Cr}(\text{tpy})(\text{HLT}11)][\text{PF}_6]_4$ (figure 3.44) which shows broad peaks in the cyclic voltammogram. In the square wave measurement, always two serried signals were observed. We explained that with slightly different reduction potentials for the two different ligands, as was reported for similar $\{\text{Cr}[\text{bpy}]_3\}^{3+}$ complexes (2.4, p. 24).

Recent results from *Wiegardt et al.*⁵² indicate that all redox processes are ligand based and chromium remains in the 3+ oxidation state (table 3.9). The study is based on X-ray, magnetic susceptibility and X-band EPR results for the complex $[\text{Cr}(\text{tpy})_2][\text{PF}_6]_3$ in its four oxidation states. This stands in contrast to the common explanation in several publications^{51,118,121,122,132} that the first reduction forms the low-spin Cr(II) complex. We have not confirmed whether this formulation will also hold for the complexes with substituted tpy ligands.

The complexes containing *N,N*-diphenylaniline tpy ligands also show reversible oxidation processes (table 3.8, figures 3.40, 3.41 and 3.42). These processes are also ligand based and correspond to the data obtained for the free ligands. The oxidation potentials for the free ligands

were 0.917 V for LT5 and 0.402 and 0.984 for LT6 (measured in MeCN with respect to Fc/Fc⁺ and [ⁿBu₄N][PF₆] as supporting electrolyte at a scan rate of 0.1 V s⁻¹.)

Table 3.9: The composition of {Cr(tpy)₂}ⁿ (n = 3+, 2+, 1+ and 0) according to *Wieghardt et al.*⁵²

3+	2+	1+	0
$[\text{Cr}^{III}(\text{tpy}^0)_2][\text{PF}_6]_3$	$[\text{Cr}^{III}(\text{tpy}^\bullet)(\text{tpy}^0)][\text{PF}_6]_2$	$[\text{Cr}^{III}(\text{tpy}^\bullet)_2][\text{PF}_6]$	$[\text{Cr}^{III}(\text{tpy}^\bullet)(\text{tpy}^{\bullet\bullet})]$
S = 3/2	S = 1	S = 1/2	S = 0

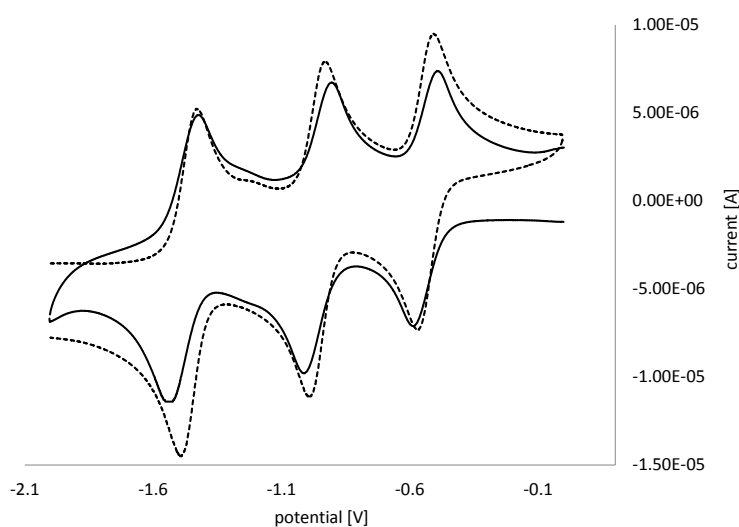


Figure 3.39: Cyclic voltammograms for [Cr(tpy)₂][PF₆]₃ (solid line) and [Cr(tpy)(5,5''-Me₂tpy)][PF₆]₃ (dotted line). Measured in MeCN solution with respect to Fc/Fc⁺ and [ⁿBu₄N][PF₆] as supporting electrolyte at a scan rate of 0.1 V s⁻¹.

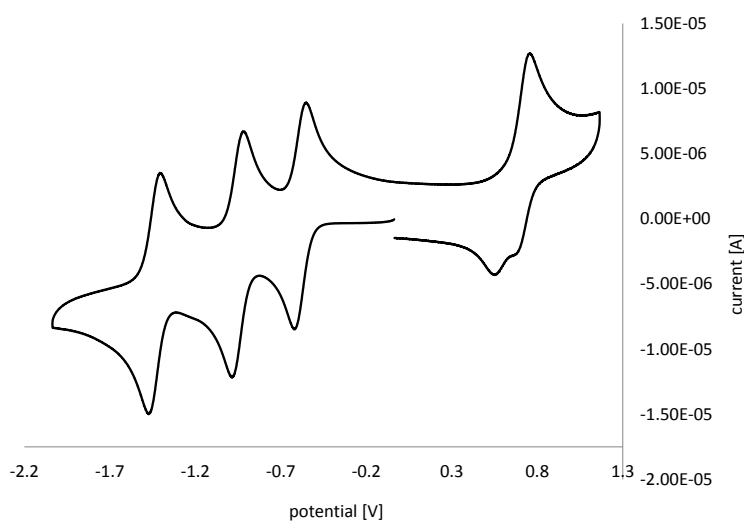


Figure 3.40: Cyclic voltammogram for $[\text{Cr}(4'-(4\text{-tolyl})\text{tpy})(\text{LT5})][\text{CF}_3\text{SO}_3]_3$. With respect to Fc/Fc^+ , measured in MeCN solution with $[\text{nBu}_4\text{N}][\text{PF}_6]$ as supporting electrolyte and a scan rate of 0.1 V s^{-1} .

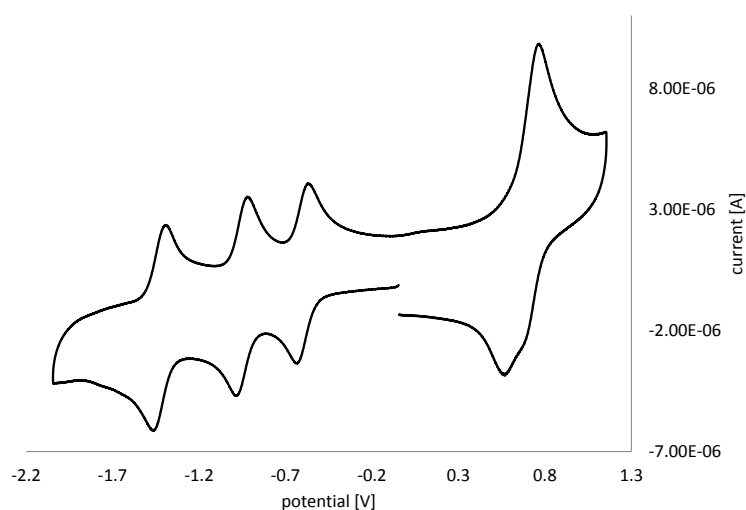


Figure 3.41: Cyclic voltammogram for $[\text{Cr}(\text{LT5})_2][\text{CF}_3\text{SO}_3]_3$. Measured in MeCN with respect to Fc/Fc^+ and $[\text{nBu}_4\text{N}][\text{PF}_6]$ as supporting electrolyte at a scan rate of 0.1 V s^{-1} .

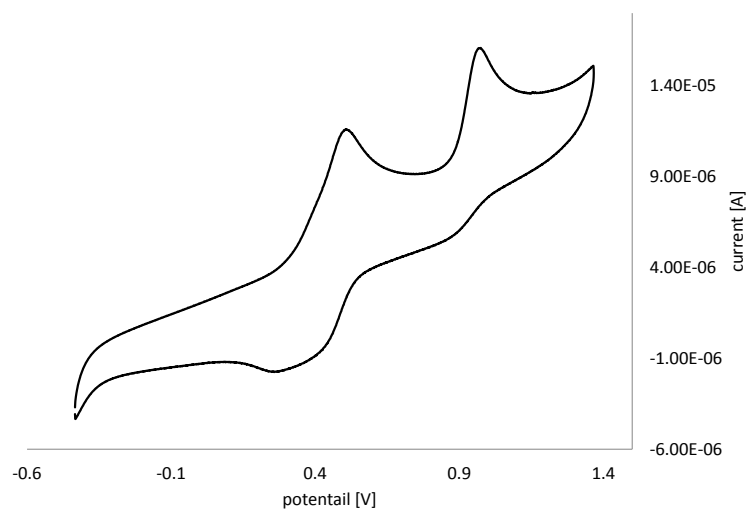


Figure 3.42: Cyclic voltammogram of the oxidation processes for [Cr(tpy)(LT6)][CF₃SO₃]₃. Measured in MeCN with respect to Fc/Fc⁺ and [nBu₄N][PF₆] as supporting electrolyte at a scan rate of 0.1 V s⁻¹.

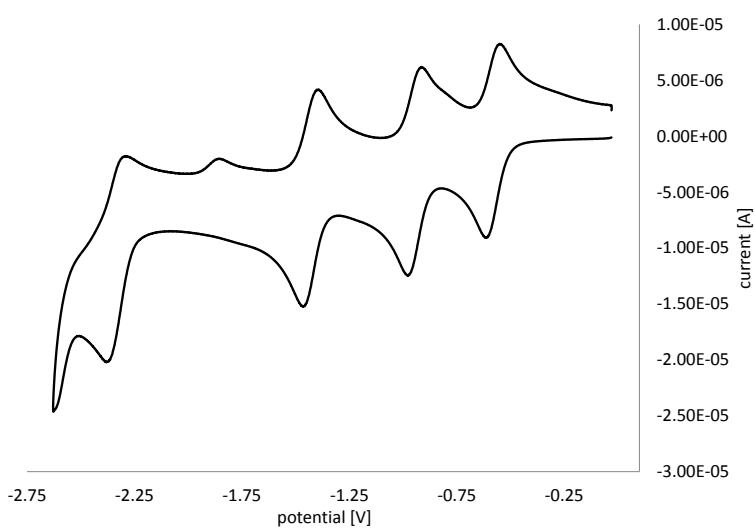


Figure 3.43: Cyclic voltammogram of the four reversible reduction processes for [Cr(4'-(4-tolyl)tpy)(LT5)][CF₃SO₃]₃. Measured in MeCN with respect to Fc/Fc⁺ and [nBu₄N][PF₆] as supporting electrolyte at a scan rate of 0.1 V s⁻¹.

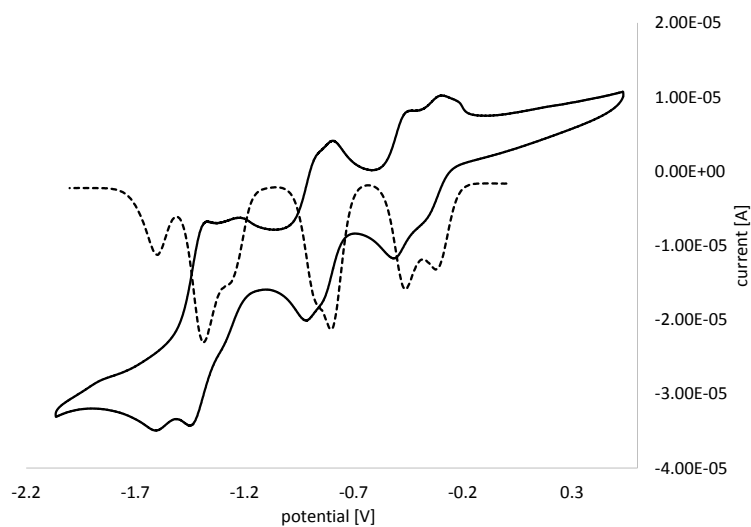


Figure 3.44: Cyclic voltammogram (solid line) and square wave (dashed line) of the reduction processes for $[\text{Cr}(\text{tpy})(\text{HLT11})][\text{PF}_6]_4$. Measured in MeCN with respect to Fc/Fc^+ and $[\text{nBu}_4\text{N}][\text{PF}_6]$ as supporting electrolyte at a scan rate of 0.1 V s^{-1} .

3.7 EPR measurements

Since chromium(III) compounds (d^3) are paramagnetic ($S = 3/2$), electron paramagnetic resonance (EPR) spectroscopy provides an additional analytical method. This work was carried out in collaboration with *Prof. Dr. Cornelia Palivan* (Department of Chemistry, University of Basel). Figure 3.45 shows the EPR measurements of the pure powder samples of $[\text{Cr}(\text{tpy})_2][\text{PF}_6]_3$ and $[\text{Cr}(\text{tpy})(5,5''\text{-Me}_2\text{tpy})][\text{PF}_6]_3$. The obtained signals are broad, but comparable with the spectrum reported in the literature for $[\text{Cr}(\text{tpy})_2][\text{PF}_6]_3$.¹⁵⁰

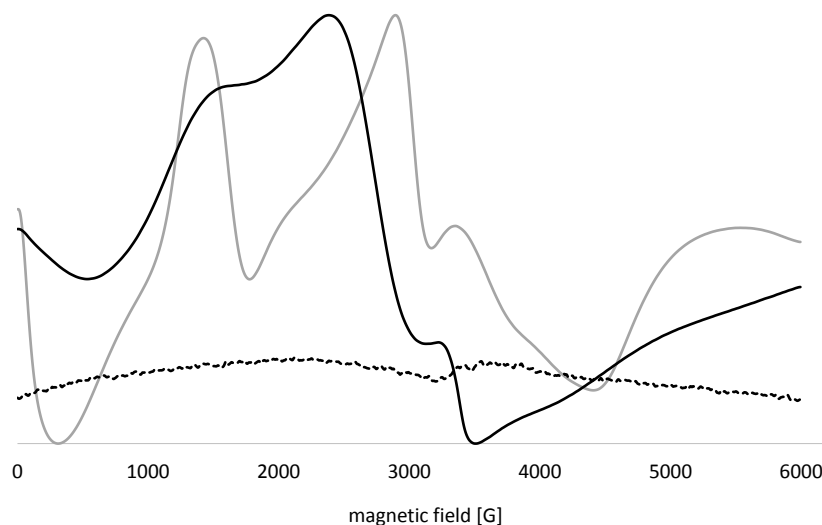


Figure 3.45: EPR spectra (at 295 K and 10 mW microwave power, conversion time 61.12 ms), of powder samples of $[\text{Cr}(\text{tpy})_2][\text{PF}_6]_3$ (black solid line), $[\text{Cr}(\text{tpy})(5,5''\text{-Me}_2\text{tpy})][\text{PF}_6]_3$ (grey solid line) and $[\text{Co}(\text{tpy})_2][\text{PF}_6]_3$ (black dashed line).

With the objective of obtaining a fine splitting of the spectra, magnetically diluted samples were made. Therefore the corresponding cobalt(III) complexes (diamagnetic, and hence EPR silent) were synthesised (4.1, p. 95). In a first attempt, the homoleptic $[\text{Co}(\text{tpy})_2]^{3+}$ complex was used to dilute both heteroleptic and homoleptic $\{\text{Cr}(\text{tpy})_2\}^{3+}$ complex samples. The magnetically diluted samples were prepared by dissolving the chromium(III) and cobalt(III) complexes in the same solvent, followed by 5 minutes stirring and then slow evaporation. The EPR spectrum of the powder mixture was then measured.¹⁵⁰ Figure 3.46 shows the EPR spectrum for the magnetically diluted samples of $[\text{Cr}(\text{tpy})_2][\text{PF}_6]_3$ and $[\text{Cr}(\text{tpy})(5,5''\text{-Me}_2\text{tpy})][\text{PF}_6]_3$. $[\text{Co}(\text{tpy})_2][\text{PF}_6]_3$ was doped with 2 % of $\{\text{Cr}(\text{tpy})_2\}^{3+}$. Although the signals are better resolved, attempts to simulate the spectra were not possible. An assumed problem was that the mixtures were not homogeneous; the different solubilities of the two complexes ($\{\text{Cr}(\text{tpy})_2\}^{3+}$ and $[\text{Co}(\text{tpy})_2]^{3+}$) could be the reason for this. Therefore several attempts with different solvents (MeCN, $(\text{CH}_3)_2\text{CO}$, DMF and water) and different percentages of the chromium(III) complex were made but were unsuccessful.

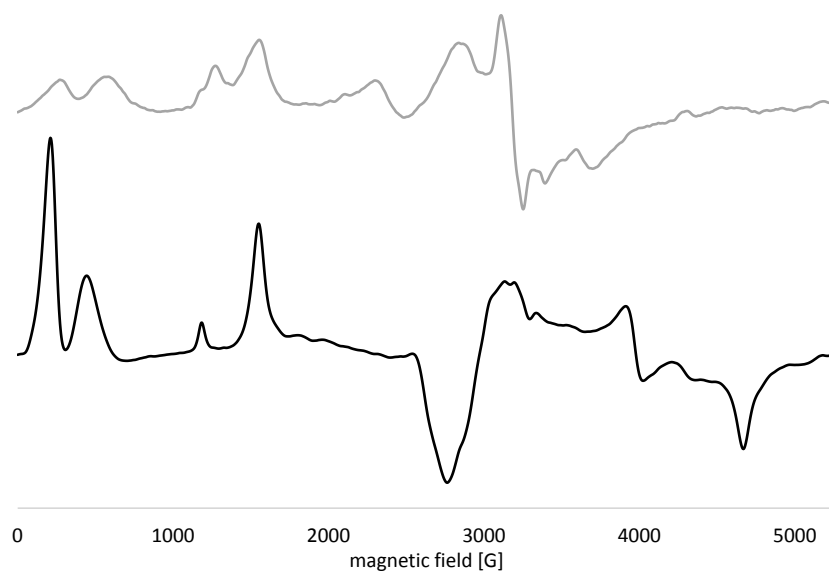


Figure 3.46: EPR spectra (at 295 K and 10 mW microwave power, conversion time 61.12 ms) of magnetically diluted powder samples of 2 % [Cr(tpy)₂][PF₆]₃ in [Co(tpy)₂][PF₆]₃ (black line) and 2 % [Cr(tpy)(5,5''-Me₂tpy)][PF₆]₃ in [Co(tpy)₂][PF₆]₃ (grey line).

3.8 DSC trials with bis(terpyridine)chromium(III) complexes

To the best of our knowledge no examples of chromium(III) complexes as dyes in DSCs (dye-sensitised solar cells) were known to date. However, *Waltz* and *Lilie* already mentioned in 1983 the possible potential of $\{\text{Cr}(\text{bpy})_3\}^{3+}$ for solar energy conversion.⁶¹ *Damrauer* and *Shores* investigated the photophysical properties of the heteroleptic $[\text{Cr}(\text{bpy})_2(4\text{-dmc})][\text{BF}_4]_3$ (4-dmc = dimethyl [2,2'-bipyridine]-4,4'-dicarboxylate) as a potential sensitizer in DSC devices. They evaluated the strongly oxidizing excited state found for the reported complex combined with the long lifetime of the excited state as promising premises for an application in DSCs, whereby no DSC results were reported.⁶²

Chromium compounds are used as a dopant in TiO_2 .^{151,152} Further *Taghavinia et. al* recently reported a Cr-Pt counter electrode, as an alternative to the platinum coated ITO (indium tin oxide) or FTO (fluorine doped tin oxide) counter electrode. The Cr-Pt counter electrode consists of a chromium coating (cube-like morphology) as a rough coating which provides high surface for electro-deposited platinum.¹⁵³

3.8.1 Dye-sensitized solar cell trials

The broad absorption of $[\text{Cr}(4'-(4\text{-tolyl})\text{tpy})(\text{LT5})][\text{CF}_3\text{SO}_3]_3$ (figure 3.25, p. 53) and a HOMO - LUMO gap of 1.2 eV (from electrochemistry in MeCN (3.6, p. 59) and 1.5 eV (from absorption measurements in MeCN) made the complexes with diphenylaniline terpyridine ligands strong candidates for DSC applications. Since the dye has to be closely adsorbed on the surface of the semiconductor for a workable and efficient DSC,^{68,154} a complex with an anchoring ligand had to be synthesised. Since carboxylic acid is the standard anchoring group for sensitizers⁶⁸ 4-([2,2':6',2''-terpyridin]-4'-yl)phthalic acid (LT10) was chosen as anchoring ligand and $[\text{Cr}(\text{LT5})(\text{LT10})][\text{CF}_3\text{SO}_3]_3$ synthesised (figure 3.47 and 6.4.3.22, p. 140).

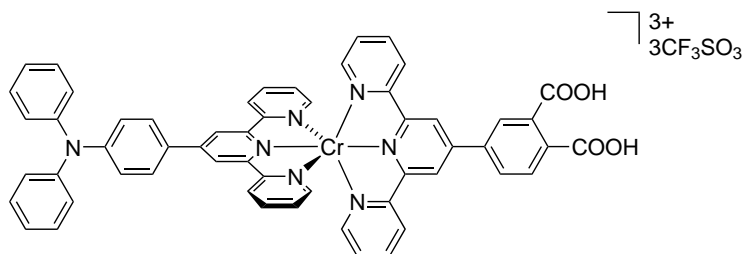


Figure 3.47: Structure of $[\text{Cr}(\text{LT5})(\text{LT10})][\text{CF}_3\text{SO}_3]_3$.

3.8.2 DSC fabrication and characterisation

The DSCs were prepared using an adapted method of *Grätzel et al.*¹⁵⁵ As photoanode commercial *Test Cell Titania Electrodes* from *Solaronix* were used. The electrodes were first rinsed with EtOH, then sintered for 30 min at 450 °C and cooled to around 80 °C. Then the electrodes were immersed into a dye solution (for details compare: table 3.10). The electrodes were then rinsed with the solvent in which they had been dipped and EtOH. Also a reference cell was prepared applying the procedure described above and using commercial N719¹⁵⁶ from *Solaronix*. Commercial *Test Cell Platinum Electrodes* from *Solaronix* were used as counter electrodes, after heating them for 30 min at 450 °C. The two electrodes were assembled using a thermoplastic hot-melt sealing foil (*Test Cell Gaskets* from *Solaronix*) by pressing them together while heating. Two different electrolytes based on I_2/I_3^- and $\text{Co}^{2+}/\text{Co}^{3+}$ were used (for the compositions

compare table 3.11). The electrolytes were filled into the cells by vacuum backfilling. The hole on the counter electrode was then sealed using the thermoplastic hot-melt sealing foil (*Test Cell Sealings* from *Solaronix*) and a cover glass (*Test Cell Caps* from *Solaronix*). The cells were masked and measured using a SolarSim 150 ($1000 \text{ W m}^{-2} = 1 \text{ sun}$). The power of the simulated light was calibrated using a reference Si cell.

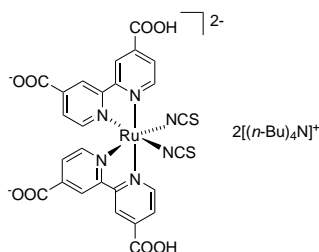


Figure 3.48: Standard dye N719.¹⁵⁶

3.8.3 DSC trials

The parameters of the DSC assembling trials are summarised in table 3.10 and the results listed in table 3.11.

With $[\text{Cr}(\text{LT5})(\text{LT10})][\text{CF}_3\text{SO}_3]_3$ and I_2/I_3^- as electrolyte two sets of two cells each were realised. The electrodes of DSCs-A were dipped for one night in the dye solution, whereas the electrodes for DSCs-B were immersed for 5 days (table 3.10). After the dipping and washing of the anode the TiO_2 layer was coloured dark red, indicating that some of the dye was adsorbed on the TiO_2 . However only a very low short circuit current (*e.g.*: well performing copper(I) complexes: >1 , and N719 >12)³⁹ and open circuit voltage (*e.g.*: well performing copper(I) complexes: >500 , and N719 ~ 750)³⁹ was observed. Also no improvement could be achieved after two and six days respectively. Unfortunately, a precipitation of the electrolyte was observed, in some cells after 1 h.

In an alternative approach (DSC-C) the anode was first dipped in a DMSO solution of the anchoring ligand (LT10) overnight. After washing with DMSO and EtOH, the electrode was immersed for 5 days in a MeCN solution of $[\text{Cr}(\text{LT5})(\text{CF}_3\text{SO}_3)_3]$. The idea in this approach was that the anchoring ligand adsorbs first on the TiO_2 and coordinates in the second step to $[\text{Cr}(\text{LT5})(\text{CF}_3\text{SO}_3)_3]$ and forms $[\text{Cr}(\text{LT5})(\text{LT10})][\text{CF}_3\text{SO}_3]_3$ (scheme 3.8). The pale red coloured TiO_2 layer indicated that some complex was adsorbed on the TiO_2 surface. But the efficiencies were as low as for DSC-A and DSC-B.

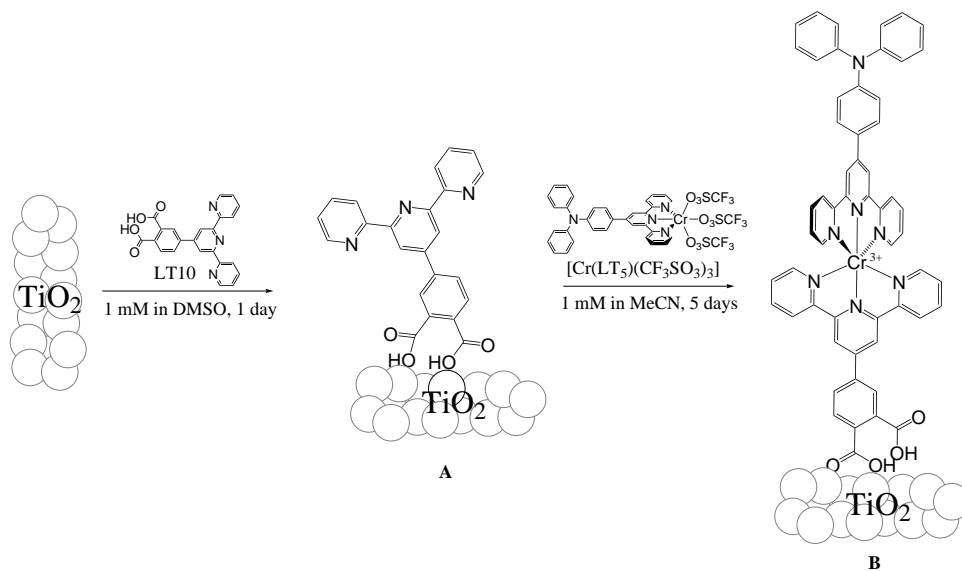
In a further trial the homoleptic $[\text{Cr}(\text{LT5})_2][\text{CF}_3\text{SO}_3]_3$ without anchoring ligand was used as dye. Since the TiO_2 layer was coloured after the dipping an adsorption of the complex occurred. In this approach the efficiencies are even worse.

As a blank measurement (DSC-blank) a cell without a dye, only filled with electrolyte, was measured. For this cell even higher efficiencies were received than for the cells with dye. The standard cell (standard-N719) with the standard dye N719 showed as proof of principle that the cells work.

As mentioned above, a precipitation was observed after a short time in the I_2/I_3^- electrolyte, in the cells containing chromium complexes. In all chromium complex containing cells mentioned above a precipitation in the electrolyte was observed, whereas no precipitation was observed in the cells of the DSC-blank and standard N719 attempts within a week.

But also the two trials with $\text{Co}^{2+}/\text{Co}^{3+}$ as alternative electrolyte (DSC-E and DSC-F) were not successful.

The complex with the anchoring ligand ($[\text{Cr}(\text{LT5})(\text{LT10})][\text{CF}_3\text{SO}_3]_3$) adsorbed on the TiO_2 but no current was generated and the efficiency was therefore very low. Also the other attempts showed very low currents and efficiencies. Since we found that $\{\text{Cr}(\text{tpy})_2\}^{3+}$ complexes are kinetically not inert and are labile in the presence of base and F^- , a decomposition of the complex is a possible reason for the failure of the cells. A further problem could be the precipitation in the electrolyte.



Scheme 3.8: Preparation of the anodes for trial DSC-C: In the first step the free anchoring ligand (LT10) is adsorbed on the TiO_2 surface (**A**). In the second step, the complex $[\text{Cr}(\text{LT5})(\text{LT10})]^{3+}$ is formed directly on the TiO_2 layer (**B**).

Table 3.10: Conditions for the preparation of DSC-A to DSC-F and standard-N719.

trial	electrodes immersed in	electrolyte
DSC-A	0.45 mM MeCN solution of [Cr(LT5)(LT10)](CF ₃ SO ₃) ₃ for 1 night	I ₂ /I ₃ ⁻
DSC-B	0.45 mM MeCN solution of [Cr(LT5)(LT10)](CF ₃ SO ₃) ₃ for 5 days	I ₂ /I ₃ ⁻
DSC-C	step 1: 1 mM DMSO solution of LT10 for 1 night step 2: 1 mM MeCN solution of [Cr(LT5)(CF ₃ SO ₃) ₃] for 5 days	I ₂ /I ₃ ⁻
DSC-D	0.40 mM MeCN solution of [Cr(LT5) ₂](CF ₃ SO ₃) ₃ for 1 night	I ₂ /I ₃ ⁻
DSC-E	0.45 mM MeCN solution [#] of [Cr(LT5)(LT10)](CF ₃ SO ₃) ₃ for 1 night	Co ²⁺ /Co ³⁺
DSC-F	0.60 mM MeCN solution of [Cr(LT5)(LT10)](CF ₃ SO ₃) ₃ for 1 night	Co ²⁺ /Co ³⁺
standard-N719	0.50 mM EtOH solution of N719 for 1 night	I ₂ /I ₃ ⁻
#: 20 days old solution		

Table 3.11: Measured characteristic parameters for DSC-A to DSC-F, DSC-blank and standard-N719.

attempt		electrolyte	J_{SC} [mA/cm ²]	V_{OC} [mV]	ff [%]	η [%]
DSC-A cell 1	fresh	I_2/I_3^-	0.07	229	55.5	0.009
DSC-A cell 2	fresh	I_2/I_3^-	0.10	247	56.8	0.013
DSC-A cell 1	2 days old	I_2/I_3^-	0.08	241	54.7	0.011
DSC-A cell 2	2 days old	I_2/I_3^-	0.10	224	55.3	0.013
DSC-A cell 2	6 days old	I_2/I_3^-	0.09	246	56.0	0.012
DSC-B cell 1	fresh	I_2/I_3^-	0.10	242	53.5	0.012
DSC-B cell 2	fresh	I_2/I_3^-	0.10	233	54.5	0.012
DSC-B cell 1	2 days old	I_2/I_3^-	0.12	262	51.4	0.016
DSC-B cell 2	2 days old	I_2/I_3^-	0.10	238	55.4	0.013
DSC-C cell 1	fresh	I_2/I_3^-	0.15	222	53.3	0.019
DSC-C cell 2	fresh	I_2/I_3^-	0.16	330	50.8	0.028
DSC-C cell 1	2 days old	I_2/I_3^-	0.10	154	53.7	0.008
DSC-D	fresh	I_2/I_3^-	0.05	150	50.2	0.004
DSC-blank	fresh	I_2/I_3^-	0.31	415	49.2	0.064
DSC-blank	2 days old	I_2/I_3^-	0.29	394	43.4	0.050
standard-N719	fresh	I_2/I_3^-	16.31	627	72.9	7.45
standard-N719	2 days old	I_2/I_3^-	16.38	640	73.5	7.704
DSC-E	fresh	Co^{2+}/Co^{3+}	0.04	135	34.9	0.002
DSC-F	fresh	Co^{2+}/Co^{3+}	0.06	90	31.4	0.002

composition of the electrolytes:

I_2/I_3^- : LiI (0.1 mol·l⁻¹), I_2 (0.05 mol·l⁻¹), 1-methylbenzimidazole (0.5 mol·l⁻¹) and 1-butyl-3-methylimidazolium iodide (0.6 mol·l⁻¹) in methoxypropionitrile

Co^{2+}/Co^{3+} : [Co(bpy)₃][PF₆]₂ (0.2 mol·l⁻¹), [Co(bpy)₃][PF₆]₃ (0.05 mol·l⁻¹), LiClO₄ (0.1 mol·l⁻¹) and 4-*tert*-butylpyridine (0.2 mol·l⁻¹) in MeCN

3.9 X-ray structures

In November 2013, the Cambridge Structural Database¹⁵⁷ (Conquest v. 1.16, CSD v. 5.35¹⁵⁸) contained only four complexes containing $\{\text{Cr}(\text{tpy})_2\}$ units. And only in one example has chromium the oxidation state 3+: $[\text{Cr}(\text{tpy})_2][\text{ClO}_4]_3 \cdot \text{H}_2\text{O}$.^{159,160} Further are reported structures of: $[\text{Cr}(\text{tpy})_2][\text{PF}_6]_2 \cdot \text{MeCN}$,⁵² $[\text{Cr}(\text{tpy})_2][\text{PF}_6]$ ⁵² and $[\text{Cr}(\text{tpy})_2]$.⁵²

Single crystals were obtained using three different approaches: slow diffusion of Et_2O into an MeCN solution of the complex, slow diffusion of hexane into an acetone solution of the complex or slow evaporation of a MeOH solution of the complex. For details compare tables 3.12, 3.13, 3.16 and 3.17. Single crystals of two homoleptic complexes were obtained from solutions of heteroleptic complexes ($[\text{Cr}(5,5''\text{-Me}_2\text{tpy})_2][\text{CF}_3\text{O}_3\text{S}]_3$ and $[\text{Cr}(\text{LT1})_2][\text{CF}_3\text{SO}_3]_3$). This is consistent with the lability of the complexes and the observed ligand exchange (3.2, p. 38, and 3.3, p. 43). Although the interactions among the cations and the anions and solvent molecules are dominant, several cations show also interactions between the cations. Therefore, π - π and $\text{CH}\dots\pi$ complete the $\text{CH}\dots\text{N}$ and $\text{CH}\dots\text{F}$ interactions in the packing.

3.9.1 Homoleptic complexes

Table 3.12: Crystallographic data of homoleptic $\{\text{Cr}(\text{tpy})_2\}^{3+}$ complexes, part I

compound	$[\text{Cr}(\text{tpy})_2][\text{PF}_6]_3$	$[\text{Cr}(4'-(4\text{-toly})\text{tpy})_2][\text{CF}_3\text{SO}_3]_3$	$[\text{Cr}(\text{LT}3)_2][\text{PF}_6]_3$
formula moiety	$2(\text{C}_{30}\text{H}_{22}\text{CrN}_6)$, $6(\text{F}_6\text{P})$, $5(\text{C}_2\text{H}_3\text{N})$	$\text{C}_{44}\text{H}_{34}\text{CrN}_6$, $3(\text{CF}_3\text{O}_3\text{S})$, $2(\text{C}_2\text{H}_3\text{N})$	$\text{C}_{50}\text{H}_{34}\text{CrN}_6$, $3(\text{F}_6\text{P})$, $0.2(\text{C}_2\text{H}_3\text{N})$
formula weight $[\text{g mol}^{-1}]$	2112.1	1228.12	1222.16
crystal colour and habit	yellow, plate	yellow, needle	orange, block
crystal system	orthorhombic	monoclinic	triclinic
space group	Pbca	C2/c	P $\bar{1}$
a, b, c [\AA]	22.0190(11) 32.5520(17) 47.334(3)	14.5535(8) 17.1633(11) 21.9247(14)	11.4677(5) 14.9613(6) 15.2475(6)
α, β, γ [$^\circ$]	90 90 90	90 108.308(4) 90	100.0920(10) 108.6350(10) 92.1140(10)
U [\AA^3]	33927(3)	5199.3(6)	2428.41(17)
Dc [Mg m^{-3}]	1.654	1.569	1.671
Z	16	4	2
$\mu(\text{Cu-K}\alpha)$ [mm^{-1}]	4.390	3.802	3.920
T [K]	123(2)	123(2)	123
refln. collected	161369	17034	25679
unique refln.	30417	4644	8765
refln. for refinement	19918	3700	8274
parameters	2406	404	861
threshold	$I > 2.0\sigma$	$I > 2.0\sigma$	$I > 2.0\sigma$
R1 (R1 all data)	0.0782 (0.1232)	0.0383 (0.0539)	0.0580 (0.0596)
wR2 (wR2 all data)	0.1973 (0.2219)	0.0906 (0.0984)	0.0683 (0.0689)
goodness of fit	1.056	1.019	1.0213
crystal growing	diffusion MeCN/Et ₂ O	MeOH slow evapora- tion	diffusion MeCN/Et ₂ O

Table 3.13: Crystallographic data of homoleptic $\{\text{Cr}(\text{tpy})_2\}^{3+}$ complexes, part II

compound	$[\text{Cr}(5,5''\text{-Me}_2\text{tpy})_2][\text{CF}_3\text{SO}_3]_3$	$[\text{Cr}(\text{HLT11})(\text{LT11})][\text{PF}_6]_4$	$[\text{Cr}(\text{LT1})_2][\text{CF}_3\text{SO}_3]_3$
formula moiety	$\text{C}_{34}\text{H}_{30}\text{CrN}_6, 3(\text{CF}_3\text{O}_3\text{S}), \text{H}_2\text{O}$	$\text{C}_{40}\text{H}_{29}\text{CrN}_8, 4(\text{F}_6\text{P})$	$\text{C}_{120}\text{H}_{113}\text{Cr}_2\text{F}_{18}\text{N}_{19}\text{O}_{18.50}\text{S}_6$
formula weight $[\text{g mol}^{-1}]$	1039.9	1253.56	2755.65
crystal colour and habit	orange, needle	yellow, block	red, block
crystal system	monoclinic	triclinic	triclinic
space group	$\text{P } 2_1/\text{n}$	$\text{P}\bar{1}$	$\text{P}\bar{1}$
a, b, c [\AA]	9.5697(12) 18.148(2) 23.573(3)	10.2844(14) 19.644(3) 24.538(3)	11.5505(5) 14.0824(6) 20.7389(8)
α, β, γ [$^\circ$]	90 92.963(9) 90	76.099(9) 80.775(8) 78.789(8)	106.9770(10) 97.252(2) 94.309(2)
U [\AA^3]	4088.5(9)	4686.7(11)	3178.2(2)
Dc [Mg m^{-3}]	1.689	1.571	1.440
Z	4	4	1
$\mu(\text{M-K}\alpha)$ [mm^{-1}]	4.708 (M=Cu)	0.458 (M=Mo)	3.183 (M=Cu)
T [K]	123(2)	123(2)	123(2)
refln. collected	22707	59218	48955
unique refln.	7137	18272	11290
refln. for refinement	3598	9196	10982
parameters	605	1393	985
threshold	$I > 2.0\sigma$	$I > 2.0\sigma$	$I > 2.0\sigma$
R1 (r1 all data)	0.0660 (0.1579)	0.0880 (0.1827)	0.0378 (0.0387)
wR2 (wR2 all data)	0.1268 (0.1608)	0.2486 (0.3175)	0.1073 (0.1089)
goodness of fit	0.96	1.061	1.032
crystal growing	diffusion MeCN/Et ₂ O	diffusion MeCN/Et ₂ O	diffusion MeCN/Et ₂ O
notes		obtained from heteroleptic bulk complex $[\text{Cr}(5,5''\text{-Me}_2\text{tpy})(\text{LT4})][\text{CF}_3\text{SO}_3]_3$	received from heteroleptic bulk complex $[\text{Cr}(\text{LT1})(\text{LT4})][\text{CF}_3\text{SO}_3]_3$

The two complexes $2\{[\text{Cr}(\text{tpy})_2][\text{PF}_6]_3\}\cdot 5\text{MeCN}$ and $[\text{Cr}(5,5''\text{-Me}_2\text{tpy})_2][\text{CF}_3\text{SO}_3]_3\cdot \text{H}_2\text{O}$, both with a non-extended tpy core show no interactions between the cations. The crystal packing is dominated by $\text{CH}\dots\text{F}$, $\text{CH}\dots\text{N}$ and $\text{CH}\dots\text{O}$ interactions between the cations and the anions and the solvent molecules respectively.

3.9.1.1 Structure of $2\{[\text{Cr}(\text{tpy})_2][\text{PF}_6]_3\}\cdot 5\text{MeCN}$

$2\{[\text{Cr}(\text{tpy})_2][\text{PF}_6]_3\}\cdot 5\text{MeCN}$ crystallises in the orthorhombic space group $Pbca$ with four independent cations (figure 3.49) in the asymmetric unit ($Z'=4$). The deviations in the metrical parameters of the four cations are small (compare table 3.14). The two tpy domains are arranged nearly orthogonal; the angle between the least squares planes lies between 84.5° and 89.5° (compare table 3.14).

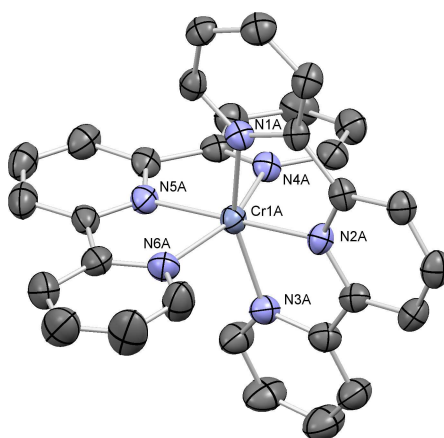
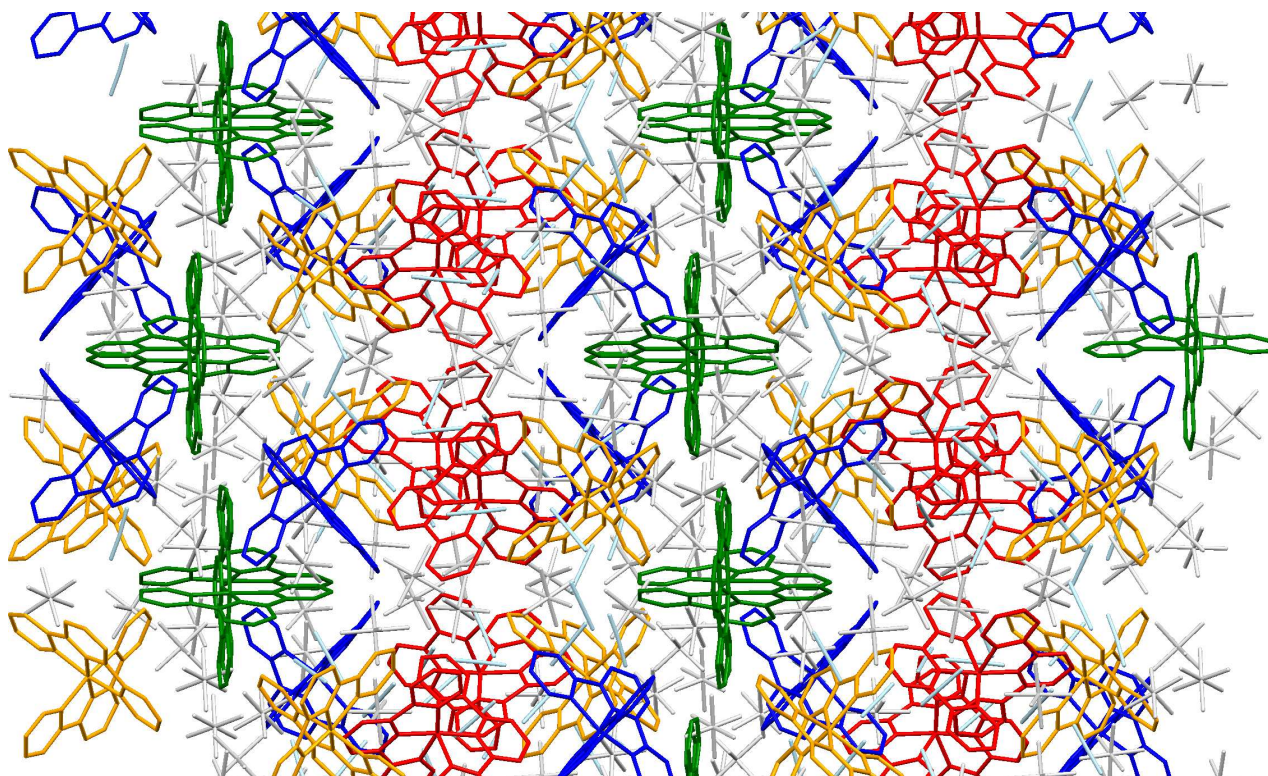


Figure 3.49: Structure of one of the four independent $[\text{Cr}(\text{tpy})_2]^{3+}$ cations with ellipsoids plotted at 50 % probability level. H atoms, counter ions and solvent molecules are omitted for clarity. Bond lengths and angles for all four cations are reported in table 3.14.

Table 3.14: Metrical parameters for the four independent cations of $2\{[\text{Cr}(\text{tpy})_2][\text{PF}_6]_3\}\cdot 5\text{MeCN}$

cation a:		cation b:		cation c:		cation d:	
bond	[Å]	bond	[Å]	bond	[Å]	bond	[Å]
Cr1A-N1A	2.054(3)	Cr1B-N1B	2.055(3)	Cr1C-N1C	2.099(4)	Cr1D-N1D	2.039(4)
Cr1A-N2A	1.985(3)	Cr1B-N2B	1.976(3)	Cr1C-N2C	2.003(4)	Cr1D-N2D	1.981(4)
Cr1A-N3A	2.058(4)	Cr1B-N3B	2.057(3)	Cr1C-N3C	2.035(4)	Cr1D-N3D	2.049(4)
Cr1A-N4A	2.042(3)	Cr1B-N4B	2.062(3)	Cr1C-N4C	2.063(4)	Cr1D-N4D	2.053(4)
Cr1A-N5A	1.987(3)	Cr1B-N5B	1.989(3)	Cr1C-N5C	1.983(3)	Cr1D-N5D	1.978(4)
Cr1A-N6A	2.062(4)	Cr1B-N6B	2.042(3)	Cr1C-N6C	2.049(3)	Cr1D-N6D	2.057(4)
angle	[°]	angle	[°]	angle	[°]	angle	[°]
N2A-Cr1A-N1A	78.78(14)	N2B-Cr1B-N1B	79.01(13)	N2C-Cr1C-N1C	77.39(15)	N2D-Cr1D-N1D	78.80(15)
N2A-Cr1A-N3A	78.34(14)	N2B-Cr1B-N3B	79.29(14)	N2C-Cr1C-N3C	79.59(17)	N2D-Cr1D-N3D	79.41(15)
N1A-Cr1A-N3A	157.06(14)	N1B-Cr1B-N3B	158.24(13)	N3C-Cr1C-N1C	156.93(16)	N1D-Cr1D-N3D	157.98(16)
N5A-Cr1A-N4A	79.00(14)	N5B-Cr1B-N4B	79.12(13)	N5C-Cr1C-N4C	78.37(14)	N5D-Cr1D-N4D	78.43(15)
N5A-Cr1A-N6A	78.22(15)	N5B-Cr1B-N6B	78.97(14)	N5C-Cr1C-N6C	78.92(14)	N5D-Cr1D-N6D	79.38(15)
N4A-Cr1A-N6A	157.17(14)	N6B-Cr1B-N4B	157.98(13)	N6C-Cr1C-N4C	157.19(14)	N4D-Cr1D-N6D	157.76(15)
angle [°] between tpy domains:							
cation a:	84.77	cation b:	89.57	cation c:	89.15	cation d:	87.3

Figure 3.50: Packing of $2\{[\text{Cr}(\text{tpy})_2][\text{PF}_6]_3\}\cdot 5\text{MeCN}$. The four independent cations are shown in blue (A), green (B), yellow (C) and red (D), the anions (PF_6^-) in light grey and the solvent molecules (MeCN) in light blue. H atoms were omitted for clarity.

3.9.1.2 Structure of $[\text{Cr}(5,5''\text{-Me}_2\text{tpy})_2][\text{CF}_3\text{SO}_3]_3\cdot\text{H}_2\text{O}$

$[\text{Cr}(5,5''\text{-Me}_2\text{tpy})_2][\text{CF}_3\text{SO}_3]_3\cdot\text{H}_2\text{O}$ crystallises in the monoclinic $P2_1/n$ space group. The two tpy domains are arranged nearly orthogonal (angle between least squares planes = 89.2°) and the metrical parameters (compare caption to figure 3.51) are comparable with this reported for $2\{[\text{Cr}(\text{tpy})_2][\text{PF}_6]_3\}\cdot 5\text{MeCN}$. The accommodation of three $[\text{CF}_3\text{SO}_3]^-$ anions and one water molecule per complex cation prevents the formation of inter-cation tpy embraces,^{161,162} and therefore the principal packing interactions involve CH...F and CH...O contacts (figure 3.52).

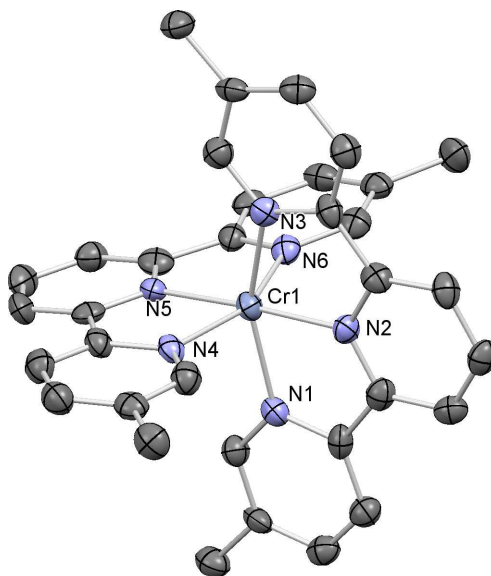


Figure 3.51: Structure of the cation in $[\text{Cr}(5,5''\text{-Me}_2\text{tpy})_2][\text{CF}_3\text{SO}_3]_3$ with ellipsoids plotted at 50 % probability level. H atoms, counter ions and solvent molecules are omitted for clarity. Selected bond lengths [\AA]: Cr1-N1 = 2.083(5), Cr1-N2 = 1.983(5), Cr1-N3 = 2.056(5), Cr1-N4 = 2.062(5), Cr1-N5 = 1.988(5), Cr1-N6 = 2.065(5); and bond angles [$^\circ$]: N1-Cr1-N2 = 78.7(2), N3-Cr1-N2 = 78.2(2), N1-Cr1-N3 = 156.92(19), N4-Cr1-N5 = 78.22(19), N6-Cr1-N5 = 78.04(19), N4-Cr1-N6 = 155.94(19).

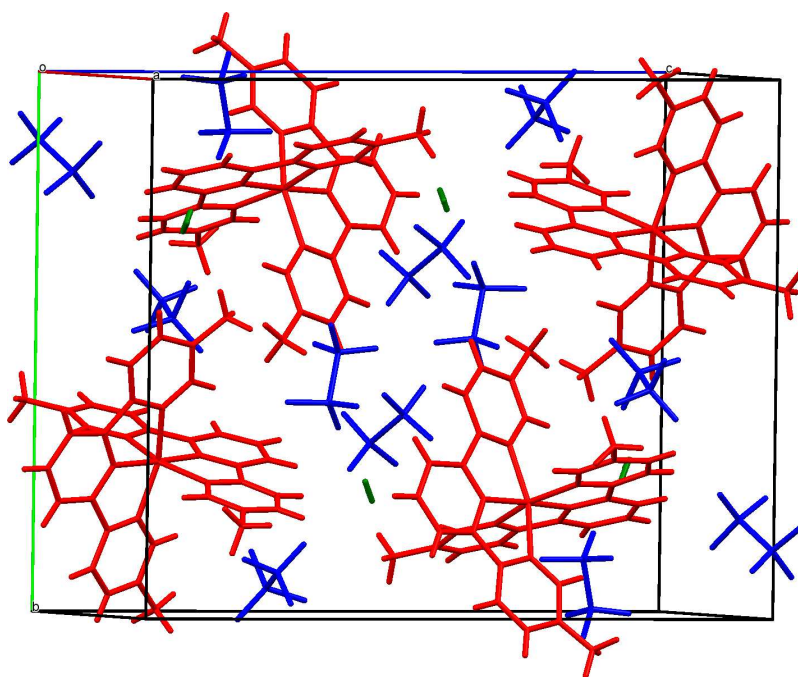


Figure 3.52: Packing for $[\text{Cr}(5,5''\text{-Me}_2\text{tpy})_2][\text{CF}_3\text{SO}_3]_3\cdot\text{H}_2\text{O}$. Colour code: cation (red), counter anion (blue) and water (green).

The further homoleptic complexes include tpy-ligands which are substituted at the 4'-position with at least one aromatic ring. This rings are twisted compared with the tpy domain in order to minimise the repulsions between the *ortho*-hydrogen atoms and to optimise π - π -interactions between the cations. The torsion angles are between 17.4° and 39.7° (compare table 3.15). In these examples interactions among the cations can be assigned, based on the structural information.¹¹⁹ But the principal packing interactions are CH...F, CH...O and CH...N contacts with the counter anions and solvent molecules accommodated in the packing.

Table 3.15: Torsion angles between the tpy domain and the aromatic ring at the 4'-position.

$[\text{Cr}(4'-(4\text{-tolyl})\text{tpy})_2][\text{CF}_3\text{SO}_3]_3\cdot 2\text{MeCN}$	tpy(N1-N3)-tolyl(C16)	17.4°
$[\text{Cr}(\text{LT}3)_2][\text{PF}_6]_3\cdot 0.2\text{MeCN}$	tpy(N1-N3)-naph(C16)	39.7°
	tpy(N4-N6)-naph(C41)	21.4°
$[\text{Cr}(\text{HLT}11)(\text{LT}11)][\text{PF}_6]_4$	tpy(N1A-N3A)-py(N4A)	28.9°
	tpy(N5A-N7A)-py(N8A)	37.3°
	tpy(N1B-N3B)-py(N4B)	23.0°
	tpy(N5B-N7B)-py(N8B)	34.6°
$[\text{Cr}(\text{LT}1)_2][\text{CF}_3\text{SO}_3]_3$	tpy(N1-N3)-phen(C16)	17.6°
	tpy(N4-N6)-phen(C41)	18.6°

3.9.1.3 Structure of $5\{[\text{Cr}(\text{LT}3)_2][\text{PF}_6]_3\}\cdot\text{MeCN}$

$5\{[\text{Cr}(\text{LT}3)_2][\text{PF}_6]_3\}\cdot\text{MeCN}$ crystallises in the triclinic space group $P\bar{1}$. Figure 3.53 shows an ORTEP representation of the cation $[\text{Cr}(\text{LT}3)_2]^{3+}$. It is noticeable that the two naphthalene units are twisted differently with respect to the tpy domains (21.4° respectively 39.7°). This complex shows also two different π - π interactions among two complexes involving the naphthyl groups (figure 3.54).¹¹⁹ The naphthyls containing C16 overlap with the plane of the rings being coparallel by symmetry (centre of inversion) with a distance of the least squares planes of 3.53 \AA . The naphthyl groups are offset with each other (figure 3.55). The second interaction involves the 2^{nd} ligand on the complex. The naphthyl group containing C41 interacts with the pyridine ring containing N6. This π - π interaction has to be less strong, since the angle between the two least square planes is 21.1° . The distance between the two calculated ring centroids is 3.84 \AA and the shortest distance between a least square plane (pyridine containing N6) and a centroid (naphthyl containing C41) is 3.26 \AA . As a consequence of these two different interactions, the cations are packed in chains where the orientation of each link changes in an alternating manner (figure 3.56). These chains do not interact directly with one another (figure 3.57).

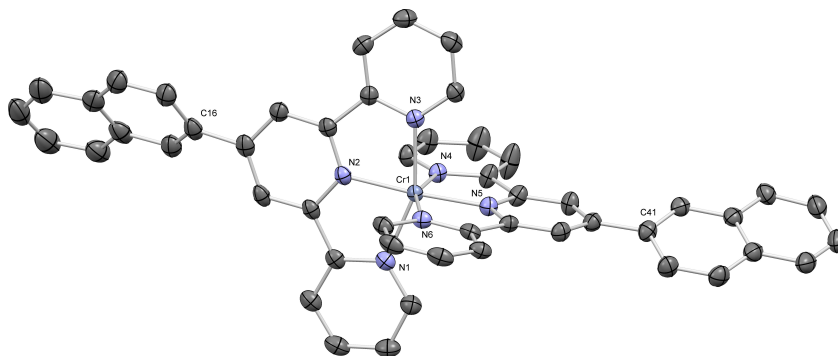


Figure 3.53: Structure of the cation in $[\text{Cr}(\text{LT}3)_2][\text{PF}_6]_3$ with ellipsoids plotted at 50 % probability level. H atoms, counter ions and solvent molecules are omitted for clarity. Selected bond lengths [\AA]: Cr1-N1 = 2.058(2), Cr1-N2 = 1.967(2), Cr1-N3 = 2.061(2), Cr1-N4 = 2.055(2), Cr1-N5 = 1.971(2), Cr1-N6 = 2.047(2); and bond angles [$^\circ$]: N1-Cr1-N2 = 78.68(8), N3-Cr1-N2 = 78.95(8), N1-Cr1-N3 = 157.59(9), N4-Cr1-N5 = 79.07(8), N6-Cr1-N5 = 78.46(8), N4-Cr1-N6 = 157.53(9).

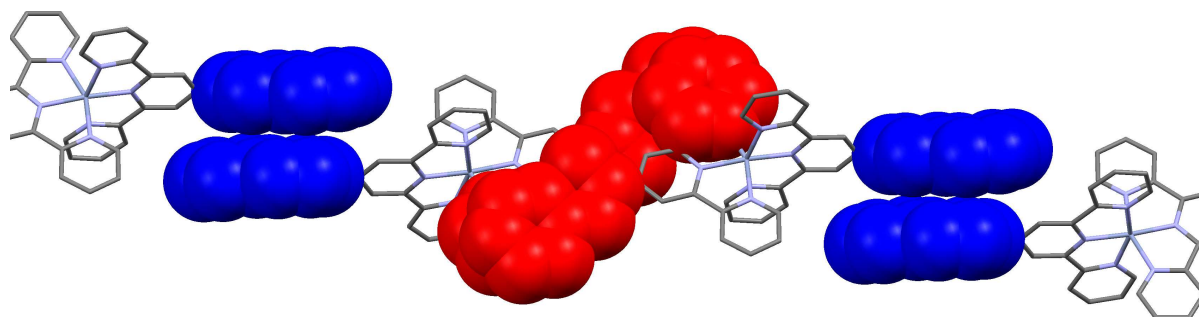


Figure 3.54: Face-to-face interaction contacts in $[\text{Cr}(\text{LT}3)_2][\text{PF}_6]_3$. The interactions between the naphthyls containing C16 are highlighted in blue, the interactions between the naphthyl group containing C41 and the ring containing N6 in red.

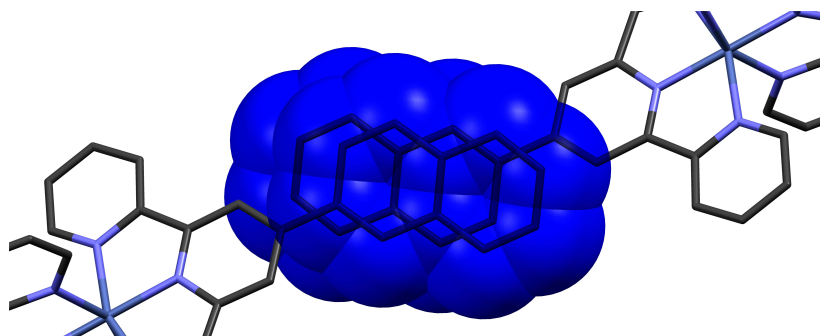


Figure 3.55: Face-to-face interaction contacts in $[\text{Cr}(\text{LT}3)_2][\text{PF}_6]_3$. Superposition of the stick and the spacefill presentation shows the stacked face-to-face interaction. The distance between the least square planes is 3.53 Å and the planes are parallel (angle = 0°) to each other.

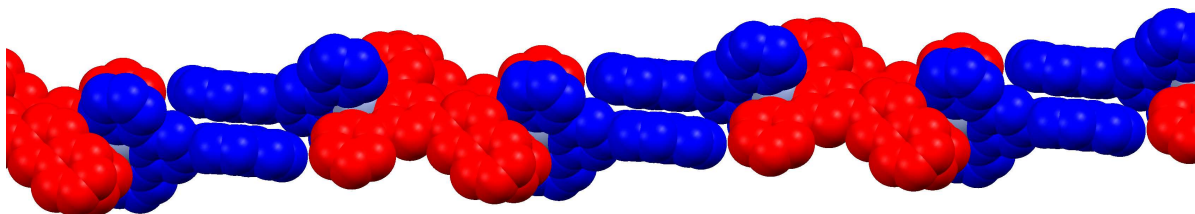


Figure 3.56: Illustration of a chain formed by the $[\text{Cr}(\text{LT}3)_2]^{3+}$ -cations. Counter ions, H atoms and solvent molecules are omitted for clarity. The ligands containing C16 are presented in blue, those containing C41 in red.

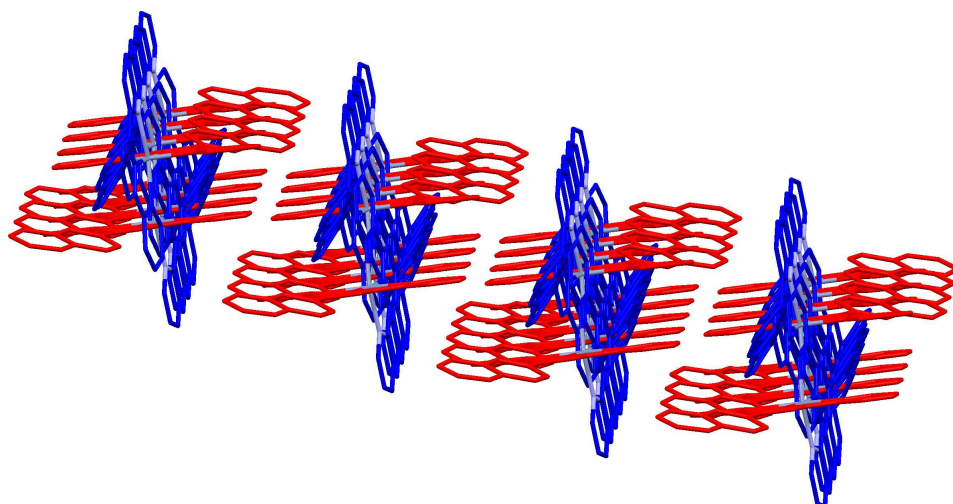


Figure 3.57: View along the independent chains formed by the $[\text{Cr}(\text{LT}3)_2]^{3+}$ -cations. Counter ions, H atoms and solvent molecules are omitted for clarity. The ligands containing C16 are presented in blue, those containing C41 in red.

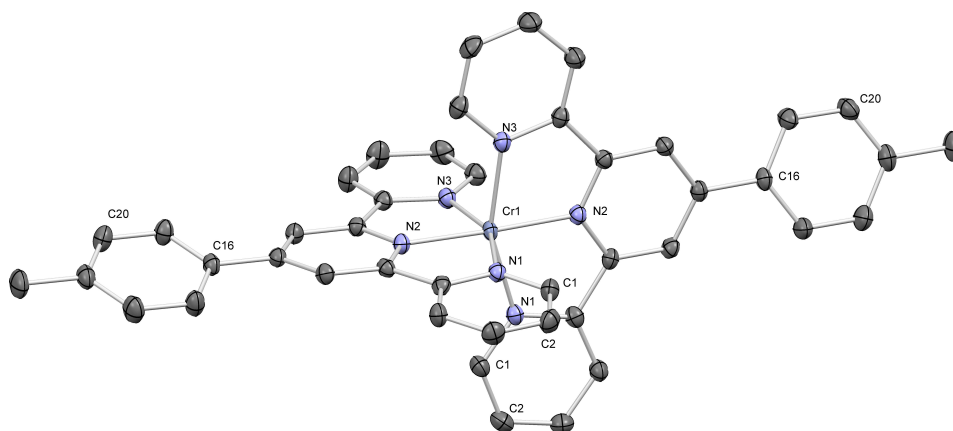
3.9.1.4 Structure of $[\text{Cr}(4'-(4\text{-tolyl})\text{tpy})_2][\text{CF}_3\text{SO}_3]_3 \cdot 2\text{MeCN}$ 

Figure 3.58: Structure of the cation in $[\text{Cr}(4'-(4\text{-tolyl})\text{tpy})_2][\text{CF}_3\text{SO}_3]_3 \cdot 2\text{MeCN}$ with ellipsoids plotted at 50 % probability level. H atoms, counter ions and solvent molecules are omitted for clarity. Selected bond lengths [\AA]: Cr1-N1 = 2.062(2), Cr1-N2 = 1.9717(18), Cr1-N3 = 2.055(2); and bond angles [$^\circ$]: N1-Cr1-N2 = 78.79(8), N3-Cr1-N2 = 78.59(8), N1-Cr1-N3 = 157.27(7).

$[\text{Cr}(4'-(4\text{-tolyl})\text{tpy})_2][\text{CF}_3\text{SO}_3]_3 \cdot 2\text{MeCN}$ crystallises in the monoclinic $C2/c$ space group (figure 3.58). The metrical parameters of the two ligands in this complex are identical, because a 2-fold axis goes through the metal centre. Between two cations, π - π plane to plane and $\text{CH}\dots\pi$ interactions can be observed. The face-to-face interaction between the pyridine-ring containing N3 and the phenyl-ring containing C16 can be classified as moderate since the two least squares planes are not parallel. The angle between the planes is 17.4° . The distance between the calculated centroids (of the rings containing N3 and C16) is 3.71 \AA and the shortest distance between a centroid and a plane 3.40 \AA (centroid of the ring containing C16 and plane of the ring containing N3). Additional $\text{CH}\dots\pi$ interactions C20H...C1 and C20H...C2 (2.79 \AA respectively 2.82 \AA) between the pyridine-ring containing N1 and the phenyl-ring increase the cation-cation-interactions (figure 3.59).¹¹⁹

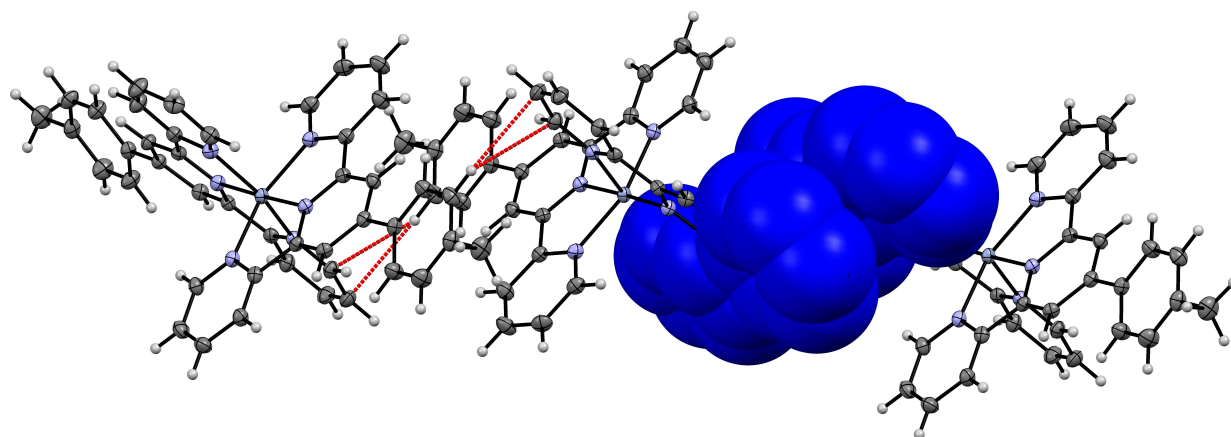


Figure 3.59: Interaction contacts in $[\text{Cr}(4'-(4\text{-tolyl})\text{tpy})_2][\text{CF}_3\text{SO}_3]_3 \cdot 2\text{MeCN}$. The face to face interaction (blue space-filling) and the $\text{CH}\dots\pi$ interactions (red) are shown separately. H atoms, counter ions and solvent molecules are omitted for clarity.

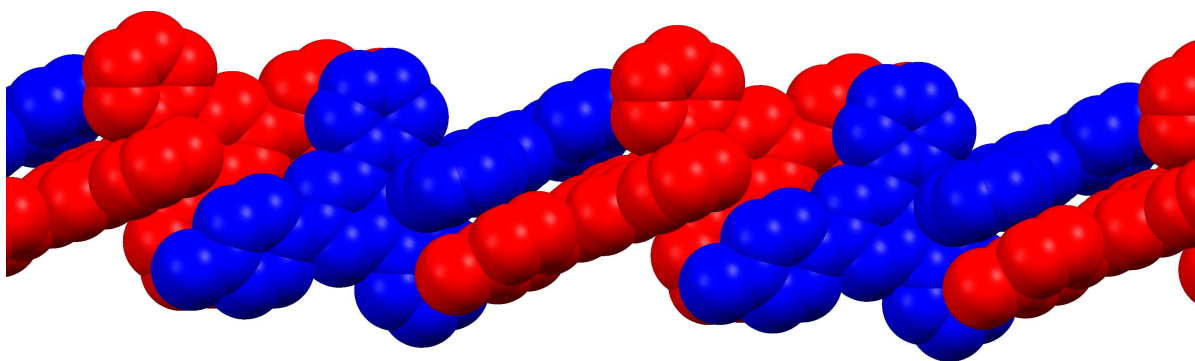


Figure 3.60: Chain-shaped packing of $[\text{Cr}(4'-(4\text{-tolyl})\text{tpy})_2][\text{CF}_3\text{SO}_3]_3 \cdot 2\text{MeCN}$. The cations were coloured alternately to improve the clearness. H atoms, counter ions and solvent molecules are omitted for clarity.

3.9.1.5 Structure of $[\text{Cr}(\text{LT1})_2][\text{CF}_3\text{SO}_3]_3$

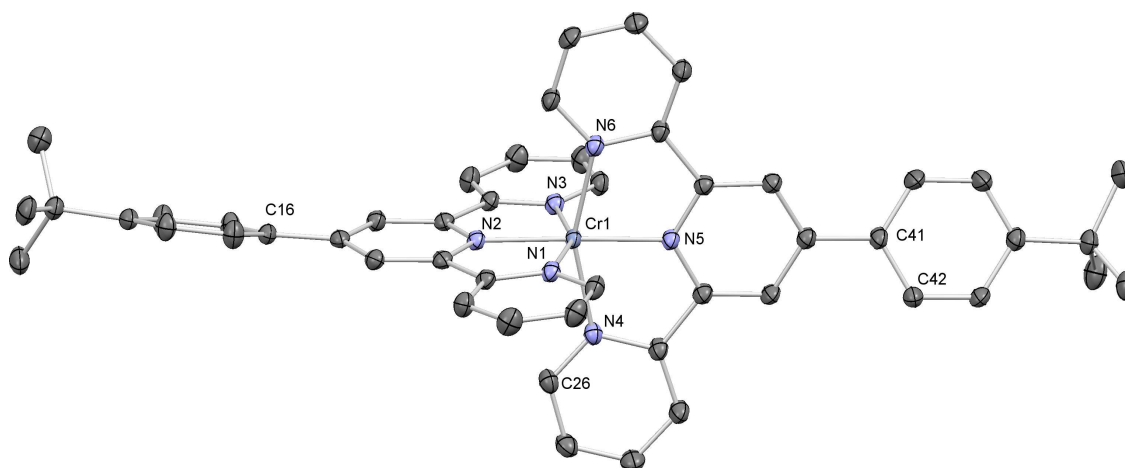


Figure 3.61: The structure of the cation in $[\text{Cr}(\text{LT1})_2][\text{CF}_3\text{SO}_3]_3$ with ellipsoids plotted at 50 % probability level. H atoms, counter ions and solvent molecules are omitted for clarity. Selected bond lengths [Å]: Cr1-N1 = 2.0580(16), Cr1-N2 = 1.9815(15), Cr1-N3 = 2.0622(15), Cr1-N4 = 2.0691(16), Cr1-N5 = 1.9836(15), Cr1-N6 = 2.0555(15); and bond angles [°]: N1-Cr1-N2 = 78.32(6), N3-Cr1-N2 = 78.30(6), N1-Cr1-N3 = 156.59(6), N4-Cr1-N5 = 78.19(6), N6-Cr1-N5 = 78.29(6), N4-Cr1-N6 = 156.37(6).

$[\text{Cr}(\text{LT1})_2][\text{CF}_3\text{SO}_3]_3$ crystallises in the triclinic $\bar{P}1$ space group (figure 3.61). These cations interact in a similar way as those in $[\text{Cr}(4'-(4\text{-tolyl})\text{tpy})_2][\text{CF}_3\text{SO}_3]_3 \cdot 2\text{MeCN}$. But since the two ligands are crystallographically independent, the complex is not symmetric and therefore two slightly different interactions are present (compare figure 3.62). Based on the geometrical data the interactions have to be categorised as weaker compared to those in the previously mentioned complex. The angles between the least squares planes are 20.3° (rings containing N6 and C41) and 20.5° (rings containing N3 and C16). The distances between the centroids are 3.85 Å (rings containing N6 and C41) and 4.12 Å (rings containing N3 and C16). 4.12 Å is really too long for a significant π -stacking interaction. And the minimal distances between a

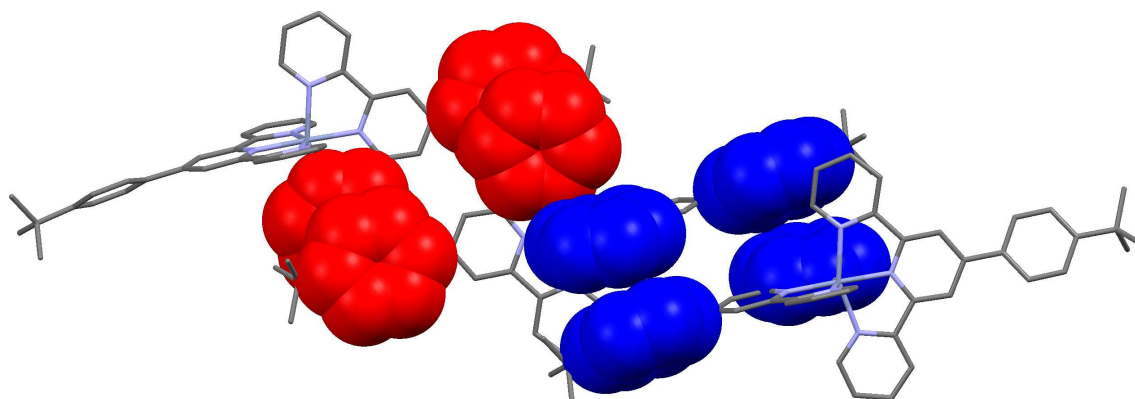


Figure 3.62: $[\text{Cr}(\text{LT1})_2][\text{CF}_3\text{SO}_3]_3$: Face-to-face stacking between the cations, between the rings containing N3 and C16 (red) and N6 and C41 (blue).

plane and a centroid are 3.50 Å (rings containing N3 and C16) and 3.57 Å (rings containing N6 and C41).¹¹⁹ This has the consequence that the orientation of the complex in the chain-shaped packing changes alternately, like in $[\text{Cr}(\text{LT3})_2][\text{PF}_6]_3 \cdot 0.2\text{MeCN}$. The solvent molecules and anions in this structure are badly disordered and could not be modelled in a satisfactory way.

3.9.1.6 Structure of $[\text{Cr}(\text{HLT11})(\text{LT11})][\text{PF}_6]_4$

The preliminary data show that the unit cell of $[\text{Cr}(\text{HLT11})(\text{LT11})][\text{PF}_6]_4$ contains two independent cations (figure 3.63). The cations are displayed as ball and stick since the anisotropic refinement was not possible for all atoms. The distance between the cations is too big to interact by π - π or $\text{CH}\dots\pi$ interactions.¹¹⁹ A possible reason for this observation is the presence of one additional PF_6^- anion in the packing, since one of the non-coordinating pyridine rings is protonated. In contrast to the complexes reported above there are no solvent molecules in the lattice (figure 3.65). The angle between the two tpy domains is 75.4° (cation A) and 77.7° (cation B) respectively. This is a bigger deviation from the orthogonal position, compared with the other reported complexes. The non-coordinating pyridine rings containing N4A and N4B are protonated. In contrast the other non-coordinating pyridine rings containing N8A and N8B are not protonated. There is an interaction between adjacent cations through N-H...N hydrogen bonds between the protonated and not protonated units. As a consequence, the cations form chains (figure 3.64) with alternating cations A and B as building blocks.

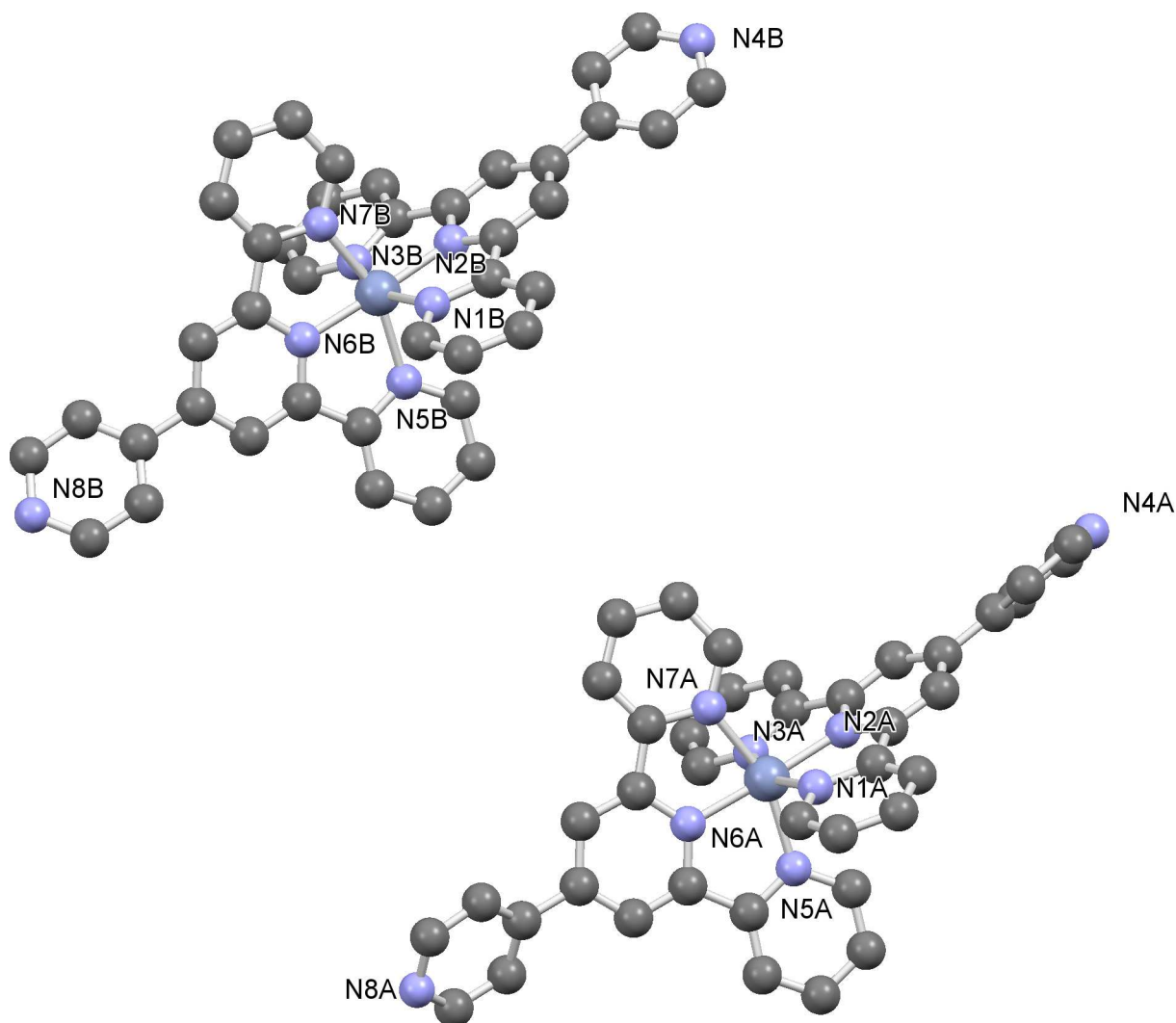


Figure 3.63: Two independent cations in $[\text{Cr}(\text{HLT11})(\text{LT11})][\text{PF}_6]_4$ plotted as ball and stick. H atoms and counter ions are omitted for clarity. Selected bond lengths [\AA]: Cr1A-N1A = 2.042(7), Cr1A-N2A = 1.984(6), Cr1A-N3A = 2.053(7), Cr1A-N5A = 2.055(7), Cr1A-N6A = 1.986(6), Cr1A-N7A = 2.056(7); Cr1B-N1B = 2.035(7), Cr1B-N2B = 1.986(6), Cr1B-N3B = 2.058(7), Cr1B-N5B = 2.064(7), Cr1B-N6B = 1.969(6), Cr1B-N7B = 2.073(7); and bond angles [$^\circ$]: N1A-Cr1A-N2A = 77.9(2), N3A-Cr1A-N2A = 78.8(2), N1A-Cr1A-N3A = 156.6(3), N5A-Cr1A-N6A = 78.8(3), N7A-Cr1A-N6A = 78.6(3), N5A-Cr1A-N7A = 157.3(2), N1B-Cr1B-N2B = 78.1(3), N3B-Cr1B-N2B = 78.6(3), N1B-Cr1B-N3B = 156.7(3), N5B-Cr1B-N6B = 79.1(3), N7B-Cr1B-N6B = 77.9(3), N5B-Cr1B-N7B = 156.9(3).

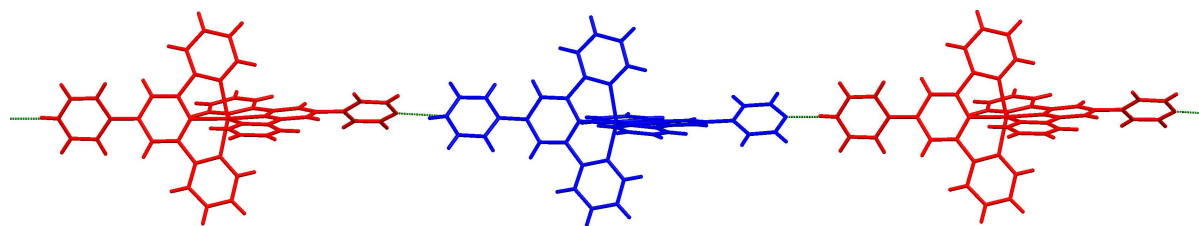


Figure 3.64: Nitrogen-hydrogen connections between protonated and non-protonated pyridine rings build a linear hydrogen-bonded polymer. The $[\text{Cr}(\text{HLT11})(\text{LT11})]^{4+}$ cations A (red) and B (blue) alternate as building blocks of the chain. Bond distances [\AA]: N4A-H...N4B: 1.80 and N4B-H...N8A: 1.79.

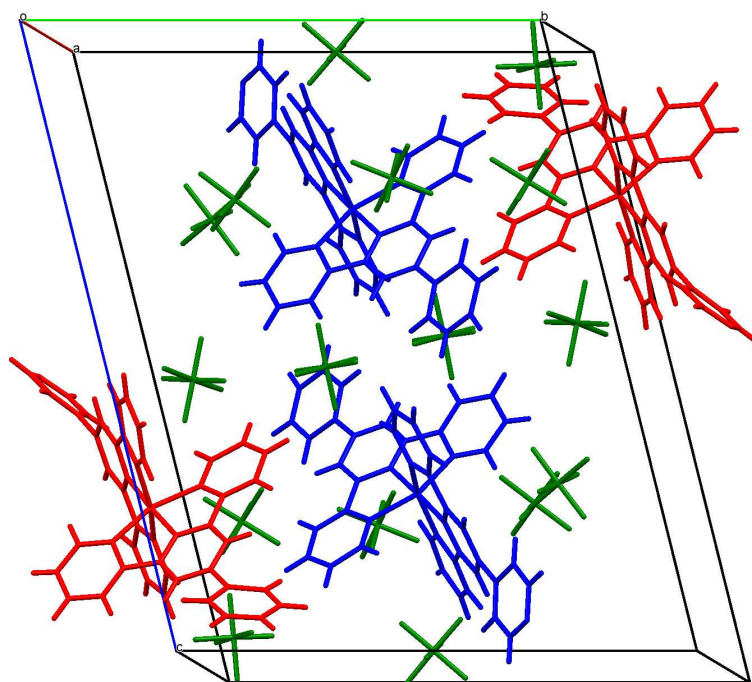


Figure 3.65: Packing for $[\text{Cr}(\text{HLT11})(\text{LT11})][\text{PF}_6]_4$. Colour code: cation A (red), cation B (blue) and anion PF_6^- (green).

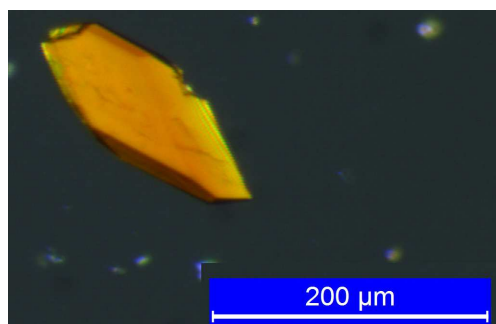


Figure 3.66: Light microscope picture of a $[\text{Cr}(\text{HLT11})(\text{LT11})][\text{PF}_6]_4$ plate.

3.9.2 Heteroleptic complexes

Although several crystal growth trials were accomplished with all the synthesised heteroleptic bis(terpyridine)chromium(III) complexes, measurable crystals were only obtained for cations with one unsubstituted tpy.

Table 3.16: Crystallographic data for heteroleptic $\{\text{Cr}(\text{tpy})_2\}^{3+}$ complexes, part I

compound	$[\text{Cr}(\text{tpy})(4'-(4\text{-toly})\text{tpy})][\text{PF}_6]_3$	$[\text{Cr}(\text{tpy})(\text{HLT11})][\text{PF}_6]_3[\text{CF}_3\text{SO}_3]$	$[\text{Cr}(\text{tpy})(5,5''\text{-Me}_2\text{tpy})][\text{PF}_6]_3$
formula moiety	$\text{C}_{37}\text{H}_{28}\text{CrN}_6$, $3(\text{F}_6\text{P})$, $3(\text{C}_2\text{H}_3\text{N})$	$\text{C}_{35}\text{H}_{26}\text{CrN}_7$, $3(\text{F}_6\text{P})$, $\text{CF}_3\text{O}_3\text{S}$	$\text{C}_{32}\text{H}_{26}\text{CrN}_6$, $3(\text{F}_6\text{P})$, $3(\text{C}_2\text{H}_3\text{N})$
formula weight	1166.71	1180.62	1104.66
crystal colour and habit [g mol ⁻¹]	orange, block	orange, plate	orange, block
crystal system	monoclinic	monoclinic	orthorhombic
space group	Cc	C2/c	Pbca
a, b, c [°A]	14.8008(10) 16.1020(10) 21.0282(14)	13.0909(10) 27.138(2), 12.3651(10)	12.6552(9) 19.1818(13) 36.810(3)
α , β , γ [°]	90 106.033(5) 90	90 94.194(2) 90	90 90 90
U [Å ³]	4816.56	4381.0(6)	8935.61
Dc [Mg m ⁻³]	1.609	1.790	1.642
Z	4	4	8
$\mu(\text{M-K}\alpha)$ [mm ⁻¹]	0.451 (M=Mo)	0.556 (M=Mo)	4.199 (M=Cu)
T [K]	123	123(2)	123(2)
refln. collected	53498	41505	117869
unique refln.	17525	6362	8050
refln. for refinement	12289	4933	7612
parameters	668	471	627
threshold	$I > 3.0\sigma$	$I > 2.0\sigma$	$I > 2.0\sigma$
R1 (r1 all data)	0.0384 (0.0509)	0.0694 (0.0857)	0.0339 (0.0356)
wR2 (wR2 all data)	0.0389 (0.0621)	0.1883 (0.2065)	0.0908 (0.0921)
goodness of fit	1.0984	1.033	1.053
crystal growing	diffusion acetone/ hexane	diffusion MeCN/Et ₂ O	diffusion MeCN/Et ₂ O

Table 3.17: Crystallographic data for heteroleptic Cr(tpy)₂ complexes, part II

compound	[Cr(tpy)(LT7)][PF ₆] ₃	[Cr(tpy)(LT8)][PF ₆] ₃	[Cr(tpy)(LT9)][PF ₆] ₃
formula moiety	C ₃₇ H ₂₅ CrN ₇ , 3(F ₆ P), 3(C ₃ H ₆ O)	C ₃₄ H ₂₄ CrF ₁₈ N ₆ OP ₃	C ₃₇ H ₂₈ CrN ₆ S, 3(F ₆ P), 2(C ₂ H ₃ N)
formula weight [g mol ⁻¹]	1228.78	1019.5	1157.72
crystal colour and habit	orange, block	orange, plates	orange, needle
crystal system	monoclinic	triclinic	triclinic
space group	P2 ₁ /c	P $\bar{1}$	P $\bar{1}$
a, b, c [Å]	9.4797(5) 27.4574(15) 19.5291(10)	12.715(2) 18.720(4) 20.255(4)	12.3948(7) 12.5942(8) 17.4369(10)
α, β, γ [°]	90 96.296(3) 90	96.984(6) 100.216(6) 104.519(9)	73.761(3) 76.298(3) 63.737(3)
U [Å ³]	5052.5(5)	4522.8(16)	2323.3(2)
Dc [Mg m ⁻³]	1.615	1.497	1.655
Z	4	4	2
Mu(M-K α) [mm ⁻¹]	0.438 (M=Mo)	0.468 (M=Mo)	4.474 (M=Cu)
T [K]	123(2)	123(2)	123
refn. collected	98720	42394	27428
unique refn.	12182	16318	8169
refn. for refinement	10177	9460	7237
parameters	709	1287	652
threshold	I > 2.0 σ	I > 2.0 σ	I > 0.0 σ
R1 (r1 all data)	0.0389 (0.0513)	0.0876 (0.1588)	0.0592 (0.0618)
wR2 (wR2 all data)	0.1379 (0.1161)	0.2325 (0.3050)	0.0641 (0.0706)
goodness of fit	1.075	1.072	1.0891
crystal growing	diffusion MeCN/Et ₂ O	diffusion MeCN/Et ₂ O	diffusion MeCN/Et ₂ O

3.9.2.1 [Cr(tpy)(5,5''-Me₂tpy)][PF₆]₃·3MeCN

[Cr(tpy)(5,5''-Me₂tpy)][PF₆]₃·3MeCN crystallises in the orthorhombic space group Pbc_a (figure 3.67). The two tpy domains are arranged in an angle of 85.8° (angle of the least squares planes). The three anions (PF₆⁻) and three solvent molecules (MeCN) are ordered and their accommodation in the lattice prevents inter-cation embraces. Therefore the principal packing interactions are CH...F and CH...N contacts between the cation and the anions and the solvent molecules respectively.

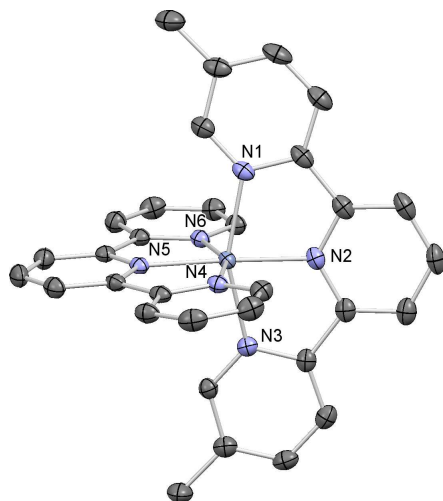


Figure 3.67: The cation in [Cr(tpy)(5,5''-Me₂tpy)][PF₆]₃ with ellipsoids plotted at 50 % probability level. Counter ions, H atoms and solvent molecules are omitted for clarity. Selected bond lengths [Å]: Cr1-N1 = 2.0655(15), Cr1-N2 = 1.9887(15), Cr1-N3 = 2.0648(15), Cr1-N4 = 2.0715(15), Cr1-N5 = 1.9836(15), Cr1-N6 = 2.0579(15); and bond angles [°]: N1-Cr1-N2 = 78.53(6), N2-Cr1-N3 = 78.45(6), N1-Cr1-N3 = 156.24(6), N4-Cr1-N5 = 78.49(6), N6-Cr1-N5 = 78.65(6), N4-Cr1-N6 = 157.14(6).

3.9.2.2 [Cr(tpy)(HLT11)][PF₆]₃[CF₃SO₃]

[Cr(tpy)(HLT11)][PF₆]₃[CF₃SO₃] crystallises in the monoclinic space group C2/c (figure 3.68). The non-coordinating pyridine is protonated as seen in the homoleptic complex [(HLT11)(LT11)][PF₆]₄ (page 81). An additional analogy to this homoleptic complex is that the lattice is solvent free. The two tpy domains are nearly perfectly arranged orthogonally (angle between the least squares planes: 89.2°). As in the structure described above there are no direct contacts between the cations. The principal packing interactions are CH...F interactions with the anions. The presence of three PF₆⁻ and one CF₃SO₃⁻ anion shows that there was no complete anion exchange. The pyridyl of ligand LT11 is disorderd. The twist angle between the tpy domain and the pyridyl-ring is 30.6° (I) and 31.5° (II) respectively, but in the opposite direction (angles between the least squares planes, compare figure 3.69). The occupancies of the two disorderd positions are 53% (I) and 47% (II).

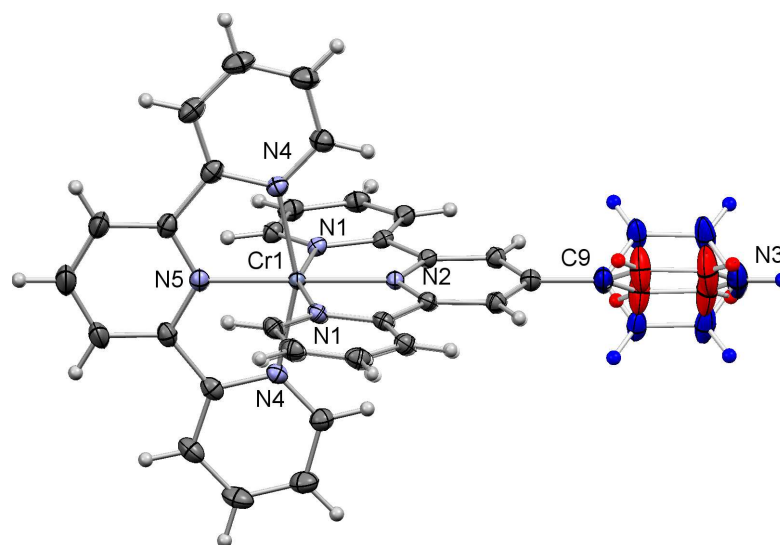


Figure 3.68: The cation in $[\text{Cr}(\text{tpy})(\text{HLT11})][\text{PF}_6]_3[\text{CF}_3\text{SO}_3]$ with ellipsoids plotted at 50 % probability level. Counter anions are omitted for clarity. Selected bond lengths [\AA]: Cr1-N1 = 2.0644(18), Cr1-N2 = 1.988(2), Cr1-N4 = 2.0571(17), Cr1-N5 = 1.983(2); and bond angles [$^\circ$]: N1-Cr1-N2 = 78.39(5), N1-Cr1-N1 = 156.77(10), N4-Cr1-N5 = 78.73(5), N4-Cr1-N4 = 157.45(10). The pyridine-ring containing N3 is disordered: red (I) and blue (II).

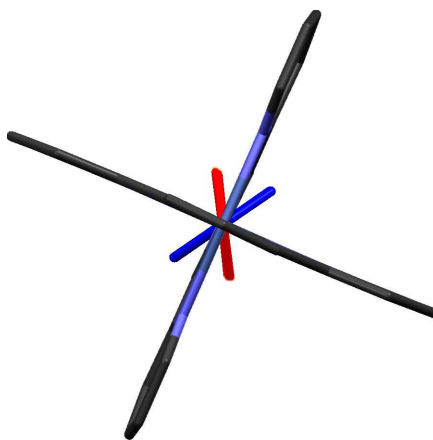


Figure 3.69: The two tpy domains are arranged in an angle of 89.2° . The pyridine-ring is twisted compared with the tpy domain: red (I): 30.56° and blue (II): 31.5°

3.9.2.3 Structure of $[\text{Cr}(\text{tpy})(\text{LT7})][\text{PF}_6]_3 \cdot 3\text{Me}_2\text{CO}$

$[\text{Cr}(\text{tpy})(\text{LT7})][\text{PF}_6]_3 \cdot 3\text{Me}_2\text{CO}$ crystallises in the monoclinic space group $\text{P}2_1/\text{c}$ (figure 3.70). The two tpy domains are arranged at an angle of 89.8° . The phenyl-ring (containing C16) is twisted through 26.3° with respect to the tpy domain. The phenyl-rings containing C16 of adjacent cations stand perfectly parallel to each other with a distance of 3.74 \AA (distance between the least squares planes and the centroids). The rings are co-parallel because of symmetry; an inversion center is located in the middle between the two phenyl-rings. Beside these face-to-face π - π -interactions, CH...N interactions between C26H and N7 (2.66 \AA) plus C38H and N7 (2.60 \AA) are present.¹¹⁹ The consequence is that each pair of cations is inter-connected by face-to-face and two CH...N (C38H...N7) interactions. Further, each pair is connected to four

pairs via CH...N (C26H...N7) connections (figure 3.71).

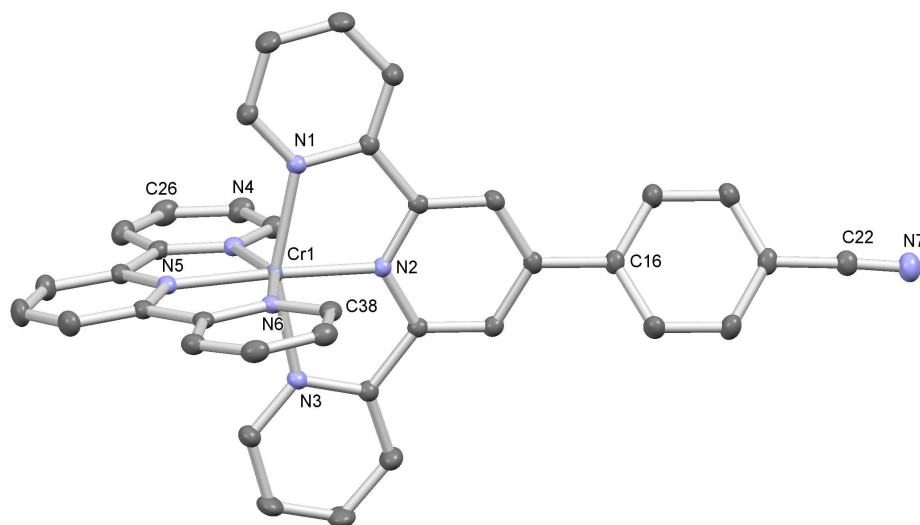


Figure 3.70: $[\text{Cr}(\text{LT7})(\text{tpy})][\text{PF}_6]_3 \cdot 3\text{C}_3\text{H}_6\text{O}$ with ellipsoids plotted at 50 % probability level. H atoms, counter ions and solvent molecules are omitted for clarity. Selected bond lengths [\AA]: Cr1-N1 = 2.0627(16), Cr1-N2 = 1.9843(16), Cr1-N3 = 2.0557(16), Cr1-N4 = 2.0504(16), Cr1-N5 = 1.9850(16), Cr1-N6 = 2.0584(16); and bond angles [$^\circ$]: N1-Cr1-N2 = 78.40(6), N3-Cr1-N2 = 78.64(6), N1-Cr1-N3 = 157.03(6), N4-Cr1-N5 = 79.03(7), N6-Cr1-N5 = 78.32(6), N4-Cr1-N6 = 157.34(7).

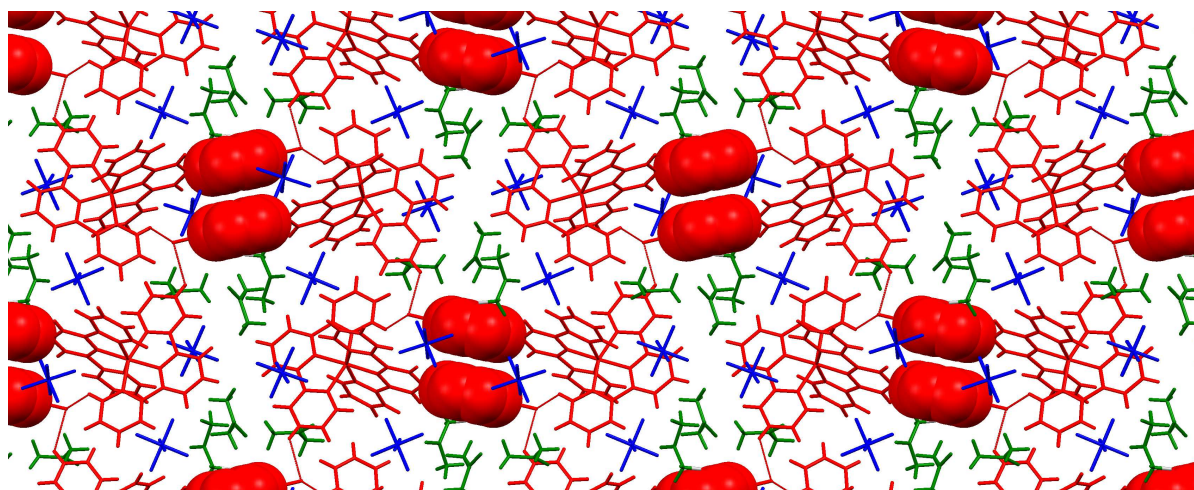


Figure 3.71: $[\text{Cr}(\text{LT7})(\text{tpy})][\text{PF}_6]_3 \cdot 3\text{Me}_2\text{CO}$ packing with face-to-face π - π interactions between the phenyl-rings (spacefill) and CH...N interactions (thin red lines). Colour code: red: cation, blue: counter anion PF_6^- and green: acetone.

3.9.2.4 [Cr(tpy)(LT9)][PF₆]₃·2MeCN

[Cr(tpy)(LT9)][PF₆]₃·2MeCN crystallises in the triclinic space group $P\bar{1}$ (figure 3.72). The two tpy domains are arranged in an angle of 88.0°. The phenyl-ring containing C31 is twisted through 18.6° with respect to the tpy domain. The interactions between the cations are similar to those reported for [Cr(4'-(4-tolyl)tpy)₂][CF₃SO₃]₃·2MeCN. A moderate π - π interaction is present between the pyridyl-ring (containing N6) and the phenyl-ring (containing C31). The angle between the least squares planes is 14.9° and the shortest distance between a centroid and a least squares plane is 3.49 Å (centroid of the phenyl-ring and least squares plane of the pyridyl-ring). The distance between the two centroids is 3.71 Å (figure 3.73).¹¹⁹

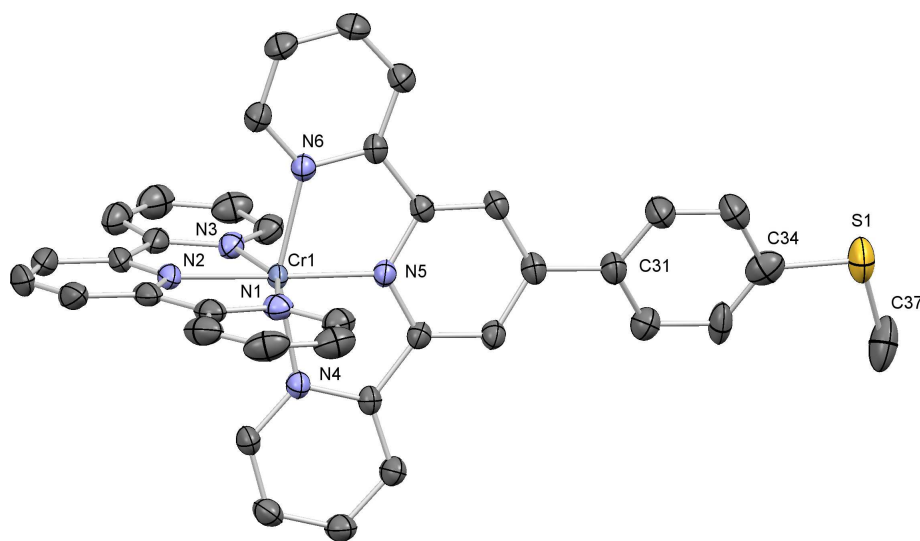


Figure 3.72: The cation in [Cr(tpy)(LT9)][PF₆]₃·2MeCN with ellipsoids plotted at 50 % probability level. H atoms, counter ions and solvent molecules are omitted for clarity. Selected bond lengths [Å]: Cr1-N1 = 2.052(3), Cr1-N2 = 2.001(2), Cr1-N3 = 2.074(3), Cr1-N4 = 2.071(3), Cr1-N5 = 1.981(2), Cr1-N6 = 2.064(3); and bond angles [°]: N1-Cr1-N2 = 78.41(11), N3-Cr1-N2 = 77.99(11), N1-Cr1-N3 = 156.40(11), N4-Cr1-N5 = 78.01(10), N6-Cr1-N5 = 78.35(10), N4-Cr1-N6 = 156.31(10), C34-S1-C37 = 103.9(2).

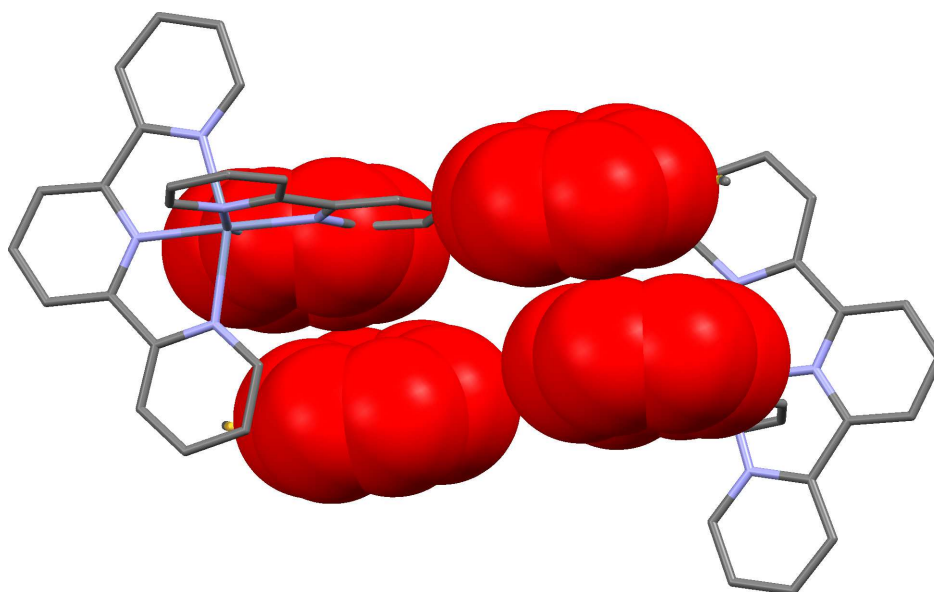


Figure 3.73: Face-to-face contacts in $[\text{Cr}(\text{tpy})(\text{LT9})][\text{PF}_6]_3 \cdot 2\text{MeCN}$: π - π packing between the pyridyl-ring containing N6 and the phenyl-ring containing C31. Counter anions, solvent molecules and H atoms are omitted for clarity.

3.9.2.5 $[\text{Cr}(\text{tpy})(4'-(4\text{-tolyl})\text{tpy})][\text{PF}_6]_3 \cdot 3\text{MeCN}$

$[\text{Cr}(\text{tpy})(4'-(4\text{-tolyl})\text{tpy})][\text{PF}_6]_3 \cdot 3\text{MeCN}$ crystallises in the monoclinic space group Cc (figure 3.74). The tpy domains are arranged in an angle of 88.9° . The phenyl-ring is twisted with respect to the tpy domain by 23.4° . The contacts between two cations can either be classified as face-to-face or edge-to-face but the tolyl-ring of one cation is accommodated within the cleft (85.2°) formed by two pyridine-rings (containing N1 and N4) of the other cation. The closest $\text{CH}\dots\pi$ interactions are 3.40 to 3.50 Å (figure 3.75).¹¹⁹

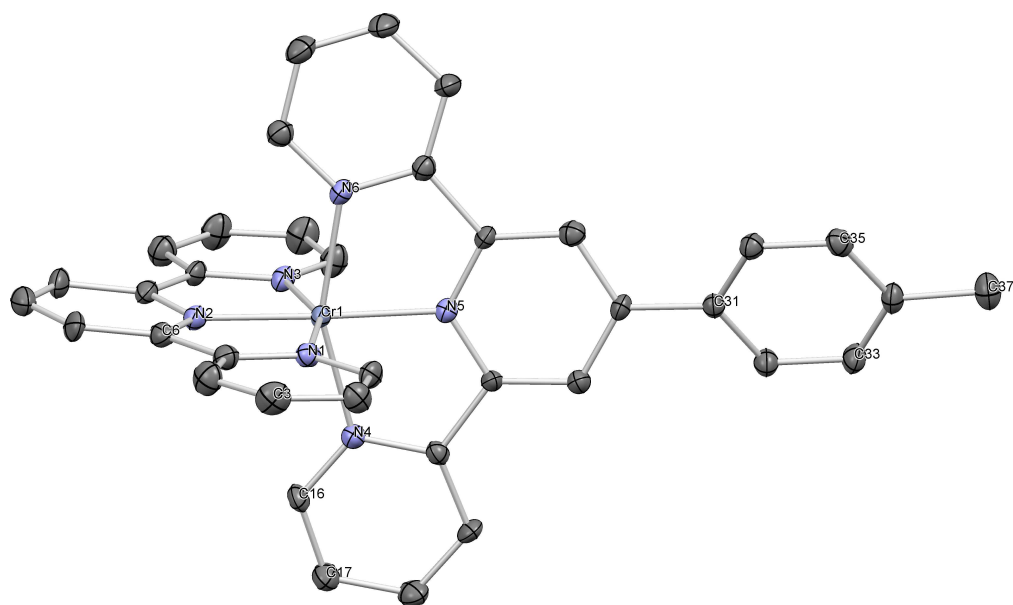


Figure 3.74: The cation in $[\text{Cr}(\text{tpy})(4'-(4\text{-tolyl})\text{tpy})][\text{PF}_6]_3$ with ellipsoids plotted at 50 % probability level. Counter ions, H atoms and solvent molecules are omitted for clarity. Selected bond lengths [\AA]: Cr1-N1 = 2.054(2), Cr1-N2 = 1.986(2), Cr1-N3 = 2.061(2), Cr1-N4 = 2.064(2), Cr1-N5 = 1.979(2), Cr1-N6 = 2.052(2); and bond angles [$^\circ$]: N1-Cr1-N2 = 78.83(9), N2-Cr1-N3 = 78.73(9), N1-Cr1-N3 = 157.56(9), N4-Cr1-N5 = 77.90(9), N6-Cr1-N5 = 78.67(9), N4-Cr1-N6 = 156.44(9).

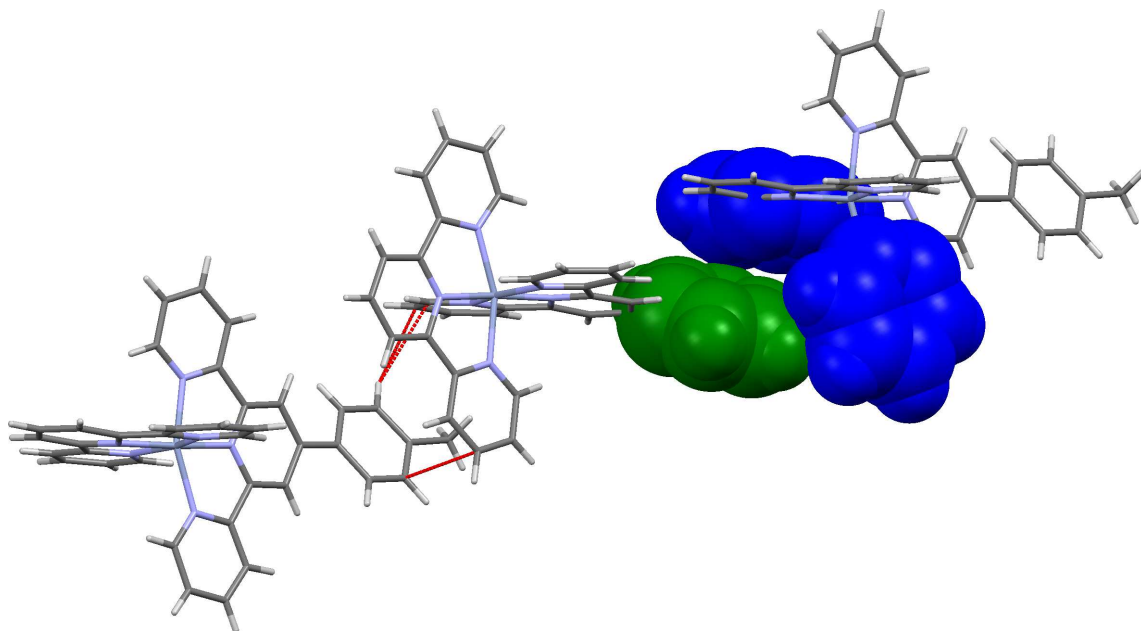


Figure 3.75: Short contacts in $[\text{Cr}(\text{tpy})(4'-(4\text{-tolyl})\text{tpy})][\text{PF}_6]_3 \cdot \text{MeCN}$. Tolyl unit (green) in the cleft formed by the two pyridine rings containing N1 and N4 (blue). CH... π interactions are highlighted in red.

3.9.2.6 Structure of $[\text{Cr}(\text{tpy})(\text{LT8})][\text{PF}_6]_3$

$[\text{Cr}(\text{tpy})(\text{LT8})][\text{PF}_6]_3$ crystallises in the triclinic space group $P\bar{1}$. The structure determination is only preliminary. The asymmetric unit contains two different cations A and B (figure 3.76). The two tpy domains are arranged in an angle of 85.6° (cation A) and 89.6° (cation B) respectively. The furan-rings are twisted compared with the corresponding tpy domains by: 7.1° (cation A) and 15.2° (cation B). The interactions between two equivalent cations are similar to those described in $[\text{Cr}(\text{LT9})(\text{tpy})][\text{PF}_6]_3 \cdot 2\text{MeCN}$. The angles between the least squares planes are quite different in the two face-to-face interactions: 3.5° (rings containing N3A and O1A) and 16.05° (rings containing N1B and O1B). The shortest distance between a centroid and a plane are 3.32 \AA (cation A) and 3.66 \AA (cation B). Additionally to these interactions, a weak π - π contact can be found between the two cation pairs, namely between the rings containing O1B and N1A. The angle between the least squares planes is 9.8° and the shortest distance between a plane and a centroid is 3.57 \AA .

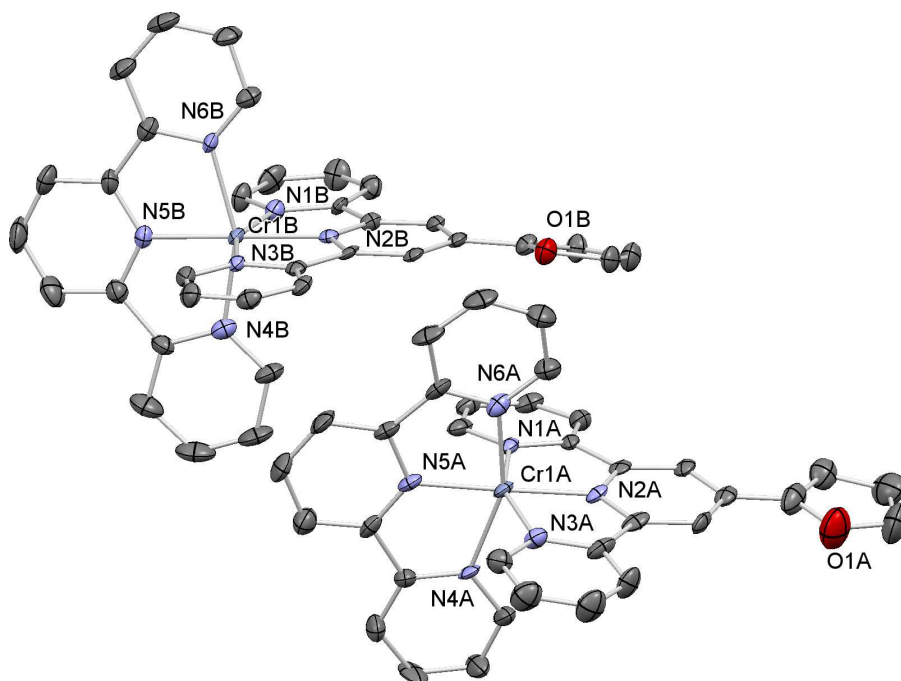


Figure 3.76: The two independent cations in $[\text{Cr}(\text{tpy})(\text{LT8})][\text{PF}_6]_3$ with ellipsoids plotted at 50 % probability level. H atoms, counter ions and solvent molecules are omitted for clarity. Selected bond lengths [\AA]: Cr1A-N1A = 2.060(6), Cr1A-N2A = 1.988(6), Cr1A-N3A = 2.067(6), Cr1A-N4A = 2.077(6), Cr1A-N5A = 1.986(6), Cr1A-N6A = 2.059(6); Cr1B-N1B = 2.067(6), Cr1B-N2B = 1.974(6), Cr1B-N3B = 2.069(6), Cr1B-N4B = 2.056(6), Cr1B-N5B = 1.987(6), Cr1B-N6B = 2.077(6); and bond angles [$^\circ$]: N1A-Cr1A-N2A = 78.3(2), N3A-Cr1A-N2A = 78.6(2), N1A-Cr1A-N3A = 156.8(2), N4A-Cr1A-N5A = 77.9(2), N6A-Cr1A-N5A = 78.8(2), N4A-Cr1A-N4A = 156.8(2), N1B-Cr1B-N2B = 78.6(2), N3B-Cr1B-N2B = 78.3(2), N1B-Cr1B-N3B = 156.9(2), N4B-Cr1B-N5B = 78.7(2), N6B-Cr1B-N5B = 78.2(2), N4B-Cr1B-N6B = 156.9(2).

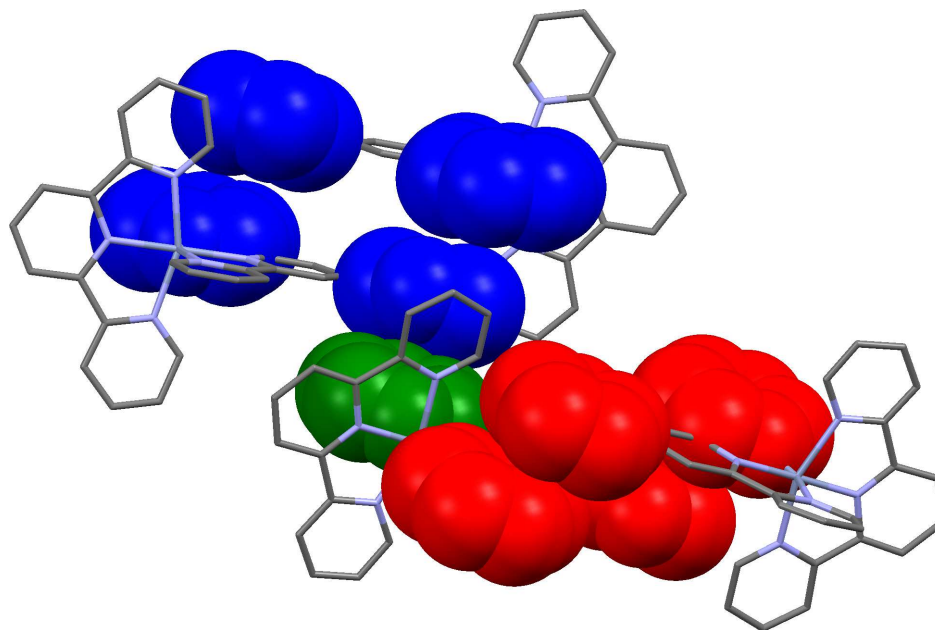


Figure 3.77: Interactions between cations in $[\text{Cr}(\text{tpy})(\text{LT8})][\text{PF}_6]_3$. The plane-to-plane interactions between the rings containing N3A and O1A (red) and N1B and O1B (blue) can be classified as good. However the interactions between N1A and O1B (green - blue) are weak. Counter anions, solvent molecules and H atoms omitted for clarity.

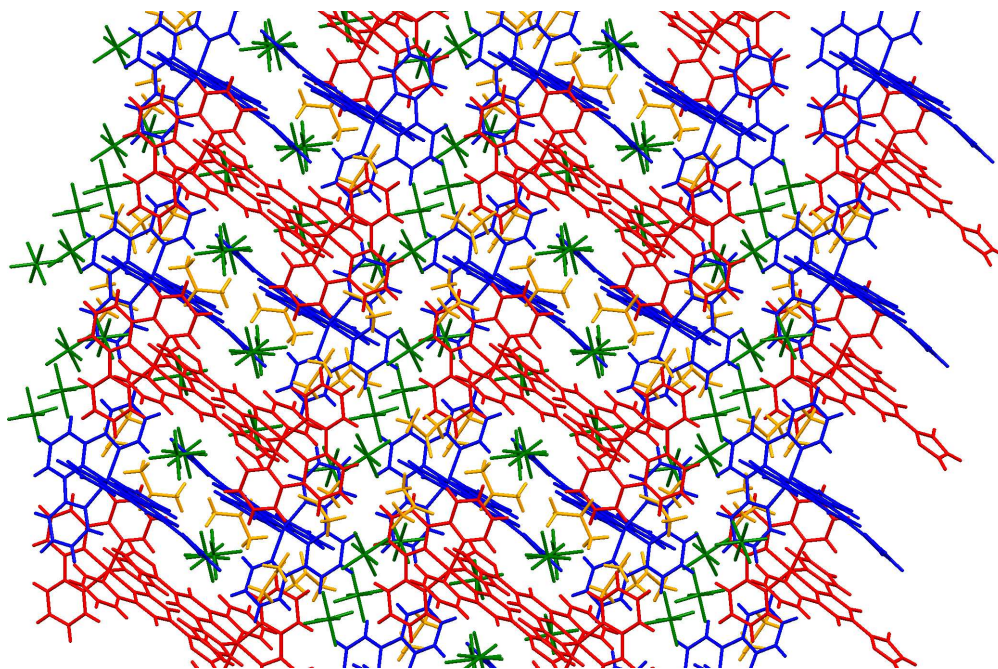


Figure 3.78: $[\text{Cr}(\text{LT8})(\text{tpy})][\text{PF}_6]_3$: The cations A (red) and B (blue) form layers. Additional colour codes: PF_6^- counter anions (green) and solvent molecules (acetone, orange).

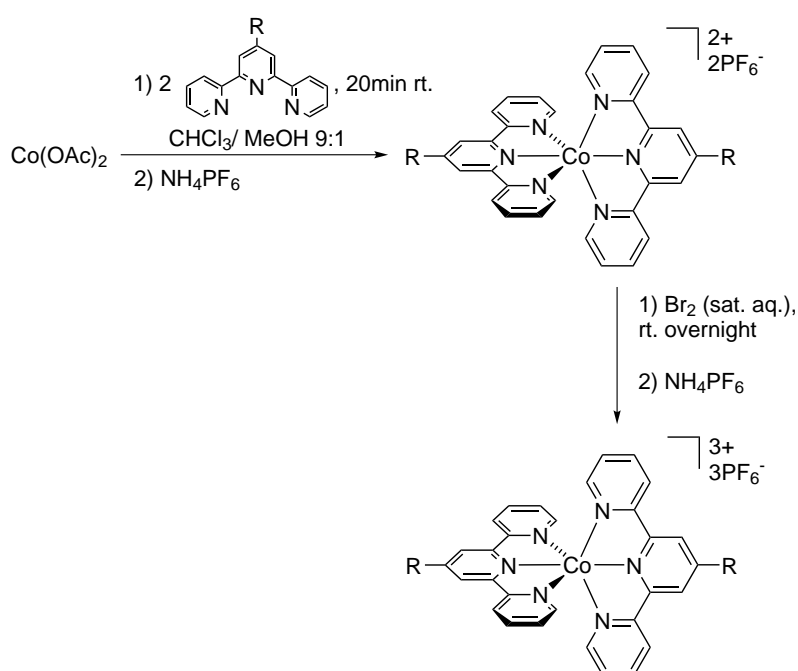
Chapter 4

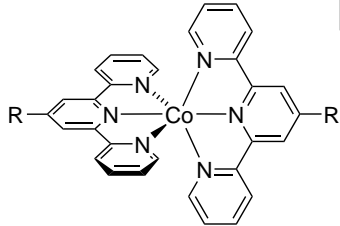
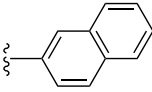
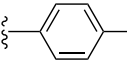
Bis(terpyridine)cobalt(III) complexes

4.1 Synthesis of the bis(terpyridine)cobalt(III) complexes

For the powder EPR measurements diamagnetic analogues of the $\{\text{Cr}(\text{tpy})_2\}^{3+}$ complexes were necessary to prepare magnetically diluted samples (3.7, p. 63). Therefore three different homoleptic $\{\text{Co}(\text{tpy})_2\}^{3+}$ were synthesised (scheme 4.1).

The complexes with $\{\text{Co}(\text{tpy})_2\}^{3+}$ cores have been synthesised according to an established protocol (scheme 4.1) in our group.¹⁶² In the first step the $\{\text{Co}(\text{tpy})_2\}^{2+}$ complex is synthesised. $\text{Co}(\text{OAc})_2 \cdot 4\text{H}_2\text{O}$ and two equivalents of the tpy ligand are stirred for 20 min at room temperature in a $\text{CHCl}_3/\text{MeOH}$ mixture (9:1). The $\{\text{Co}(\text{tpy})_2\}^{2+}$ intermediate was oxidised in a saturated aqueous bromine solution overnight at room temperature, to receive the target $\{\text{Co}(\text{tpy})_2\}^{3+}$ complex.



	<p>R = H</p> <p>exp.: 6.5.1 (p. 141) published earlier by our group^{162,163}</p>	<p>R = </p> <p>exp.: 6.5.2 (p. 141)</p>	<p>R = </p> <p>exp.: 6.5.3 (p. 142)</p>
---	---	---	--

Scheme 4.1: Synthesis pathway to $\{\text{Co}(\text{tpy})_2\}^{3+}$ complexes and overview of the synthesised complexes (exp. = link to the experimental)

Chapter 5

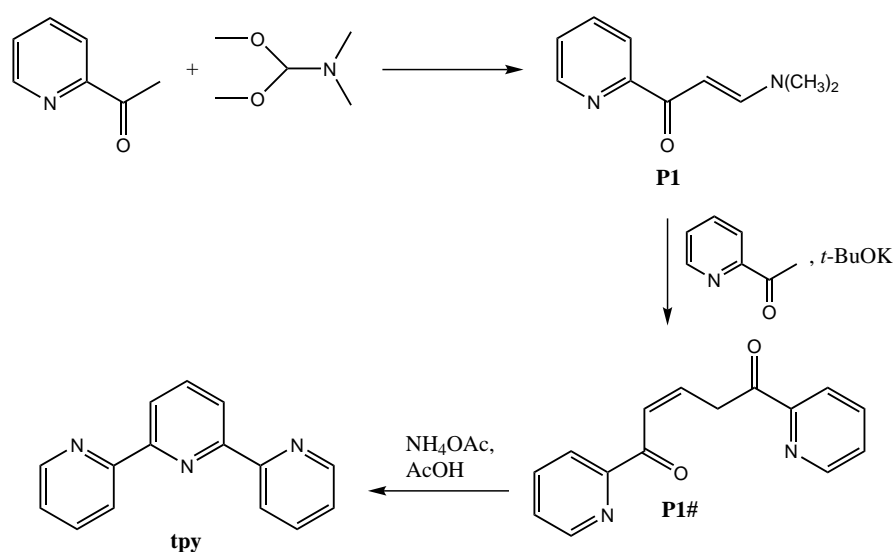
Terpyridine ligand synthesis

5.1 Synthesis of the tpy ligands

2,2':6',2''-Terpyridine (tpy) and derivatives thereof were all synthesised using different ring-assembly methodologies.³⁴

5.1.1 2,2':6',2''-Terpyridine (tpy)

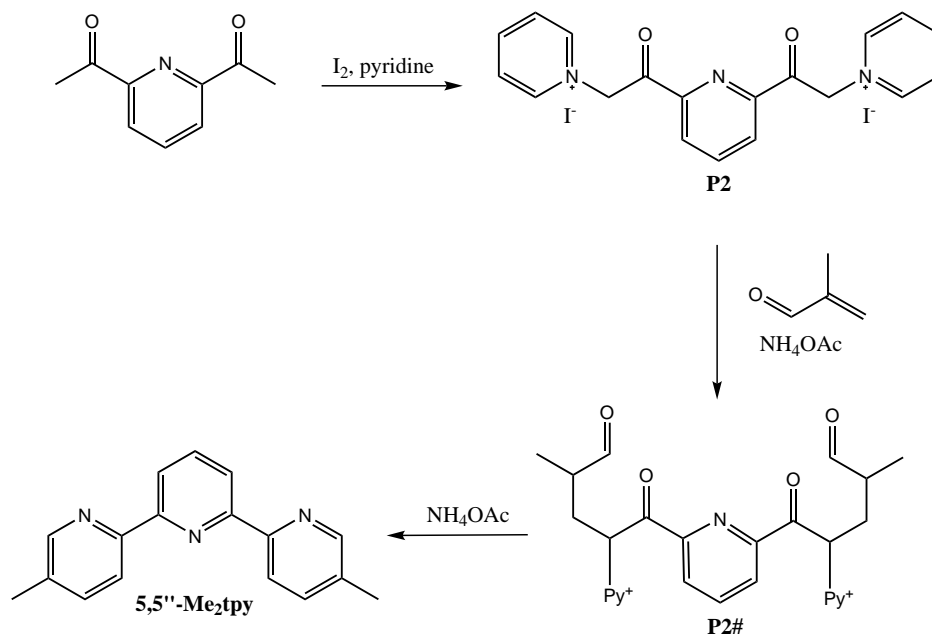
The unsubstituted 2,2':6',2''-terpyridine (tpy) was synthesised by a two step synthesis reported by *Jameson et al.*¹⁶⁴ In the first step the enaminone **P1** (scheme 5.1) is prepared by the reaction of 2-acetylpyridine and *N,N*-dimethylformamide dimethyl acetal. In the second step, the potassium enolate of 2-acetylpyridine reacts with enaminone **P1**, with subsequent loss of dimethyl amine. Closure of the resulting, not isolated, intermediate (Z)-1,5-di(pyridin-2-yl)pent-2-ene-1,5-dione (**P1#**) with ammonium acetate gives 2,2':6',2''-terpyridine (**tpy**). The overall yield is very low, and was in our case 3.1 %.



Scheme 5.1: Synthesis route for 2,2':6',2''-terpyridine (tpy)

5.1.1.1 5,5''-Dimethyl-2,2':6',2''-terpyridine (5,5''-Me₂tpy)

5,5''-Dimethyl-2,2':6',2''-terpyridine (5,5''-Me₂tpy) was synthesised in a two step reaction according to the protocol of *Sasaki et al.*¹⁶⁵ In the first step of this *Kröhnke* reaction¹⁶⁶ the pyridinium salt (**P2**, scheme 5.2) was synthesised by heating 2,6-diacetylpyridine and elemental iodine in pyridine.^{165,167} In the second step methacrolein in formamide forms the (not isolated) intermediate **P2#**.¹⁶⁸ The closure of the two rings with ammonium acetate gives 5,5''-dimethyl-2,2':6',2''-terpyridine (5,5''-Me₂tpy). The overall yield is moderate, and was in our synthesis 55.2 %.

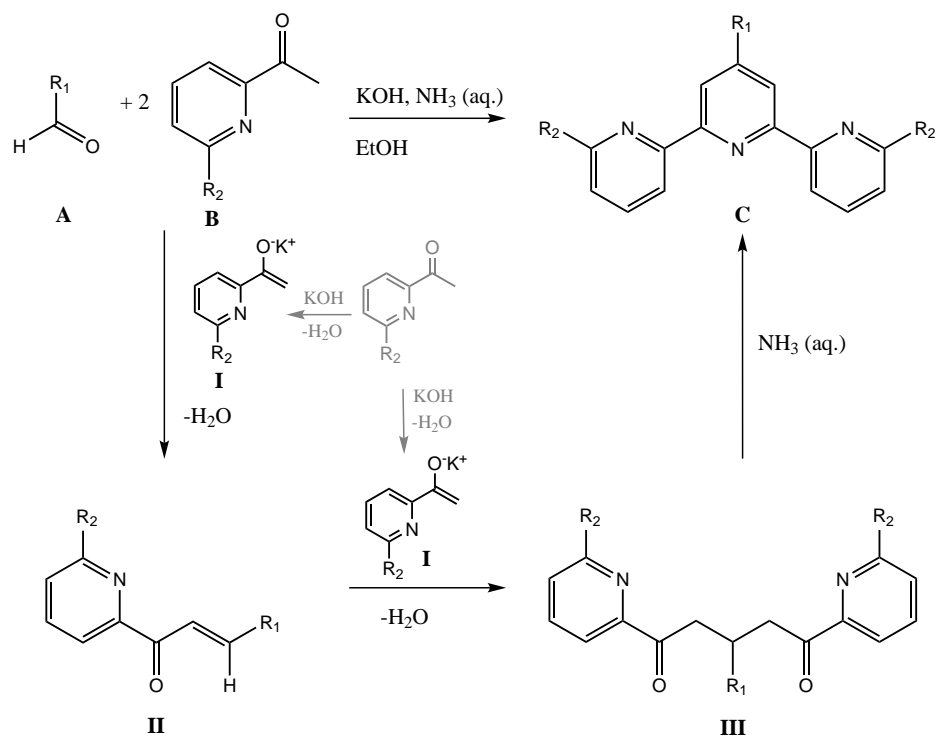


Scheme 5.2: 5,5''-dimethyl-2,2':6',2''-terpyridine (5,5''-Me₂tpy)

5.1.1.2 2,2':6',2''-Terpyridines (tpy) substituted at the 4'-position

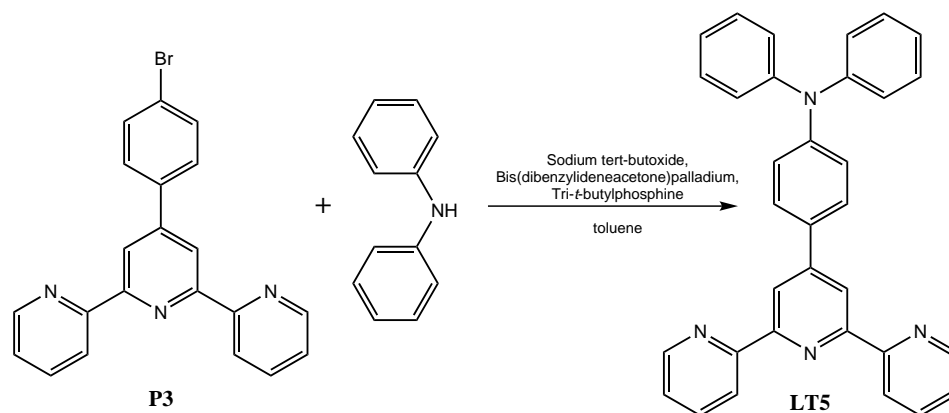
2,2':6',2''-Terpyridines (tpy) which are substituted at the 4'-position were synthesised according to the protocol of *Wang et al.*¹⁶⁹ In an one-pot synthesis, aryl aldehyde (**A**, scheme 5.3) and two equivalents 2-acetylpyridine molecules (**B**) react under basic conditions with ammonia as the nitrogen source to give a 4'-substituted terpyridine (**C**). The enolate (**I**) of 2-acetylpyridine (**B**) can be generated by potassium hydroxide. The intermediate **II** is formed via an aldol condensation¹⁷⁰ of the aryl aldehyde **A** and the first equivalent of the enolate **I**. In the subsequent *Michael*-addition the diketone **III** is formed.¹⁷⁰ In the final ring closing step with aqueous ammonia, the target product was obtained in moderate yields.

The synthesised ligands 4'-(4-tolyl)tpy, LT1 – LT3 and P3 (table in scheme 5.3) were known in the literature.^{169,171,172} To the best of our knowledge, ligand LT4 was not reported before. Also no examples of the reaction starting with 2-acetylpyridine substituted at the 6,6''-positions are published. The yields of these reactions lie between 24.9 and 52.6 % (table in scheme 5.3). The lowest yield is for the synthesis of the sterically more hindered tpy which is substituted at the 6,6''-positions (LT4).



label:	R ₁ :	R ₂ :	yield:	literature:
4'-(4-tolyl)tpy		H	52.6%	Tang <i>et al.</i> ¹⁷¹
LT1		H	37.8%	Constable <i>et al.</i> ¹⁷³
LT2		H	27.7 %	Wang <i>et al.</i> ¹⁶⁹
LT3		H	33.8 %	McMillin <i>et al.</i> ¹³⁹
P3		H	42.2 %	Wang <i>et al.</i> ¹⁶⁹
LT4		Me	24.9 %	not reported

Scheme 5.3: Synthesis of 2,2':6',2''-terpyridines (tpy) substituted in the 4'-position.

5.1.1.3 Synthesis of 4-([2,2':6',2''-terpyridin]-4'-yl)-*N,N*-diphenylaniline (LT5)Scheme 5.4: Synthesis of 4-([2,2':6',2''-terpyridin]-4'-yl)-*N,N*-diphenylaniline (LT5).

Ligand LT5 was first reported by *Goodall et al.*¹⁷² An improved synthetic strategy was previously reported by our group.³⁸ In a palladium catalysed *Buchwald-Hartwig*-coupling^{174,175} 4'-(4-bromophenyl)-2,2':6',2''-terpyridine (P3) reacts with diphenylamine. The overall yield of this two step synthesis is moderate (29.6 %).

5.1.2 Further terpyridine ligands

The following ligands (figure 5.1) were available in the laboratory and used for the synthesis of $\{\text{Cr}(\text{tpy})_2\}^{3+}$. They were synthesised by current or former members of our group or students in the lab course (inorganic chemistry lab course, 4th semester, at the University of Basel).

4-([2,2':6',2''-Terpyridin]-4'-yl)-*N,N*-bis(4-methoxyphenyl)aniline (LT6)

↔ Synthesised by Nik Hostettler.³⁸

4-([2,2':6',2''-Terpyridin]-4'-yl)benzotrile (LT7)

↔ Synthesised by Frank Schaeper.

4'-(Furan-2-yl)-2,2':6',2''-terpyridine (LT8)

↔ Synthesised by Frank Schaeper.¹⁷⁶

4'-(4-(Methylthio)phenyl)-2,2':6',2''-terpyridine (LT9)

↔ Synthesised by Federica Reinders¹⁷⁷

4-([2,2':6',2''-Terpyridin]-4'-yl)phthalic acid (LT10)

↔ Synthesised by Ralf Schmitt.³⁸

4'-(Pyridin-4-yl)-2,2':6',2''-terpyridine (LT11)

↔ Synthesised by students in the lab course, using the protocol of *Wang et al.*¹⁶⁹

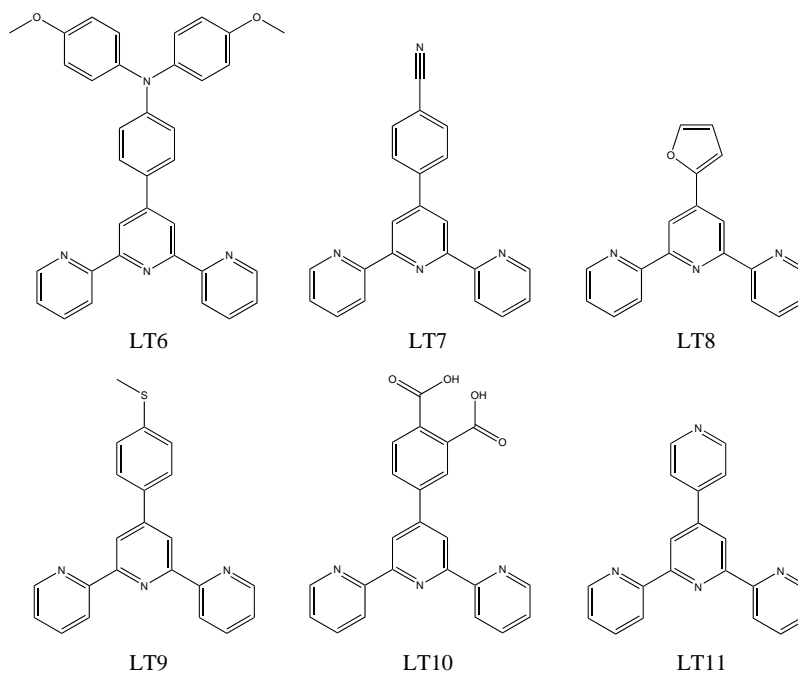


Figure 5.1: Ligands LT6 to LT11 were available in the lab.

5.2 X-ray structure

5.2.1 Structure of $2\{[H_2LT4][CF_3SO_3]_2\}\cdot Et_2O$

The ligand LT4 crystallised in the double protonated form (figure 5.2). The torsion angle between the pyridine rings containing N1 and N2 is 10.6° and between the pyridine ring containing N2 and the phenyl ring (containing C10) is 27.4° . A two fold axis goes through the molecule (axis N2 - C10 - C14). The protons on C14 (50:50) and the CF_3 -moiety of the anion (60:40) are disordered. The anions pack close to the protonated pyridine rings (figure 5.3). The shortest N-H...O distance is 2.09 Å. The ligands form layers controlled by π - π plane to plane interactions between the pyridine rings containing N1. The space between two rows is forced by the toluene moieties and the tubes so formed are occupied by the solvent molecules.

Table 5.1: Crystallographic data of $2\{[H_2LT4][CF_3SO_3]_2\}\cdot Et_2O$

formula moiety	$2(C_{24}H_{23}N_3),$ $4(CF_3O_3S), C_4H_{10}O$	$\mu(Cu-K\alpha)$ [mm^{-1}]	2.227
formula weight	1377.35	T [K]	123
crystal colour and habit	green, block	refln. collected	24747
crystal system	monoclinic	unique refln.	2932
space group	C 2/c	refln. for refinement	2856
	11.4673(5)	parameters	260
a, b, c [Å]	31.9948(13)	threshold	$I > 2.0\sigma$
	8.8068(4)	R1 (R1 all data)	0.0489 (0.0489)
	90.00	wR2 (wR2 all data)	0.1417 (0.1421)
α, β, γ [°]	93.523(2)	goodness of fit	1.107
		crystal growing:	diffusion
			MeCN/ Et_2O
U [Å ³]	90.00		
Dc [Mg m ⁻³]	3225.1(2)		
	1.418		

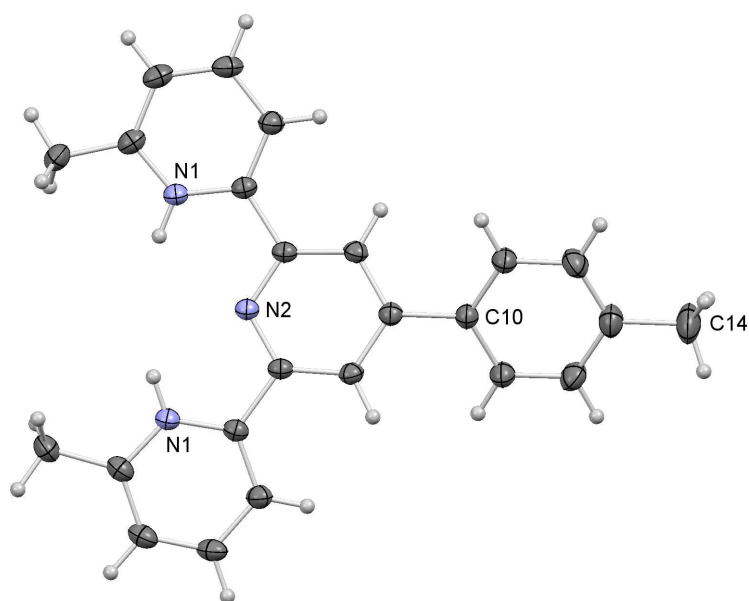


Figure 5.2: $2\{[\text{H}_2\text{LT4}][\text{CF}_3\text{SO}_3]_2\}\cdot\text{Et}_2\text{O}$ with ellipsoids plotted at 50 % probability level. Counter ions and solvent molecules are omitted for clarity. Only one of the disordered positions of the protons on C14 is shown.

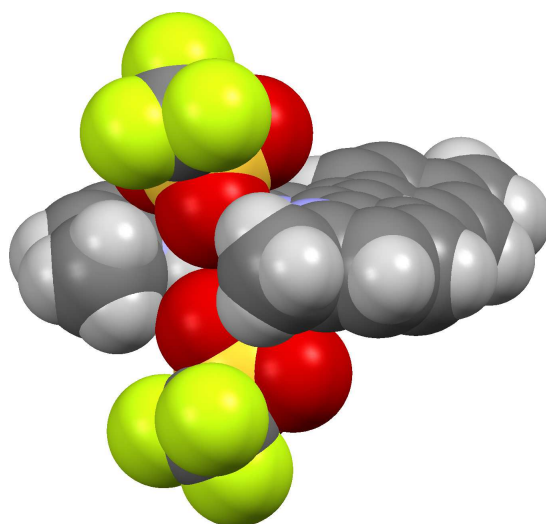


Figure 5.3: Position of the two anions ($[\text{CF}_3\text{SO}_3]^-$) near to the protonated pyridine rings of $[\text{H}_2\text{LT4}]^{2+}$. Only the main form of the disordered anions is shown. The solvent molecule is omitted for clarity.

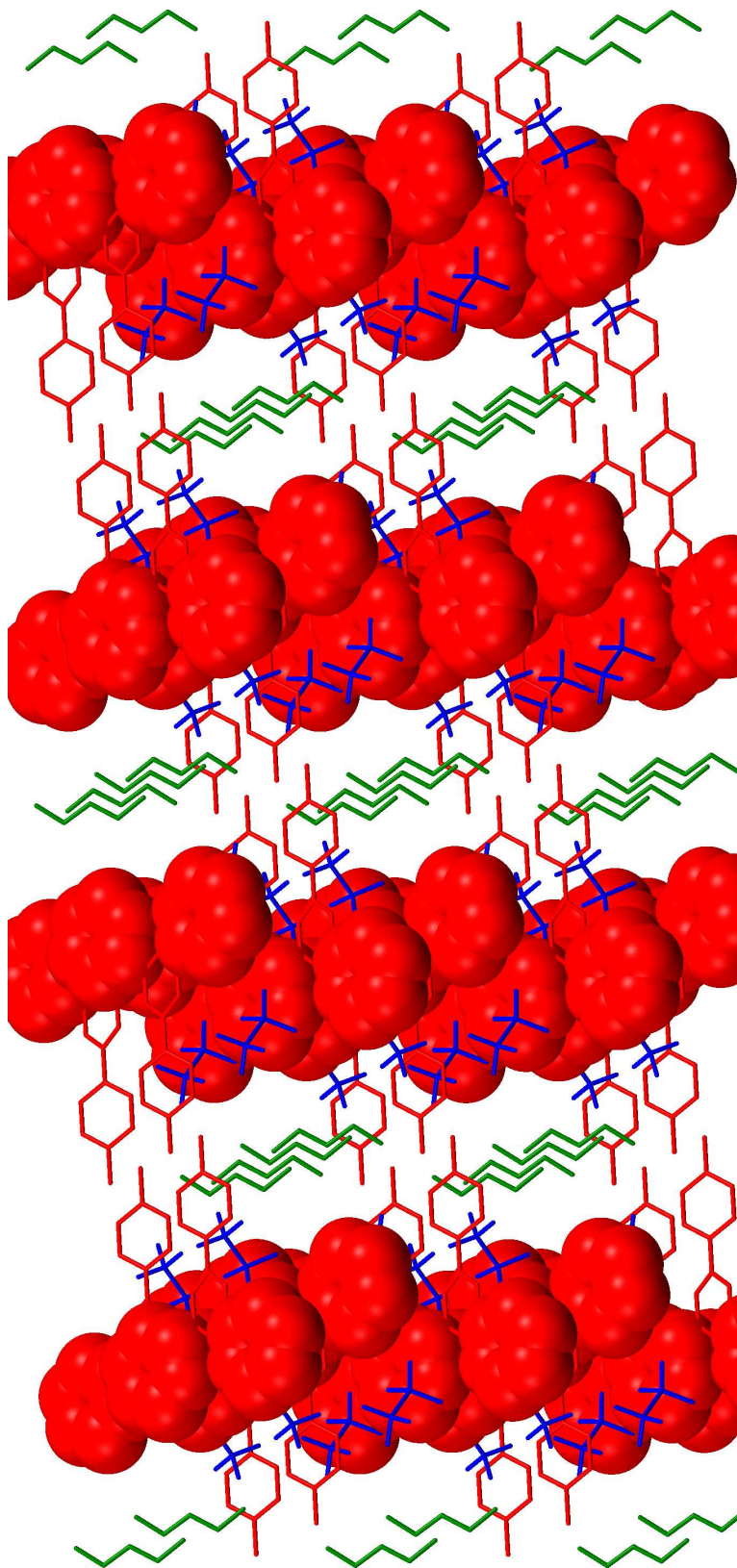


Figure 5.4: Packing of $2\{[H_2LT4][CF_3SO_3]_2\} \cdot Et_2O$. The pyridine rings containing N1 are highlighted in the spacefill style. Colour code: red: cation, blue: anion and green solvent molecule.

Chapter 6

Experimental

6.1 General experimental

If not mentioned otherwise, all starting chemicals were commercially available. They were of reagent grade, and used without further purification. The used solvents were purchased as dry solvents (crown cap), in reagent grade or were distilled.

nuclear magnetic resonance (NMR): ^1H , $^{13}\text{C}\{^1\text{H}\}$ and ^{19}F NMR were recorded on a Bruker AM250 (250 MHz), Bruker DRX400 (400 MHz) or a Bruker DRX500 (500 MHz) spectrometers, respectively on Bruker AvanceIII-250 (250 MHz), AvanceIII-400 (400 MHz) and AvanceIII-500 spectrometers (500 MHz). For the assignment of the ^1H and $^{13}\text{C}\{^1\text{H}\}$ spectra, COSY, DEPT-135, HMBC and HMQC experiments were conducted on the Bruker AvanceIII-500 (500 MHz). For ^1H and $^{13}\text{C}\{^1\text{H}\}$ NMR measurements, the chemical shifts δ are relative and internally referenced to the residual peak of the solvent (acetonitrile: ^1H : 1.940, ^{13}C : 118.690 and chloroform: ^1H : 7.240, ^{13}C : 77.230)ⁱ. All measurements were run at room temperature (295 K (500MHz), 300 K (250 and 400MHz)).

All reported triplets (t) are from the origin not triplets but not resolved doublet of doublets with a very similar coupling constant.

infrared spectroscopy (IR): Infrared spectra were recorded on a Shimadzu FTIR-8400S (with Golden Gate ATR) or on a Perkin Elmer Spectrum Two spectrophotometer (with Universal ATR two) spectrophotometer. Solid samples were measured using the attenuated total reflection (ATR) technique.

electrospray ionisation mass spectrometry (ESI-MS): Mass spectra were measured (in methanol) on a Bruker Esquire 3000^{plus} by *Dr. G. Schneider* or *R. Schmitt*.

matrix-assisted laser desorption/ionization mass spectrometry (MALDI-MS): mass spectra were measured, with 4-nitroaniline as matrix, on a Bruker Daltonics microflex by *S. Müller*.

UV-VIS spectroscopy: UV-VIS spectroscopy measurements were done on an Agilent Technologies UV-Visible 8453 spectrophotometer or on a Varian Cary 5000 spectrophotometer. The measurements were done in HPLC-grade solvents.

ⁱsource: MestReNova, there referenced as *Budavari et al.*¹⁷⁸

photoluminescence: The photoluminescence measurements were performed on a Shimadzu RF-5301PC spectrofluorophotometer.

photoluminescence lifetime: The lifetime of the photoluminescence was measured with an Edinburgh Instruments mini- τ -apparatus, equipped with an EPL-405 picosecond pulsed diode laser ($\lambda_{ex} = 404.2$ nm, pulse width = 78.2 ps, Edinburgh Instruments) with the appropriate wavelength filter, or with a compact fluorescence lifetime spectrometer C11367-11 from Hamamatsu.

elemental analysis (EA): The elemental analyses were measured by *S. Mittelheisser* on an Elementar Vario Micro Cube instrument, or by *W. Kirsch* with a Leco CHN-900 microanalyser.

electrochemistry: Electrochemical measurements were made on a CH Instruments 900B potentiostat. The samples were dissolved in HPLC grade MeCN (10^{-4} to 10^{-5} mol dm $^{-3}$) containing 0.1 mol dm $^{-3}$ [nBu $_4$ N][PF $_6$] as supporting electrolyte. The following electrodes were applied: working (glassy carbon), counter (platinum wire) and pseudo reference (silver wire). Ferrocene was used as internal reference added at the end of the experiments.

X-ray diffraction: Data were collected on a Bruker-Nonius APEX2 diffractometer with data reduction, solution and refinement using the programs APEX2,¹⁷⁹ SIR92¹⁸⁰ and CRYSTALS¹⁸¹ or SHELXL97 or SHELX-13.¹⁸² Visualisation and structural analyses were performed with the software CCDC Mercury (versions 3.0 and 3.3).^{158,183}

sun simulator: The properties of the DSCs were measured with a SolarSim150 (100 W m $^{-2}$ = 1 sun).

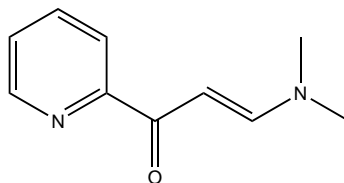
microwave reaction: Microwave reactions were carried out in a Biotage Initiator 8 reactor.

electron paramagnetic resonance (EPR): EPR measurements were performed by *Dr. M. Spulber* or *Dr. R. Mayap Talom* on a Bruker CW EPR Elexsys-500 spectrometer equipped with a variable temperature unit. The spectra were recorded at 295 K and 100 K with the following parameters: microwave power 10 mW, conversion time 61.12 ms, number of scans up to 60, resolution 2048 points, modulation amplitude in the range of 5 G, sweep width 6000 G.

6.2 Synthesis of terpyridine ligands

6.2.1 Synthesis of precursors for terpyridine ligands

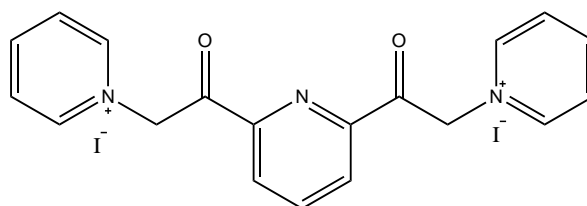
6.2.1.1 3-(Dimethylamino)-1-(pyridin-2-yl)prop-2-en-1-one (P1)



2-Acetylpyridine (17.2 ml, 153 mmol) and *N,N*-dimethylformamide dimethyl acetal (25.0 ml, 187 mmol) were dissolved in toluene (100 ml) and heated to reflux. Methanol was removed with a *Dean-Stark* apparatus. The colour changed to dark red. After 8 h 45 min the reaction was stopped, and allowed to cool to room temperature. The precipitate was separated by filtration and the filtrate stored at 4 °C. Additional precipitate was filtered and the solution refluxed for an additional 8 h. The solution was again stored overnight at room temperature and the separation of the product was carried out as described above. Finally the volume of the solvent was reduced, then cyclohexane was added and again stored at 4 °C overnight. The precipitate was separated by filtration. All solid precipitate of the yellow product were combined (14.3 g, 81.2 mmol, 53.1 %).

$^1\text{H NMR}$ (250 MHz, 298 K, chloroform-*d*) δ /ppm = 8.63 (1 H, ddd, $J = 4.8, 1.8, 0.9$ Hz), 8.14 (1 H, dt, $J = 7.9, 1.1$ Hz), 7.91 (1 H, d, $J = 12.7$ Hz), 7.79 (1 H, td, $J = 7.7, 1.8$ Hz), 7.35 (1 H, ddd, $J = 7.5, 4.8, 1.3$ Hz), 6.45 (1 H, d, $J = 12.7$ Hz), 3.08 (6 H, d, $J = 45.1$ Hz). $^1\text{H NMR}$ spectroscopic data agree with literature data.¹⁶⁴

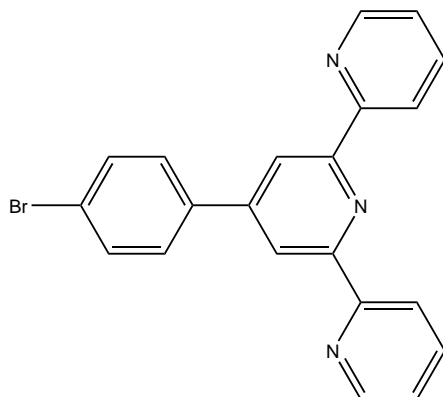
6.2.1.2 1,1'-(Pyridine-2,6-diylbis(2-oxoethane-2,1-diyl))bis(pyridin-1-ium) iodide (P2)



This reaction was executed under a nitrogen atmosphere. 2,6-Diacetylpyridine (2.00 g, 12.3 mmol) and iodine (6.38 g, 25.1 mmol) were separately dissolved in dry pyridine (9 ml each). The iodine solution was then added to the 2,6-diacetylpyridine solution and heated at 100 °C for 6 h. After a short time, the precipitate inhibited the stirring, therefore additional pyridine (5 ml) was added to the reaction mixture. After cooling to room temperature, the crude product was filtered. Recrystallisation from 95 % ethanol gave the beige product (5.12 g, 8.93 mmol, 72.9 %).

$^1\text{H NMR}$ (250 MHz, 298 K, acetonitrile-*d*₃) δ /ppm = 9.16 – 8.86 (4 H, m), 8.67 (2 H, tt, $J = 7.9, 1.4$ Hz), 8.47 – 8.24 (3 H, m), 8.25 – 8.04 (4 H, m), 6.98 (4 H, dd, $J = 2.9, 1.2$ Hz). $^1\text{H NMR}$ spectroscopic data agree with literature data.¹⁸⁴

6.2.1.3 4'-(4-Bromophenyl)-2,2':6',2''-terpyridine (P3)



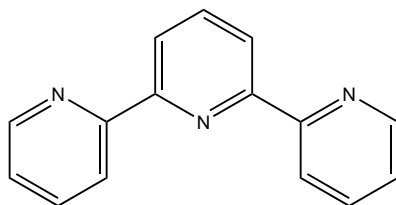
2-Acetylpyridine (4.49 ml, 40.0 mmol) and solid potassium hydroxide (2.24 g, 40.0 mmol) were dissolved in a water/ ethanol mixture (1:1, 100 ml). After stirring at room temperature for 10 min 1-(5-bromopyridin-2-yl)ethan-1-one (3.70 g, 20.0 mmol) was added and allowed to stir for 1 h at room temperature. The colour changed from pale yellow to pale red. Solid potassium hydroxide (3.08 g, 54.9 mmol) was added and the colour turned red. Then aqueous NH_3 (2 ml, conc. 32%) was added and the reaction mixture was heated at reflux for 5 h. The pale yellow precipitate was filtered and washed with cold ethanol. The crude product was recrystallised from ethanol to yield a white powder (3.27 g, 8.22 mmol, 42.2 %).

Although the ^1H NMR spectrum showed some minor impurities, the product was used as the precursor for the synthesis of LT5.

^1H NMR (250 MHz, 298 K, chloroform-d) δ/ppm = 8.73 (2 H, ddd, J = 4.8, 1.8, 0.9 Hz), 8.71 (2 H, s), 8.68 (2 H, dt, J = 8.0, 1.1 Hz), 7.89 (2 H, ddd, J = 8.0, 7.5, 1.8 Hz), 7.82 – 7.73 (2 H, m), 7.68 – 7.61 (2 H, m), 7.37 (2 H, ddd, J = 7.2, 4.6, 1.1 Hz). ^1H NMR spectroscopic data agree with literature data.¹⁸⁵

6.2.2 Terpyridine ligands

6.2.2.1 2,2':6',2''-Terpyridine (tpy)

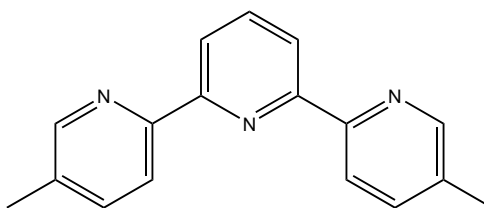


This reaction was executed under a nitrogen atmosphere. 2-Acetylpyridine (9.84 g, 81.2 mmol) and potassium *tert*-butoxide (18.2 g, 162 mmol) were suspended in anhydrous THF (500 ml). After stirring for 2 h at room temperature P1 (14.3 g, 81.2 mmol) was added and a colour change occurred from yellow to dark red. The reaction mixture was stirred overnight at room temperature. Then ammonium acetate (18.2 g, 162 mmol) was added successively followed by acetic acid (250 ml). The colour changed to black and after 15 min the reaction mixture was completely dissolved. The THF and as much as possible of the acetic acid were removed on the rotary evaporator, leaving a black, oily residue. The residue was suspended in water

(500 ml) and solid sodium carbonate was added until effervescing stopped. The mixture was extracted three times with dichloromethane (200 ml). The combined organic phases were dried over magnesium sulfate, filtered and evaporated to a black oil. The crude product was purified with a silica column (long and wide) using toluene as eluent. The combined fractions were recrystallised from hot hexane to remove some insoluble red residue. Tpy was isolated as a white powder (1.13 g, 4.83 mmol, 5.94 %).

$^1\text{H NMR}$ (400 MHz, 298 K, chloroform-d) δ/ppm = 8.71 (2 H, ddd, J = 4.8, 1.8, 0.9 Hz), 8.63 (2 H, dt, J = 8.0, 1.1 Hz), 8.46 (2 H, d, J = 7.8 Hz), 7.97 (1 H, t, J = 7.8 Hz), 7.86 (2 H, ddd, J = 8.0, 7.5, 1.8 Hz), 7.34 (2 H, ddd, J = 7.5, 4.8, 1.2 Hz). $^1\text{H NMR}$ spectroscopic data agree with literature data.¹⁶⁴

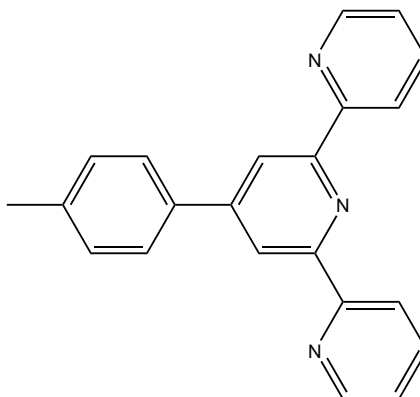
6.2.2.2 5,5''-Dimethyl-2,2':6',2''-terpyridine (5,5''-Me₂tpy)



To a solution P2 (5.10 g, 8.90 mmol) in formamide (60 ml), ammonium acetate (10.3 g, 133 mmol) and methacrolein (2.06 ml, 2.00 mmol) were added. Heating at 100 °C overnight yielded after short time in a precipitate. After cooling to room temperature, the precipitate was filtered, washed with water and dried. 5,5''-Me₂tpy was isolated as a white powder (1.76 g, 6.73 mmol, 75.7 %).

$^1\text{H NMR}$ (400 MHz, 298 K, chloroform-d) δ/ppm = 8.57 – 8.47 (4 H, m), 8.38 (2 H, d, J = 7.8 Hz), 7.92 (1 H, t, J = 7.8 Hz), 7.71 – 7.60 (2 H, m), 2.42 (6 H, d, J = 0.7 Hz). $^1\text{H NMR}$ spectroscopic data agree with the literature data.¹⁶⁵

6.2.2.3 4'-(4-Tolyl)-2,2':6',2''-terpyridine (4'-(4-tolyl)tpy)

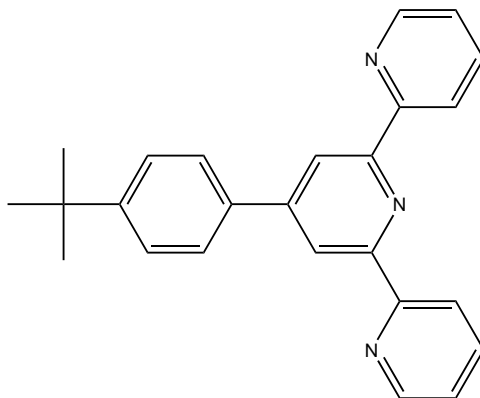


2-Acetylpyridine (4.50 ml, 40.1 mmol) and 4-methylbenzaldehyde (2.38 ml, 20.1 mmol) were dissolved in ethanol (100 ml). Solid potassium hydroxide (3.08 g, 54.9 mmol) was added and the colour turned red. After all potassium hydroxide was dissolved, aqueous NH₃ (60 ml, conc. 32%) was added and stirred overnight at 35°C. The formed pale yellow precipitate was filtered and washed with cold ethanol. The crude product was recrystallised from ethanol to yield white

needles (3.41 g, 10.6 mmol, 52.6 %).

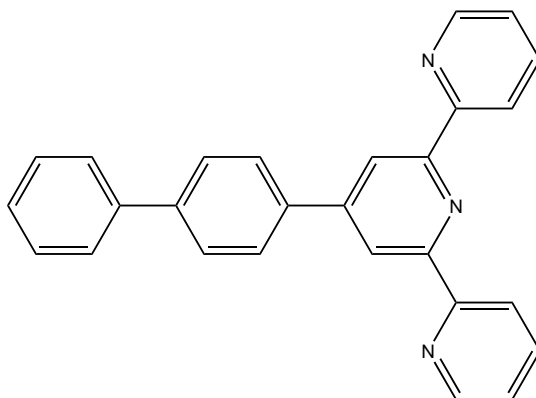
$^1\text{H NMR}$ (250 MHz, 298 K, chloroform-d) δ/ppm = 8.79 – 8.68 (4 H, m), 8.67 (2 H, dt, J = 8.0, 1.1 Hz), 7.94 – 7.77 (4 H, m), 7.30 - 7.33 (4 H, m), 2.43 (3 H, s). $^1\text{H NMR}$ spectroscopic data agree with the literature data.¹⁷¹

6.2.2.4 4'-(4-(*tert*-Butyl)phenyl)-2,2':6',2''-terpyridine (LT1)



2-Acetylpyridine (2.24 ml, 20.0 mmol) and 4-*tert*-butylbenzaldehyde (1.94 ml, 10.0 mmol) were dissolved in ethanol (50 ml). Solid potassium hydroxide (1.12 g, 20.0 mmol) was added and the colour turned red. After all the potassium hydroxide had dissolved, aqueous NH_3 (1 ml, conc. 32%) was added and the mixture was stirred overnight at room temperature. The pale yellow precipitate was filtered and washed with cold ethanol. The crude product was recrystallised from ethanol with some drops of chloroform to yield a white powder (1.38 g, 3.78 mmol, 37.8%). $^1\text{H NMR}$ (400 MHz, 298 K, chloroform-d) δ/ppm = 8.76 – 8.71 (4 H, m), 8.67 (2 H, dt, J = 8.1, 1.1 Hz), 7.92 – 7.83 (4 H, m), 7.56 – 7.49 (2 H, m), 7.35 (2 H, ddd, J = 7.5, 4.8, 1.2 Hz), 1.38 (9 H, s). $^1\text{H NMR}$ spectroscopic data agree with literature data.¹⁷³

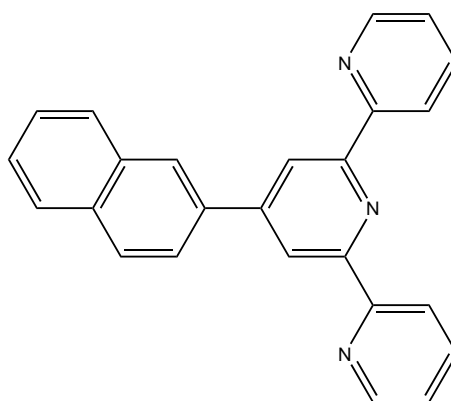
6.2.2.5 4'-([1,1'-Biphenyl]-4-yl)-2,2':6',2''-terpyridine (LT2)



The compound was prepared by the same method as LT1. 2-Acetylpyridine (2.24 ml, 20.0 mmol) and [1,1'-biphenyl]-4-carbaldehyde (1.82 g, 10.0 mmol) were dissolved in ethanol (50 ml). Then solid potassium hydroxide (1.12 g, 20.0 mmol) and aqueous NH_3 (30 ml, conc. 32%) were added. The target product was isolated as a white powder (1.07 g, 2.77 mmol, 27.7%).

$^1\text{H NMR}$ (400 MHz, 298 K, chloroform- d) δ/ppm = 8.80 (2 H, s), 8.75 (2 H, ddd, J = 4.8, 1.9, 0.9 Hz), 8.69 (2 H, dt, J = 7.9, 1.1 Hz), 8.07 – 7.97 (2 H, m), 7.89 (2 H, td, J = 7.7, 1.8 Hz), 7.78 – 7.72 (2 H, m), 7.71 – 7.65 (2 H, m), 7.53 – 7.45 (2 H, m), 7.42 – 7.33 (3 H, m). $^1\text{H NMR}$ spectroscopic data agree with literature data.¹⁸⁶

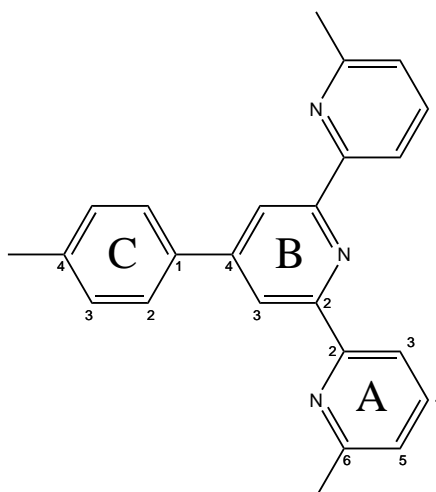
6.2.2.6 4'-(Naphthalen-2-yl)-2,2':6',2''-terpyridine (LT3)



The compound was prepared by the same method as LT1. 2-Acetylpyridine (2.24 ml, 20.0 mmol) and 2-naphthaldehyde (1.36 ml, 10.0 mmol) were dissolved in ethanol (50 ml). Then solid potassium hydroxide (1.12 g, 20.0 mmol) and aqueous NH_3 (1 ml, conc. 32%) were added. The target product was isolated as a white needles (1.22 g, 3.38 mmol, 33.8%).

$^1\text{H NMR}$ (250 MHz, 298 K, chloroform- d) δ/ppm = 8.94 – 8.84 (2 H, m), 8.75 - 8.77 (2 H, m), 8.69 - 8.73 (2 H, m), 8.42 (1 H, s), 8.12 – 7.82 (6 H, m), 7.62 – 7.49 (2 H, m), 7.38 (2 H, ddd, J = 7.5, 4.8, 1.3 Hz). $^1\text{H NMR}$ spectroscopic data agree with literature data.¹³⁹

6.2.2.7 6,6''-Dimethyl-4'-(*p*-tolyl)-2,2':6',2''-terpyridine (LT4)

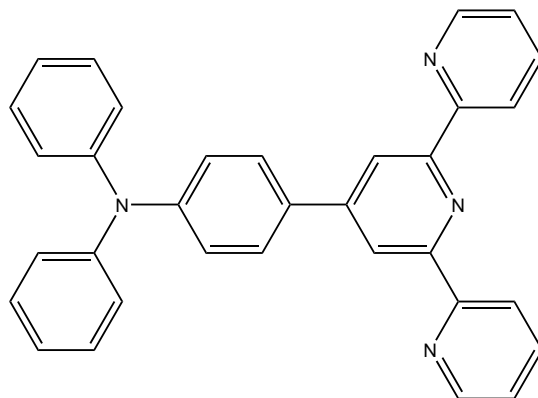


The compound was prepared by the same method as LT1. 1-(6-Methylpyridin-2-yl)ethan-1-one (1.57 ml, 12.0 mmol) and 4-methylbenzaldehyde (0.710 ml, 6.00 mmol) were dissolved in ethanol (30 ml). Then solid potassium hydroxide (673 mg, 12.0 mmol) and aqueous NH_3 (1 ml, conc. 32%) were added. The crude product was redissolved in CH_2Cl_2 and washed three times

with water, dried over MgSO_4 and evaporated to dryness. The residue was recrystallised from ethanol with some drops of chloroform. The target product was isolated as a white powder (526 mg, 1.50 mmol, 24.9%).

$^1\text{H NMR}$ (400 MHz, 298 K, chloroform- d) δ/ppm = 8.71 (s, 2H, B_3), 8.44 (d, J = 7.8 Hz, 2H, A_3), 7.91 – 7.78 (m, 2H, C_2), 7.75 (t, J = 7.7 Hz, 2H, A_4), 7.35 - 7.32 (m, 2H, C_3), 7.20 (d, J = 7.6 Hz, 2H, A_5), 2.67 (s, 6H, A_{Me}), 2.44 (s, 3H, C_{Me}). $^{13}\text{C}\{^1\text{H}\}$ NMR (101 MHz, 298 K, chloroform- d) δ/ppm = 158.0 (A_6), 156.3 (A_2/B_2), 156.0 (A_2/B_2), 150.2 (B_4), 139.0 (C_4), 137.1 (A_4), 136.1 (C_1), 129.7 (C_3), 127.3 (C_2), 123.4 (A_5), 118.8 (B_3), 118.5 (A_3), 24.9 (A_{Me}), 21.4 (C_{Me}). **IR:** (solid, ν/cm^{-1}) 539 (s), 564 (m), 586 (w), 630 (m), 639 (m), 651 (m), 662 (s), 719 (w), 739 (m), 747 (s), 750 (s), 759 (m), 764 (m), 799 (s), 822 (m), 896 (m), 991 (w), 1019 (w), 1038 (w), 1064 (w), 1086 (w), 1115 (w), 1125 (w), 1156 (w), 1187 (w), 1212 (w), 1258 (w), 1269 (w), 1387 (m), 1391 (m), 1412 (m), 1464 (m), 1516 (m), 1540 (m), 1569 (s), 1572 (s), 1580 (m), 1605 (w), 1613 (w), 2921 (w), 3989 (m). **EA:** Found C 81.84, H 6.02, N 11.96; $\text{C}_{24}\text{H}_{21}\text{N}_3$ requires C 82.02, H 6.06, N 12.27.

6.2.2.8 4-([2,2':6',2''-Terpyridin]-4'-yl)-*N,N*-diphenylaniline (LT5)



This reaction was executed under a nitrogen atmosphere. P3 (3.27 g, 8.42 mmol) and diphenylamine (1.43 g, 8.42 mmol) were suspended in toluene (60 ml). After adding sodium *tert*-butoxide (1.05 g, 10.9 mmol) the colour changed to orange. Bis(dibenzylideneacetone)palladium (96.9 mg, 0.168 mmol) and tri-*tert*-butylphosphine (13.8 mg, 0.168 mmol) were suspended separately in toluene (4 ml) and added to the reaction mixture with a syringe. The solution turned purple and was heated at 100 °C for 16 h. The reaction mixture was filtered hot through celite. The solution was evaporated to dryness and washed with ethanol. The crude product was then recrystallised twice from ethanol and some drops of chloroform. The target product was isolated as a brown powder (2.79 g, 5.86 mmol, 69.6%).

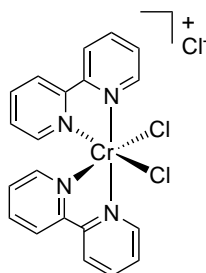
$^1\text{H NMR}$ (400 MHz, 298 K, chloroform- d) δ/ppm = 8.74 – 8.69 (m, 4H), 8.67 (dt, J = 8.0, 1.1 Hz, 2H), 7.88 (ddd, J = 8.0, 7.5, 1.8 Hz, 2H), 7.82 – 7.76 (m, 2H), 7.37 – 7.27 (m, 6H), 7.19 – 7.13 (m, 6H), 7.11 – 7.04 (m, 2H). $^1\text{H NMR}$ spectroscopic data agree with literature data.¹⁸⁶

6.3 Synthesis of tris(diimine)chromium(III) complexes

All bipyridine ligands were available commercially and used without further purification.

6.3.1 Synthesis of the $\{\text{Cr}(\text{NN})_2\text{Cl}_2\}\text{Cl}^-$ type precursors

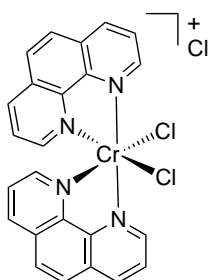
6.3.1.1 $[\text{Cr}(\text{bpy})_2\text{Cl}_2]\text{Cl}$



Anhydrous CrCl_3 (3.00 g, 18.9 mmol) and bpy (9.40 g, 60.2 mmol) were suspended in EtOH (100 ml). The reaction mixture was heated to reflux, and then traces of zinc powder were added. After a short time, the mixture turned black. The reaction was heated at reflux for 2.5 h, then the reaction mixture was cooled in an ice bath, yielding a green precipitate. The precipitate was recrystallised from water and filtered hot. $[\text{Cr}(\text{bpy})_2\text{Cl}_2]\text{Cl}$ was isolated as a pale brown solid (2.99 g, 9.52 mmol, 50.3 %).

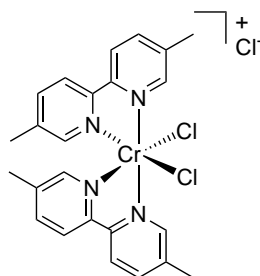
IR: (solid, ν/cm^{-1}) 648 (w), 654 (m), 669 (m), 730 (s), 741 (w), 765 (s), 770 (s), 804 (s), 821 (s), 852 (w), 904 (w), 1015 (w), 1033 (m), 1113 (w), 1175 (w), 1242 (w), 1280 (w), 1321 (w), 1430 (w), 1446 (m), 1472 (w), 1504 (w), 1568 (w), 1606 (m), 3119 (w).

6.3.1.2 $[\text{Cr}(\text{phen})_2\text{Cl}_2]\text{Cl}$



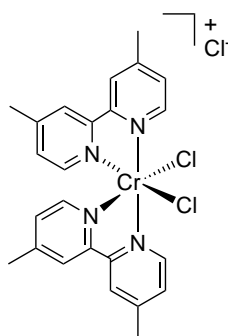
Anhydrous CrCl_3 (3.00 g, 18.9 mmol) and phen (10.3 g, 56.8 mmol) were suspended in EtOH (100 ml). The reaction mixture was heated to reflux, and then zinc powder (18.6 mg, 0.284 mmol) was added. After a short time, the mixture turned black. The reaction was heated at reflux for 30 min, then the reaction mixture was cooled to 0 °C, yielding a green precipitate. The precipitate was recrystallised from water and filtered hot. $[\text{Cr}(\text{phen})_2\text{Cl}_2]\text{Cl}$ was isolated as a greyish solid (8.36 g, 16.1 mmol, 85.0 %).

IR: (solid, ν/cm^{-1}) 513 (s), 654 (w), 717 (s), 740 (m), 784 (w), 830 (w), 851 (s), 876 (m), 913 (w), 1107 (w), 1151 (w), 1211 (w), 1308 (w), 1341 (w), 1425 (m), 1519 (m), 1581 (w), 1606 (w), 1630 (w), 3044 (w), 3351 (w).

6.3.1.3 $[\text{Cr}(5,5'\text{-Me}_2\text{bpy})_2\text{Cl}_2]\text{Cl}$ 

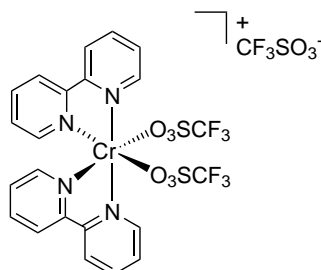
Anhydrous CrCl_3 (516 mg, 3.26 mmol) and 5,5'- Me_2bpy (1.50 g, 8.14 mmol) were suspended in EtOH (15 ml). The reaction mixture was heated to reflux, and then zinc powder (3.19 mg, 0.0488 mmol) was added. After a short time, the mixture turned black. The reaction was heated at reflux for 45 min, then the reaction mixture was cooled to room temperature, yielding a green precipitate. The precipitate was recrystallised from water and filtered hot. $[\text{Cr}(5,5'\text{-Me}_2\text{bpy})_2\text{Cl}_2]\text{Cl}$ was isolated as a bark green solid (526 mg, 1.33 mmol, 40.9 %).

MS: (ESI, m/z): 490.1 $[\text{M}-\text{Cl}]^+$ (calc. 490.08). **IR:** (solid, ν/cm^{-1}) 651 (m), 662 (s), 670 (m), 727 (s), 768 (w), 826 (m), 852 (s), 857 (w), 918 (w), 927 (w), 999 (m), 1003 (w), 1040 (m), 1056 (s), 1060 (w), 1144 (m), 1146 (w), 1155 (w), 1232 (m), 1251 (m), 1295 (w), 1320 (m), 1390 (m), 1447 (w), 1474 (m), 1504 (m), 1578 (m), 1599 (w), 1610 (w), 2953 (w), 3013 (w). **EA:** Found C 53.96, H 4.44, N 10.38; $\text{C}_{24}\text{H}_{24}\text{Cl}_3\text{CrN}_4 \cdot 0.5\text{H}_2\text{O}$ requires C 53.80, H 4.70, N 10.46.

6.3.1.4 $[\text{Cr}(4,4'\text{-Me}_2\text{bpy})_2\text{Cl}_2]\text{Cl}$ 

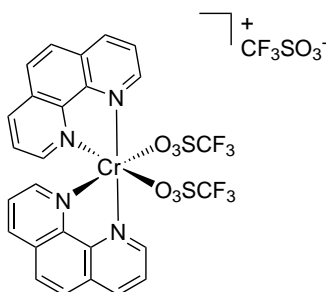
Anhydrous CrCl_3 (573 mg, 3.62 mmol) and 4,4'- Me_2bpy (2.00 g, 10.9 mmol) were suspended in EtOH (20 ml). The reaction mixture was heated to reflux, and then zinc powder (3.55 mg, 0.0543 mmol) was added. After a short time, the mixture turned black. The reaction was heated at reflux for 20 min, then the reaction mixture was cooled at room temperature, yielding a green precipitate. The precipitate was recrystallised from water and filtered hot. $[\text{Cr}(4,4'\text{-Me}_2\text{bpy})_2\text{Cl}_2]\text{Cl}$ was isolated as a greyish solid (415 mg, 0.788 mmol, 21.8 %).

MS: (ESI, m/z): 490.2 $[\text{M}-\text{Cl}]^+$ (calc. 490.08). **IR:** (solid, ν/cm^{-1}) 562 (m), 828 (s), 903 (m), 926 (m), 1028 (s), 1239 (s), 1243 (m), 1279 (m), 1308 (m), 1377 (w), 1411 (m), 1412 (m), 1484 (m), 1486 (m), 1553 (m), 1615 (s), 3005 (w), 3398 (w). **EA:** Found C 52.46, H 4.96, N 10.53; $\text{C}_{24}\text{H}_{24}\text{Cl}_3\text{CrN}_4 \cdot \text{H}_2\text{O}$ requires C 52.91, H 4.70, N 10.46.

6.3.2 Synthesis of the $\{\text{Cr}(\text{NN})_2(\text{CF}_3\text{SO}_3)_2\}(\text{CF}_3\text{SO}_3)^-$ type precursors6.3.2.1 $[\text{Cr}(\text{bpy})_2(\text{CF}_3\text{SO}_3)_2][\text{CF}_3\text{SO}_3]$ 

$[\text{Cr}(\text{bpy})_2\text{Cl}_2]\text{Cl}$ (1.00 g, 2.13 mmol) was dissolved in $\text{CF}_3\text{SO}_3\text{H}$ (5.0 ml, 56 mmol) and the dark red solution was stirred overnight at room temperature. The reaction was then cooled to 0 °C and Et_2O (90 ml) was added, yielding an orange precipitate. The solid was separated by filtration, washed with Et_2O and dried under an air stream. $[\text{Cr}(\text{bpy})_2(\text{CF}_3\text{SO}_3)_2][\text{CF}_3\text{SO}_3]$ was isolated as a pale orange solid (1.66 g, 2.05 mmol, 96.2 %).

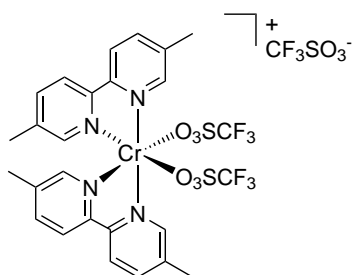
IR: (solid, ν/cm^{-1}) 621 (s), 633 (s), 727 (s), 768 (s), 772 (m), 971 (m), 998 (s), 1013 (s), 1030 (s), 1074 (w), 1151 (m), 1159 (s), 1177 (m), 1192 (m), 1198 (m), 1234 (m), 1261 (m), 1274 (m), 1343 (s), 1448 (m), 1474 (m), 1503 (w), 1570 (w), 1605 (m), 1700 (w).

6.3.2.2 $[\text{Cr}(\text{phen})_2(\text{CF}_3\text{SO}_3)_2][\text{CF}_3\text{SO}_3]$ 

$[\text{Cr}(\text{phen})_2\text{Cl}_2]\text{Cl}$ (1.50 g, 2.89 mmol) was dissolved in $\text{CF}_3\text{SO}_3\text{H}$ (7.0 ml, 79 mmol) and the dark red solution was stirred overnight at room temperature. The reaction was then cooled to 0 °C and Et_2O (90 ml) was added, yielding a dark red precipitate. The solid was separated by filtration, washed with Et_2O and dried under an air stream. $[\text{Cr}(\text{phen})_2(\text{CF}_3\text{SO}_3)_2][\text{CF}_3\text{SO}_3]$ was isolated as a pale purple solid (1.98 g, 2.83 mmol, 97.9 %).

IR: (solid, ν/cm^{-1}) 632 (s), 720 (s), 741 (m), 848 (s), 877 (m), 1026 (s), 1109 (s), 1145 (s), 1221 (s), 1241 (s), 1285 (s), 1415 (w), 1428 (m), 1497 (w), 1522 (m), 1585 (w), 1609 (w), 1636 (w), 3066 (w), 3101 (w), 3294 (w).

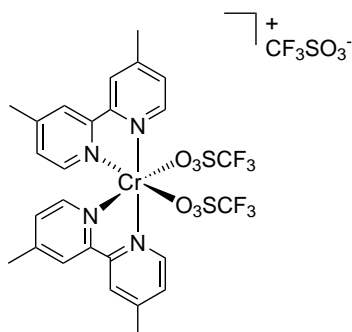
6.3.2.3 $[\text{Cr}(5,5'\text{-Me}_2\text{bpy})_2(\text{CF}_3\text{SO}_3)_2][\text{CF}_3\text{SO}_3]$



$[\text{Cr}(5,5'\text{-Me}_2\text{bpy})_2\text{Cl}_2]\text{Cl}$ (112 mg, 0.213 mmol) was dissolved in $\text{CF}_3\text{SO}_3\text{H}$ (0.5 ml, 6 mmol) and the dark red solution was stirred overnight at room temperature. The reaction was then cooled to 0°C and Et_2O (50 ml) was added, yielding an orange precipitate. The solid was separated by filtration, washed with Et_2O and dried under an air stream. $[\text{Cr}(5,5'\text{-Me}_2\text{bpy})_2(\text{CF}_3\text{SO}_3)_2][\text{CF}_3\text{SO}_3]$ was isolated as an orange solid (121 mg, 0.172 mmol, 80.6 %).

IR: (solid, ν/cm^{-1}) 631 (s), 667 (w), 725 (m), 759 (m), 833 (m), 839 (m), 852 (m), 1021 (s), 1059 (m), 1161 (s), 1200 (m), 1230 (m), 1287 (m), 1311 (m), 1393 (w), 1475 (m), 1605 (w), 2852 (w), 3045 (w), 3363 (w). **EA:** Found C 35.22, H 3.62, N 6.33; $\text{C}_{27}\text{H}_{24}\text{CrF}_9\text{N}_4\text{O}_9\text{S}_3 \cdot 2\text{H}_2\text{O}$ requires C 35.88, H 3.12, N 6.20.

6.3.2.4 $[\text{Cr}(4,4'\text{-Me}_2\text{bpy})_2(\text{CF}_3\text{SO}_3)_2][\text{CF}_3\text{SO}_3]$

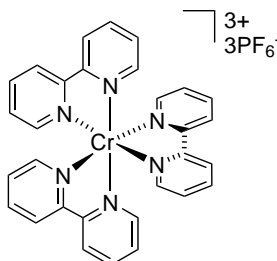


$[\text{Cr}(4,4'\text{-Me}_2\text{bpy})_2\text{Cl}_2]\text{Cl}$ (350 mg, 0.664 mmol) was dissolved in $\text{CF}_3\text{SO}_3\text{H}$ (1.5 ml, 17 mmol) and the dark red solution was stirred overnight at room temperature. The reaction was then cooled to 0°C and Et_2O (100 ml) was added, yielding a dark red precipitate. The solid was separated by filtration, washed with Et_2O and dried under an air stream. $[\text{Cr}(4,4'\text{-Me}_2\text{bpy})_2(\text{CF}_3\text{SO}_3)_2][\text{CF}_3\text{SO}_3]$ was isolated as an orange solid (391 mg, 0.551 mmol, 82.9 %).

IR: (solid, ν/cm^{-1}) 512 (s), 567 (s), 628 (s), 729 (w), 759 (m), 821 (m), 827 (m), 926 (w), 1020 (s), 1153 (s), 1170 (s), 1203 (s), 1234 (m), 1294 (s), 1416 (w), 1445 (w), 1486 (w), 1500 (w), 1553 (w), 1616 (m), 1625 (m), 2964 (w). **EA:** Found C 35.98, H 3.27, N 6.47; $\text{C}_{27}\text{H}_{24}\text{CrF}_9\text{N}_4\text{O}_9\text{S}_3 \cdot 1.5\text{H}_2\text{O}$ requires C 36.25, H 3.04, N 6.26.

6.3.3 Synthesis of the $\{\text{Cr}(\text{NN})_3\}$ complexes

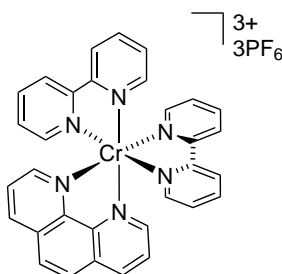
6.3.3.1 $[\text{Cr}(\text{bpy})_3][\text{PF}_6]_3$



$[\text{Cr}(\text{bpy})_2\text{Cl}_2]\text{Cl}$ (188 mg, 0.399 mmol) was dissolved in $\text{CF}_3\text{SO}_3\text{H}$ (1.4 ml, 16 mmol) and the dark red solution was stirred at room temperature overnight. The reaction was then cooled to 0°C and Et_2O (20 ml) was added, yielding a dark red precipitate of $[\text{Cr}(\text{bpy})_2(\text{CF}_3\text{SO}_3)_2][\text{CF}_3\text{SO}_3]$. This was separated by filtration onto a *Schlenk* frit, was washed with Et_2O and dried under a flow of N_2 . The flask attached to the *Schlenk* frit was replaced by a two necked round-bottom flask containing solid bpy (68.7 mg, 0.440 mmol). MeCN (25 ml) was used to dissolve $[\text{Cr}(\text{bpy})_2(\text{CF}_3\text{SO}_3)_2][\text{CF}_3\text{SO}_3]$ and transfer it to the reaction flask. The reaction mixture was heated at reflux for 4 h and the colour changed to yellow-orange. Solvent was evaporated, the residue redissolved in MeOH (3 ml) and the mixture was sonicated for 20 min. The solution was then filtered and the filtrate poured into a MeOH solution of excess NH_4PF_6 . The yellow precipitate formed was separated by filtration, and was washed with Et_2O . $[\text{Cr}(\text{bpy})_3][\text{PF}_6]_3$ was isolated as a pale yellow powder (233 mg, 0.244 mmol, 61.0 %).

IR: (solid, ν / cm^{-1}) 648 (w), 654 (m), 669 (m), 731 (s), 742 (w), 766 (s), 771 (s), 804 (s), 822 (s), 852 (w), 905 (w), 1015 (w), 1034 (m), 1114 (w), 1176 (w), 1242 (w), 1281 (w), 1321 (w), 1430 (w), 1447 (m), 1473 (w), 1504 (w), 1568 (w), 1607 (m), 3120 (w). **UV-VIS I:** (MeCN, $1.0 \times 10^{-5} \text{ mol dm}^{-3}$) λ / nm 235 sh ($\epsilon / \text{dm}^3 \text{ mol}^{-1} \text{ cm}^{-1}$ 41300), 244 sh (34400), 265 (18000), 277 (16400), 306 sh (23700), 313 (25500), 345 (8900), 363 (5400). **UV-VIS II:** (H_2O , $1.0 \times 10^{-5} \text{ mol dm}^{-3}$) λ / nm 234 sh ($\epsilon / \text{dm}^3 \text{ mol}^{-1} \text{ cm}^{-1}$ 27750), 276 (10750), 310 (19250), 344 sh (5350), 358 sh (3550), 420 (350). **EA:** Found C 37.65, H 2.68, N 8.81; $\text{C}_{30}\text{H}_{24}\text{CrF}_{18}\text{N}_6\text{P}_3$ requires C 37.71, H 2.53, N 8.80.

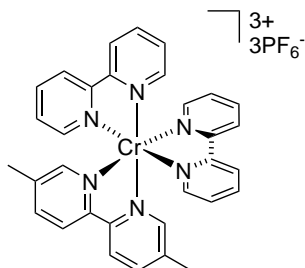
6.3.3.2 $[\text{Cr}(\text{bpy})_2(\text{phen})][\text{PF}_6]_3$



$[\text{Cr}(\text{bpy})_2(\text{CF}_3\text{SO}_3)_2][\text{CF}_3\text{SO}_3]$ (50.0 mg, 0.0616 mmol) and phen (27.3 mg, 0.173 mmol) were suspended in CH_2Cl_2 (5 ml). The reaction mixture was heated at reflux (10 h) and a yellow precipitate formed. This was separated by filtration, dissolved in H_2O (20 ml) and precipitated with an excess of NH_4PF_6 . The yellow precipitate that formed was separated by filtration,

and was washed with Et₂O. [Cr(bpy)₂(phen)][PF₆]₃ was isolated as a yellow powder. The bulk sample could not be obtained pure, but an X-ray structure could be determined (2.5.2, p. 29).

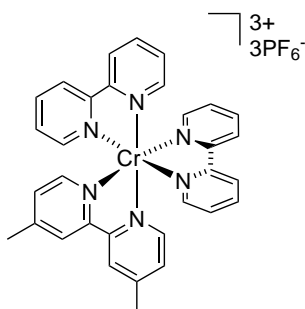
6.3.3.3 [Cr(bpy)₂(5,5'-Me₂bpy)][PF₆]₃



[Cr(bpy)₂(CF₃SO₃)₂][CF₃SO₃] (200 mg, 0.246 mmol) and 5,5'-Me₂bpy (47.8 mg, 0.259 mmol) were dissolved in MeCN (15 ml). The reaction mixture was heated at reflux for 6 h and the colour changed to yellow-orange. Solvent was evaporated, the residue redissolved in water (4 ml) and the mixture was sonicated for 20 min. The solution was then filtered and the filtrate poured into an aqueous solution of excess NH₄PF₆. The yellow precipitate that formed was separated by filtration, and was washed with Et₂O. [Cr(bpy)₃][PF₆]₃ was isolated as a yellow powder (191 mg, 0.194 mmol, 79.1 %).

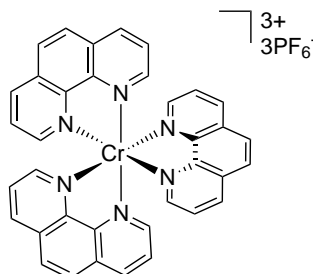
IR: (solid, ν/cm^{-1}) 554 (m), 752 (m), 800 (s), 928 (w), 1033 (m), 1224 (w), 1251 (w), 1280 (w), 1311 (w), 1417 (w), 1484 (w), 1499 (w), 1555 (w), 1616 (m), 3098 (w), 3658 (w). **UV-VIS:** (H₂O, 1.0×10^{-5} mol dm⁻³) λ / nm 237 sh (ϵ / dm³ mol⁻¹ cm⁻¹ 32400), 313 (20750), 324 sh (13700), 358 sh (4400). **EA:** Found C 38.83, H 2.90, N 8.50; C₃₂H₂₈CrF₁₈N₆P₃ requires C 39.08, H 2.87, N 8.55.

6.3.3.4 [Cr(bpy)₂(4,4'-Me₂bpy)][PF₆]₃



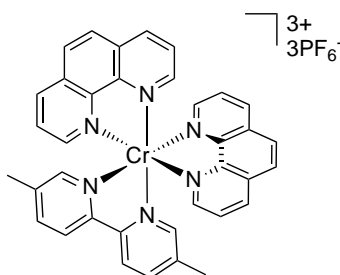
[Cr(bpy)₂(CF₃SO₃)₂][CF₃SO₃] (169 mg, 0.208 mmol) and 4,4'-Me₂bpy (40.4 mg, 0.219 mmol) were dissolved in MeCN (12 ml). The reaction mixture was heated at reflux for 5 h 45 min and the colour changed to yellow. Solvent was evaporated, the residue redissolved in water (3 ml) and the mixture was sonicated for 20 min. The solution was then filtered and the filtrate poured into an aqueous solution of excess NH₄PF₆. The yellow precipitate that formed was separated by filtration, and was washed with Et₂O. [Cr(bpy)₃][PF₆]₃ was isolated as a yellow powder (139 mg, 0.141 mmol, 57.5 %). **IR:** (solid, ν/cm^{-1}) 652 (w), 668 (w), 730 (m), 740 (m), 764 (m), 817 (s), 1033 (m), 1111 (w), 1169 (w), 1241 (w), 1321 (w), 1447 (m), 1473 (m), 1501 (m), 1598 (w), 1606 (m), 3098 (w). **EA:** Found C 37.86, H 2.90, N 8.48; C₃₂H₂₈CrF₁₈N₆P₃·1.5H₂O requires C

38.03, H 3.09, N 8.32.

6.3.3.5 $[\text{Cr}(\text{phen})_3][\text{PF}_6]_3$ 

$[\text{Cr}(\text{phen})_2(\text{CF}_3\text{SO}_3)_2][\text{CF}_3\text{SO}_3]$ (280 mg, 0.400 mmol) and phen (144 mg, 0.800 mmol) was suspended in CH_2Cl_2 (12 ml). The reaction mixture was heated at 110 °C and 10 bar in the microwave reactor (1 h 30 min) and a yellow precipitate formed. This was separated by filtration and washed with CH_2Cl_2 . Then the intermediate was dissolved in H_2O (20 ml), filtered and precipitated with an excess of NH_4PF_6 . The yellow precipitate that formed was separated by filtration, and was washed with H_2O and Et_2O . The precipitate was recrystallised from water. $[\text{Cr}(\text{phen})_3][\text{PF}_6]_3$ was isolated as a yellow powder (0.116 mg, 0.113 mmol, 28.3 %).

IR: (solid, ν/cm^{-1}) 554 (s), 656 (m), 713 (m), 717 (m), 822 (s), 880 (m), 1112 (w), 1155 (w), 1227 (w), 1312 (w), 1416 (w), 1429 (m), 1524 (m), 1584 (w), 1609 (w), 1636 (w), 3110 (w), 3570 (w). **UV-VIS:** (MeCN, 1.0×10^{-5} mol dm^{-3}) λ / nm 211 sh (ϵ / $\text{dm}^3 \text{mol}^{-1} \text{cm}^{-1}$ 82700), 222 sh (76900), 268 (57500), 283 sh (35850), 352 (3300), 322 (10800). **EA:** Found C 41.58, H 2.31, N 7.96; $\text{C}_{36}\text{H}_{24}\text{CrF}_{18}\text{N}_6\text{P}_3 \cdot 0.5\text{H}_2\text{O}$ requires C 41.72, H 2.43, N 8.11.

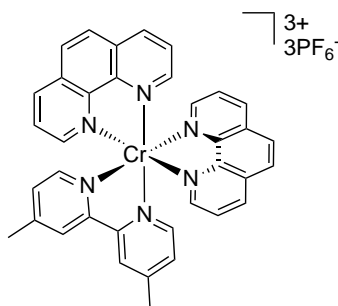
6.3.3.6 $[\text{Cr}(\text{phen})_2(5,5'\text{-Me}_2\text{bpy})][\text{PF}_6]_3$ 

$[\text{Cr}(\text{phen})_2(\text{CF}_3\text{SO}_3)_2][\text{CF}_3\text{SO}_3]$ (280 mg, 0.400 mmol) and 5,5'- Me_2bpy (88.4 mg, 0.480 mmol) were suspended in CH_2Cl_2 (12 ml). The reaction mixture was heated at 110 °C and 10 bar in the microwave reactor (1 h) and a yellow precipitate formed. This was separated by filtration, dissolved in H_2O (20 ml) and precipitated with an excess of NH_4PF_6 . The yellow precipitate that formed was separated by filtration, and was washed with Et_2O . The precipitate was recrystallised from water and filtered hot. The precipitate was then dissolved in a small amount of acetone, filtered and overlaid with Et_2O . $[\text{Cr}(\text{phen})_2(5,5'\text{-Me}_2\text{bpy})][\text{PF}_6]_3$ was isolated as a yellow powder (65.4 mg, 0.0634 mmol, 19.5 %).

IR: (solid, ν/cm^{-1}) 554 (m), 658 (w), 702 (m), 716 (m), 725 (m), 742 (m), 754 (m), 769 (m), 777 (m), 780 (m), 827 (s), 879 (m), 1063 (m), 1113 (m), 1156 (m), 1227 (w), 1246 (w), 1319

(w), 1432 (m), 1478 (m), 1523 (m), 1584 (w), 1605 (w), 1634 (w), 3099 (w). **UV-VIS:** (H_2O , $1.0 \times 10^{-5} \text{ mol dm}^{-3}$) λ / nm 226 sh ($\epsilon / \text{dm}^3 \text{ mol}^{-1} \text{ cm}^{-1}$ 55650), 268 (41400), 284 sh (25350), 326 sh (12200), 362 sh (4000). **EA:** Found C 41.77, H 2.64, N 8.13; $\text{C}_{36}\text{H}_{28}\text{CrF}_{18}\text{N}_6\text{P}_3$ requires C 41.92, H 2.74, N 8.15.

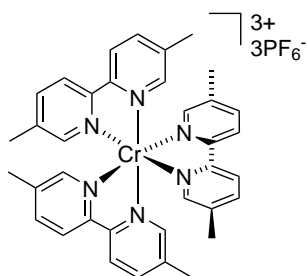
6.3.3.7 $[\text{Cr}(\text{phen})_2(4,4'\text{-Me}_2\text{bpy})][\text{PF}_6]_3$



$[\text{Cr}(\text{phen})_2(\text{CF}_3\text{SO}_3)_2][\text{CF}_3\text{SO}_3]$ (405 mg, 0.471 mmol) and 4,4'-Me₂bpy (117 mg, 0.637 mmol) were dissolved in MeCN (30 ml). The reaction mixture was heated at reflux for 5 h 15 min and the colour changed to yellow. Solvent was evaporated, the residue redissolved in MeOH (4 ml) and the mixture was sonicated for 20 min. The solution was then filtered and the filtrate poured into a MeOH solution of excess NH_4PF_6 . The beige precipitate that formed was separated by filtration, and was washed with Et_2O . $[\text{Cr}(\text{phen})_2(4,4'\text{-Me}_2\text{bpy})][\text{PF}_6]_3$ was isolated as a beige powder (314 mg, 0.305 mmol, 64.7 %).

IR: (solid, ν/cm^{-1}) 554 (s), 635 (m), 719 (m), 741 (m), 823 (s), 879 (w), 1032 (m), 1113 (w), 1153 (w), 1225 (w), 1255 (m), 1285 (w), 1429 (m), 1522 (m), 1616 (w), 3108 (w). **UV-VIS:** (H_2O , $1.0 \times 10^{-5} \text{ mol dm}^{-3}$) λ / nm 226 sh ($\epsilon / \text{dm}^3 \text{ mol}^{-1} \text{ cm}^{-1}$ 70800), 273 (48450), 304 sh (19050), 360 sh (3370). **EA:** Found C 41.37, H 2.90, N 7.99; $\text{C}_{36}\text{H}_{28}\text{CrF}_{18}\text{N}_6\text{P}_3 \cdot 0.5\text{H}_2\text{O}$ requires C 41.55, V 2.81, N 8.07.

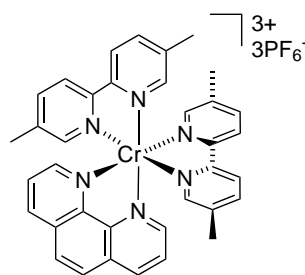
6.3.3.8 $[\text{Cr}(5,5'\text{-Me}_2\text{bpy})_3][\text{PF}_6]_3$



$[\text{Cr}(5,5'\text{-Me}_2\text{bpy})_2(\text{CF}_3\text{SO}_3)_2][\text{CF}_3\text{SO}_3]$ (189 mg, 0.219 mmol) and 5,5'-Me₂bpy (51.7 mg, 0.281 mmol) were dissolved in MeCN (15 ml). The reaction mixture was heated at reflux for 4h 20 min and the colour changed to yellow. Solvent was evaporated, the residue redissolved in MeOH (6 ml) and the mixture was sonicated for 20 min. The solution was then filtered and an excess of NH_4PF_6 was added. The yellow precipitate that formed was separated by filtration, and was washed with Et_2O . $[\text{Cr}(5,5'\text{-Me}_2\text{bpy})_3][\text{PF}_6]_3$ was isolated as a yellow powder (193 mg, 0.186 mmol, 85.4 %).

IR: (solid, ν/cm^{-1}) 666 (m), 722 (m), 759 (w), 816 (s), 827 (s), 1060 (m), 1169 (w), 1237 (w), 1246 (w), 1319 (w), 1386 (w), 1448 (w), 1476 (m), 1510 (w), 1607 (w), 1700 (w), 2366 (w). **UV-VIS:** (H_2O , $1.0 \times 10^{-5} \text{ mol dm}^{-3}$) λ / nm 245 ($\epsilon / \text{dm}^3 \text{ mol}^{-1} \text{ cm}^{-1}$ 46350), 293 (22750), 325 sh (26650), 377 sh (4550). **EA:** Found C 41.49, H 3.37, N 8.13; $\text{C}_{36}\text{H}_{36}\text{CrF}_{18}\text{N}_6\text{P}_3$ requires C 41.59, H 3.49, N 8.08.

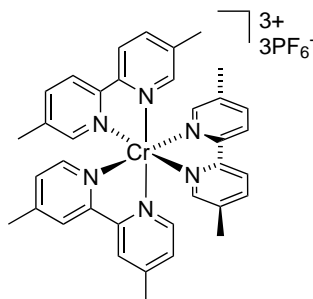
6.3.3.9 $[\text{Cr}(5,5'\text{-Me}_2\text{bpy})_2(\text{phen})][\text{PF}_6]_3$



$[\text{Cr}(5,5'\text{-Me}_2\text{bpy})_2(\text{CF}_3\text{SO}_3)_2][\text{CF}_3\text{SO}_3]$ (159 mg, 0.183 mmol) and phen (42.6 mg, 0.237 mmol) were dissolved in MeCN (12 ml). The reaction mixture was heated at reflux for 3 h and the colour changed to yellow. Solvent was evaporated, the residue redissolved in water (5 ml) and the mixture was sonicated for 20 min. The solution was then filtered and an excess of NH_4PF_6 was added. The yellow precipitate that formed was separated by filtration, and was washed with Et_2O . $[\text{Cr}(5,5'\text{-Me}_2\text{bpy})_3][\text{PF}_6]_3$ was isolated as a yellow powder (118 mg, 0.114 mmol, 62.2 %).

IR: (solid, ν/cm^{-1}) 555 (s), 620 (m), 638 (m), 659 (m), 667 (m), 717 (s), 726 (s), 742 (m), 814 (s), 879 (w), 1031 (w), 1060 (w), 1113 (w), 1147 (m), 1163 (m), 1238 (m), 1288 (w), 1318 (w), 1386 (w), 1417 (w), 1431 (w), 1447 (w), 1453 (w), 1457 (w), 1477 (m), 1509 (w), 1524 (w), 1547 (w), 1585 (w), 1609 (w), 3101 (w). **EA:** Found C 42.02, H 3.28, m 8.06; $\text{C}_{36}\text{H}_{32}\text{CrF}_{18}\text{N}_6\text{P}_3$ requires C 41.75, H 3.11, N 8.12.

6.3.3.10 $[\text{Cr}(5,5'\text{-Me}_2\text{bpy})_2(4,4'\text{-Me}_2\text{bpy})][\text{PF}_6]_3$

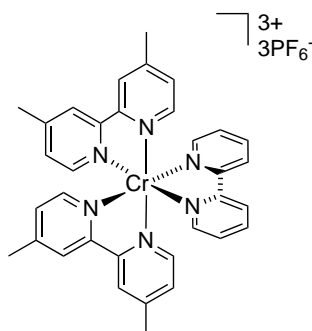


$[\text{Cr}(5,5'\text{-Me}_2\text{bpy})_2(\text{CF}_3\text{SO}_3)_2][\text{CF}_3\text{SO}_3]$ (80.0 mg, 0.0922 mmol) and 4,4'-Me₂bpy (21.9 mg, 0.119 mmol) were dissolved in MeCN (12 ml). The reaction mixture was heated at reflux for 7 h and the colour changed to yellow. Solvent was evaporated, the residue redissolved in water (3 ml) and the mixture was sonicated for 30 min. The solution was then filtered and an excess of NH_4PF_6 was added. The yellow precipitate that formed was separated by filtration,

and was washed with Et₂O. [Cr(5,5'-Me₂bpy)₂(4,4'-Me₂bpy)][PF₆]₃ was isolated as a yellow powder (55.8 mg, 0.0537 mmol, 58.2 %).

IR: (solid, ν/cm^{-1}) 557 (s), 668 (m), 701 (w), 723 (m), 726 (m), 820 (s), 1035 (w), 1060 (w), 1161 (w), 1237 (w), 1286 (w), 1319 (w), 1394 (w), 1437 (w), 1476 (m), 1505 (w), 1615 (w), 3075 (w). **EA:** found C 41.17, H 3.63, N 7.91; C₃₆H₃₆CrF₁₈N₆P₃·0.5H₂O requires C 41.23, H 3.56, N 8.01.

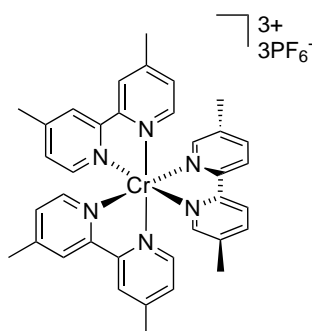
6.3.3.11 [Cr(4,4'-Me₂bpy)₂(bpy)][PF₆]₃



[Cr(4,4'-Me₂bpy)₂(CF₃SO₃)₂][CF₃SO₃] (46.4 mg, 0.0535 mmol) and bpy (10.4 mg, 0.0667 mmol) were dissolved in MeCN (5 ml). The reaction mixture was heated at reflux (9 h) and the colour changed to yellow. Solvent was evaporated, the residue redissolved in water (1 ml) and the mixture was sonicated for 30 min. The solution was then filtered and an excess of NH₄PF₆ was added. The yellow precipitate that formed was separated by filtration, and was washed with Et₂O. [Cr(4,4'-Me₂bpy)₂(bpy)][PF₆]₃ was isolated as a yellow-orange powder (10.7 mg, 0.0106 mmol, 19.8 %).

EA: Found C 39.72, H 3.30, N 8.25; C₃₄H₃₂CrF₁₈N₆P₃·0.5H₂O requires C 40.01, H 3.26, N 8.23.

6.3.3.12 [Cr(4,4'-Me₂bpy)₂(5,5'-Me₂bpy)][PF₆]₃



[Cr(4,4'-Me₂bpy)₂(CF₃SO₃)₂][CF₃SO₃] (81.0 mg, 0.093 mmol) and 4,4'-Me₂bpy (22.1 mg, 0.120 mmol) were dissolved in MeCN (12 ml). The reaction mixture was heated at reflux for 6 h 20 min and the colour changed to yellow. Solvent was evaporated, the residue redissolved into water (2 ml) and the mixture was sonicated for 20 min. The solution was then filtered and the filtrate poured in an aqueous solution of excess NH₄PF₆. The yellow precipitate that formed was separated by filtration, and was washed with Et₂O. [Cr(4,4'-Me₂bpy)₂(5,5'-Me₂bpy)][PF₆]₃

was isolated as a yellow-orange powder (72.4 mg, 0.0696 mmol, 74.6 %).

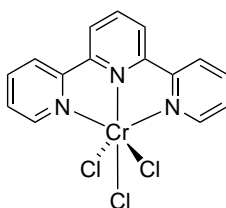
IR: (solid, ν/cm^{-1}) 554 (s), 740 (m), 818 (s), 928 (w), 1032 (m), 1164 (w), 1248 (w), 1282 (w), 1415 (w), 1478 (w), 1556 (w), 1616 (m), 1738 (w), 3082 (w), 3648 (w). **EA:** Found C 41.15, H 3.65, N 8.00; $\text{C}_{36}\text{H}_{36}\text{CrF}_{18}\text{N}_6\text{P}_3 \cdot 0.5\text{H}_2\text{O}$ requires C 41.23, H 3.56, N 8.01.

6.4 Synthesis of bis(terpyridine)chromium(III) complexes

6.4.1 Synthesis of the precursors of type: $\{\text{Cr}(\text{tpy})\text{Cl}_3\}$

All reactions were performed under inert conditions (N_2). For the reaction steps dry solvents (crown cap) from Sigma Aldrich were used. Anhydrous CrCl_3 was obtained from Acros Organics and used as received.

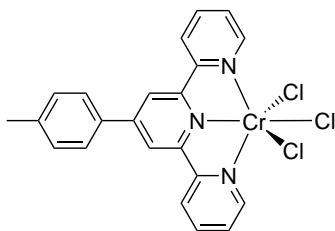
6.4.1.1 $[\text{Cr}(\text{tpy})\text{Cl}_3]$



Anhydrous CrCl_3 (185 mg, 1.15 mmol) and tpy (350 mg, 1.50 mmol) were suspended in EtOH (10 ml). The reaction mixture was heated to reflux, and then granulated zinc (21.0 mg, 0.320 mmol) was added. After a short time, the mixture turned black and a green precipitate was formed. The reaction was heated at reflux for 6.5 h, then the reaction mixture was filtered, leaving excess zinc behind in the reaction flask. The green precipitate collected on the filter-frit was washed with EtOH. $[\text{Cr}(\text{tpy})\text{Cl}_3]$ (415 mg, 1.06 mmol, 91.7 %) was used in the next step without further purification.

IR: (solid, ν/cm^{-1}) 453 (m), 489 (w), 513 (w), 558 (m), 654 (s), 675 (w), 734 (m), 783 (vs), 827 (w), 889 (w), 905 (w), 926 (w), 980 (w), 1025 (s), 1040 (m), 1050 (m), 1069 (w), 1099 (w), 1137 (w), 1158 (m), 1171 (w), 1186 (w), 1242 (m), 1291 (w), 1302 (w), 1317 (m), 1402 (w), 1446 (s), 1475 (s), 1500 (w), 1572 (w), 1600 (w), 3064 (w). **EA:** Found C 46.01, H 3.00, N 11.00; $\text{C}_{15}\text{H}_{11}\text{Cl}_3\text{CrN}_3$ requires C 46.00, H 2.83, N 10.73.

6.4.1.2 $[\text{Cr}(4'-(4\text{-tolyl})\text{tpy})\text{Cl}_3]$

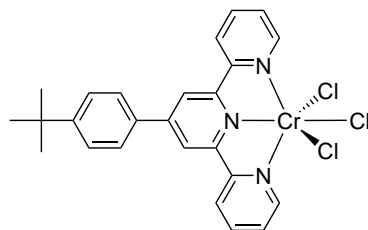


The compound was prepared by the same method as $[\text{Cr}(\text{tpy})\text{Cl}_3]$, starting with anhydrous CrCl_3 (761 mg, 4.76 mmol) and 4'-(4-tolyl)tpy (2.00 g, 6.18 mmol) suspended in EtOH (60 ml). Granulated zinc (68.2 mg, 1.05 mmol) was added and heated at reflux for 4 h 15 min. $[\text{Cr}(4'-(4\text{-tolyl})\text{tpy})\text{Cl}_3]$ was used in the next step without further purification.

IR: (solid, ν/cm^{-1}) 501 (s), 519 (m), 612 (w), 650 (w), 661 (s), 690 (s), 695 (s), 719 (w), 728 (s), 751 (s), 790 (s), 827 (w), 834 (s), 890 (m), 899 (w), 1017 (w), 1026 (s), 1034 (w), 1066 (w), 1078 (w), 1099 (w), 1186 (w), 1205 (m), 1244 (s), 1262 (w), 1271 (w), 1289 (w), 1338 (m), 1367 (w), 1411 (m), 1436 (w), 1446 (w), 1467 (m), 1489 (m), 1520 (m), 1547 (w), 1568 (m), 1576

(s), 1582 (s), 1603 (m), 3059 (w), 3061 (w), 3998 (w). **EA:** Found C 54.96, H 3.86, N 8.58; $C_{22}H_{17}Cl_3CrN_3$ requires C 54.85, H 3.56, N 8.72.

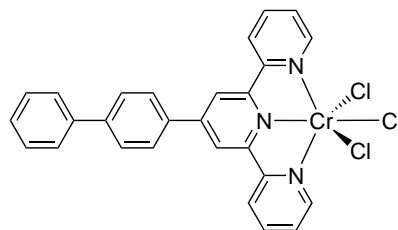
6.4.1.3 [Cr(LT1)Cl₃]



The compound was prepared by the same method as [Cr(tpy)Cl₃], starting with anhydrous CrCl₃ (168 mg, 1.05 mmol) and 4'-(4-(*tert*-butyl)phenyl)-2,2':6',2''-terpyridine (LT1) (500 mg, 1.37 mmol) suspended in EtOH (15 ml). Granulated zinc (15.1 mg, 0.231 mmol) was added and heated at reflux for 6 h. [Cr(LT1)Cl₃] was used in the next step without further purification.

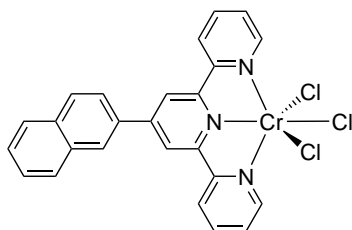
IR: (solid, ν/cm^{-1}) 545 (m), 651 (w), 660 (m), 684 (w), 718 (w), 731 (m), 758 (m), 797 (s), 829 (w), 895 (w), 981 (w), 1012 (w), 1025 (s), 1043 (w), 1066 (w), 1099 (w), 1120 (w), 1165 (w), 1206 (w), 1213 (w), 1248 (w), 1277 (w), 1303 (w), 1363 (w), 1406 (m), 1432 (w), 1464 (w), 1475 (m), 1549 (w), 1601 (s), 2870 (w), 2908 (w), 2964 (w), 3069 (w). **EA:** Found C 57.04, H 4.68, N 8.05; $C_{25}H_{23}Cl_3CrN_3$ requires C 57.32, H 4.43, N 8.02.

6.4.1.4 [Cr(LT2)Cl₃]



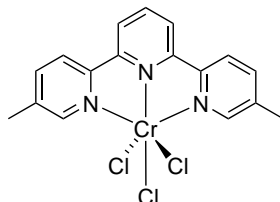
The compound was prepared by the same method as [Cr(tpy)Cl₃], starting with anhydrous CrCl₃ (188 mg, 1.18 mmol) and 4'-([1,1'-biphenyl]-4-yl)-2,2':6',2''-terpyridine (LT2) (590 mg, 1.53 mmol) suspended in EtOH (15 ml). Granulated zinc (16.9 mg, 0.259 mmol) was added and heated at reflux for 5 h 15 min. [Cr(LT2)Cl₃] was used in the next step without further purification.

IR: (solid, ν/cm^{-1}) 509 (s), 625 (w), 659 (w), 689 (m), 730 (m), 741 (w), 766 (m), 792 (s), 825 (w), 841 (w), 846 (w), 887 (w), 898 (w), 971 (w), 1004 (w), 1026 (m), 1036 (w), 1051 (w), 1067 (w), 1095 (w), 1163 (w), 1209 (w), 1243 (w), 1302 (w), 1366 (w), 1402 (w), 1424 (w), 1448 (w), 1471 (w), 1491 (w), 1542 (w), 1565 (w), 1598 (m), 1613 (w), 3060 (w), 3569 (w), 3991 (m). **EA:** Found C 58.87, H 3.83, N 7.74; $C_{27}H_{19}Cl_3CrN_3 \cdot 0.5H_2O$ requires C 58.66, H 3.65, N 7.60.

6.4.1.5 [Cr(LT3)Cl₃]

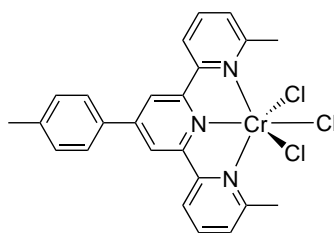
The compound was prepared by the same method as [Cr(tpy)Cl₃], starting with anhydrous CrCl₃ (188 mg, 1.18 mmol) and 4'-(naphthalen-2-yl)-2,2':6',2''-terpyridine (LT3) (550 mg, 1.53 mmol) suspended in EtOH (15 ml). Granulated zinc (16.9 mg, 0.259 mmol) was added and heated at reflux for 6 h. [Cr(LT3)Cl₃] was used in the next step without further purification.

IR: (solid, ν/cm^{-1}) 500 (s), 502 (s), 506 (s), 577 (m), 607 (m), 651 (m), 659 (s), 666 (w), 690 (s), 721 (w), 728 (s), 751 (s), 763 (m), 772 (m), 775 (m), 787 (s), 817 (s), 865 (s), 883 (m), 891 (m), 904 (w), 947 (w), 956 (w), 969 (w), 1005 (w), 1026 (s), 1034 (m), 1043 (w), 1051 (w), 1066 (w), 1093 (w), 1104 (w), 1161 (w), 1168 (w), 1203 (w), 1223 (w), 1249 (m), 1290 (w), 1302 (w), 1347 (w), 1362 (w), 1381 (w), 1418 (m), 1442 (m), 1456 (w), 1475 (s), 1548 (m), 1565 (m), 1601 (s), 3062 (w), 3383 (w), 3995 (m). **EA:** Found C 55.54, H 3.63, N 7.78; C₂₅H₁₇Cl₃CrN₃·1.5H₂O requires C 55.12, H 3.70, N 7.71.

6.4.1.6 [Cr(5,5''-Me₂tpy)Cl₃]

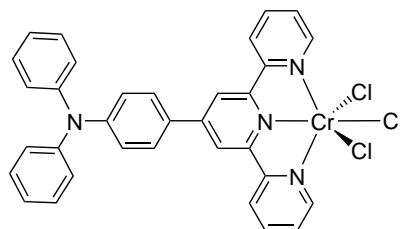
The compound was prepared by the same method as [Cr(tpy)Cl₃], starting with anhydrous CrCl₃ (72.3 mg, 0.452 mmol) and 5,5''-dimethyl-2,2':6',2''-terpyridine (5,5''-Me₂tpy) (130 mg, 0.497 mmol) suspended in EtOH (9 ml). Granulated zinc (6.50 mg, 99.5 μmol) was added and heated at reflux for 6 h. [Cr(5,5''-Me₂tpy)Cl₃] was used in the next step without further purification.

EA: Found C 48.02, H 3.80, N 10.00; C₁₇H₁₅Cl₃CrN₃·0.5H₂O requires C 47.63, H 3.76, N 9.80.

6.4.1.7 [Cr(LT4)Cl₃]

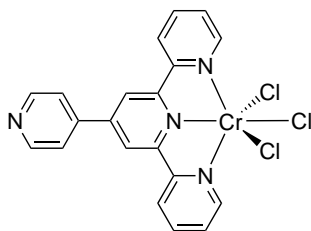
The compound was prepared by the same method as [Cr(tpy)Cl₃], starting with anhydrous CrCl₃ (124 mg, 0.854 mmol) and 6,6''-dimethyl-4'-(*p*-tolyl)-2,2':6',2''-terpyridine (LT4) (300 mg, 0.776 mmol) suspended in EtOH (12.5 ml). Granulated zinc (11.2 mg, 0.171 mmol) was added and heated at reflux for 7 h 45 min. [Cr(LT4)Cl₃] was used in the next step without further purification.

IR: (solid, ν/cm^{-1}) 584 (m), 632 (m), 658 (s), 674 (w), 711 (w), 744 (m), 751 (m), 767 (m), 797 (s), 811 (s), 892 (m), 904 (w), 943 (w), 959 (w), 991 (w), 1002 (w), 1010 (m), 1018 (m), 1036 (m), 1048 (w), 1119 (w), 1128 (w), 1163 (w), 1175 (m), 1191 (w), 1229 (w), 1243 (w), 1373 (w), 1406 (w), 1419 (w), 1428 (m), 1443 (m), 1447 (m), 1454 (m), 1483 (m), 1518 (w), 1549 (m), 1554 (m), 1569 (m), 1606 (s), 3078 (w), 3994 (m). **EA:** Found C 56.21, H 4.26, N 8.31; C₂₄H₂₁Cl₃CrN₃ requires C 56.54, H 4.15, N 8.24.

6.4.1.8 [Cr(LT5)Cl₃]

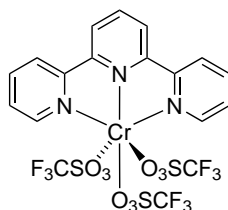
The compound was prepared by the same method as [Cr(tpy)Cl₃], starting with anhydrous CrCl₃ (188 mg, 1.18 mmol) and 4-([2,2':6',2''-terpyridin]-4'-yl)-*N,N*-diphenylaniline (LT5) (731 mg, 1.53 mmol) suspended in EtOH (15 ml). Granulated zinc (16.9 mg, 0.259 mmol) was added and heated at reflux for 6 h. [Cr(LT5)Cl₃] was used in the next step without further purification.

IR: (solid, ν/cm^{-1}) 501 (s), 519 (m), 612 (w), 650 (w), 661 (s), 690 (s), 695 (s), 719 (w), 728 (s), 751 (s), 790 (s), 827 (w), 834 (s), 890 (m), 899 (w), 1017 (w), 1026 (s), 1034 (w), 1066 (w), 1078 (w), 1099 (w), 1186 (w), 1205 (m), 1244 (s), 1262 (w), 1271 (w), 1289 (w), 1338 (m), 1367 (w), 1411 (m), 1436 (w), 1446 (w), 1467 (m), 1489 (m), 1520 (m), 1547 (w), 1568 (m), 1576 (s), 1582 (s), 1603 (m), 3059 (w), 3061 (w), 3998 (w). **EA:** Found C 62.57, H 4.07, N 9.07; C₃₃H₂₄Cl₃CrN₄ requires C 62.43, H 3.81, N 8.82.

6.4.1.9 [Cr(LT11)Cl₃]

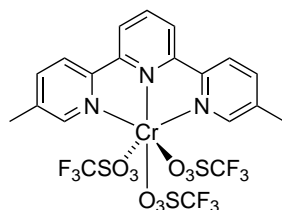
The compound was prepared by the same method as [Cr(tpy)Cl₃], starting with anhydrous CrCl₃ (185 mg, 1.15 mmol) and 4'-(pyridin-4-yl)-2,2':6',2''-terpyridine (LT11) (430 mg, 1.39 mmol) suspended in EtOH (10 ml). Granulated zinc (7.60 mg, 0.116 mmol) was added and heated at reflux for 6 h 15 min. [Cr(LT11)Cl₃] was used in the next step without further purification.

EA: Found C 51.28, H 3.29, N 11.71; C₂₀H₁₄Cl₃CrN₃ requires C 51.28, H 3.29, N 11.71.

6.4.2 Synthesis of the precursors of the type {Cr(tpy)(CF₃SO₃)₃}6.4.2.1 [Cr(tpy)(CF₃SO₃)₃]

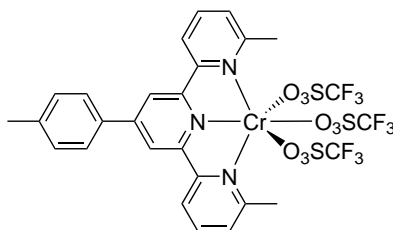
[Cr(tpy)Cl₃] (27.5 mg, 0.0700 mmol) was dissolved in CF₃SO₃H (0.3 ml, 2.80 mmol) and the dark red solution was stirred overnight at room temperature. The reaction was then cooled to 0 °C and Et₂O (20 ml) was added, yielding a dark red precipitate. The solid was separated by filtration, washed with Et₂O and dried under an air stream. [Cr(tpy)(CF₃SO₃)₃] was isolated as a dark red solid (28.0 mg, 0.038 mmol, 54.2 %).

IR: (solid, ν/cm^{-1}) 515 (s), 534 (m), 571 (m), 604 (s), 622 (vs), 661 (m), 682 (w), 734 (m), 766 (m), 777 (s), 829 (w), 905 (m), 989 (vs), 1031 (s), 1054 (w), 1096 (w), 1104 (w), 1157 (vs), 1171 (vs), 1196 (vs), 1236 (s), 1230 (w), 1309 (w), 1325 (m), 1345 (s), 1408 (w), 1450 (w), 1484 (w), 1508 (w), 1574 (w), 1605 (w), 3093 (w). **EA:** Found C 29.62, H 1.77, N 5.74; C₁₈H₁₁CrF₉N₃O₉S₃ requires C 29.52, H 1.51, N 5.74.

6.4.2.2 [Cr(5,5''-Me₂tpy)(CF₃SO₃)₃]

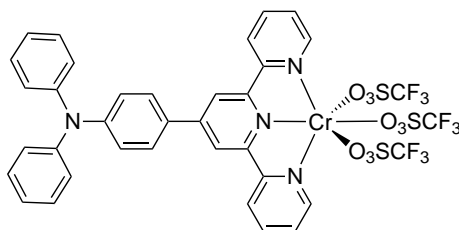
[Cr(5,5''-Me₂tpy)Cl₃] (100 mg, 0.238 mmol) was dissolved in CF₃SO₃H (0.8 ml, 9.53 mmol) and the dark red solution was stirred overnight at room temperature. The reaction was then cooled to 0 °C and Et₂O (20 ml) was added, yielding a dark red precipitate. The solid was separated by filtration, washed with Et₂O and dried under an air stream. [Cr(5,5''-Me₂tpy)(CF₃SO₃)₃] was isolated as a dark red solid and used for further reactions without characterisation.

6.4.2.3 [Cr(LT4)(CF₃SO₃)₃]



[Cr(LT4)Cl₃] (250 mg, 0.490 mmol) was dissolved in CF₃SO₃H (1.7 ml, 16.6 mmol) and the dark red solution was stirred overnight at room temperature. The reaction was then cooled to 0 °C and Et₂O (40 ml) was added, yielding a dark red precipitate. The solid was separated by filtration, washed with Et₂O and dried under an air stream. [Cr(LT4)(CF₃SO₃)₃] was isolated as a dark red solid and used for further reactions without characterisation.

6.4.2.4 [Cr(LT5)(CF₃SO₃)₃]

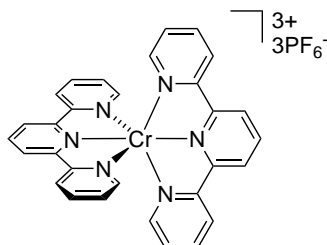


[Cr(LT5)Cl₃] (75.0 mg, 0.118 mmol) was dissolved in CF₃SO₃H (0.4 ml, 4.4 mmol) and the dark red solution was stirred overnight at room temperature. The reaction was then cooled to 0 °C and Et₂O (20 ml) was added, yielding a dark red precipitate. The solid was separated by filtration, washed with Et₂O and dried under an air stream. [Cr(LT5)(CF₃SO₃)₃] was isolated as a dark red solid (72.8 mg, 0.0746 mmol, 67.8 %).

EA: Found C 43.96, H 2.71, N 6.03; C₃₆H₂₄CrF₉N₄O₉S₃·0.5H₂O requires C 43.91, H 2.56, N 5.74.

6.4.3 Synthesis of the bis(terpyridine)chromium(III) complexes

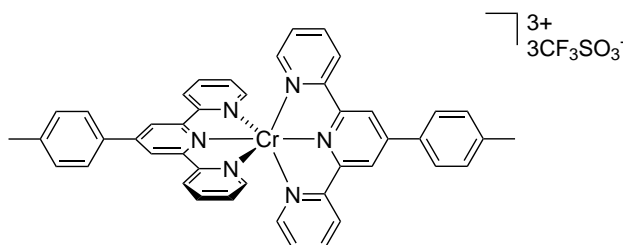
6.4.3.1 $[\text{Cr}(\text{tpy})_2][\text{PF}_6]_3$



$[\text{Cr}(\text{tpy})\text{Cl}_3]$ (200 mg, 0.511 mmol) was dissolved in $\text{CF}_3\text{SO}_3\text{H}$ (1.8 ml, 20.4 mmol) and the dark red solution was stirred at room temperature overnight. The reaction was then cooled to 0°C and Et_2O (20 ml) was added, yielding a dark red precipitate of $[\text{Cr}(\text{tpy})(\text{CF}_3\text{SO}_3)_3]$. This was separated by filtration onto a *Schlenk* frit, was washed with Et_2O and dried under a flow of N_2 . The flask attached to the *Schlenk* frit was replaced by a two necked round-bottomed flask containing solid 2,2':6',2''-terpyridine (tpy) (131 mg, 0.562 mmol). MeCN (10 ml) was used to dissolve $[\text{Cr}(\text{tpy})(\text{CF}_3\text{SO}_3)_3]$ and transfer it to the reaction flask. The reaction mixture was heated at reflux (3.75 h) and the colour changed to yellow-orange. Solvent was evaporated, the residue redissolved in MeOH (2 ml) and the mixture was sonicated for 20 min. The solution was then filtered and the filtrate poured into an MeOH solution of excess NH_4PF_6 . The yellow precipitate that formed was separated by filtration, and was washed with hexane and Et_2O . $[\text{Cr}(\text{tpy})_2][\text{PF}_6]_3$ was isolated as a yellow powder (278 mg, 0.292 mmol, 57.0 %).

IR: (solid, ν/cm^{-1}) 552 (s), 555 (vs), 660 (m), 772 (s), 779 (m), 802 (m), 824 (vs), 1028 (m), 1099 (w), 1247 (w), 1325 (m), 1448 (m), 1480 (m), 1506 (w), 1560 (w), 1603 (m). **MS:** MALDI-TOF m/z 809.3 $[\text{M}-\text{PF}_6]^+$ (calc. 808.1). **UV-VIS:** (H_2O , 1.0×10^{-5} mol dm^{-3}) λ / nm 265 (ϵ / $\text{dm}^3 \text{mol}^{-1} \text{cm}^{-1}$ 29400), 282 sh (21700), 324 (14400), 334 (14900), 347 (15300), 363 (16700). **EA:** Found C 38.18, H 2.58, N 8.86; $\text{C}_{30}\text{H}_{22}\text{CrF}_{18}\text{N}_6\text{P}_3$ requires C 37.79, H 2.33, N 8.81.

6.4.3.2 $[\text{Cr}(4'-(4\text{-tolyl})\text{tpy})_2][\text{CF}_3\text{SO}_3]_3$

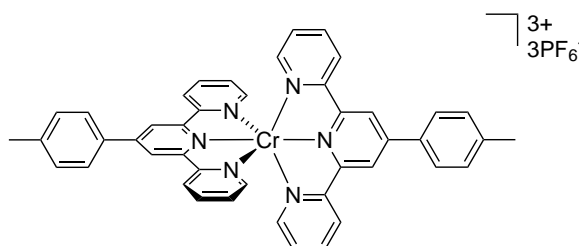


The compound was prepared by the same method as $[\text{Cr}(\text{tpy})_2][\text{PF}_6]_3$, starting with $[\text{Cr}(4'-(4\text{-tolyl})\text{tpy})\text{Cl}_3]$ (164 mg, 0.341 mmol) and $\text{CF}_3\text{SO}_3\text{H}$ (1.2 ml, 14 mmol) in the first step, and then 4'-(*p*-tolyl)-2,2':6',2''-terpyridine (4'-(4-tolyl)tpy) (121 mg, 0.375 mmol) and a reaction time of 6 h 20 min in the second step. The target product precipitated during the reaction. This was filtered and recrystallised from hot MeCN. $[\text{Cr}(4'-(4\text{-tolyl})\text{tpy})_2][\text{CF}_3\text{SO}_3]_3$ was isolated as an orange solid (302 mg, 0.263 mmol, 77.0 %).

IR: (solid, ν/cm^{-1}) 500 (s), 505 (s), 517 (s), 529 (m), 572 (m), 613 (m), 625 (s), 634 (s), 662

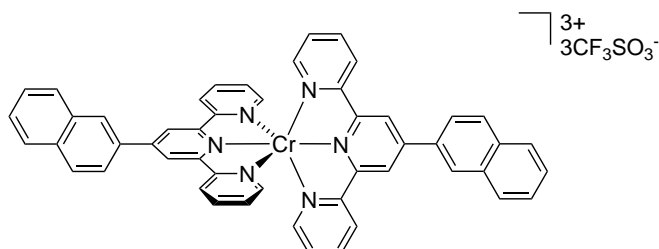
(w), 693 (w), 727 (w), 778 (m), 788 (m), 823 (m), 949 (w), 996 (m), 1027 (s), 1097 (w), 1116 (m), 1138 (m), 1158 (s), 1210 (m), 1222 (m), 1249 (s), 1363 (w), 1406 (w), 1435 (w), 1478 (w), 1533 (w), 1539 (w), 1601 (s), 1618 (w), 3066 (w). **EA:** Found C 49.34, H 3.40, N 8.70; $C_{47}H_{34}CrF_9N_6O_9S_3 \cdot H_2O$ requires C 49.36, H 3.27, N 8.63.

6.4.3.3 $[Cr(4'-(4\text{-tolyl})tpy)_2][PF_6]_3$

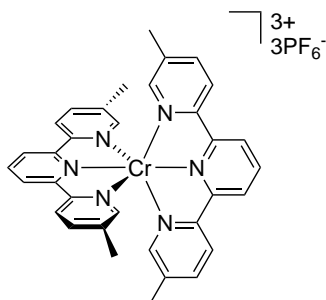


The compound was prepared by the same method as $[Cr(4'-(4\text{-tolyl})tpy)_2][CF_3SO_3]_3$, starting with $[Cr(4'-(4\text{-tolyl})tpy)Cl_3]$ (193 mg, 0.400 mmol) and CF_3SO_3H (1.4 ml, 16 mmol) in the first step, and then 4'-(*p*-tolyl)-2,2':6',2''-terpyridine (4'-(4-tolyl)tpy) (142 mg, 0.440 mmol) and a reaction time of 6 h in the second step. In this reaction a counter ion exchange was conducted. The crude product was dissolved in MeOH, filtered and poured into a MeOH solution of excess NH_4PF_6 . The resulting precipitate was filtered and washed with cold MeOH. The bulk product could not be obtained pure, but an X-ray structure could be determined (3.9.1.4, p. 79).

6.4.3.4 $[Cr(LT3)_2][PF_6]_3$

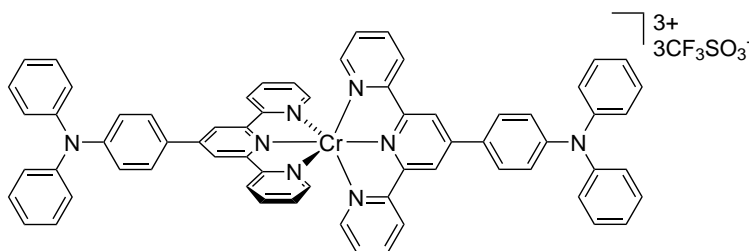


The compound was prepared by the same method as $[Cr(tpy)_2][PF_6]_3$, starting with $[Cr(LT3)Cl_3]$ (100 mg, 0.195 mmol) and CF_3SO_3H (0.70 ml, 7.8 mmol) in the first step, and then 4'-(naphthalen-2-yl)-2,2':6',2''-terpyridine (LT3) (77.3 mg, 0.215 mmol) and a reaction time of 7 h in the second step. The counterion $[Cr(4'-(4\text{-tolyl})tpy)_2][PF_6]_3$ was isolated as an orange solid (302 mg, 0.263 mmol, 77.0%). The bulk product could not be obtained pure, but an X-ray structure could be determined (3.9.1.3, p. 77).

6.4.3.5 $[\text{Cr}(5,5''\text{-Me}_2\text{tpy})_2][\text{PF}_6]_3$ 

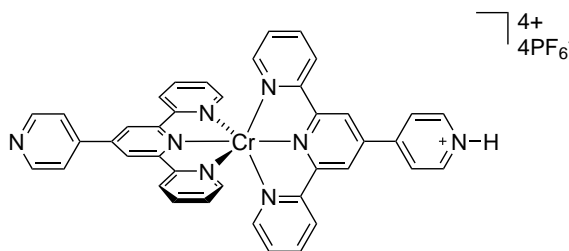
A microwave vial was charged with $[\text{Cr}(5,5''\text{-Me}_2\text{tpy})(\text{CF}_3\text{SO}_3)_3]$ (26.5 mg, 34.8 μmol), 5,5''-dimethyl-2,2':6',2''-terpyridine (5,5''-Me₂tpy) (10 mg, 38.3 μmol) and MeCN (4 ml). The reaction was heated in the microwave reactor at 150 °C and 11 bar for 2 h. Then the solvent was evaporated and the residue redissolved in MeOH. The solution was filtered into a MeOH solution with excess of NH_4PF_6 . The solution was stored overnight at 4 °C, resulting in a yellow precipitate (16.0 mg, 15.8 μmol , 45.5 %).

EA: Found C 39.02, H 3.50, N 8.45; $\text{C}_{34}\text{H}_{30}\text{CrF}_{18}\text{N}_6 \cdot 2\text{H}_2\text{O}$ requires C 39.05, H 3.28, N 8.03.

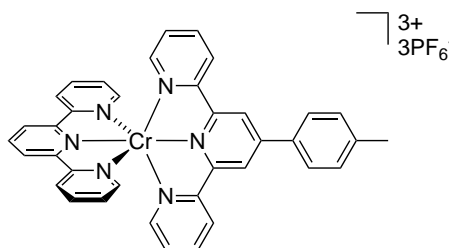
6.4.3.6 $[\text{Cr}(\text{LT}5)_2][\text{CF}_3\text{SO}_3]_3$ 

A mixture of $[\text{Cr}(\text{LT}5)(\text{CF}_3\text{SO}_3)_3]$ (50.0 mg, 51.2 μmol) and 4-([2,2':6',2''-terpyridin]-4'-yl)-*N,N*-diphenylamine (LT5) (26.9 mg, 56.4 μmol) in MeCN (2 ml) was heated at reflux for 7 h. The crude product was recrystallised from EtOH to yield a dark red precipitate (18.2 mg, 12.5 μmol , 24.4 %).

IR: (solid, ν/cm^{-1}) 503 (s), 570 (m), 635 (s), 661 (m), 691 (m), 717 (m), 749 (m), 786 (m), 829 (m), 1026 (s), 1068 (m), 1094 (m), 1120 (m), 1142 (s), 1198 (s), 1222 (s), 1240 (s), 1332 (m), 1366 (m), 1418 (m), 1439 (m), 1476 (s), 1520 (m), 1568 (s), 1575 (s), 1605 (m), 3075 (w), 3497 (w). **EA:** Found C 56.24, H 3.64, N 7.83; $\text{C}_{69}\text{H}_{51}\text{CrF}_9\text{N}_8\text{S}_3\text{O}_9 \cdot 1\text{H}_2\text{O}$ requires C 56.24, H 3.63, N 7.61.

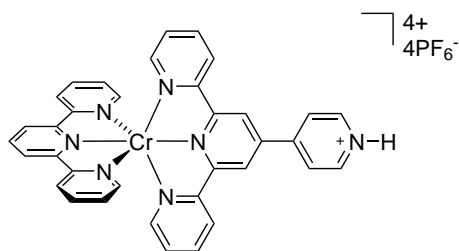
6.4.3.7 $[\text{Cr}(\text{HLT11})(\text{LT11})][\text{PF}_6]_4$ 

The compound was prepared by the same method as $[\text{Cr}(\text{tpy})_2][\text{PF}_6]_3$, starting with $[\text{Cr}(\text{LT11})\text{Cl}_3]$ (200 mg, 0.427 mmol) and $\text{CF}_3\text{SO}_3\text{H}$ (1.5 ml, 17 mmol) in the first step, and then 4'-(pyridin-4-yl)-2,2':6',2''-terpyridine (LT11) (146 mg, 0.469 mmol) and a reaction time of 4 h in the second step. To remove some remaining zinc powder from the first step the solution was filtered through a paper filter and celite respectively. The X-ray structure confirmed that a protonated complex was isolated. The bulk product could not be obtained pure, but a X-ray structure could be determined (3.9.1.6, p. 81).

6.4.3.8 $[\text{Cr}(\text{tpy})(4'-(4\text{-tolyl})\text{tpy})][\text{PF}_6]_3$ 

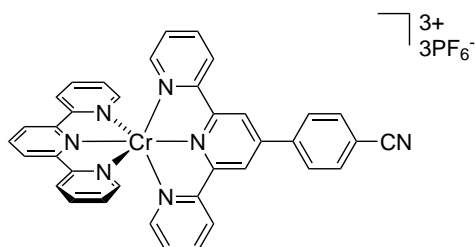
The compound was prepared by the same method as $[\text{Cr}(\text{tpy})_2][\text{PF}_6]_3$, starting with $[\text{Cr}(\text{tpy})\text{Cl}_3]$ (165 mg, 0.421 mmol) and $\text{CF}_3\text{SO}_3\text{H}$ (1.5 ml, 16.9 mmol) in the first step, and then 4'-(4-tolyl)tpy (150 mg, 0.463 mmol) and a reaction time of 4 h 40 min in the second step. $[\text{Cr}(\text{tpy})(4'-(4\text{-tolyl})\text{tpy})][\text{PF}_6]_3$ was isolated as an orange solid (304 mg, 0.291 mmol, 69.1 %).

IR: (solid, ν/cm^{-1}) 602 (w), 660 (m), 725 (m), 741 (w), 772 (s), 789 (w), 818 (vs), 828 (vs), 1028 (m), 1038 (w), 1047 (w), 1098 (w), 1171 (w), 1249 (w), 1327 (w), 1437 (w), 1447 (w), 1482 (m), 1549 (w), 1571 (w), 1605 (m), 1700 (s). **UV-VIS:** (H_2O , $1.0 \times 10^{-5} \text{ mol dm}^{-3}$) λ / nm 267 ($\epsilon / \text{dm}^3 \text{ mol}^{-1} \text{ cm}^{-1}$ 25700), 284 (23100), 347 (24150), 363 sh (20900). **EA:** Found C 42.00, H 2.55, N 8.04; $\text{C}_{37}\text{H}_{28}\text{CrF}_{18}\text{N}_6\text{P}_3 \cdot \text{MeOH}$ requires C 42.43, H 3.00, N 7.81.

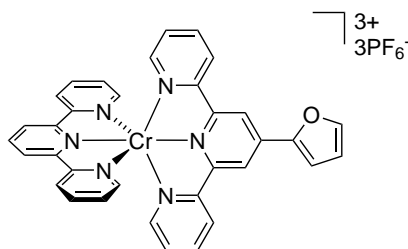
6.4.3.9 $[\text{Cr}(\text{tpy})(\text{HLT11})][\text{PF}_6]_4$ 

The compound was prepared by the same method as $[\text{Cr}(\text{tpy})_2][\text{PF}_6]_3$, starting with $[\text{Cr}(\text{tpy})\text{Cl}_3]$ (157 mg, 0.400 mmol) and $\text{CF}_3\text{SO}_3\text{H}$ (1.4 ml, 16 mmol) in the first step, and then 4'-(pyridin-4-yl)-2,2':6',2''-terpyridine (LT11) (137 mg, 0.440 mmol) and a reaction time of 5 h 30 min in the second step. The X-ray structure and the elemental analysis results indicate that the protonated complex was isolated. $[\text{Cr}(\text{tpy})(\text{HLT11})][\text{PF}_6]_4$ was isolated as a yellow powder (413 mg, 0.359 mmol, 89.6 %).

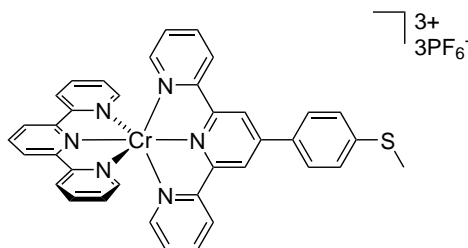
IR: (solid, ν/cm^{-1}) 503 (s), 554 (s), 619 (w), 639 (m), 661 (s), 676 (w), 728 (s), 731 (s), 772 (s), 821 (s), 1028 (s), 1101 (w), 1170 (w), 1247 (s), 1284 (w), 1329 (w), 1413 (w), 1433 (w), 1451 (w), 1482 (s), 1509 (w), 1543 (w), 1564 (w), 1573 (w), 1599 (s), 1609 (s), 1623 (w), 3109 (w), 3320 (w), 3583 (w), 3657 (w). **EA:** Found C 35.17, H 2.43, N 8.60; $\text{C}_{35}\text{H}_{26}\text{CrF}_{24}\text{N}_7\text{P}_4 \cdot \text{H}_2\text{O}$ requires C 35.22, H 2.28, N 8.22.

6.4.3.10 $[\text{Cr}(\text{tpy})(\text{LT7})][\text{PF}_6]_4$ 

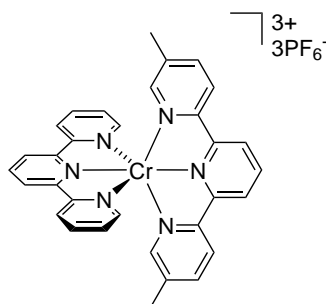
The compound was prepared by the same method as $[\text{Cr}(\text{tpy})_2][\text{PF}_6]_3$, starting with $[\text{Cr}(\text{tpy})\text{Cl}_3]$ (202 mg, 0.516 mmol) and $\text{CF}_3\text{SO}_3\text{H}$ (1.8 ml, 21 mmol) in the first step, and then 4'-(4-isocyanophenyl)-2,2':6',2''-terpyridine (LT7) (190 mg, 0.567 mmol) and a reaction time of 4 h 30 min in the second step. The bulk product could not be obtained pure, but an X-ray structure could be determined (3.9.2.3, p. 87).

6.4.3.11 $[\text{Cr}(\text{tpy})(\text{LT8})][\text{PF}_6]_3$ 

The compound was prepared by the same method as $[\text{Cr}(\text{tpy})_2][\text{PF}_6]_3$, starting with $[\text{Cr}(\text{tpy})\text{Cl}_3]$ (202 mg, 0.516 mmol) and $\text{CF}_3\text{SO}_3\text{H}$ (1.8 ml, 21 mmol) in the first step, and then 4'-(furan-2-yl)-2,2':6',2''-terpyridine (LT8) (170 mg, 0.567 mmol) and a reaction time of 7 h 15 min in the second step. The bulk product could not be obtained pure, but an X-ray structure could be determined (3.9.2.6, p. 92).

6.4.3.12 $[\text{Cr}(\text{tpy})(\text{LT9})][\text{PF}_6]_3$ 

The compound was prepared by the same method as $[\text{Cr}(\text{tpy})_2][\text{PF}_6]_3$, starting with $[\text{Cr}(\text{tpy})\text{Cl}_3]$ (132 mg, 0.336 mmol) and $\text{CF}_3\text{SO}_3\text{H}$ (1.2 ml, 13.4 mmol) in the first step, and then 4'-(methylthio)-2,2':6',2''-terpyridine (LT9) (131 mg, 0.369 mmol) and a reaction time of 5 h in the second step. The bulk product could not be obtained pure, but an X-ray structure could be determined (3.9.2.4, p. 89).

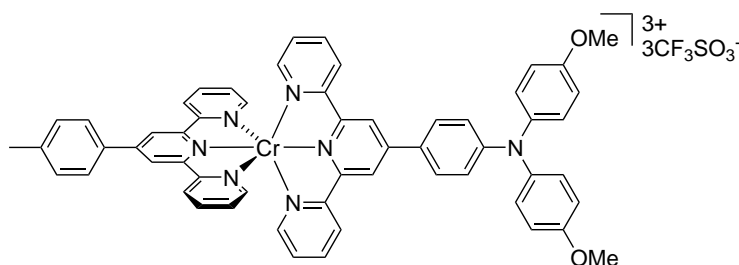
6.4.3.13 $[\text{Cr}(\text{tpy})(5,5''\text{-Me}_2\text{tpy})][\text{PF}_6]_3$ 

The compound was prepared by the same method as $[\text{Cr}(\text{tpy})_2][\text{PF}_6]_3$, starting with $[\text{Cr}(\text{tpy})\text{Cl}_3]$ (95.4 mg, 0.244 mmol) and $\text{CF}_3\text{SO}_3\text{H}$ (0.8 ml, 9.74 mmol) in the first step, and then 5,5''-Me₂tpy (70.0 mg, 0.268 mmol) and a reaction time of 4 h 45 min in the second step. $[\text{Cr}(\text{tpy})(5,5''\text{-Me}_2\text{tpy})][\text{PF}_6]_2$

was isolated as an orange solid (215 mg, 0.219 mmol, 89.8 %).

IR: (solid, ν/cm^{-1}) 603 (m), 636 (w), 661 (m), 671 (m), 700 (m), 729 (s), 741 (s), 767 (s), 783 (s), 790 (s), 813 (s), 901 (w), 1029 (m), 1045 (w), 1052 (m), 1064 (w), 1100 (w), 1117 (w), 1156 (w), 1172 (w), 1197 (w), 1234 (w), 1245 (w), 1257 (w), 1309 (w), 1332 (w), 1339 (w), 1384 (w), 1398 (w), 1456 (m), 1482 (m), 1512 (w), 1559 (m), 1575 (w), 1602 (m), 1609 (m), 1700 (w), 2356 (w), 3095 (w), 3999 (w). **MS:** MALDI-TOF m/z 706.4 (calc. for $[\text{M}^+2\text{PF}_6]^-$ 691.1), 830.7 (calc. for $[\text{M}-\text{PF}_6]^+$ 836.1). **UV-VIS:** (H_2O , $1.0 \times 10^{-5} \text{ mol dm}^{-3}$) λ / nm 264 ($\epsilon / \text{dm}^3 \text{ mol}^{-1} \text{ cm}^{-1}$ 31100), 286 sh (22300), 323 (16100), 334 (17050), 362 (14150), 362 (14150). **EA:** Found C 38.73, H 3.21, N 8.53; $\text{C}_{32}\text{H}_{26}\text{CrF}_{18}\text{N}_6\text{P}_3 \cdot \text{H}_2\text{O}$ requires C 38.45, H 2.82, N 8.41.

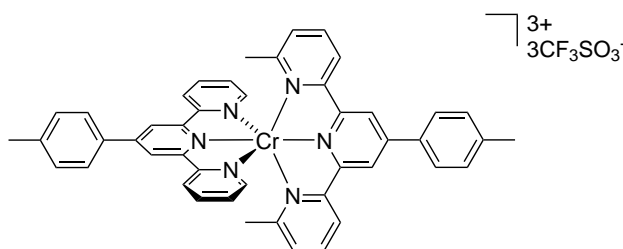
6.4.3.14 $[\text{Cr}(\text{LT6})(4'-(4\text{-tolyl})\text{tpy})][\text{CF}_3\text{SO}_3]_3$



The compound was prepared by the same method as $\text{Cr}(4'-(4\text{-tolyl})\text{tpy})_2][\text{CF}_3\text{SO}_3]_3$, starting with $[\text{Cr}(4'-(4\text{-tolyl})\text{tpy})\text{Cl}_3]$ (34.8 mg, 72.2 μmol) and $\text{CF}_3\text{SO}_3\text{H}$ (0.5 ml, 5.6 mmol) in the first step, and then 4-([2,2':6',2''-terpyridin]-4'-yl)-*N,N*-bis(4-methoxyphenyl)aniline (LT6) (42.6 mg, 79.4 μmol) and a reaction time of 6 h in the second step. $[\text{Cr}(\text{LT6})(4'-(4\text{-tolyl})\text{tpy})][\text{CF}_3\text{SO}_3]_3$ was isolated as a dark red solid (85.7 mg, 63.1 μmol , 43.7 %).

EA: Found C 52.77, H 3.85, N 6.99; $\text{C}_{60}\text{H}_{45}\text{CrF}_9\text{N}_7\text{S}_3\text{O}_{11} \cdot \text{MeOH}$ requires C 52.66, H 3.55, N 7.05.

6.4.3.15 $[\text{Cr}(4'-(4\text{-tolyl})\text{tpy})(\text{LT4})][\text{CF}_3\text{SO}_3]_3$

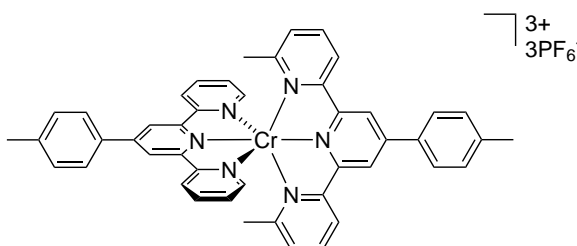


The compound was prepared by the same method as $\text{Cr}(4'-(4\text{-tolyl})\text{tpy})_2][\text{CF}_3\text{SO}_3]_3$, starting with $[\text{Cr}(4'-(4\text{-tolyl})\text{tpy})\text{Cl}_3]$ (48.2 mg, 0.100 mmol) and $\text{CF}_3\text{SO}_3\text{H}$ (0.36 ml, 4.0 mmol) in the first step, and then 6,6''-dimethyl-4'-(*p*-tolyl)-2,2':6',2''-terpyridine (LT4) (38.7 mg, 0.110 mmol) and a reaction time of 5 h 30 min in the second step. $[\text{Cr}(4'-(4\text{-tolyl})\text{tpy})(\text{LT4})][\text{CF}_3\text{SO}_3]_3$ was isolated as an orange solid. The crude product was recrystallised from EtOH (31.7 mg, 0.0185 mmol, 19.4 %).

IR: (solid, ν/cm^{-1}) 516 (m), 571 (m), 593 (w), 633 (s), 691 (w), 728 (w), 747 (w), 755 (w), 788 (m), 802 (m), 818 (m), 883 (w), 1000 (m), 1027 (s), 1099 (w), 1121 (m), 1141 (s), 1196

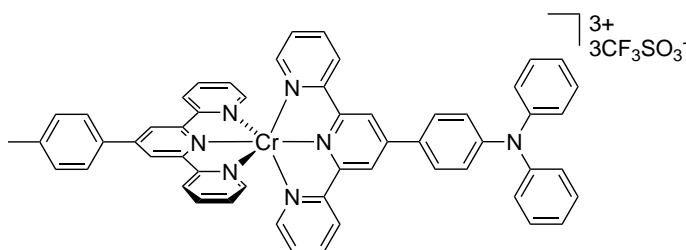
(w), 1223 (s), 1247 (s), 1369 (w), 1408 (w), 1433 (m), 1480 (w), 1540 (w), 1545 (m), 1570 (w), 1607 (m), 3084 (m), 3498 (w). **EA:** Found C 49.35, H 3.62, N 7.18; $C_{49}H_{38}CrF_9N_{60}O_9S_3 \cdot H_2O$ requires C 49.38, H 3.38, N 7.05.

6.4.3.16 $[Cr(4'-(4\text{-tolyl})\text{tpy})(\text{LT4})][PF_6]_3$



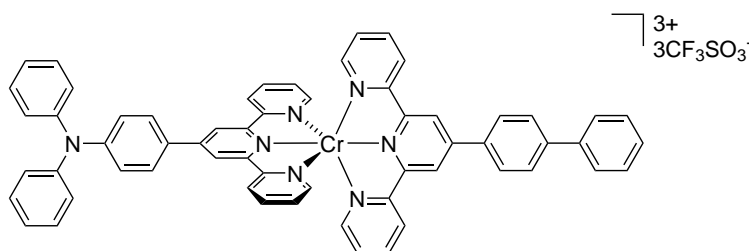
The crude product of $[Cr(4'-(4\text{-tolyl})\text{tpy})(\text{LT4})][CF_3SO_3]_3$ (66.0 mg, 0.0511 mmol) was dissolved in MeOH, filtered and the filtrate poured into a MeOH solution of excess NH_4PF_6 . The yellow precipitate that formed was separated by filtration, and was washed with hexane and Et_2O . $[Cr(4'-(4\text{-tolyl})\text{tpy})(\text{LT4})][PF_6]_3$ was isolated as a yellow powder (43.4 mg, 3.72 μmol , 6.61 %) **IR:** (solid, ν/cm^{-1}) 505 (s), 555 (s), 591 (w), 637 (w), 663 (w), 691 (w), 740 (m), 748 (m), 788 (s), 817 (s), 826 (s), 829 (s), 1015 (w), 1029 (m), 1036 (m), 1096 (w), 1167 (w), 1194 (w), 1248 (w), 1276 (w), 1374 (w), 1407 (w), 1436 (m), 1480 (m), 1549 (m), 1572 (w), 1600 (m), 3116 (w). **EA:** Found C 46.16, H 3.86, N 6.93; $C_{46}H_{38}CrF_{18}N_6P_3S \cdot 2H_2O$ requires C 46.13, H 3.54, N 7.02.

6.4.3.17 $[Cr(4'-(4\text{-tolyl})\text{tpy})(\text{LT5})][CF_3SO_3]_3$



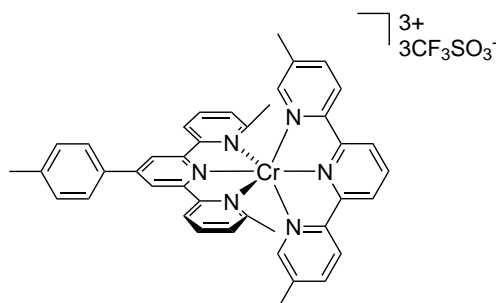
The compound was prepared by the same method as $[Cr(4'-(4\text{-tolyl})\text{tpy})_2][CF_3SO_3]_3$, starting with $[Cr(4'-(4\text{-tolyl})Cl_3]$ (91.9 mg, 0.191 mmol) and CF_3SO_3H (1.7 ml, 7.6 mmol) in the first step, and then 4-([2,2':6',2''-terpyridin]-4'-yl)-*N,N*-diphenylaniline (LT5) (100 mg, 0.210 mmol) and a reaction time of 5 h 30 min in the second step. $[Cr(4'-(4\text{-tolyl})\text{tpy})(\text{LT5})][CF_3SO_3]_3$ was isolated as a dark red solid (236 mg, 0.182 mmol, 95.2 %).

IR: (solid, ν/cm^{-1}) 573 (m), 635 (s), 662 (m), 693 (m), 725 (w), 755 (m), 786 (m), 823 (w), 846 (w), 885 (w), 1026 (s), 1068 (w), 1096 (m), 1147 (s), 1198 (m), 1222 (s), 1244 (s), 1336 (w), 1367 (w), 1423 (m), 1464 (m), 1475 (m), 1478 (m), 1520 (w), 1538 (m), 1564 (m), 1569 (m), 1579 (m), 1602 (m), 3071 (w), 3498 (w). **EA:** Found C 51.99, H 3.36, N 7.42; $C_{58}H_{41}CrF_9N_7S_3O_9 \cdot 2H_2O$ requires C 52.17, H 3.45, N 7.42.

6.4.3.18 $[\text{Cr}(\text{LT2})(\text{LT5})][\text{CF}_3\text{SO}_3]_3$ 

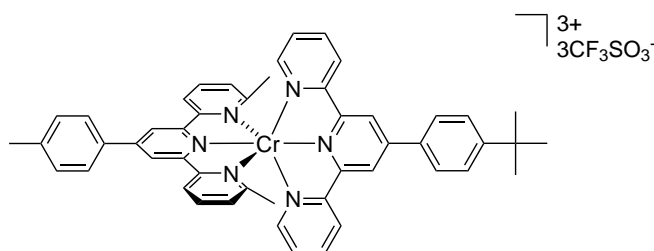
The compound was prepared by the same method as $[\text{Cr}(4'-(4\text{-tolyl})\text{tpy})_2][\text{CF}_3\text{SO}_3]_3$, starting with $[\text{Cr}(\text{LT2})\text{Cl}_3]$ (104 mg, 0.191 mmol) and $\text{CF}_3\text{SO}_3\text{H}$ (1.7 ml, 7.6 mmol) in the first step, and then 4-([2,2':6',2''-terpyridin]-4'-yl)-*N,N*-diphenylaniline (LT5) (100 mg, 0.210 mmol) and a reaction time of 5 h 30 min in the second step. $[\text{Cr}(\text{LT2})(\text{LT5})][\text{CF}_3\text{SO}_3]_3$ was isolated as a dark red solid (64.9 mg, 47.7 μmol , 50.0 %).

IR: (solid, ν/cm^{-1}) 500 (s), 505 (s), 571 (m), 604 (m), 633 (s), 661 (m), 692 (m), 717 (w), 727 (m), 754 (m), 768 (m), 787 (m), 826 (w), 839 (w), 890 (w), 1025 (s), 1095 (m), 1144 (m), 1201 (m), 1223 (m), 1242 (s), 1333 (w), 1367 (w), 1419 (m), 1436 (m), 1477 (m), 1522 (w), 1540 (m), 1569 (m), 1578 (m), 1601 (m), 3066 (w), 3492 (w). **EA:** Found C 54.12, H 3.29, N 7.38; $\text{C}_{63}\text{H}_{43}\text{CrF}_9\text{N}_7\text{S}_3\text{O}_9 \cdot 1.5\text{H}_2\text{O}$ requires C 54.51, H 3.34, N 7.06.

6.4.3.19 $[\text{Cr}(5,5''\text{-Me}_2\text{tpy})(\text{LT4})][\text{CF}_3\text{SO}_3]_3$ 

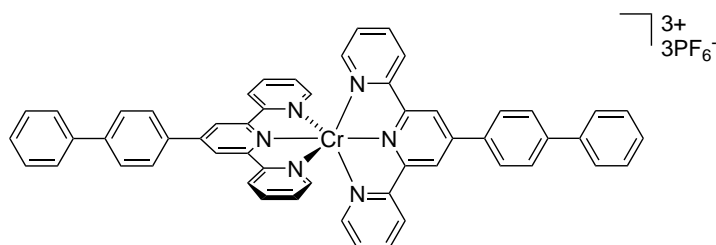
A microwave vial was charged with $[\text{Cr}(\text{LT4})(\text{CF}_3\text{SO}_3)_3]$ (29.6 mg, 34.8 μmol), 5,5''-dimethyl-2,2':6',2''-terpyridine (5,5''-Me₂tpy) (10 mg, 38.3 μmol) and MeCN (4 ml). The reaction mixture was heated in the microwave reactor at 150 °C and 11 bar for 2 h. Then the solvent was evaporated and one part of the batch was isolated as yellow triflate-salt (17.5 mg, 15.7 μmol , 45.2 %). The remaining of the batch was used for different solubility tests.

IR: (solid, ν/cm^{-1}) 520 (m), 572 (m), 634 (s), 704 (w), 730 (w), 743 (w), 758 (w), 792 (w), 802 (m), 804 (m), 809 (m), 857 (w), 879 (w), 994 (w), 1026 (w), 1102 (w), 1118 (w), 1145 (m), 1149 (m), 1150 (m), 1154 (m), 1174 (m), 1224 (m), 1244 (m), 1271 (m), 1333 (w), 1366 (w), 1393 (w), 1456 (w), 1489 (w), 1524 (w), 1602 (m), 1616 (w), 1631 (w), 3094 (w). **EA:** Found C 47.26, H 3.92, N 7.46; $\text{C}_{44}\text{H}_{36}\text{CrF}_9\text{N}_6\text{O}_9\text{S}_3 \cdot \text{MeOH}$ requires C 47.24, H 3.52, N 7.35.

6.4.3.20 $[\text{Cr}(\text{LT1})(\text{LT4})][\text{CF}_3\text{SO}_3]_3$ 

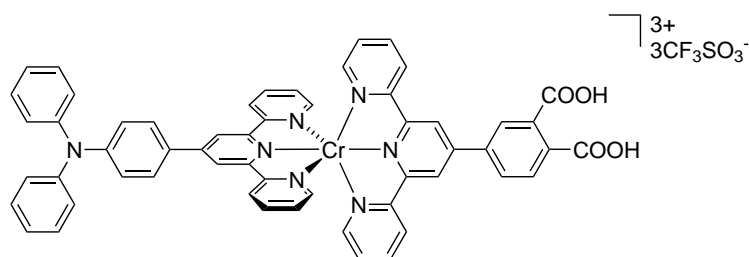
The compound was prepared by the same method as $[\text{Cr}(4'-(4\text{-tolyl})\text{tpy})_2][\text{CF}_3\text{SO}_3]_3$, starting with $[\text{Cr}(\text{LT4})\text{Cl}_3]$ (21 mg, 41.2 μmol) and $\text{CF}_3\text{SO}_3\text{H}$ (0.3 ml, 3.3 mmol) in the first step, and then 4'-(4-(*tert*-butyl)phenyl)-2,2':6',2''-terpyridine (LT1) (16.6 mg, 45.3 μmol) and a reaction time of 6 h in the second step. The crude product was recrystallised from EtOH. $[\text{Cr}(\text{LT1})(\text{LT4})][\text{CF}_3\text{SO}_3]_3$ was isolated as an orange solid (10.2 mg, 8.39 μmol , 20.4 %).

IR: (solid, ν/cm^{-1}) 500 (w), 520 (m), 547 (w), 572 (m), 631 (s), 662 (w), 688 (w), 716 (w), 727 (w), 743 (w), 755 (w), 790 (m), 813 (m), 837 (w), 849 (w), 885 (w), 931 (w), 997 (w), 1026 (s), 1045 (w), 1059 (w), 1067 (w), 1098 (w), 1155 (s), 1223 (s), 1244 (s), 1271 (s), 1366 (w), 1406 (w), 1436 (m), 1480 (m), 1520 (w), 1531 (w), 1543 (w), 1569 (w), 1602 (m), 1633 (w), 2968 (w), 3085 (w). **EA:** Found C 50.41, H 4.07, N 7.03; $\text{C}_{52}\text{H}_{44}\text{CrF}_9\text{N}_6\text{O}_9\text{S}_3 \cdot 1.5 \text{H}_2\text{O}$ requires C 50.24, H 3.81, N 6.76.

6.4.3.21 $[\text{Cr}(\text{LT2})_2][\text{PF}_6]_3$ 

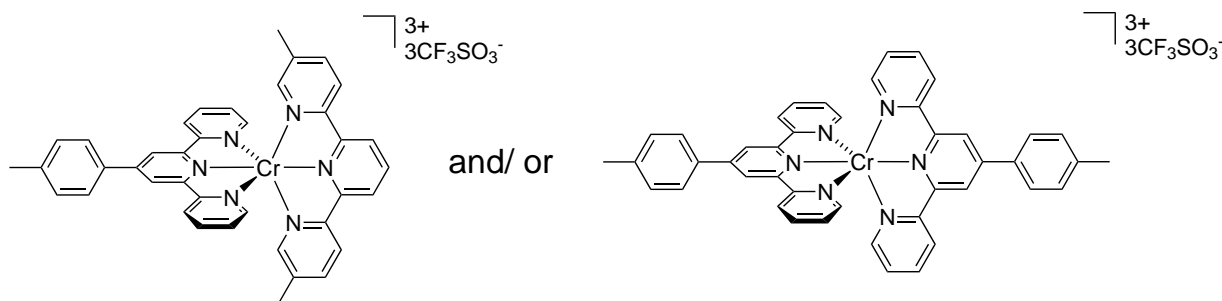
The compound was prepared by the same method as $[\text{Cr}(\text{tpy})_2][\text{PF}_6]_3$, starting with $[\text{Cr}(\text{LT2})\text{Cl}_3]$ (104 mg, 0.191 mmol) and $\text{CF}_3\text{SO}_3\text{H}$ (0.78 ml, 7.6 mmol) in the first step, and then 4'-([1,1'-biphenyl]-4-yl)-2,2':6',2''-terpyridine (LT2) (81.0 mg, 0.210 mmol) and a reaction time of 7 h in the second step. To exchange the counter ion the crude $[\text{Cr}(\text{LT2})_2][\text{CF}_3\text{SO}_3]_3$ was dissolved in methanol, filtered and poured into a MeOH solution of excess NH_4PF_6 . $[\text{Cr}(\text{LT2})_2][\text{PF}_6]_3$ was isolated as an orange solid (93.7 mg, 0.0744 mmol, 39.0 %).

IR: (solid, ν/cm^{-1}) 501 (s), 508 (s), 513 (s), 546 (m), 555 (s), 663 (w), 693 (m), 699 (w), 727 (m), 740 (m), 759 (m), 766 (m), 787 (m), 828 (s), 1005 (w), 1028 (w), 1097 (w), 1156 (w), 1165 (w), 1247 (w), 1301 (w), 1369 (w), 1406 (w), 1432 (w), 1479 (m), 1542 (w), 1599 (m), 3085 (w). **EA:** Found C 51.02, H 3.27, N 7.03; $\text{C}_{54}\text{H}_{38}\text{CrF}_{18}\text{N}_6\text{P}_3 \cdot 0.5\text{H}_2\text{O}$ requires C 51.19, H 3.10, N 6.63.

6.4.3.22 $[\text{Cr}(\text{LT5})(\text{LT10})][\text{CF}_3\text{SO}_3]_3$ 

4-([2,2':6',2''-terpyridin]-4'-yl)phthalic acid (LT10) (17.5 mg, 40.0 μmol) was suspended in MeCN (8 ml) and heated at reflux. After 1 h some of the ligand was dissolved and the solution turned pale yellow. Then $[\text{Cr}(\text{LT4})(\text{CF}_3\text{SO}_3)_3]$ (17.5 mg, 44.0 μmol) was added and heated the reaction at reflux for 10 h. The crude product was filtered and the solvent evaporated, to yield a dark red powder (40.1 mg, 29.2 μmol , 73 %).

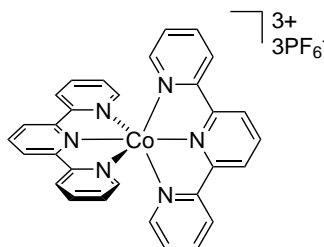
IR: (solid, ν/cm^{-1}) 501 (s), 513 (s), 571 (m), 613 (m), 636 (s), 689 (w), 699 (m), 729 (w), 744 (w), 758 (m), 786 (m), 827 (w), 977 (w), 993 (m), 1026 (s), 1068 (w), 1097 (m), 1154 (s), 1224 (s), 1245 (s), 1336 (w), 1419 (w), 1478 (m), 1489 (w), 1520 (w), 1532 (w), 1541 (w), 1559 (w), 1569 (m), 1580 (m), 1599 (m), 1712 (w), 2921 (w), 3067 (w). **EA:** Found C 49.50, H 3.56, N 7.15; $\text{C}_{59}\text{H}_{39}\text{CrF}_9\text{N}_7\text{O}_{13}\text{S}_3 \cdot 3\text{H}_2\text{O}$ requires C 49.65, H 3.18, N 6.87.

6.4.3.23 $[\text{Cr}(4'-(4\text{-tolyl})\text{tpy})(5,5''\text{-Me}_2\text{tpy})][\text{CF}_3\text{SO}_3]_3$ (trial)

A microwave vial was charged with $[\text{Cr}(4'-(4\text{-tolyl})\text{tpy})(\text{CF}_3\text{SO}_3)_3]$ (28.6 mg, 34.8 μmol), 5,5''-dimethyl-2,2':6',2''-terpyridine (5,5''-Me₂tpy) (10 mg, 38.3 μmol) and 4 ml MeCN. The reaction was heated in the microwave reactor at 150°C at 11 bar for 1 h. Then the solvent was evaporated and redissolved in MeOH. The solution was filtered and evaporated to dryness. The bulk product could not be obtained pure and X-ray growing trials gave the homoleptic $[\text{Cr}(4'-(4\text{-tolyl})\text{tpy})_2][\text{CF}_3\text{SO}_3]_3$ (3.3, p. 43).

6.5 Synthesis of the bis(terpyridine)cobalt(III) complexes

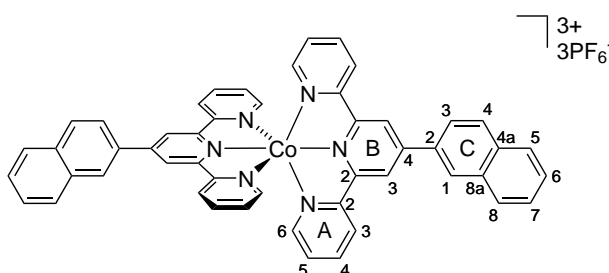
6.5.1 $[\text{Co}(\text{tpy})_2][\text{PF}_6]_3$



$\text{Co}(\text{OAc})_2 \cdot 4\text{H}_2\text{O}$ (53.2 mg, 0.214 mmol) and tpy (101 mg, 0.433 mmol) were dissolved in $\text{CHCl}_3/\text{MeOH}$ (9:1, 20 ml). The orange solution was stirred at room temperature for 50 min, the colour turned to dark red. An excess of NH_4PF_6 in MeOH was added to precipitate the intermediate. The precipitation was collected by filtration through celite, and washed in MeOH and Et_2O . The residue was redissolved in MeCN, and the solvent removed by evaporation. The intermediate $[\text{Co}(\text{tpy})_2][\text{PF}_6]_2$ was isolated as a brown solid. $[\text{Co}(\text{tpy})_2][\text{PF}_6]_2$ was suspended in water (10 ml) and a saturated solution of aqueous Br_2 (10 drops neat Br_2 in 10 ml H_2O) was added. The orange reaction mixture was stirred for 20 h at room temperature. An excess of NH_4PF_6 in H_2O was added and stirred for 20 min. The precipitation was filtered through celite and washed with H_2O , EtOH and Et_2O . The residue was redissolved with MeCN, and the solvent removed by evaporation. $[\text{Co}(\text{tpy})_2][\text{PF}_6]_3$ was isolated as an orange solid (61.9 mg, 0.0645 mmol, 30.1 %).

$^1\text{H-NMR}$ (250 MHz, 298 K, MeCN- d_3) $\delta/\text{ppm} = 9.14 - 8.95$ (m, 6H), 8.59 (dd, $J = 7.9, 1.5$ Hz, 4H), 8.22 (td, $J = 7.8, 1.3$ Hz, 4H), 7.47 - 7.36 (m, 4H), 7.22 (dd, $J = 5.8, 1.3$ Hz, 4H). ^1H NMR spectroscopic data agree with literature data.¹⁶²

6.5.2 $[\text{Co}(\text{LT3})_2][\text{PF}_6]_3$



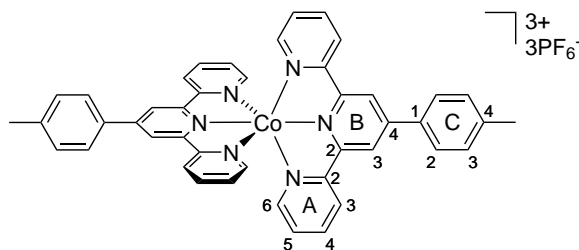
The compound was prepared by the same method as $[\text{Co}(\text{tpy})_2][\text{PF}_6]_3$. $\text{Co}(\text{OAc})_2 \cdot 4\text{H}_2\text{O}$ (99.6 mg, 0.400 mmol) and 4'-(naphthalen-2-yl)-2,2':6',2''-terpyridine (LT3) (290 mg, 0.806 mmol) were dissolved in $\text{CHCl}_3/\text{MeOH}$ (9:1, 40 ml) and stirred at room temperature for 1 h. The dark red intermediate $[\text{Co}(4'-(4\text{-tolyl})\text{tpy})_2][\text{PF}_6]_2$ was then suspended in H_2O (20 ml) and oxidised by adding a saturated solution of aqueous Br_2 (20 drops neat Br_2 in 20 ml H_2O) and stirring for 23 h at room temperature. $[\text{Co}(\text{LT3})_2][\text{PF}_6]_3$ was isolated as an orange solid (409 mg, 0.337 mmol, 84.3 %).

$^1\text{H-NMR}$ (500 MHz, 295 K, MeCN- d_3) $\delta/\text{ppm} = 9.43$ (s, 4H, B₃), 8.97 (d, $J = 2.0$ Hz, 2H, C₁), 8.78 (dt, $J = 8.0, 1.0$ Hz, 4H, A₃), 8.41 (dd, $J = 8.6, 2.0$ Hz, 2H, C₃), 8.39 - 8.33 (m, 2H,

C₄), 8.34 – 8.23 (m, 6H, A₄&C₈), 8.20 – 8.12 (m, 2H, C₅), 7.84 – 7.74 (m, 4H, C₆&7), 7.52 – 7.42 (m, 8H, A₄&5). ¹³C{¹H}-NMR (126 MHz, 295 K, MeCN-d₃) δ/ppm = 125.4 (C₃), 126.5 (B₃), 128.3 (A₃), 128.8 (C_{6/7}), 129.1 (C₅), 129.9 (C_{6/7}), 130.4 (C₈), 130.7 (C₁), 131.1 (C₄), 131.9 (A_{5/6}), 133.2 (C₂), 134.3 (C_{8a}), 136.0 (C_{4a}), 144.2 (A₄), 153.5 (A_{5/6}), 157.2 (two signals, A₂&B₂), 158.7 (B₄).

IR: (solid, ν/cm⁻¹) 500 (w), 553 (s), 567 (w), 590 (w), 610 (w), 620 (w), 628 (w), 654 (w), 663 (m), 667 (m), 670 (w), 688 (w), 695 (m), 725 (s), 741 (s), 749 (s), 757 (s), 784 (s), 826 (s), 904 (w), 948 (w), 970 (w), 1031 (w), 1049 (w), 1060 (w), 1101 (w), 1135 (w), 1169 (w), 1203 (w), 1223 (w), 1252 (w), 1297 (w), 1364 (w), 1423 (w), 1444 (w), 1482 (m), 1559 (m), 1609 (m), 3102 (w). **EA:** Found C 48.52, H 2.83, N 6.93; C₅₀H₃₄CoF₁₈N₆P₃·H₂O requires C 48.80, H 2.95, N 6.83.

6.5.3 [Co(4'-(4-tolyl)tpy)₂][PF₆]₃



The compound was prepared by the same method as [Co(tpy)₂][PF₆]₃. Co(OAc)₂·4H₂O (99.6 mg, 0.400 mmol) and 4'-(*p*-tolyl)-2,2':6',2''-terpyridine (4'-(4-tolyl)tpy) (261 mg, 0.806 mmol) were dissolved in CHCl₃/ MeOH (9:1, 40 ml) and stirred at room temperature for 1 h. The dark red intermediate [Co(4'-(4-tolyl)tpy)₂][PF₆] was then suspended in H₂O (20 ml) and oxidised by adding a saturated solution of aqueous Br₂ (20 drops neat Br₂ in 20 ml H₂O) and stirring for 23 h at room temperature. [Co(4'-(4-tolyl)₂][PF₆]₃ was isolated as an orange solid (437 mg, 0.383 mmol, 95.8 %).

¹H-NMR (500 MHz, 295 K, MeCN-d₃) δ/ppm = 9.24 (s, 4H, B₃), 8.71 (ddd, J = 7.9, 1.5, 0.6 Hz, 4H, A₃), 8.29 – 8.21 (m, 8H, A₄&C₂), 7.68 (dd, J = 8.5, 0.7 Hz, 4H, C₃), 7.45 – 7.41 (m, 4H, A₅), 7.39 (ddd, J = 5.8, 1.4, 0.6 Hz, 4H, A₆), 2.58 (s, 6H, C_{Me}). ¹³C{¹H}-NMR (126 MHz, 295 K, MeCN-d₃) δ/ppm = 158.8 (B₄), 157.3 (B₂), 157.1 (A₂), 153.4 (A₆), 144.7 (C₄), 144.1 (A₄), 133.1 (C₁), 131.8 (A₅), 131.7 (C₃), 129.4 (C₂), 128.2 (A₃), 126.0 (B₃), 21.6 (C_{Me}).

IR: (solid, ν/cm⁻¹) 500 (s), 503 (s), 556 (s), 625 (w), 654 (w), 662 (m), 695 (w), 716 (m), 727 (m), 742 (m), 751 (m), 786 (s), 820 (s), 833 (s), 879 (w), 899 (w), 976 (w), 1017 (w), 1030 (m), 1060 (w), 1104 (w), 1170 (w), 1197 (w), 1251 (w), 1374 (w), 1405 (w), 1424 (w), 1435 (m), 1484 (m), 1558 (w), 1604 (m), 1617 (m), 3097 (w).

Conclusion

The synthesis and characterisation of 25 new chromium(III) complexes with polypyridyl ligands have been presented in this PhD-thesis (7 tris(diimine)chromium(III) complexes and 18 bis(terpyridine)chromium(III) complexes). A new three step synthesis route for the preparation of $\{\text{Cr}(\text{tpy})_2\}^{3+}$ complexes was developed. Starting with anhydrous CrCl_3 , $\{\text{Cr}(\text{tpy})\text{Cl}_3\}$ was prepared, followed by exchange of the Cl^- counter anions to CF_3SO_3^- to yield $\{\text{Cr}(\text{tpy})(\text{CF}_3\text{SO}_3)_3\}$. In the last step, the second tpy ligand is added to get $\{\text{Cr}(\text{tpy})_2\}^{3+}$. The successive addition of the two tpy ligands gives the possibility to synthesise heteroleptic $\{\text{Cr}(\text{tpy}_A)(\text{tpy}_B)\}^{3+}$ complexes. These are the first reported examples of heteroleptic bis(terpyridine)chromium(III) complexes. The structures of several heteroleptic complexes could be confirmed with X-ray analysis. Altogether, 17 crystal structures (homoleptic and heteroleptic, 6 tris(diimine)chromium(III) complexes and 12 bis(terpyridine)chromium(III) complexes) could be determined.

Despite the fact that the Cr^{3+} ion (d^3) is widely recognised as a kinetically inert metal centre, we observed a sensitive liability of the complexes in the presence of F^- or in an alkaline environment. The residues of these decompositions could be confirmed as $\{\text{Cr}(\text{tpy})\text{F}_3\}$ and $\{\text{Cr}(\text{tpy})(\text{OH})_3\}$ respectively. These findings led to an explanation of the photoluminescence observations done previously. It was already known that the photoluminescence properties of $\{\text{Cr}(\text{tpy})_2\}^{3+}$ are quite different from those of $\{\text{Cr}(\text{bpy})_3\}^{3+}$. We found that the majority of the observed emission could be assigned as deriving from small quantities of neutral or protonated free ligand.

The $\{\text{Cr}(\text{tpy})_2\}^{3+}$ complexes containing at least one *N,N*-diphenylaniline-tpy showed a broad and solvatochromic absorption. Although the broad absorption makes these complexes strong candidates for DSC applications, all trials were unsuccessful. Also, the application of $\{\text{Cr}(\text{bpy})_3\}^{3+}$ complexes in LEC devices was unsuccessful.

Bibliography

- [1] *Formeln und Tafeln*, ed. D. Mathematikkommission and D. Physikkommission, Orell Füssli, Zürich, 9th edn., 2001.
- [2] *Conversion Factors*, National Institute of Standards and Technology, <http://www.nist.gov/pml/data/wavenum/appendix.cfm>, 2010.
- [3] N. Eastaugh, V. Walsh, T. Chaplin and R. Siddall, *Pigment Compendium - A Dictionary of Historical Pigments*, Elsevier Butterworth-Heinemann, Oxford, 1st edn., 2004.
- [4] G. Schwedt, *Chem. unserer Zeit*, 2011, **45**, 294–295.
- [5] D. A. Herlod and R. L. Fitzgerald, in *Handbook on Metals in Clinical and Analytical Chemistry*, ed. H. G. Seiler, A. Siegel and H. Siegel, Marcel Dekker, New York, 1st edn., 1994, ch. 25.
- [6] *High-Purity Chromium Metal: Supply Issues for Gas-Turbine Superalloys*, The National Academies Press, 1995.
- [7] L. R. Nelson, *The Journal of the South African Institute of Mining and Metallurgy*, 1996, 135–144.
- [8] A. F. Holleman, E. Wiberg and N. Wiberg, *Lehrbuch der Anorganischen Chemie*, Walter de Gruyter, Berlin, 102nd edn., 2007.
- [9] G. Anger, J. Halstenberger, K. Hochgeschwender, C. Scherhag, U. Korallus, H. Knopf, P. Schmidt and M. Ohlinger, in *Ullman's Encyclopedia of Industrial Chemistry*, WILEY-VCH, Weinheim, 2012, pp. 157–191.
- [10] A. Stwertka, *Guide to the Elements*, Oxford University Press, Oxford, 2nd edn., 2002.
- [11] C. Blanford, *Chromium: yellow US school buses, gemstones and shiny chrome car parts (podcast Royal Society of Chemistry)*, 2010.
- [12] J. F. Papp, in *U.S. Geological Survey Minerals Yearbook 2011*, U.S. Geological Survey, 2013, pp. 17.1 – 17.22.
- [13] *Mineral Commodity Summaries 2013*, U.S. Department of the Interior, Reston, 2013.
- [14] D. G. Barceloux and D. Barceloux, *Clin. Toxicol.*, 1999, **37**, 173–194.
- [15] L. Pauling, *General Chemistry*, Dover Publications, Mineola, 3rd edn., 1970.
- [16] R. Cheng, Z. Liu, L. Zhong, X. He, P. Qiu, M. Terano, M. S. Eisen, S. L. Scott, B. Liu and Abstract, in *Polyolefins : 50 years after Ziegler and Natta I Polyethylene and Polypropylene*, ed. W. Kaminsky, Springer, Heidelberg, 2013.

- [17] T. H. Maiman, *Nature*, 1960, **187**, 493–494.
- [18] R. T. Krebs, *The History and Use of Our Earth's Chemical Elements - A Reference Guide*, Greenwood Press, Westport, 2nd edn., 2006.
- [19] L. H. Gade, *Koordinationschemie*, WILEY-VCH, Weinheim, 1st edn., 1998.
- [20] A. D. Convington, *Tanning Chemistry - The Science of Leather*, Royal Society of Chemistry, Cambridge, 1st edn., 2009.
- [21] J. B. Vincent, *J. Chem. Soc., Dalton Trans.*, 2010, **39**, 3787–3794.
- [22] K. R. Di Bona, S. Love, N. R. Rhodes, D. McAdory, S. H. Sinha, N. Kern, J. Kent, J. Strickland, A. Wilson, J. Beaird, J. Ramage, J. F. Rasco and J. B. Vincent, *J. Biol. Inorg. Chem.*, 2011, **16**, 381–390.
- [23] C. E. Housecroft and A. G. Sharpe, *Inorganic Chemistry*, Pearson Education Limited, Essex, 2nd edn., 2005.
- [24] G. E. Rodgers, *Descriptive Inorganic, Coordination and Solid-State Chemistry*, Cengage Learning, Boston, 3rd edn., 2012.
- [25] L. H. Gade, *Chem. unserer Zeit*, 2002, **36**, 168–175.
- [26] E. C. Constable and C. E. Housecroft, *Chem. Soc. Rev.*, 2013, **42**, 1429–1439.
- [27] A. Werner, Nobel Lecture, Stockholm, 1913.
- [28] P. Pfeiffer, *Z. anorg. Chem.*, 1908, **58**, 317–324.
- [29] F. Blau, *Ber. Dtsch. Chem. Ges.*, 1888, **21**, 1077–1078.
- [30] G. T. Morgan and F. H. Burstall, *J. Chem. Soc.*, 1932, 20.
- [31] *SciFinder*, American Chemical Society, <https://scifinder.cas.org>, 2014.
- [32] E. C. Constable, *Coord. Chem. Rev.*, 1989, **93**, 205–223.
- [33] P. A. Smith and L. C. Fraser, in *Comprehensive Coordination Chemistry II volume 1*, ed. J. A. McCleverty and T. J. Meyer, Elsevier Pergamon, Amsterdam, 2003, ch. 1.
- [34] U. S. Schubert, A. Winter and G. R. Newkome, *Terpyridine-based Materials: For Catalytic, Optoelectronic and Life Science Applications*, WILEY-VCH, Weinheim, 1st edn., 2011.
- [35] S. P. Faulkner, R. P. Gambrell and S. L. Ashby, *Water Quality Technical Note*, 1996, 1–10.
- [36] Z.-Q. Liang, C.-X. Wang, J.-X. Yang, H.-W. Gao, Y.-P. Tian, X.-T. Tao and M.-H. Jiang, *New J. Chem.*, 2007, **31**, 906.
- [37] K. Kalyanasundaram, *Coord. Chem. Rev.*, 1998, **177**, 347–414.
- [38] B. Bozic-Weber, E. C. Constable, N. Hostettler, C. E. Housecroft, R. Schmitt and E. Schoenhofer, *Chem. Commun.*, 2012, **48**, 5727–5729.
- [39] B. Bozic-Weber, E. C. Constable and C. E. Housecroft, *Coord. Chem. Rev.*, 2013, **257**, 3089–3106.

- [40] R. D. Costa, E. Ortí, H. J. Bolink, F. Monti, G. Accorsi and N. Armaroli, *Angew. Chem. Int. Ed.*, 2012, **51**, 8178–8211.
- [41] T. White, J. Knoll, S. Arachchige and K. Brewer, *Materials*, 2011, **5**, 27–46.
- [42] E. C. Constable, *Chem. Soc. Rev.*, 2007, **36**, 246–253.
- [43] M. Isaacs, A. G. Sykes and S. Ronco, *Inorg. Chim. Acta.*, 2006, **359**, 3847–3854.
- [44] C. C. Scarborough, S. Sproules, T. Weyhermüller, S. DeBeer and K. Wieghardt, *Inorg. Chem.*, 2011, **50**, 12446–12462.
- [45] R. Sriram, M. S. Henry and M. Z. Hoffman, *Inorg. Chem.*, 1979, **18**, 1727–1730.
- [46] J. Lilie, W. L. Waltz, S. H. Lee and L. L. Gregor, *Inorg. Chem.*, 1986, **25**, 4487–4492.
- [47] M. Maestri, F. Bolletta, L. Moggi, V. Balzani, M. S. Henry and M. Z. Hoffman, *J. Am. Chem. Soc.*, 1978, **100**, 2694–2701.
- [48] S. J. Milder, J. S. Gold and D. S. Kliger, *Inorg. Chem.*, 1990, **29**, 2506–2511.
- [49] A. Tiyabhorn and K. O. Zahir, *Can. J. Chem.*, 1996, **74**, 336–340.
- [50] K. Takada, G. D. Storrier, F. Pariente and H. D. Abruña, *J. Phys. Chem. B*, 1998, **102**, 1387–1396.
- [51] V. G. Vaidyanathan and B. U. Nair, *Eur. J. Inorg. Chem.*, 2004, **2004**, 1840–1846.
- [52] C. C. Scarborough, K. M. Lancaster, S. DeBeer, T. Weyhermüller, S. Sproules and K. Wieghardt, *Inorg. Chem.*, 2012, **51**, 3718–3732.
- [53] E. Bequerel, *La lumière, ses causes et ses effects*, 1867.
- [54] L. S. Forster, *Chem. Rev.*, 1990, **90**, 331–353.
- [55] V. Balzani, G. Bergamini, S. Campagna and F. Puntoriero, *Top Curr Chem*, 2007, 37–67.
- [56] A. D. Kirk, *Chem. Rev.*, 1999, **99**, 1607–1640.
- [57] *Bundesrat legt Eckpunkte für Klimapolitik nach 2020 fest*, Federal Office for the Environment, www.bafu.admin.ch, 2014.
- [58] R. D. Costa, D. Tordera, E. Ortí, H. J. Bolink, J. Schönle, S. Graber, C. E. Housecroft, E. C. Constable and J. A. Zampese, *J. Mater. Chem.*, 2011, **21**, 16108–16118.
- [59] *Periodic table*, Royal Society of Chemistry, www.rsc.org/periodic-table, 2014.
- [60] www.metalprices.org, 2014.
- [61] J. Lilie and W. L. Waltz, *Inorg. Chem.*, 1983, **22**, 1473–1478.
- [62] A. M. McDaniel, H.-W. Tseng, N. H. Damrauer and M. P. Shores, *Inorg. Chem.*, 2010, **49**, 7981–7991.
- [63] BFE, Bundesamt für Energie, Endverbrauch erneuerbare Energien, nach Energieträgern und Technologien 1990 - 2012 T8.2.5.1, Bern, 2013.
- [64] BFE, Bundesamt für Energie, Schweizerische Elektrizitätsstatistik 2012, Bern, 2013.

- [65] D. Wöhrle and O. R. Hild, *Chem. Unserer Zeit*, 2010, **44**, 174–189.
- [66] B. O'Regan and M. Grätzel, *Nature*, 1991, **353**, 737–740.
- [67] T. Bessho, E. C. Constable, M. Graetzel, A. Hernandez Redondo, C. E. Housecroft, W. Kylberg, M. K. Nazeeruddin, M. Neuburger and S. Schaffner, *Chem. Commun.*, 2008, 3717–3719.
- [68] A. Hagfeldt, G. Boschloo, L. Sun, L. Kloo and H. Pettersson, *Chem. Rev.*, 2010, **110**, 6595–6663.
- [69] M. Grätzel, *J. Photochem. Photobiol. A*, 2004, **164**, 3–14.
- [70] M. M. Richter, *Chem. Rev.*, 2004, **104**, 3003–3036.
- [71] E. F. Schubert, J. K. Kim, H. Luo and J.-Q. Xi, *Rep. Prog. Phys.*, 2006, **69**, 3069–3099.
- [72] C. J. Humphreys, *MRS Bull.*, 2008, **33**, 459–471.
- [73] Q. Pei, G. Yu, C. Zhang, Y. Yang and A. J. Heeger, *Science*, 1995, **269**, 1086–1088.
- [74] Q. Pei, G. Yu, C. Zhang and A. J. Heeger, *J. Am. Chem. Soc.*, 1996, **118**, 3922–3929.
- [75] K. M. Maness, R. H. Terrill, T. J. Meyer, R. W. Murray and R. M. Wightman, *J. Am. Chem. Soc.*, 1996, **118**, 10609–10616.
- [76] J. D. Slinker, A. A. Gorodetsky, M. S. Lowry, J. Wang, S. Parker, R. Rohl, S. Bernhard and G. G. Malliaras, *J. Am. Chem. Soc.*, 2004, **126**, 2763–2767.
- [77] A. B. Tamayo, S. Garon, T. Sajoto, P. I. Djurovich, I. M. Tsyba, R. Bau and M. E. Thompson, *Inorg. Chem.*, 2005, **44**, 8723–8732.
- [78] M. S. Lowry and S. Bernhard, *Chem. Eur. J.*, 2006, **12**, 7970–7977.
- [79] H.-C. Su, H.-F. Chen, F.-C. Fang, C.-C. Liu, C.-C. Wu, K.-T. Wong, Y.-H. Liu and S.-M. Peng, *J. Am. Chem. Soc.*, 2008, **130**, 3413–3419.
- [80] C. Ulbricht, B. Beyer, C. Friebe, A. Winter and U. S. Schubert, *Adv. Mater.*, 2009, **21**, 4418–4441.
- [81] R. D. Costa, F. J. Céspedes-Guirao, E. Ortí, H. J. Bolink, J. Gierschner, F. Fernández-Lázaro and A. Sastre-Santos, *Chem. Commun.*, 2009, 3886–3888.
- [82] R. D. Costa, E. Ortí, D. Tordera, A. Pertegás, H. J. Bolink, S. Graber, C. E. Housecroft, L. Sachno, M. Neuburger and E. C. Constable, *Adv. Energy Mater.*, 2011, **1**, 282–290.
- [83] W.-L. Jia, Y.-F. Hu, J. Gao and S. Wang, *Dalton Trans.*, 2006, 1721–1728.
- [84] H. J. Bolink, E. Coronado, R. D. Costa, P. Gaviña, E. Ortí and S. Tatay, *Inorg. Chem.*, 2009, **48**, 3907–3909.
- [85] D. Pucci, A. Bellusci, A. Crispini, M. Ghedini, N. Godbert, E. I. Szerb and A. M. Talarico, *J. Mater. Chem.*, 2009, **19**, 7643–7649.
- [86] H. Rudmann, S. Shimada and M. F. Rubner, *J. Am. Chem. Soc.*, 2002, **124**, 4918–4921.
- [87] O. Moudam, A. Kaeser, B. Delavaux-Nicot, C. Duhayon, M. Holler, G. Accorsi, N. Armaroli, I. Séguy, J. Navarro, P. Destruel and J.-F. Nierengarten, *Chem. Commun.*, 2007, **3092**, 3077–3079.

- [88] Q. Zhang, Q. Zhou, Y. Cheng, L. Wang, D. Ma, X. Jing and F. Wang, *Adv. Funct. Mater.*, 2006, **16**, 1203–1208.
- [89] J. D. Slinker, J. Rivnay, J. S. Moskowitz, J. B. Parker, S. Bernhard, H. D. Abruna and G. G. Malliaras, *J. Mater. Chem.*, 2007, **17**, 2976–2988.
- [90] I. Andrés-Tomé, J. Fyson, F. B. Dias, A. P. Monkman, G. Iacobellis and P. Coppo, *Dalton Trans.*, 2012, **41**, 8669–8674.
- [91] R. Starosta, U. K. Komarnicka and M. Puchalska, *J. Lumin.*, 2013, **143**, 137–144.
- [92] B. R. Baker and B. D. Mehta, *Inorg. Chem.*, 1965, **4**, 848–854.
- [93] A. Hauser, M. Maeder, W. T. Robinson, R. Murugesan and J. Ferguson, *Inorg. Chem.*, 1987, **26**, 1331–1338.
- [94] W. R. Robinson, *J. Chem. Educ.*, 1985, **62**, 1001.
- [95] L. R. Ocone and B. Block, *Inorg. Synth.*, 1966, **8**, 125–132.
- [96] N. Turova, *Inorganic Chemistry in Tables*, Springer, Heidelberg, 1st edn., 2011.
- [97] R. S. Nyholm and F. H. Burstall, *J. Chem. Soc.*, 1952, 3570–3579.
- [98] C. K. Ryu and J. F. Endicott, *Inorg. Chem.*, 1988, **27**, 2203–2214.
- [99] K. D. Barker, K. A. Barnett, S. M. Connell, J. W. Glaeser, A. J. Wallace, J. Wildsmith, B. J. Herbert, J. F. Wheeler and N. A. Kane-Maguire, *Inorg. Chim. Acta*, 2001, **316**, 41–49.
- [100] J. T. Veal, W. E. Hatfield and D. J. Hodgson, *Acta Crystallogr. Sect. B-Struct. Sci.*, 1973, **29**, 12–20.
- [101] R. P. Scaringe, P. Singh, R. P. Eckberg, W. E. Hatfield and D. J. Hodgson, *Inorg. Chem.*, 1975, **14**, 1127–1133.
- [102] N. Kane-Maguire and J. Hallock, *Inorg. Chim. Acta.*, 1979, **35**, L309–L311.
- [103] H. Dreves, *Z. anorg. allg. Chem.*, 1991, **605**, 145–150.
- [104] T. Kauffmann, J. König and A. Woltermann, *Chem. Ber.*, 1976, **109**, 3864–3868.
- [105] C. Dietrich-Buchecker, P. A. Marnot and J. P. Sauvage, *Tetrahedron Lett.*, 1982, 5291–5294.
- [106] E. Schönhofer, *Master thesis: Transition metal complexes for electroluminescent devices*, University of Basel, Basel, 2010.
- [107] P. Kopecky, *Inauguraldissertation: New Oligopyridine Ligands for Transition Metal Complexes and Their Applications*, University of Basel, Basel, 2012.
- [108] R. A. Marusak, K. Doan and S. D. Cummings, *Integrated approach to coordination chemistry an inorganic laboratory guide*, WILEY-INTERSCIENCE, Hoboken, 1st edn., 2007, pp. 202–206.
- [109] N. Serpone, M. A. Jamieson, M. S. Henry, M. Z. Hoffman, F. Bolletta and M. Maestri, *J. Am. Chem. Soc.*, 1979, **101**, 2907–2916.

- [110] E. König and S. Herzog, *J. Inorg. Nucl. Chem.*, 1970, **32**, 585–599.
- [111] M. A. Jamieson, C. H. Langford, N. Serpone and M. W. Hersey, *The Journal of Physical Chemistry*, 1983, **87**, 1004–1008.
- [112] J. R. Lakowicz, *Principles of Fluorescence Spectroscopy*, Springer, New York, 3rd edn., 2006.
- [113] M. Maestri, F. Bolletta, N. Serpone, L. Moggi and V. Balzani, *Inorg. Chem.*, 1976, **15**, 2048–2051.
- [114] M. A. Jamieson, N. Serpone and M. Maestri, *Inorg. Chem.*, 1978, **17**, 2432–2436.
- [115] M. S. Henry and M. Z. Hoffman, *J. Phys. Chem.*, 1979, **83**, 618–625.
- [116] D. Vonlanthen, *personal communication*, 2012.
- [117] S. Vasudevan, J. a. Smith, M. Wojdyla, A. DiTrapani, P. E. Kruger, T. McCabe, N. C. Fletcher, S. J. Quinn and J. M. Kelly, *Dalton Trans.*, 2010, **39**, 3990–3998.
- [118] P. Zanello, *Inorganic Electrochemistry*, Royal Society of Chemistry, Cambridge, 1st edn., 2003, pp. 230–236.
- [119] C. Janiak, *J. Chem. Soc., Dalton Trans.*, 2000, 3885–3896.
- [120] K. V. Goodwin, W. T. Pennington and J. D. Petersen, *Inorg. Chem.*, 1989, **28**, 2016–2018.
- [121] M. C. Hughes, D. J. Macero and J. Rao, *Inorg. Chim. Acta.*, 1981, **49**, 241–245.
- [122] M. C. Hughes and D. J. Macero, *Inorg. Chem.*, 1975, **15**, 2040–2044.
- [123] H. Riesen and L. Wallace, *PhysChemComm*, 2003, **6**, 9–11.
- [124] J. A. Broomhead, J. Evans, W. D. Grumiey and M. Sterns, *Dalton Trans.*, 1977, **2**, 173–176.
- [125] M. A. Jamieson, N. Serpone, M. S. Henry and M. Z. Hoffman, *Inorg. Chem.*, 1979, **18**, 214–216.
- [126] M. Hesse, H. Meier and B. Zeeh, *Spektroskopische Methoden in der organischen Chemie*, Thieme, Stuttgart, 6th edn., 2002.
- [127] *Spectral Database for Organic Compounds (SDBS)*, SDBS No.: 40029, http://sdfs.db.aist.go.jp/sdfs/cgi-bin/direct_frame_top.cgi, (accessed April 10th, 2014).
- [128] R. Fernandez-Galan, B. R. Manzano, A. Otero, M. Lanfranchi and M. A. Pellinghelli, *Inorg. Chem.*, 1994, **33**, 2309–2312.
- [129] T. Birk, M. J. Magnussen, S. Piligkos, H. Weihe, A. Holten and J. Bendix, *J. Fluor. Chem.*, 2010, **131**, 898–906.
- [130] G. U. Priimov, P. Moore, P. K. Maritim, P. K. Butalanyi and N. W. Alcock, *Dalton Trans.*, 2000, **1**, 445–449.
- [131] E. C. Constable, *Adv. Inorg. Chem.*, 1986, **30**, 69–121.
- [132] J. M. Rao, M. C. Hughes and D. J. Macero, *Inorg. Chim. Acta*, 1976, **18**, 127–131.

- [133] B. Brunschwig and N. Sutin, *J. Am. Chem. Soc.*, 1978, **100**, 7568–7577.
- [134] N. Yoshikawa, S. Yamabe, N. Kanehisa, H. Takashima and K. Tsukahara, *J. Phys. Org. Chem.*, 2009, **22**, 410–417.
- [135] N. Yoshikawa, S. Yamabe, N. Kanehisa, T. Inoue, H. Takashima and K. Tsukahara, *J. Phys. Org. Chem.*, 2010, 431–439.
- [136] K. A. Walters, Y.-J. Kim and J. T. Hupp, *J. Electroanal. Chem.*, 2003, **554–555**, 449–458.
- [137] N. Armaroli, L. D. Cola, V. Balzani, J.-P. Sauvage, C. Dietrich-Buchecker and J. M. Kern, *J. Chem. Soc. Faraday Trans.*, 1992, **88**, 553–556.
- [138] F. W. Vance and J. T. Hupp, *J. Am. Chem. Soc.*, 1999, **121**, 4047–4053.
- [139] J. F. Michalec, S. A. Bejune, D. G. Cuttell, G. C. Summerton, J. A. Gertenbach, J. S. Field, R. J. Haines and D. R. McMillin, *Inorg. Chem.*, 2001, **40**, 2193–200.
- [140] L. Xiao, Y. Xu, M. Yan, D. Galipeau, X. Peng and X. Yan, *J. Phys. Chem. A*, 2010, **114**, 9090–9097.
- [141] K. C. D. Robson, B. D. Koivisto, T. J. Gordon, T. Baumgartner and C. P. Berlinguette, *Inorg. Chem.*, 2010, **49**, 5335–5337.
- [142] J. Collin and S. Guillerez, *Coord. Chem. Rev.*, 1991, **111**, 291–296.
- [143] W. Leslie, R. A. Poole, P. R. Murray, L. J. Yellowlees, A. Beeby and J. G. Williams, *Polyhedron*, 2004, **23**, 2769–2777.
- [144] E. Baranoff, I. M. Dixon, J.-P. Collin, J.-P. Sauvage, B. Ventura and L. Flamigni, *Inorg. Chem.*, 2004, **43**, 3057–3066.
- [145] X. Chen, Q. Zhou, Y. Cheng, Y. Geng, D. Ma, Z. Xie and L. Wang, *J. Lumin.*, 2007, **126**, 81–90.
- [146] X. Chen, Y. Ding, Y. Cheng and L. Wang, *Synth. Met.*, 2010, **160**, 625–630.
- [147] M. C. Rezende, in *Encyclopedia of Supramolecular Chemistry - volume 2*, ed. J. L. Atwood and J. W. Steed, Marcel Dekker, New York, 2004, p. 1330.
- [148] P. A. Krieger, *High Purity Solvent Guide*, Burdick and Jackson Laboratories, Michigan, 1st edn., 1984.
- [149] M. C. Hughes and D. J. Macero, *Inorg. Chem.*, 1976, **15**, 2040–2044.
- [150] U. Casellato, R. Graziani, R. P. Bonomo and A. J. Di Bilio, *J. Chem. Soc., Dalton Trans.*, 1991, 23.
- [151] J. C. Yu, G. Li, X. Wang, X. Hu, C. W. Leung and Z. Zhang, *Chem. Commun.*, 2006, 2717–2719.
- [152] S. P. Berglund, S. Hoang, R. L. Minter, R. R. Fullon and C. B. Mullins, *J. Phys. Chem. BC*, 2013, **117**, 25248–25258.
- [153] F. Behrouznejad and N. Taghavinia, *Journal of Power Sources*, 2014, **260**, 299–306.
- [154] K. Murakoshi, G. Kano, Y. Wada, S. Yanagida, H. Miyazaki, M. Matsumoto and S. Murasawa, *Journal of Electroanalytical Chemistry*, 1995, **396**, 27–34.

- [155] S. Ito, T. N. Murakami, P. Comte, P. Liska, C. Grätzel, M. K. Nazeeruddin and M. Grätzel, *Thin Solid Films*, 2008, **516**, 4613–4619.
- [156] K. Kalyanasundaram and M. Nazeeruddin, *Chem. Phys. Lett.*, 1992, **193**, 292–297.
- [157] F. H. Allen, *Acta Crystallogr. Sect. B-Struct. Sci.*, 2002, **58**, 380.
- [158] I. J. Bruno, J. C. Cole, P. R. Edgington, M. K. Kessler, C. F. Macrae, P. McCabe, J. Pearson and R. Taylor, *Acta Crystallogr. Sect. B-Struct. Sci.*, 2002, **58**, 389.
- [159] W. A. Wickramasinghe, P. H. Bird, M. A. Jamieson and N. Serpone, *J. Chem. Soc., Chem. Commun.*, 1979, 798.
- [160] W. A. Wickramasinghe, P. H. Bird and N. Serpone, *Inorg. Chem.*, 1982, **21**, 2694–2698.
- [161] J. McMurtrie and I. Dance, *CrystEngComm*, 2005, **7**, 216.
- [162] E. C. Constable, K. Harris, C. E. Housecroft, M. Neuburger and J. A. Zampese, *CrystEngComm*, 2010, **12**, 2949.
- [163] H. S. Chow, E. C. Constable, C. E. Housecroft, K. J. Kulicke and Y. Tao, *Dalton Trans.*, 2005, 236–237.
- [164] D. L. Jameson and L. E. Guise, *Tetrahedron Lett.*, 1991, **32**, 1999–2002.
- [165] I. Sasaki, J. C. Daran and G. G. A. Balavoine, *Synthesis*, 1999, 815–820.
- [166] F. Kröhnke, *Synthesis*, 1976, 1–24.
- [167] M. Ziegler, V. Monney, H. Stoeckli-Evans, A. von Zelewsky, I. Sasaki, G. Dupic, J.-C. Daran and G. G. A. Balavoine, *Dalton Trans.*, 1999, 667–675.
- [168] C.-G. Yan, X.-M. Cai, Q.-F. Wang, T.-Y. Wang and M. Zheng, *Org. Biomol. Chem.*, 2007, **5**, 945–951.
- [169] J. Wang and G. S. Hanan, *Synlett*, 2005, 1251–1254.
- [170] K. P. C. Vollhardt and N. E. Schore, *Organische Chemie*, 4th edn., 2005.
- [171] B. Tang, F. Yu, P. Li, L. Tong, X. Duan, T. Xie and X. Wang, *J. Am. Chem. Soc.*, 2009, **131**, 3016–3023.
- [172] W. Goodall and J. A. G. Williams, *Chem. Commun.*, 2001, 2514–2515.
- [173] E. C. Constable, P. Harverson, D. F. Smith and L. A. Whall, *Tetrahedron*, 1994, **50**, 7799–7806.
- [174] A. S. Guram and S. L. Buchwald, *J. Am. Chem. Soc.*, 1994, **116**, 7901–7902.
- [175] F. Paul, J. Patt and J. F. Hartwig, *J. Am. Chem. Soc.*, 1994, **116**, 5969–5970.
- [176] E. C. Constable, E. L. Dunphy, C. E. Housecroft, M. Neuburger, S. Schaffner, F. Schaper and S. R. Batten, *Dalton Trans.*, 2007, 4323–4332.
- [177] E. C. Constable, C. E. Housecroft, E. Medlycott, M. Neuburger, F. Reinders, S. Reymann and S. Schaffner, *Inorganic Chemistry Communications*, 2008, **11**, 518–520.
- [178] *The Merck Index an encyclopedia of chemicals, drugs, and biologicals*, ed. S. Budavari, M. J. O’Neil, A. Smith and P. E. Heckelmann, Merck & CO, Rahway, 11th edn., 1989.

- [179] *APEX2, version 2 User Manual, M86-E01078*, Bruker Analytical X-ray Systems, Madison, 2006.
- [180] A. Altomare, G. Cascarano, C. Giacovazzo, A. Guagliardi, M. C. Burla, G. Polidori and M. Camalli, *J. Appl. Cryst.*, 1994, **27**, 435.
- [181] P. W. Betteridge, J. R. Carruthers, R. I. Cooper, K. Prout and D. J. Watkin, *J. Appl. Cryst.*, 2003, **36**, 1487.
- [182] G. M. Sheldrick, *Acta Crystallogr., Sect. A: Fundam. Crystallogr.*, 2008, **64**, 112–122.
- [183] C. F. Macrae, I. J. Bruno, J. A. Chisholm, P. R. Edgington, P. McCabe, E. Pidcock, L. Rodriguez-Monge, R. Taylor, J. van de Streek and P. A. Wood, *J. Appl. Cryst.*, 2008, **41**, 466–470.
- [184] V.-M. Mikkala, M. Helenius, I. Hemmilä, J. Kankare and H. Takalo, *Helv. Chim. Acta*, 1993, **76**, 1361–1378.
- [185] W. Spahni and G. Calzagerri, *Helv. Chim. Acta*, 1984, **67**, 450–454.
- [186] W. Goodall, K. Wild, K. J. Arm and J. A. G. Williams, *J. Chem. Soc., Perkin Trans. 2*, 2002, 1669–1681.

Appendix A: X-ray structures: CIF file labels and CCDC numbers

Table 6.1: CIF files labels and CCDC number (P = preliminary data):

compound:	CIF file label	CCDC number
tris(diimine)chromium(III) complexes		
[Cr(bpy) ₃][PF ₆] ₃ ·MeCN	JS132	
[Cr(bpy) ₂ (phen)][PF ₆] ₃ ·3MeCN	JS145	
[Cr(bpy) ₂ (5,5'-Me ₂ bpy)][PF ₆] ₃ ·2Me ₂ CO	JS202 P	
4{[Cr(4,4'-Me ₂ bpy) ₂ (bpy)][PF ₆] ₃ }·12MeCN·H ₂ O	JS217	
[Cr(4,4'-Me ₂ bpy) ₂ (bpy)][PF ₆] ₃ ·2MeCN	JS217	
[Cr(5,5'-Me ₂ bpy) ₃][PF ₆] ₃	JS227 P	
bis(terpyridine)chromium(III) complexes		
2{[Cr(tpy) ₂][PF ₆] ₃ }·5MeCN	JS274	981376
[Cr(4'-(4-tolyl)tpy) ₂][CF ₃ SO ₃] ₃ ·2MeCN	JS323	
[Cr(LT1) ₂][CF ₃ SO ₃] ₃	JS357 P	
5{[Cr(LT5) ₂][CF ₃ SO ₃] ₃ }·MeCN	JS388	
[Cr(5,5''-Me ₂ tpy) ₂][CF ₃ SO ₃] ₃ ·H ₂ O	JS383	
[Cr(LT11)(HLT11)][PF ₆] ₄	JS258 P	
[Cr(tpy)(4'-(4-tolyl)tpy)][PF ₆] ₃ ·3MeCN	JS275	981377
[Cr(tpy)(HLT11)][PF ₆] ₄	JS294 P	
[Cr(tpy)(5,5''-Me ₂ tpy)][PF ₆] ₃ ·3MeCN	JS295	981378
[Cr(tpy)(LT7)][PF ₆] ₃ ·Me ₂ CO	JS299	
[Cr(tpy)(LT8)][PF ₆] ₃	JS301 P	
[Cr(tpy)(LT9)][PF ₆] ₃ ·2MeCN	JS303	
2{[H ₂ LT4][CF ₃ SO ₃] ₂ }·Et ₂ O	JS360	